Firing up the tumor: drug repurposing uncovers novel role of 5-Nonyloxytryptamine in boosting immunotherapies and uncovering ferroptosis inducing functions of volasertib in B-ALL

Inaugural dissertation

for the attainment of the title of doctor

in the Faculty of Mathematics and Natural Sciences

at the Heinrich Heine University Düsseldorf

presented by

Paweł Stachura

from Radom, Poland

Dusseldorf, July 2024

from the institute for Molecular Medicine II

and

Department of Pediatric Oncology, Hematology and Clinical Immunology

at the Heinrich Heine University Düsseldorf

Published by permission of the

Faculty of Mathematics and Natural Sciences at

Heinrich Heine University Düsseldorf

Supervisor: Prof. Dr. Philipp Lang

Co-supervisor: Prof. Dr. Arndt Borkhardt

Date of the oral examination:

Table of Contents

This cumulative thesis is based on articles obtained during doctoral study:

1. **Senescent Tumor CD8$^+$ T Cells: Mechanisms of Induction and Challenges to Immunotherapy.**
   Liu W*, **Stachura P***, Xu HC, Bhatia S, Borkhardt A, Lang PA, Pandyra AA. 2020 Sep 30;12(10):2828. doi: 10.3390/cancers12102828. PMID: 33008037; PMCID: PMC7601312.
   Journal: Cancers (Basel). IF: 5.6

   Contribution:
   Paweł Stachura performed a data search and edited the manuscript.

2. **Unleashing T cell anti-tumor immunity: new potential for 5-Nonloxytryptamine as an agent mediating MHC-I upregulation in tumors**.
   Stachura P*, Liu W*, Xu HC, Wlodarczyk A, Stencel O, Pandey P, Vogt M, Bhatia S, Picard D, Remke M, Lang KS, Häussinger D, Homey B, Lang PA, Borkhardt A, Pandyra AA.
   2023 Aug 15;22(1):136. doi: 10.1186/s12943-023-01833-8. PMID: 37582744; PMCID: PMC10426104.
   Journal: Molecular Cancer. IF: 37.3

   Contribution:
   Paweł Stachura performed 30% of experiments, contributed in data analysis, methodology, writing parts of the manuscript and editing the manuscript. Paweł Stachura performed *in vitro* work with cancer cells: assessing cell death upon treatment with multiple compounds, flow cytometry analysis, gene and protein expression with qPCR and immunoblot, fluorescent microscopy, designing and cloning of sgRNA plasmids, generation and analysis of knock-down and knock-out clones and synergy responses in combinatorial treatment. Paweł Stachura performed *in vivo* tumor growth experiments with compound treatment also in combination with antibody-based cell depletion of CD8$^+$ T cells and anti-PD1 blockade. Paweł Stachura performed flow cytometry of tumors and lymph

nodes, histological, immunoblot and qPCR genes and proteins assessment and analysis of tumors. Paweł Stachura infected mice with LCMV, purified T cells and performed co-culture experiments, analyzing cytokines expression by flow cytometry upon compounds treatment. Paweł Stachura contributed to experiments included in every figure of this publication.

3. **Deep transfer learning approach for automated cell death classification reveals novel ferroptosis-inducing agents in subsets of B-ALL.**
   Stachura P, Lu Z, Kronberg R, Xu HC, Liu W, Tu JW, Scharov K, Kameri E, Picard P, von Karstedt S, Fischer U, Bhatia S, Lang PA, Borkhardt A and Pandyra AA
   Submitted on 7th March 2024 for publication in Cell Death and Disease. IF: 9.2

   Contribution:
   Paweł Stachura performed 40% of the experiments, analyzed the data and contributed in conceptualization, methodology and writing the manuscript. Paweł Stachura performed the *in vitro* experiments, optimized and assessed cell death induction analyzed with flow cytometry and fluorescent microscopy, gene expression with qPCR upon compounds treatment in multiple cell lines. Paweł Stachura contributed to deep transfer based program development by optimizing and performing cell death induction, generating Incucyte images, performing drug screening, visualization and statistical analyses. Paweł Stachura generated the C1498 cell line expressing GFP and luciferase. *In vivo*, Paweł Stachura performed all *in vivo* experiments. Paweł Stachura assessed flow cytometry and gene expression data of patient-derived cancer samples upon compound treatment. Paweł Stachura contributed to experiments included in every figure of this manuscript.

*Contributed equally; IF from 2023

Publications not included in this doctoral thesis:

1. **Repurposing the serotonin agonist Tegaserod as an anticancer agent in melanoma: molecular mechanisms and clinical implications**
   Liu W*, **Stachura P***, Xu HC, Umesh Ganesh N, Cox F, Wang R, Lang KS, Gopalakrishnan J, Häussinger D, Homey B, Lang PA, Pandyra AA
   2020 Feb 21;39(1):38. doi: 10.1186/s13046-020-1539-7. PMID: 32085796; PMCID: PMC7035645.
   Journal: Journal of Experimental & Clinical Cancer Research. IF: 11.4

2. **Cyclic AMP-hydrolyzing phosphodiesterase inhibitors potentiate statin-induced cancer cell death**
   Longo J*, Pandyra AA*, **Stachura P**, Minden MD, Schimmer AD, Penn LZ
   2020 Oct;14(10):2533-2545. doi: 10.1002/1878-0261.12775. Epub 2020 Aug 25. PMID: 32749766; PMCID: PMC7530792.
   Journal: Molecular Oncology. IF: 6.6

3. **The role of ADAM17 during liver damage**
   Al-Salihi M, Bornikoel A, Zhuang Y, **Stachura P**, Scheller J, Lang KS, Lang PA
   2021 Jun 30;402(9):1115-1128. doi: 10.1515/hsz-2021-0149. PMID: 34192832.
   Journal: Biological Chemistry. IF: 2.9

4. **Deep Transfer Learning Approach for Automatic Recognition of Drug Toxicity and Inhibition of SARS-CoV-2**
   Werner J, Kronberg RM, **Stachura P**, Ostermann PN, Müller L, Schaal H, Bhatia S, Kather JN, Borkhardt A, Pandyra AA, Lang KS, Lang PA
   2021 Apr 2;13(4):610. doi: 10.3390/v13040610. PMID: 33918368; PMCID: PMC8066066.
   Journal: Viruses by MDPI. IF: 3.8

5. **BAFF Attenuates Immunosuppressive Monocytes in the Melanoma Tumor Microenvironment**

   Liu W, **Stachura P**, Xu HC, Váraljai R, Shinde P, Ganesh NU, Mack M, Van Lierop A, Huang A, Sundaram B, Lang KS, Picard D, Fischer U, Remke M, Homey B, Roesch A, Häussinger D, Lang PA, Borkhardt A, Pandyra AA

   2022 Jan 15;82(2):264-277. doi: 10.1158/0008-5472.CAN-21-1171. Epub 2021 Nov 22. PMID: 34810198; PMCID: PMC9397630.

   Journal: Cancer Research. IF: 12.5

6. **Arenaviruses: Old viruses present new solutions for cancer therapy**

   Stachura P, Stencel O, Lu Z, Borkhardt A, Pandyra AA

   2023 Mar 24;14:1110522. doi: 10.3389/fimmu.2023.1110522.

   PMID: 37033933; PMCID: PMC10079900.

   Journal: Frontiers in Immunology. IF: 5.7

7. **Integrative multi-omics reveals two biologically distinct groups of pilocytic astrocytoma**

   Picard D, Felsberg J, Langini M, **Stachura P**, Qin N, Macas J, Reiss Y, Bartl J, Selt F, Sigaud R, Meyer FD, Stefanski A, Stühler K, Roque L, Roque R, Pandyra AA, Brozou T, Knobbe-Thomsen C, Plate KH, Roesch A, Milde T, Reifenberger G, Leprivier G, Faria CC, Remke M

   2023 Oct;146(4):551-564. doi: 10.1007/s00401-023-02626-5. Epub 2023Sep1.

   PMID: 37656187; PMCID: PMC10500011.

   Journal: Acta Neuropathologica. IF: 13.1

*Contributed equally; IF from 2023

Acknowledgments

It is my great honor to acknowledge people who contributed to my PhD career. This PhD journey has been a rollercoaster of experiments, late nights, and a fair amount of self-doubt. But as I reach the end, it's time to express my gratitude to those who stood by me and helped make this possible.

A special thanks to my supervisor, Prof. Philipp Lang, who took a chance on me and accepted me for this PhD. You have taught me more about immunology than I ever thought possible, and I am grateful for the knowledge and guidance. To my second supervisor, Prof. Arndt Borkhardt, thank you for welcoming me into the leukemia laboratory. The experience I gained there is invaluable. Both of You have not only imparted a vast amount of knowledge but also provided opportunities that allowed me to grow as a researcher. The many projects I could join and conferences you encouraged me to attend have been instrumental in my development.

My daily lab supervisor, Prof. Aleksandra Pandyra deserves a medal for her patience. Your daily support, both scientific, personal, and occasional reality checks kept me on track. From the countless hours spent analyzing data to the even more countless hours listening to me whine about it, you were there every step of the way. You taught me how to be a leader, showing me through your own example what it means to support a team with strength and compassion. And let's not forget your incredible ability to see light in my data where I only saw trash! While I was busy lamenting over what I was sure were failed experiments, you somehow managed to find the bright side.

And to the friends I made during my PhD: AnnaRita, Cassy, Arshia, Farhad, Julia, Julian, Meryem, Max, Wei, Zhe, Ersen, Eleni, Kati, Julian, Vera, Jia, Rebcia, Mela, Olivia and many more - you are the ones who made this journey more than just academic. You are the people I could count on daily for help, laughs, shared lunches, and those unforgettable lab-outs. We bonded over science, but also over late-night parties, spontaneous trips, and shared frustrations. Gabriel and Lorenz - You made my life here beautiful. Whether it was a quiet evening in or an all-night clubbing adventure, you were always there to remind me that life is about balance between the hard work and the fun. Thank you for the unforgettable memories we created together.

In the end, I didn't just gain a title, I gained friends. You have made Düsseldorf a place I will always carry in my heart.

To my Polish friends, both those who stayed in Poland and those who ventured abroad: Lila, Dajana, Monika, Kasia, Maja, Olga, Asia, Natlia and Paula but also Pana and Ben - thank you for keeping the connection alive across borders, you were the ones who kept my spirits high. Whether it was a quick visit or a longer stay, you always made room for me and gave me a home away from home.

Most importantly, I want to thank my family. Mom and Dad, you have always said I am lazy, but smart when I want to be. I hope this PhD proves I finally want to be more smart than lazy. Your unwavering support kept me going, even when I moved abroad to pursue this dream. To my Parents Anna and Sławomir, my sisters Emila and Iwona, my brother-in-law Łukasz, and my amazing nephews Natalia and Kacper: your warm welcome every time I returned home was like a recharge button for my soul. Thank you for always being there, cheering me on, and making me feel like a hero, even if just for getting through another chapter. Also thank you for keeping my fridge full, even from abroad. I could always count on packages with pierogi and kielbasa that made me feel a bit like at home.

List of Abbreviations

5-NL - 5-Nonyloxytryptamine

ACSL4 - Acyl-CoA synthetase long chain family member 4

AML - Acute myelogenous leukemia

AMPK - AMP-activated protein kinase

APC - Antigen-presenting cells

ATP - Adenosine triphosphate

B-ALL - B-cell acute lymphoblastic leukemia

BTK - Bruton's tyrosine kinase

CAR-T cell - Chimeric antigen receptor T cell

CGA - Cancer-germlines antigens

CML - Chronic myeloid leukemia

COX-2 - Cyclooxygenase 2

CREB - cAMP-response element binding protein

CTLA-4 - Cytotoxic T-lymphocyte associated protein 4

CXC - C-X-C chemokine

CXCR - C-X-C chemokine receptor

DAMPs - Damage-associated molecular patterns

DC - Dendritic cells

EGFR - Epidermal growth factor receptor

ER - Endoplasmic reticulum

FDA - Food and Drug Administration

Foxp3 - Forkhead box protein p3

GPX4 - Glutathione peroxidase 4

GSH – Glutathione

GZMB – GranzymeB

HMGB1 - High mobility group box 1

HTR - 5-hydroxytryptamine (serotonin) receptor

ICB - Immune checkpoint blockade

ICD - Immunogenic cell death

IFN – Interferon

IL– Interleukin

KD – Knock-down

KO – Knock-out

LAG3 - Lymphocyte-activation gene 3

MAPK - Mitogen-activated protein kinase

MHC - Major histocompatibility complex

MUFA - Monounsaturated Fatty Acids

NK – Natural killer

NSCLC - Non-small cell lung cancer

PAMPs - Pathogen-Associated Molecular Patterns

PD-1 - Programmed cell death 1

PDE – Phosphodiesterase

PD-L1 - Programmed death-ligand 1

PDX – Patient derived xenograft

PGE2 - Prostaglandin E2

PI3K - Phosphatidylinositol 3-kinase

PLK - Polo-like kinase

PUFA - Polyunsaturated fatty acid

ROS - Reactive oxygen species

SAPE-OOH - 1-steaoryl-2-15-HpETE-sn-glycero-3-phosphatidylethanolamine

TAA - Tumor associated antigens

TAM – Tumor associated macrophage

TCR - T cell receptor

TGF - Transforming growth factor

Tim3 - T-cell immunoglobulin and mucin domain 3

TKI - Tyrosine kinase inhibitor

TLR – Toll like receptor

TMB - Tumor mutation burden

TME - Tumor microenvironment

TNF - Tumor necrosis factor

Treg - T regulatory cells

TSA - Tumor specific antigens

VEGF - Vascular endothelial growth factor

SUMMARY

Recent research indicates that cancer development is influenced not only by the malignant cells themselves but also by interactions with surrounding stromal cells and immune infiltrates. The progression of cancer is facilitated by an immunosuppressive tumor microenvironment (TME), which enables immune escape. The concept of tumor "hotness," which describes the presence of an intra-tumoral T cell signature, is useful in predicting responsiveness to immunotherapies. "Hot" tumors, characterized by high immune cell infiltration, demonstrate a better prognosis when treated with immunotherapies compared to "cold" tumors that have minimal immune cell infiltration and/or exhausted/dysfunctional T cells. Enhancing tumor hotness involves modulating the TME to boost antigen presentation and T cell activation, which can be achieved by manipulating immune checkpoints, cytokine production, and immunogenic cell death pathways.

This doctoral thesis encompasses the biology and recent progress in understanding and boosting functions of dysfunctional T cells in cancer treatment. Many compounds including chemotherapeutics are now recognized for their immunomodulatory effects, warranting a reevaluation of their potential in combination therapies to improve anti-cancer immunity and tumor hotness. The immunomodulatory effects of 5-Nonyloxytryptamine (5-NL), a serotonin receptor agonist, were identified through drug screening. Initially developed for targeting serotonin receptors, 5-NL was found to enhance MHC class I expression on tumor cells, crucial for T cell recognition and elimination of tumor cells. This effect was linked to the modulation of several signaling pathways independent of classical serotonin signaling. 5-NL treatment led to activation of the AMPK pathway and subsequent phosphorylation of CREB, influencing the antigen-presenting machinery. *In vivo* settings indicate that combining 5-NL with anti-PD1 antibodies enhanced efficacy, suggesting its potential to convert "cold" tumors to "hot" tumors.

Another approach for increasing tumor hotness is the induction of immunogenic cell death (ICD) that transforms the TME from immunosuppressive to immune-activating. Ferroptosis, a form of regulated cell death characterized by lipid peroxide accumulation, has emerged as a promising strategy to enhance cancer therapy by inducing ICD. Using a deep-learning screening-based approach, volasertib, a chemotherapeutic agent, was revealed to have novel ferroptosis-inducing functions in several B-ALL cell lines, patient-derived xenograft samples and in an *in vivo* leukemia model. Volasertib treatment led to iron ion accumulation, glutathione depletion and membrane lipids peroxidation. Recent studies indicate that induction of ferroptosis has the potential to not only increase tumor immunogenicity but to also overcome chemoresistance. Combining ferroptosis inducers such as volasertib with immune checkpoint

inhibitors or other immunotherapies could improve overall treatment efficacy, particularly in immunologically cold and apoptosis-resistant cancers.

ZUSAMMENFASSUNG

Jüngste Forschungsergebnisse zeigen, dass Krebs durch ein Zusammenspiel maligner Zellen und deren Interaktion mit den umliegenden Stromazellen und infiltrierenden Immunzellen entsteht. Das Fortschreiten der Erkrankung wird durch ein immunsuppressives Tumormikromilieu (TME) begünstigt, welches eine Immunevasion des Tumors ermöglicht. "Heiße" Tumore, die durch eine hohe Immunzellinfiltration gekennzeichnet sind, zeigen bei der Behandlung mit Immuntherapien eine bessere Prognose im Vergleich zu "kalten" Tumoren, die eine minimale Immunzellinfiltration und/oder erschöpfte/dysfunktionale T-Zellen aufweisen. Die Tumorinfiltration kann durch Modulation des TME erhöht werden. Dies kann über eine Steigerung der Antigenpräsentation und T-Zell-Aktivierung durch Manipulation von Immuncheckpoints, Zytokinproduktion und immunogenen Zelltod erreicht werden.

Diese Doktorarbeit befasst sich mit der Biologie und den Fortschritten, die in den letzten Jahren zum Verständnis und der Aktivierung dysfunktionaler T-Zellen in der Krebsbehandlung beigetragen haben. Eine Vielzahl von Substanzen, unter anderem Chemotherapeutika, besitzen immunmodulatorische Effekte. Dies macht eine Neubewertung ihres Potenzials in Kombinationstherapien zur Verbesserung der Anti-Tumor-Immunität und der Tumorinfiltration erforderlich. In dieser Dissertation wurden die immunmodulatorischen Effekte von 5-Nonyloxytryptamin (5-NL), einem Serotoninrezeptor-Agonisten, durch ein Wirkstoff-Screening identifiziert. Ursprünglich wurde 5-NL zur Bindung von Serotoninrezeptoren entwickelt, erhöht jedoch auch die Expression von MHC-Klasse-I-Proteinen auf Tumorzellen, was für die T-Zell-Erkennung und Eliminierung von Tumorzellen entscheidend ist. 5-NL moduliert mehrere Signalwege, die unabhängig von der klassischen Signaltransduktion durch Serotonin sind. Die Behandlung mit 5-NL führte zur Aktivierung des AMPK-Signalwegs und zur anschließenden Phosphorylierung von CREB, welches die antigenpräsentierende Maschinerie beeinflusst. In-vivo-Studien zeigten, dass die Kombination von 5-NL mit Anti-PD1-Antikörpern deren Wirksamkeit erhöht. Dies deutet darauf hin, dass durch die Kombination beider Wirkstoffe „kalte“ zu „heißen“ Tumoren umgewandelt werden können.

Ein weiterer Ansatz zur Erhöhung der Tumorinfiltration ist die Induktion des immunogenen Zelltods (ICD), um ein immunsuppressives TME zu einem immunaktivierenden TME umzuwandeln. Ferroptose, eine Form des regulierten Zelltods, die durch die Ansammlung von Lipidperoxiden gekennzeichnet ist, hat sich als vielversprechende Strategie zur Verbesserung der Krebstherapie durch Induktion von ICD erwiesen. Mithilfe eines Deep-Learning-basierten Screenings wurde Volasertib, ein Polo-like-Kinase 1 Inhibitor, als neuer Ferroptose-induzierender Wirkstoff in mehreren B-ALL-Zelllinien, Patientenproben und in einem In-vivo-Leukämiemodell identifiziert. Die Behandlung mit Volasertib führte zur Akkumulation von Eisenionen, zur Depletion von Glutathion sowie Lipidperoxidation der Zellmembran. Studien

weisen darauf hin, dass die Induktion von Ferroptose nicht nur die Tumorimmunogenität erhöht, sondern auch Chemoresistenz überwinden kann. Die Kombination von Ferroptose-Induktoren, wie etwa Volasertib, mit Immuncheckpoint-Inhibitoren oder anderen Immuntherapien könnte daher die Krebsbehandlung verbessern, insbesondere bei immunologisch „kalten“ und Apoptose-resistenten Tumoren.

INTRODUCTION

Cancer remains one of the most challenging diseases of our times in the context of cure and treatment. According to The Global Burden of Diseases, Injuries, and Risk Factors Study (GBD) in 2019 23.6 million new cancer cases were reported and globally 10 million deaths occurred due to cancer (1). Cancer is in part a disease of aging, as mutations accumulate through a lifetime and 90% of diagnosed cases are in an age group above 50 (2). Therefore, as many people are living longer, there is a growing burden of cancer. In addition, cancer is also a leading cause of death in children and adolescents with leukemia being the most commonly diagnosed form (3). Improvements in early tumor detection, surgical techniques, research in biomarkers and targeted therapy, and many other factors have increased the survival rate of many types of cancer (4). Unfortunately, the treatment progress has not been equal in all tumor types leading to a visible disproportion in the survival. For example, the five-year cancer survival rate for prostate or breast cancer is over 90%, whereas for patients with liver or lung cancer only around 18% (5). Modern and effective anti-cancer therapies, for example, cell transfer or immune checkpoint blockade immunotherapies are not affordable for many patients or even not available in many countries (6). Not surprisingly, the number of deaths caused by cancer is the highest in low- and middle-income countries, whereas the highest rate of five year-survival in high-income countries, according to the International Agency for Research on Cancer, WHO (statistics for 2020).

Molecularly, cancer cells are characterized by intrinsically complex biological attributes that differentiate them from healthy cells. In the seminal Hanahan and Weinberg recently updated “Hallmarks of cancer” paper, a cancer cell was classically described as resisting cell death, sustaining proliferative signaling, evading growth suppressors, activating invasion and metastasis, enabling replicative immortality, inducing angiogenesis, deregulating cell metabolism, avoiding immune destruction, inducing tumor-promoting inflammation and genome instability (7). Cancer hallmarks including avoiding immune destruction and tumor-promoting inflammation led to a further important way of tumor classification according to inflammatory status, also known as “hotness”.

1. Cold and hot tumors

Tumor hotness describes the immune phenotype, which depends on high immune cell abundance, especially T- and NK cells in hot tumors and mechanisms of immune evasion in cold tumors (8). Tumors are divided into four immunoscores: hot, cold, altered immunosuppressed and altered excluded (Figure 1) (9). Hot tumors are characterized by high degree lymphocytes infiltration, measured with $CD3^+$ or $CD8^+$, but also targetable immune checkpoint activation markers PD1, LAG3, Tim3, and CTLA-4 (10). Altered immunosuppressed tumors are defined by poor T cells infiltration, but also a high immunosuppressive environment with TGF-β, IL-10, VEGF and the presence of myeloid-derived immunosuppressive and T regulatory cells (Treg) that limit recruitment and expansion of $CD8^+$ T cells (10, 11). Altered excluded tumors experience hypoxia, abnormal vasculature and epigenetic reprogramming of the tumor microenvironment (TME) to create a barrier that leads to the accumulation of T cells on the tumor border (invasive margin), enabling the penetration (9, 10). Lastly, cold tumors are characterized by the absence of infiltrating T cells within and around resulting in part from failed $CD8^+$ T cells priming due to low tumor mutational burden, poor antigen presentation, or intrinsic insensitivity to T cell killing (9). The differences in tumor immunoscores are crucial for patient treatment and adjusting therapy to the predicted responsiveness, especially in treatment with immune checkpoint blockade (ICB) (12). For example, in the case of colon cancer immunoscore has a greater prognostic value than any other clinically used system like pathologic T stage, pathologic N stage, lymphovascular invasion, tumour differentiation or microsatellite instability status (13).

In this chapter differences between cold and hot immune phenotypes of solid tumors, namely the importance of antigen presentation and its mechanism, but also the role of immune components in tumor control and stages of $CD8^+$ T cells will be described. Finally, the TME components and their interplay influencing tumor hotness will be explored.

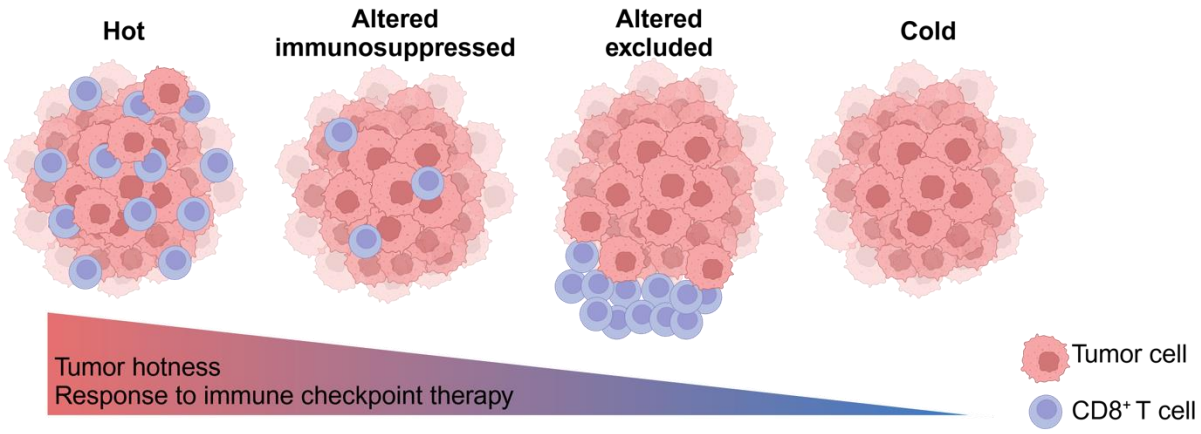

Figure 1. Schematic representation of hot, altered immunosuppressed, altered excluded and cold tumors. Tumor hotness describes $CD8^+$ T cells infiltration of the tumor, with hot tumors being highly inflamed, altered immunosuppressed with little infiltration, altered excluded with $CD8^+$ T cells on the border of the tumor and cold without infiltration. Tumor hotness correlates with responsiveness to immune checkpoint therapies. Figure created with Biorender, adapted from (14)

1.1. Tumor antigen presentation

The current classification of tumor immune phenotype is highly dependent on tumor infiltrating lymphocytes (TIL), especially $CD8^+$ T cells. High $CD8^+$ T cell infiltration is generally attributed to hot tumors (8). Cytotoxic $CD8^+$ T cells are the main players in anti-tumor immunity. Primed by antigen-presenting cells (APC), they have the ability to selectively attack cancer cells by production of cytotoxic cytokines (15). Specific $CD8^+$ anti-tumor responses can be achieved by antigen recognition presented by major histocompatibility complex class I (MHC-I) molecules on the cancer cell surface (16). MHC-I is expressed by all nucleated cells and contains beta-2 microglobulin (β_2m) in complex with HLA- A, B and C protein in humans or H2-Db and –Kb in mice (17). MHC-I assembly takes place in the endoplasmic reticulum (ER) where presented peptides are also delivered by the transporter associated with antigen processing (TAP) (18). Next, Tapsin bridges the interaction between MHC-I and TAP but also facilitates the loading of high affinity peptides on MHC-I. The created peptide-MHC-I complex is transported through the Golgi apparatus to the cell membrane (19). Important for cancer cell recognition, peptides loaded on MHC-I are derived from proteasomally degraded proteins, which failed in *de novo* ribosomal translation, and not from pre-

existing proteins. This allows for the presentation of newly synthetized proteins, potentially tumor antigens, for immediate recognition by CTLs (19). A few types of tumor antigens exist: tumor specific antigens (TSA), tumor associated antigens (TAA) and cancer-germlines antigens (CGA). TSAs are expressed in cancer cells, but not in healthy tissue as the result of mutations in DNA or virus-derived tumors, such as HPV positive tumors (20). TAA are expressed on healthy tissue but at a lower level than on cancer cells. Therefore, there is incomplete immune tolerance towards these antigens. Examples of TAA can be melanocyte differentiation antigens presented in melanomas (21) or HER-2 in ovarian tumors (22). Another class of antigens are CGA which are derived from proteins that can be expressed in germline cells, but also cancer cells with dysregulated methylation of their promoter (23).

Another important aspect of tumor hotness is tumor mutation burden (TMB). TMB is a factor representing the increased prevalence of somatic mutations that can be induced by microsatellite instability (MSI) or mismatch repair (MMR) deficiency. Genome instability with DNA repair insufficiency accumulates mutations that lead to neoantigen formation and therefore trigger immune surveillance (24). Cancers with high TMB are genetically unstable and commonly induced by carcinogens or UV light, for example, melanoma or non-small cell lung cancer (NSCLC) (25). However, a high mutational burden does not always reflect high tumor infiltration. For example, colorectal cancer and metastatic melanoma tumors are characterized by microsatellite instability but may not respond to ICB therapies due to low T-cells inflamed phenotype (26). Neoantigens and the level of antigen presentation are not the only factors important for specific anti-tumor killing. Priming and activation of $CD8^+$ T cells capable of eliciting specific anti-tumor response is also crucial and this process requires antigen cross-presentation with APCs. Cancer cells undergoing immunogenic cell death release Pathogen-Associated Molecular Patterns (PAMPs) or Damage Associated Molecular Patterns (DAMPs), which in turn can activate APCs, specifically dendritic cells (DC) (27). Activated antigen presenting cells not only produce cytokines but through overexpressed Pattern Recognition Receptors (PRRs) promote MHC-I dependent antigen cross-presentation with T cell receptor (TCR) of $CD8^+$ T cells. By expressing co-stimulatory molecules CD80 and CD86, DCs can activate the CD28 receptor of $CD8^+$ T cells (28) (Figure 2). Batf3 is a transcription factor, crucial for dendritic cells development and functional cross-presentation (29). The study by Hildner proved the essential role of DC priming $CD8^+$ T cells. The authors generated Batf3 knockout mice

and demonstrated impaired antigen cross-presentation towards CD8⁺ T cells and no tumor control in highly immunogenic tumors *in vivo* (29). Taking into consideration the importance of APCs, especially DCs in cytotoxic lymphocyte priming and activation, there are several works reporting that impaired recruitment of antigen presenting cells leads to a cold tumor phenotype (Figure 2). Spranger et al. analyzed patient metastatic melanoma samples and discovered that among those who expressed similar levels of antigens, a group of non-inflamed tumors lacked Batf-3 dendritic cell markers, pointing to a decreased number of DC in the tumor microenvironment (30). In another study Spranger showed that activated Batf-3 positive dendritic cells infiltrating tumor produce chemokine CXCL9 and CXCL10 (CXCL11 in humans), ligands of CXCR3 expressed on CD8⁺ T cells, and therefore are responsible for recruiting effector T cells to tumor side, increasing their hotness (31).

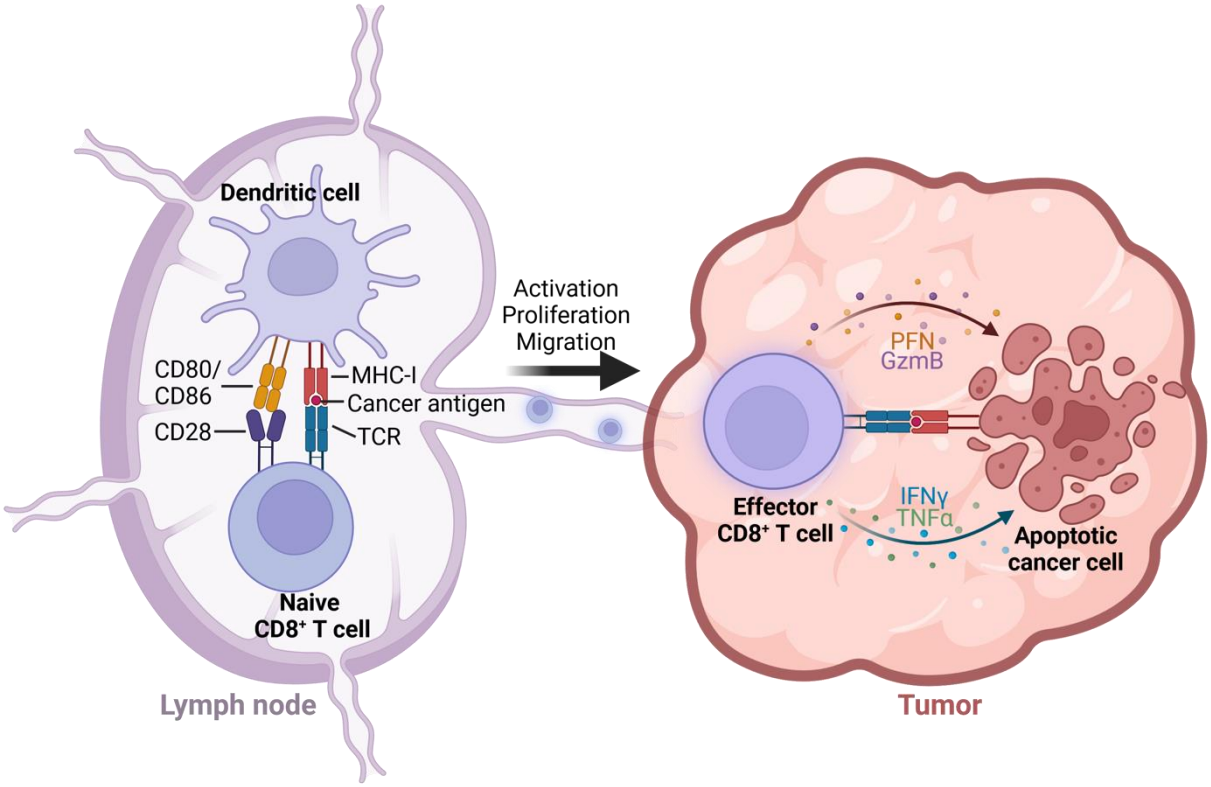

Figure 2. Dendritic cells in the lymph node present cancer antigens on MHC-I to naïve CD8⁺ T cells and activate them with CD80 and CD86, ligands of CD28. CD8⁺ T cells become activated, proliferate and migrate to the tumor bed, where, after TCR recognition release perforin (PFN), granzyme B (GzmB), interferon gamma (IFNγ) and tumor necrosis factor alfa (TNFα), inducing cancer cell death. Figure created with Biorender, adapted from (32).

Taken together, the classification of a tumor's immunoscore depends largely on the presence of TILs, particularly $CD8^+$ T cells, which play a critical role in attacking cancer cells through the recognition of antigens presented by MHC-I molecules. However, effective anti-tumor immunity also relies on the activation and priming of $CD8^+$ T cells by antigen-presenting cells, especially dendritic cells. Therefore, the importance of increasing tumor antigen presentation by modulating MHC-I expression can influence the tumor's immune phenotype and its responsiveness to immunotherapies.

1.2. Role of $CD8^+$ T cells in tumor control

Cytotoxic $CD8^+$ T cells represent the most important immune population in tumor detection and elimination. As described above, $CD8^+$ T cells function relies on the delicate interplay of innate and adaptive immune components, from priming with tumor antigen to activation of T cells. Firstly, $CD8^+$ and TCR acting as co-receptors interact with MHC-I on the surface of antigen presenting or cancer cells and get activated usually by simultaneous activation of CD28 by CD80 or CD86 ligand expressed by APC, macrophages, or activated B-cells (28). T cells can be activated by self-antigens, which could lead to autoimmune disease, but without the co-activation of the CD28 receptor, they undergo apoptosis (33). Activation of CD28 initiates recruitment of phosphatidylinositol 3-kinase (PI3K) and nuclear factor-κB (NF-κB) leading to proliferation of activated $CD8^+$ T cells, production of IL-2 and accumulation of Bcl-xL, protecting from apoptotic death (33, 34). Target cell killing by activated $CD8^+$ T cells is achieved, after recognition of antigen, by secreting IFNγ and death inducing granules, namely granzymes, PFN, cathepsin C and granulysin, which can fuse with the cancer cell membrane (35, 36) (Figure 2). Additionally, effector T cells by interacting with target cells can induce their cell death through expressed Fas ligand (FASL), which activates Fas-associated protein with death domains (FADD), leading to Caspase-dependent cell death (34, 37). Nevertheless, during cancer progression infiltrating $CD8^+$ T cell become dysfunctional by acquiring anti-tumor tolerance and differentiating from active effector into exhausted phenotype due to persistent exposure to tumor antigen (38). During T cells activation cells express immune-checkpoints molecules, which are inhibitory receptors on their surface, and which accumulate during antigen exposure (34). Immune-checkpoints molecules include: programmed cell death

receptor 1 (PD-1 or CD279) with the ligands PD-L1 and PD-L2; cytotoxic T-lymphocyte-associated protein (CTLA-4) with the ligands CD80 and CD86; lymphocyte-activation gene 3 (LAG-3), T-cell immunoglobulin and mucin domain-3 (TIM-3) and T-cell immunoreceptor with Ig and ITIM domains (TIGIT) (34). Other than exhaustion $CD8^+$ T cells can undergo a senescent state upon repetitive antigen stimulation, stress signals induced by anti-cancer therapy and aging (39). $CD8^+$ T cell exhaustion and senescence are broadly described in the article "**Senescent Tumor $CD8^+$ T Cells: Mechanisms of Induction and Challenges to Immunotherapy**" which is part of this cumulative dissertation.

1.3. Tumor microenvironment

The tumor microenvironment section outlines the interplay between cancer cells and immune components important in influencing a tumor's immunoscore. Within the TME, there are many tumor or immune derived pro- and anti-inflammatory factors. In the above "tumor antigen presentation" subchapter, antigen presentation, which is a crucial part of TME in the generation of specific anti-tumor $CD8^+$ T cells, immunosurveillance was described. Cancer cells can escape recognition by downregulation of MHC-I expression. Natural killer (NK) cells represent the main effector population of the innate system in anti-cancer immunity and express on their surface immunoreceptor tyrosine-based inhibitory motifs (ITIMs), which inhibit NK cells activity when coming in contact with MHC-I molecules. Subsequently, cancer cells with lower antigen presentation become a target for NK cells (40). Stimulation and natural killer cell activation lead to their high proliferation and conventional effector response, which is high production of cytokines IFNγ, perforin and granzymes in the tumor microenvironment (41). Additionally, tumor infiltration with NK cells was recognized to elevate inflammation by producing chemokine CCL5, CXCL1, and CXCL2 responsible for recruiting dendritic cells to the tumor bed, which increased level was correlated with increased hotness and better patient survival (42). APCs express MHC class II, through which antigen can be also presented to CD4 helper T cells, recruiting them to the tumor side (43). Primed and activated $CD4^+$ T cells can directly target cancer cells, although only these expressing MHC-II, hematological malignancies, and lymphomas (44). In the case of solid tumors, $CD4^+$ helper T cells cytotoxicity was correlated with

expressing cytokines, including interferon gamma (IFNγ) and GranzymeB (GZMB) (45). Most importantly $CD4^+$ T cells play a role in $CD8^+$ T cell priming by enhancing activation of dendritic cells by CD40/CD40L interaction, but also by directly boosting $CD8^+$ T cell activity through the release of interleukine-2 (IL-2) within the tumor microenvironment (46).

Another subgroup of T cells are the regulatory T cells (Treg). This population is important in tumor hotness due to its highly immunosuppressive properties and is characterized by the expression of forkhead box protein p3 (Foxp3) (47). Tregs repress the immune response, especially $CD8^+$, $CD4^+$ T cells and DCs by the production of inhibitory cytokines including IL-10, TGF-β, and IL-35. Additionally they can repress the function and proliferation of effector and helper T cells in direct cell to cell contact by surface expressed TGF-β, PD-L1 and CTLA-4 molecules (48). Not only T cells, but Tregs cells can mediate suppression of natural killer cells by downregulation of TIM-3 and upregulation of the NK inhibitory receptors PD-1 and the IL-1R, therefore lowering proliferation and degranulation of NK cells (49). Regulatory T cells are highly attracted to IL-2 and consume high levels of that cytokine, competing with $CD8^+$ T cells, therefore blocking the IL-2 signal was proven to be beneficial in anti-cancer therapy (50). Additionally, Tregs express on their surface nucleases CD39 and CD73 which can break extracellular ATP and ADP to AMP and produce adenosine, which is a known inhibitory molecule of receptors: A1, A2A, A2B, and A3 expressed by variety effector cells (51).

In addition to the above-mentioned lymphocytes, myeloid cells such as dendritic cells, granulocytes, monocytes and macrophages also play a role in tumor control. The important role of DCs was described in the chapter above “tumor antigen presentation”.

An important subgroup in cancer development are neutrophils which are the most abundant granulocyte population in human blood and have pro- and anti-tumoral traits (52). Neutrophils have a direct ability to promote oncogenesis by releasing ROS and additionally oxidating DNA in the inflamed tissue (53), which was additionally proven in the cancirogen induced lung cancer model, where neutrophils producing ROS were accelerating mutagenesis (54). Neutrophiles were also shown to promote tumor growth by secreting IL-1β cytokine in glioblastoma of female mice (55) or prostaglandin E_2 in RAS-driven neoplasia in the zebra fish model (56). Importantly, neutrophils can suppress other immune cells by mediators, like ROS, inducible nitric oxide synthase

and arginase 1, but also express PDL1 on their surface (57). Nevertheless, neutrophils' role in cancer development is context-specific. In two studies of spontaneous skin and intestinal tumorigenesis depletion of *cxcr2* inhibited neutrophils recruitment to the tumor bed and resulted in decreased tumor growth, supporting their immunosuppressive role (58, 59). On the other hand, depleting neutrophils through deletion of neutrophils survival factor *Mcl1* led to increased colon cancer with high intratumoral bacterial burden and increased inflammatory IL-17 cytokine (60), proving the important role in tumor control. Neutrophils can also directly attack cancer cells expressing TNF-related apoptosis-inducing ligand (TRAIL) inducing apoptosis (61), but also through release of the nitric oxide (62).

Monocytes represent a highly heterogenic and plastic subgroup of myeloid cells that react to changes in the tumor microenvironment that influence the phenotype, differentiation, and distribution of monocytes (63). Monocytes are attracted to the inflammatory side during tumorigenesis and their main functions are phagocytosis, antigen presentation, and cytokine production, but also responding to TME stimuli can differentiate into dendritic cells or macrophages (63) or directly kill cancer cells by expressing TRAIL (64). Monocytes can display anti- or pro-tumoral activities which once again is context specific. In studies of patients with breast and colorectal cancer, there was a specific $CD66b^{+}$ population of monocytes which was characterized by high phagocytic activity but also provided co-stimulation for T cells resulting in proliferation and IFN-γ secretion (65). Also, monocyte-derived tumor associated macrophages (TAMs) were shown to express high levels of Cxcl9 chemokine that were responsible for the migration of Cdxr3 positive T cells to the tumor bed (66). On the other hand, analysis of monocytes from patient breast cancer revealed an auto-stimulatory loop of tumor and TAMs whereby expression of CCL8 chemokine recruited more monocytes and by expression of TNFα induced pro-tumorgenic differentiation of these monocytes (67). Another study identified intratumoral monocytes with high expression of c-Rel of the NF-κB family that were expressing proinflammatory cytokine IL-1β together with a low level of suppressive molecule arginase 1. These c-Rel monocytes remarkably suppressed T-cell proliferation and function maintaining immunosuppressive TME (68), but also monocytes producing CCL5 were responsible for Treg tumor infiltration that greatly expressed CCR5 receptor (69). Monocytes have a clear antigen presenting role in case of infection or homeostasis (70), but in tumors they rather differentiate into monocyte-derived DC (moDC) and can successfully cross-present antigens in lymph

nodes, priming $CD8^+$ T cells (71). Nevertheless, moDC represents a minor population of monocyte origin. In a study on primary breast cancer, it was noticed that only within 5 days from tumor infiltration $CCR5^+$ classical monocytes upregulated F4/80, CD11c, MHCII, and V-CAM1 markers characteristic for TAMs (72). Tumor associated macrophages, which can be polarized into anti-tumoral phenotype (M1) or pro-tumorigenic subgroup (M2) and are differentiated between their function into host defense, wound healing and immune regulation (73). Macrophages become M1 polarized by stimulation with interferons (IFNβ or IFNγ) and TNFα, typically expressed by innate or adaptive immune cells in the first line of anti-tumor response. In turn, activated M1 macrophages express highly pro-inflammatory cytokines like IL-1, IL-6 and IL-23 (73). Additionally, macrophages possess the ability for phagocytosis and therefore both play a central role in helper and cytotoxic T cells activation by antigen cross-presentation of processed cancer epitopes (74). On the other hand, M2 type macrophages are recruited to the tumor side by transforming growth factor-β (TGFβ), macrophage colony-stimulating factor 1 (CSF1), CCL2, IL-4 and IL-1 produced by cancer cells, stromal fibroblasts, macrophages and B-cells (75). These macrophages are highly immunosuppressive by expressing PD-L1 and PD-L2 checkpoint inhibitory molecules on their surface but also secrete IL-10 and TGFβ promoting expansion of regulatory T cells within tumor microenvironment. Additionally, wound healing properties of M2 macrophages lead to the production of IL-1 and TGFβ that lead to tumor angiogenesis and therefore accelerated tumor growth (75).

Taken together, the tumor microenvironment is an extremely complex and dynamic system balancing between anti-tumoral and immunosuppressive cells and signaling interactions. The composition of the TME highly varies between tumor types and mostly depends on the infiltration of innate and adaptive immune cells and interaction with cancer cells therefore modulation of TME represents a great therapeutic opportunity.

2. Anti-cancer therapies

Conventional anti-cancer treatments include radiotherapy, chemotherapy and surgical resection in the case of solid tumors (76). Surgical removal of the tumor is the most promising treatment as it allows for the elimination of the cancer mass and it can be combined with radiation, which further destroys the unremoved cancer cells (76, 77). However, tumor resection has obvious limitations when the location of the tumor is difficult (78). Radiotherapy destroys cancer cells by the induction of DNA damage and leads to subsequent “abscopal response”, which is responsible for additional immune cells recruitment and increased adaptive immune responses (79). On the other hand, radiotherapy creates high levels of damaging reactive oxygen species (ROS) not only within the tumor but also in the tissue around it. Paradoxically, that promotes cancer metastasis by promoting the epithelial-mesenchymal transition (79, 80). Pharmacological therapies (Table 1) with classical chemotherapy targeting rapidly proliferating cells and molecularly targeted therapy that allows more precise effects on cancer cells remain a primary approach for most of the cancer types. On the other hand, there is an increasing trend in immunotherapies that boost the patient’s immune system in combating cancer. That can be achieved by increasing tumor hotness by modulating the tumor microenvironment, pharmacological induction of immunogenic cell death, targeting checkpoint inhibitors, delivering cancer antigens with vaccines, increasing inflammation with virus-based therapies, and modulating the patient’s immune cells (Figure 3) (81). Additionally, revolutionary cell-based therapy based on chimeric antigen receptor (CAR)-T cell has excellent therapeutic outcomes, especially with certain subsets of B cell leukemia or lymphoma (82). Taken together, tremendous progress has been made in advancing cancer treatment and there is a wide repertoire of treatment options including surgical techniques, chemotherapeutics, targeted agents and immunotherapies. In this chapter, anti-cancer therapies will be discussed including chemotherapies, targeted and immunotherapies, as well as different modes of cell death induction related to specific anti-cancer therapies with a focus on immunogenic ferroptosis. Lastly, this introductory chapter will specifically focus on the two emergent compounds from screening strategies, 5-Nonyloxytryptamine and volasertib that are subject of the two appended publications that comprise the main findings from the body of this thesis.

Type of the therapy	Drug Name	Mechanism of action
Chemotherapy	5-fluorouracil, fludarabine, 6-mercaptopurine, azathioprine	Purine, pyrimidine antagonists, purine analogs
	l-asparaginase	Depleting l-asparagine
	Cyclophosphamide, busulfan, chlorambucil	Alkylating agents
	Platinum-based agents: cisplatin, carboplatin, and oxaliplatin	Alkylating agents
	Irinotecan, topotecan	Topoisomerase I inhibitors
	Etoposide, teniposide, daunorubicin,	Topoisomerase II inhibitors
	Taxanes	Mitotic spindle inhibitor
Molecularly targeted therapy	gefitinib, erlotinib, afatinib and dacomitinib	EGFR tyrosine kinase inhibitors
	Crizotinib, ceritinib, lorlatinib	Anaplastic lymphoma kinase (ALK) inhibitors
	Sorafenib, sunitinib, pazopanib, regorafenib, vandetanib, cabozantinib	Growth factor receptor (GFR) inhibitors
	Imatinib	BCR-ABL tyrosine kinase inhibitor
	Ibrutinib, acalabrutinib, and zanubrutinib	Bruton's tyrosine kinase (BTK) inhibitors
	Ruxolitinib, fedratinib	Janus kinase (JAK) inhibitors
	Sotorasib	KRAS inhibitor
	Vemurafenib, cobimetinib, dabrafenib, trametinib, binimetinib	MEK inhibitor
	Sirolimus, temsirolimus, and everolimus	mTOR inhibitor
	Idelalisib, duvelisib, copanlisib, and	PI3K inhibitor
	Palbociclib, ribociclib, and abemaciclib	CDK4/6 inhibitor
	Volasertib	PLK1 inhibitor
Chemotherapeutic modulator	Thalidomide, lenalidomide, and pomalidomide	Cereblon (CRBN) inhibitor
	Azacitidine, decitabine	Hypomethylating agents
Repurposed immunomodulators	Statins: GGTI-298	Hydroxymethylglutaryl (HMG) CoA reductase inhibitor; upregulates CD80, CD86 and MHC-I on cancer cells
	Lowering blood glucose: metformin	Ubiquinone oxidoreductase; decreses PD-L1 on cancer cells, anti-metastatic
	Candesartan, losartan, olmesartan, valsartan	Angiotensin receptor blockers (ARB); decreases levels of IL-6, IL-10, VEGF and
	5-nonyloxytryptamine	HTR1D serotonin receptor agonist, upregulates MHC-I on cancer cells
Immunogenic cell death inducer	Doxorubicin, cyclophosphamide	Induces ferroptosis
	Anthracyclines, oxaliplatin	Induces immunogenic apoptosis
	Volasertib	Induces ferroptosis

Table 1. Summary of compounds used in anti-cancer therapy, segregated for the type of therapy, drug name and their mechanism of action. Listed drugs are examples mentioned in this dissertation. Highlighted on red compounds which are the subject of this work.

2.1. Chemotherapy

Chemotherapy remains the primary approach for treating cancer, and it can be categorized into various classes, such as antimetabolites, alkylating agents, mitotic spindle inhibitors, topoisomerase inhibitors, and other classes, depending on their mechanism of action (83). Chemotherapies target rapidly proliferating, including healthy cells that possess the ability for fast division, for example, digestive tract epithelium, and bone marrow stem cells (79). Antimetabolites inhibit DNA or RNA

synthesis. For example, hydroxyurea inhibits ribonucleotide reductase and therefore decreases the production of deoxyribonucleotides (84). Purine and pyrimidine antagonists, as well as purine analogs, are structurally similar to naturally occurring nucleotides and therefore are used as a substrate for DNA or RNA synthesis thereby blocking it. Examples of commonly used chemotherapeutics from this group are 5-fluorouracil, fludarabine, 6-mercaptopurine or azathioprine (83, 85). In contrast, l-asparaginase is an enzyme that cleaves the amino acid l-asparagine, which is essential for normal cell metabolism. By depleting this amino acid, l-asparaginase interferes with the metabolic processes of cancer cells, causing cell death (83). Alkylating agents engage in reactions with the nitrogen and oxygen atoms found within DNA bases, resulting in the creation of covalent alkyl bindings. These agents possess significant cytotoxicity due to their ability to inhibit most DNA polymerases, and therefore DNA synthesis or cross-linking DNA strands. Depending on their location within DNA, the various base modifications introduced by alkylating agents can alter the integrity of the genome (86). This can occur through the induction of mutagenesis, thereby increasing the likelihood of cancer development, or by blocking vital biological processes like DNA replication and transcription, potentially leading to cell death. Furthermore, specific agents can also undergo transformation into cytotoxic substances, which may activate alternate DNA repair mechanisms or trigger programmed cell death (86). Alkylating agents currently used in the clinic are cyclophosphamide, busulfan, chlorambucil or platinum-based agents, like cisplatin, carboplatin, and oxaliplatin (83). Topoisomerase I inhibitors, such as irinotecan and topotecan, along with topoisomerase II inhibitors, including etoposide, teniposide, daunorubicin, and doxorubicin, exert their anticancer effects by disrupting the activities of topoisomerases that are crucial for DNA replication. This disruption results in the formation of DNA strand breaks, which can impede the proliferation of cancerous cells (83, 87). Mitotic spindle inhibitors including taxanes, cause alterations in the function and formation of spindle microtubules. These alterations lead to the inhibition of nuclear division, causing mitotic arrest during the metaphase stage of cell division. This ultimately leads to cell death, making taxanes valuable agents in cancer treatment (83, 87). Another approach using bleomycin, which functions as an antibiotic, initiates the formation of free radicals within cancer cells. These free radicals induce DNA damage and inhibit the cell cycle in the G2 phase, thereby preventing further cell division and promoting cell death (83). Lastly, actinomycin D, an anticancer agent, intercalates itself

into DNA molecules, disrupting the transcription process. By interfering with DNA transcription, actinomycin D interferes with the synthesis of essential cellular components, ultimately leading to cell death (83). These diverse mechanisms illustrate the multifaceted approaches employed by commonly used chemotherapeutics to combat malignancies and improve patient outcomes. Despite the collateral damage induced by chemotherapies in generally targeting rapidly proliferating healthy cells, they are still the mainstay of many standard of care regimens.

2.2 Molecularly targeted therapies

Molecularly targeted therapies represent a groundbreaking advancement in cancer treatment strategies, aimed at enhancing the precision of targeting cancer cells while minimizing harm to healthy tissues. In stark contrast to conventional chemotherapy, targeted therapy offers a superior level of accuracy thereby reducing side effects and toxicity on actively dividing normal cells (88). This innovative approach encompasses the use of small molecule inhibitors and antibodies. These agents are designed to selectively hinder signal transduction pathways critical for the growth, proliferation, and survival of cancer cells. Additionally, hormonal agents have demonstrated efficacy in treating hormone receptor-dependent breast cancer and various reproductive cancers in both men and women (89, 90). Selection of the therapeutic is a result of diagnostically confirmed mutations in cancer and represents a major step in personalized medicine. Depending on the mutation or aberration in cancer, small molecules targeted therapy can be divided according to the target, like receptor tyrosine kinase inhibitors, nonreceptor tyrosine kinase inhibitors, RAS inhibitors and serine/threonine kinase inhibitors and other targeted anticancer agents (88). Receptor tyrosine kinase inhibitor targets involve epidermal growth factor receptor (EGFR) with ligands EGF, epiregulin, TGF-α, and neuregulins (91). Human EGFR is composed of subfamily proteins (ErbB1/EGFR, ErbB2/HER2, ErbB3/HER3, and ErbB4/HER4) (91) and especially HER2 component is highly overexpressed in around 25% of overall breast cancer patients (92), reported mutations in lung cancer (93) as well in glioblastoma (94) making it suitable target for therapy. Mutations in EGFR occur in the cytoplasmic domain, abnormally activating receptors without ligand-receptor interaction, whereas other cancers show overexpression of the receptor leading to high

sensitivity to the ligands (94). EGFR tyrosine kinase inhibitors (TKIs), that block EGFR' ATP-binding pocket, have been in clinical use for decades and these include gefitinib, erlotinib, afatinib and dacomitinib (90). However, approximately half of lung cancer patients develop TKI resistance (95), which led to the development of novel inhibitors targeting EGFR, for example, the orally available erlotinib (96), and monoclonal antibodies cetuximab and panitumumab approved for use in therapy of metastatic colorectal cancer (97, 98) and trastuzumab for HER2-positive breast cancer (99).

Another receptor tyrosine kinase inhibitor target is the anaplastic lymphoma kinase (ALK) that results from a chromosomal rearrangement creating a fusion protein with other oncogenes in multiple combinations, including echinoderm, microtubule-associated protein-like 4 (EML4), nucleophosmin (NPM), tropomyosin 3 (TPM3), and tropomyosin 4 (TPM4) (100). Additionally, ALK gene amplification or ALK mutations lead to overexpression of a constitutively activated ALK protein (100). Crizotinib, ceritinib and lorlatinib are clinically available ATP-cassette inhibitors of ALK used in the treatment of patients with lung cancer (101).

Other receptor tyrosine kinase inhibitors target tropomyosin receptor kinase (TRK) and fms like tyrosine kinase 3 (FLT3), but also the growth factor receptor (GFR) family receptors. Examples of clinically used GFR family inhibitors are sorafenib, sunitinib, pazopanib, regorafenib, vandetanib, cabozantinib, axitinib, tivozanib, avapritinib, erdafitinib, pemigatinib, infigratinib, derazantinib, selpercatinib, and pralsetinib. Moreover, monoclonal antibodies targeting TRK (bevacizumab and ramucirumab) or recombinant proteins (aflibercept) have been used clinically (102).

Nonreceptor tyrosine kinase inhibitors include BCR-ABL and SFK inhibitors. Oncogenic alterations in ABLs, including fusion protein formation caused by chromosome translocations in leukemia (*BCR::ABL1* in Philadelphia chromosome-positive) or chronic myeloid leukemia (CML), amplification or somatic mutations in solid tumors, constitutively activate ABL-mediated signaling pathways and promote survival, proliferation, dedifferentiation, migration, and invasion in cancer cells (103). Imatinib was designed to target BCR-ABL tyrosine kinase, key enzymes involved in numerous intracellular pathways associated with receptor-mediated growth signaling. Inhibition of these tyrosine kinases results in cellular dysfunction, followed by cell death, making these drugs effective in targeting specific cancer types (103).

Bruton's tyrosine kinase (BTK), a type of nonreceptor tyrosine kinase, holds pivotal significance in the developmental and functional processes of B cells (104). Its activation, triggered by phosphorylation, initiates a cascade involving mitogen-activated protein kinase (MAPK), nuclear factor kappa-light-chain-enhancer of activated B cells (NF-κB), and Akt pathways, regulating vital functions including B cell survival, proliferation, differentiation, and antibody secretion (104). Dysregulation of BTK is evident in various non-Hodgkin B-cell malignancies, such as chronic lymphocytic leukemia, small lymphocytic lymphoma, and mantle cell lymphoma, characterized by heightened expression and activity levels (105). Notably, inhibitors targeting BTK, such as ibrutinib, acalabrutinib, and zanubrutinib, have gained clinical approval and demonstrated efficacy in managing these disorders (106). Janus kinase (JAK) family encompasses nonreceptor tyrosine kinases like JAK1, JAK2, JAK3, and TYK2. Activation of JAK triggers phosphorylation cascades, influencing downstream signaling pathways like phosphatidylinositol-3-kinase (PI3K)/Akt, MAPK, and signal transducer and activator of transcription (STAT) transcription factors. Aberrations in JAK signaling, often attributed to activating mutations, are implicated across various solid tumors and hematological malignancies (107). Clinically approved JAK inhibitors, including ruxolitinib and fedratinib, offer therapeutic benefits in modulating dysregulated JAK signaling pathways (107).

RAS, a protein binding guanine nucleotide, holds pivotal significance in cell proliferation and differentiation. Acquired mutations in RAS lead to its continual activation (108). Among the RAS isoforms – KRAS, HRAS, and NRAS – KRAS stands out as the most frequently mutated isoform in cancer patients (109). Recently, a small molecule inhibitor sotorasib was developed to target mutated KRAS and has been approved for clinical applications (110). Activated RAS, when bound to GTP, triggers the association of RAF proteins, leading to RAF phosphorylation and subsequent activation of downstream signaling pathways involving MEKs and ERKs (111). Notably, mutations in BRAF, particularly at the V600 residue (V600E) in the activation loop, are frequently observed across various cancer types such as melanoma, papillary thyroid cancer, and colorectal cancer (111). Clinically, a combination of MEK inhibitors like vemurafenib plus cobimetinib, dabrafenib plus trametinib, and encorafenib plus binimetinib have been effectively utilized (112).

The PI3K/Akt/mTOR pathway plays a central role in regulating cellular processes including proliferation, survival, growth, and metabolism (113). Amplification of PIK3CA, loss or inactivation of PTEN, and hyperactivation of mTOR are commonly observed in various cancer types, contributing to anticancer drug resistance (113). Due to PI3K's specific expression in the hematopoietic system and its association with regulating B-cell receptor (BCR) signaling, therapeutic interventions targeting the PI3K pathway have been used in treating patients with lymphoma (114). Specifically, mTOR inhibitors, including rapamycin analogs (rapalogs) that inhibit mTORC1, have gained approval for clinical use. Examples of clinically utilized PI3K inhibitors encompass idelalisib, duvelisib, copanlisib, and alpelisib, and mTOR inhibitors such as sirolimus, temsirolimus, and everolimus have also been approved (90).

Next class inhibitors correspond to inhibitors targeting a mix of proteins controlling cell death such as PARP or Bcl-2 inhibitors. Clinically used small molecules or recently approved targeted therapies include proteasome inhibitors, and epigenetic modulators (DNA methyltransferase inhibitors and histone deacetylase inhibitors) (88).

Another approach for targeted therapy is targeting cell cycle components. Among the critical kinase families involved are Cyclin-dependent kinase (CDK), Polo-like kinase (Plk), and Aurora kinase (115). Cyclin-dependent kinases comprise a catalytic core specific to serine/threonine and form complexes with regulatory subunits called cyclins, which control kinase activity and substrate specificity (116). A key mechanism underlying the action of CDK4/6 inhibitors involves the inhibition of their phosphorylation, effectively halting cancer cell proliferation. Palbociclib, ribociclib, and abemaciclib are orally available, reversible, and selective CDK4/6 inhibitors that have been used clinically in combination with an aromatase inhibitor for the treatment of women with ER-positive and HER2-negative advanced or metastatic breast cancer (88, 117, 118). Polo-like kinase targeted therapy will be further elaborated in the subchapter "***Polo-like kinase inhibition with volasertib***".

Taken together, it is crucial to acknowledge that while these targeted therapies have demonstrated significant efficacy against different tumor types, their applicability primarily relies on identifying patients with specific targetable driver mutations or aberrations. Additionally, their effectiveness may be compromised by adverse effects, unexpected interactions with normal cells leading to toxicity, and the emergence of intrinsic or acquired drug resistance. Nevertheless, despite these limitations, targeted

therapy has delivered substantial survival benefits in certain cancer types, catalyzing a fundamental shift in cancer treatment approaches. This shift has set the stage for the advancement of precision and personalized medicine in oncology, offering a more tailored and efficacious approach to cancer management as illustrated with the example of volasertib below.

Polo-like kinase inhibition with volasertib

The Polo-like kinases (PLKs) in humans constitute a family of serine/threonine protein kinases, featuring five distinct members: PLK1, PLK2, PLK3, PLK4, and PLK5. PLK1 is activated by kinase Aurora A and plays multifaceted roles, notably in orchestrating mitotic entry, regulating centrosomes, coordinating spindle assembly, ensuring chromosome segregation, and facilitating cytokinesis (119). Acting as a master conductor, PLK1 ensures the precise progression of these cell cycle events, thereby maintaining genomic stability and proper cell division. The dysregulation of PLK1 has emerged as a significant contributor to tumorigenesis and cancer progression. Both mRNA and protein levels of PLK1 are often elevated in a variety of solid tumors as well as in acute myeloid leukemia (120). This overexpression of PLK1 has been correlated with adverse clinical outcomes, including poorer prognosis and decreased overall survival rates (121). Moreover, heightened PLK1 expression has been linked to resistance against conventional therapies in certain cases, while its inhibition has shown promise in re-sensitizing tumors to chemotherapy and radiotherapy (121). The pivotal role of Plk1 in the cell cycle and overexpression in a variety of cancers led to the development of Plk1 inhibitor volasertib (another name BI 6727). Volasertib potently inhibits Plk1, but also an inhibitory activity for two closely related kinases, Plk2 and Plk3 was reported (122). Preclinical investigations into volasertib's efficacy across a range of cancer cell lines, from colon, lung, and melanoma to various hematopoietic malignancies, prostate, urothelial, and pediatric tumors, have revealed its ability to impede cell division, ultimately leading to cell death (122). By targeting Polo-like kinase with volasertib, disruption of mitotic spindle assembly occurs, resulting in a distinctive mitotic arrest phenotype, often referred to as "Polo arrest," observed notably in prometaphase. This disruption manifests as an accumulation of phospho-histone H3 and the formation of aberrant monopolar mitotic spindles, culminating in apoptotic cell

death (123). Furthermore, volasertib has exhibited inhibitory effects on the growth and survival of cell lines derived from pediatric acute lymphoblastic leukemia patients (124).

In conclusion, PLK1 plays a critical role in cell cycle regulation and its dysregulation is closely associated with cancer development and progression. Understanding the intricate mechanisms underlying PLK1 function and its role in cancer pathogenesis provides valuable insights for the development of targeted therapies, such as volasertib, aimed at combating cancer progression and improving patient outcomes. The effect of volasertib in B cell acute lymphoblastic leukemia (B-ALL) is further discussed in the article "***Deep transfer learning approach for automated cell death classification reveals novel ferroptosis-inducing agents in subsets of B-ALL***" which is part of this cumulative thesis.

2.2. Immunotherapy

One of the best approaches in combating tumors is not only cytotoxic therapy but overall increasing tumor hotness to boost immunotherapies. Enhancing antitumor immunity can be achieved by multiple strategies. Many chemotherapeutics possess immunomodulatory traits, either by directly upregulating expression of MHC-I machinery and decreasing inhibitory PD-L1 on cancer cells, or by stimulating $CD8^+$ T cells and inhibiting Tregs (81). Modern anti-cancer therapy involves specific antibodies biding to immune checkpoint inhibitors, such as anti-PD1, anti-PDL1, anti-CTLA4, and anti-Tim3, but also targeting cancer cells by TAA and bridging interaction with $CD8^+$ T cells or NK cells. Another approach represents virotherapy, where cancer cells can be directly destroyed with a specific oncolytic virus or increase tumor hotness by noncytopathic virotherapy (125). Cell-based therapies include clinically approved generation of CAR-T cells that express a receptor against cancer antigens and therefore redirect T cells against cancer cells. Several anti-antigen receptors were tested in pre-clinical or clinical settings, such as anti-CD19 and anti-CD20 for B cell leukemia, anti-HER2 and anti-IL13Ra2 in glioblastoma and anti-HER2 and anti-MUC1 in the treatment of breast cancer (82). Specific cancer cell targeting is a major advantage of CAR T cell therapy, but also its limitation due to the limited repertoire of cancer antigens and tumor antigen escape mechanisms (82).

Additionally, there is a growing interest in inducing immunogenic regulated cell death, which leads to a release of immunogenic high mobility group box 1 (HMGB1), ATP, annexin A1, and type I interferon from cancer cells which enhance antigen uptake by dendritic cells and lead to increased T cells activation (126).

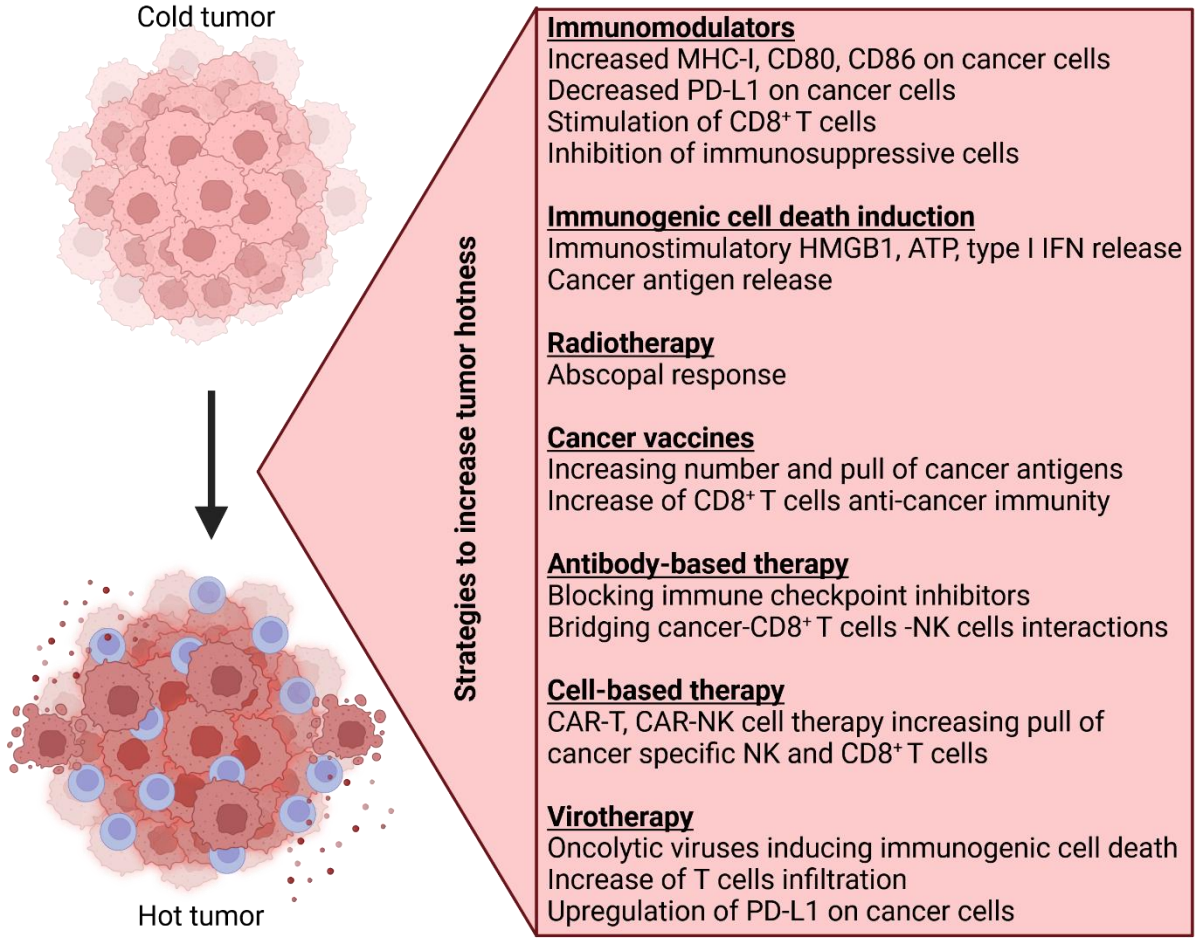

Figure 3. Schematic representation of strategies in cancer treatment leading to increasing tumor hotness. Figure created with Biorender, adapted from (81).

Taken together, increasing tumor hotness can be achieved on multiple levels from increasing cancer antigen presentation or decreasing PD-L1 expression on cancer cells, inducing immunogenic cell death, and modulating immunosuppressive myeloid cells in TME to compounds acting directly on cytotoxic T cells. The next subchapters will focus on the immunomodulatory compounds, including the effect of 5-nonyloxytryptamine as a novel immunomodulatory agent. Also, antibody-based cancer therapies, due to combinatory treatment with anti-PD1 antibodies. Additionally, ferroptosis-inducing properties of volasertib and its potential implications in immunogenic cell death will be described.

2.3.1 Antibody-based cancer immunotherapies

Currently, over a hundred antibody-based therapies are approved by the FDA for large disease plethora including cancer, infectious diseases, and autoimmune disorders (127). The success of antibody-based therapeutics depends on their relatively long half-life and ability to target any potential protein with higher specificity than chemotherapy (127). This has led to the development of advanced approaches using antibody-drug conjugates, bi-specific antibodies biding simultaneously two targets and protein-binding antibodies that can deliver specific proteins such as cytokines to the TME (127). Antibodies bind to the target antigen by the antigen-binding fragment (Fab) and interact with effector cells through their fragment crystallizable region (Fc). Antibodies act like a bridge between target cell and effector cells that express Fc receptors (FcR), which in turn leads to antibody-dependent cell-mediated cytotoxicity (ADCC) (128). In the context of cancer and designed antibodies, the effector cells expressing FcR can be NK cells, monocytes, macrophages, neutrophils, eosinophils, and dendritic cells (129). These cells can destroy cancer cells by releasing cytotoxic granules, Fas ligands and high production of ROS. In detail these cytotoxic mechanisms were described in the chapter “tumor microenvironment”. To improve NK cell interaction with cancer cells there was helpful development of bispecific antibodies targeting cancer cells and CD16A or NKp46 on NK cells. Since T cells do not express the FcR, bispecific antibodies targeting cancer cells and CD3 on T cells improved their engagement and cytotoxicity (130). Bi-specific antibodies are crucial for improving cancer patient survival, particularly in hematological malignancies. By simultaneously binding to tumor antigens and immune cells, they enhance the immune system's ability to recognize and eliminate cancer cells with greater precision. This targeted approach reduces off-target effects and minimizes damage to healthy tissues, leading to improved safety and tolerability (130). Moreover, bi-specific antibodies have shown the potential to overcome resistance mechanisms that limit the effectiveness of conventional therapies. Their ability to engage the immune system directly has resulted in significant improvements in response rates and overall survival in patients with otherwise limited treatment options (131). The most common cancer antigens used as a target for antibodies are CD19 and CD20 (Blinatumomab) for B cell leukemia, CCR4 for T cell lymphoma, growth factor receptors (EGFR, HER2) and vascular endothelial growth factor (VEGF) (132). The revolutionary Blinatumomab was first FDA approved

bispecific T-cell engager that was followed by multiple clinical trials with another bi-specific antibodies. This includes approved Glofitamab and Epcoritamab that are CD20-CD3 engagers for treatment of relapsed or refractory large B cell lymphoma and currently in clinical trials for treatment of non-Hodgkin's lymphoma and follicular lymphoma (131). Additionally approved Teclistamab, CD3-BCMA (B cell maturation antigen) engager for treatment of relapsed or refractory multiple myeloma and CD3-gp100 Tebentafusb for uveal melanoma therapy represent successful therapeutic option (131).

Since antibodies can target cancer cells with high specificity, were developed antibody-drug conjugates for more precise delivery of chemotherapeutics, decreasing off-cancer side effects. Most commonly used therapeutics linked to antibodies are anti-mitotic tubulin disruptors and DNA damaging agents such as topoisomerase I, DNA alkylating agents, RNA polymerase II and BCL-xL inhibitors (132), but also in development toll-like receptor (TLR) agonists (133). Approved antibody-drug conjugates target CD30 for Hodgkin's Lymphoma, HER2 for HER2-positive breast cancer, CD20 for BCP-ALL, CD33 for CD33-positive AML, CD79b for diffuse B-cell lymphoma, nectin-4 for urothelial cancer, trop-2 for triple-negative breast cancer, BCMA for multiple myeloma and CD19 for large B-cell lymphoma (133). These antibodies are approved with drugs like monomethyl auristatin E (MMAE), DM4, calicheamicin, DM1, and monomethyl auristatin F (MMAF) (133).

Another approach with the use of antibodies is to block immune checkpoint inhibitors and restore effector T cell functions. A few immune checkpoints have been identified including programmed cell death protein 1 (PD-1), programmed cell death 1 ligand 1 (PD-L1), cytotoxic T-lymphocyte-associated protein 4 (CTLA-4), T-cell immunoglobulin mucin receptor 3 (TIM-3), lymphocyte-activation gene 3 (LAG-3) (127). Activated TLR signaling in $CD8^+$ T cells leads to simultaneous expression of PD-1 on their surface. One of the PD-1 ligands is PD-L1 which can be expressed on immunosuppressive myeloid, but also cancer cells. Interaction between these molecules leads to inhibition of PI3K-AKT signaling, therefore inhibition of T cell activation and proliferation (134).

Another immune checkpoint molecule is CTLA-4 which can bind to B7 stimulatory molecules like CD80 and CD86 with higher affinity than T cell receptor CD28, impairing their activation. Additionally, CTLA-4 is highly overexpressed on regulatory T cells and to a lesser extent on $CD8^+$ T cells, competing and blocking B7 molecules (135).

Currently, ipilimumab is the only anti-CTLA-4 antibody approved by the FDA for the treatment of melanoma, renal cell carcinoma and colorectal cancer (127).

LAG-3 and TIM-3 are markers of T cell exhaustion, but their mechanism is not fully understood (136). For example, LAG-3 was found to engage with MHC-II, where $CD8^+$ T cell restricted TCRs are known to not interact with that molecule (136). TIM-3 has reported Galectin-9, PtdSer, HMGB1 and CEACAM1 as ligands, but the signaling pathway of each ligand is not known (136). Nevertheless, antibody blockade of LAG-3 or TIM-3 was shown to significantly decrease tumor burden in pre-clinical animal studies but also enhanced immune responses in clinical trials (137).

The disadvantages with therapies targeting tumor antigen is the limited number of identified specific cancer epitopes and antigen escape, where cancer cells downregulate the expression of MHC-I (127). Additionally, most of the cancer antigens targeted by antibodies are also expressed in healthy tissue which leads to “on-target off-tumor” side effects within healthy tissue causing inflammation and damage (138). When it comes to immune checkpoint inhibitors, it was noted that targeting one of them leads to compensatory upregulation of another. For example, mice treated with anti-PD-1 mAb had increased levels of LAG-3 and CTLA-4 whereas anti-LAG-3 antibody treatment upregulated the level of PD-1 (139). These results show the need for combinatorial treatment of immune checkpoint inhibitors. Unfortunately, highly upregulated co-expression of PD-1, CTLA-4, TIM-3, and LAG-3 leads to a terminally exhausted phenotype of $CD8^+$ T cells that cannot be any longer reversed with immune checkpoint blockade (140).

2.3.2 Immunomodulatory compounds

There is a growing number of active pharmacological compounds that were recently discovered to have additional immunostimulatory and therefore favorable combinatorial activities. For example, thalidomide, lenalidomide, and pomalidomide induce cell cycle arrest, inhibit angiogenesis, and are used in the treatment of multiple myeloma (141). Recent studies indicate that these drugs additionally stimulate T cells resulting in amplified production of IL-2 and IFNγ (142). Also, epigenetic modulators acting as hypomethylating agents, like azacitidine or decitabine approved for the treatment of myelodysplastic syndromes and acute myeloid leukemia (143), enhance the expression of cancer-specific antigens and MHC molecules therefore making cancer cell target for $CD8^+$ T cells (144). In search of potential novel immunomodulators, other clinically available compounds can also be re-evaluated for potential cancer treatment repurposing. For example, statins, hydroxymethylglutaryl (HMG) CoA reductase inhibitors in the cholesterol synthesis pathway, represent a group of drugs that are used for lowering the level of lipids in blood preventing cardiovascular diseases (145). Statins not only exhibit anti-cancer cytotoxic effects (146), but multiple studies demonstrated that statins also have the ability to act as inhibitors for Rho GTPase and Rho-dependent pathways, which are crucial for the regulation of metastasis, and immune reactions in cancer cells (147-150). For example, compound GGTI-298 was shown to upregulate surface expression of CD80, CD86 and MHC-I on melanoma cells and therefore induced strong IFNγ dependent $CD8^+$ T cell cytotoxic activity (151). Statins were also evaluated clinically and demonstrated improvement in overall survival of lipophilic statin treated elderly patients after surgical resection of epithelial ovarian cancer (152). Additionally, there are multiple studies suggesting increased all-cancer patient survival with statin treatment (153). Another example of a repurposed compound is metformin which is commonly used for lowering blood glucose in type 2 diabetes, which inhibits ubiquinone oxidoreductase in mitochondria, activating 5′-AMP-activated protein kinase (AMPK) and therefore suppressing gluconeogenesis (154). Metformin was shown to have strong immunomodulating effects in the melanoma model, where it increased the numbers of $CD8^+$ T cells but also exhibited anti-metastatic properties in mice challenged with B16F10 melanoma cells (155). Additionally, metformin was reported

to restore $CD8^+$ T cells functionality by induced degradation of PD-L1 in cancer cells (156).

Angiotensin receptor blockers (ARB), candesartan, losartan, olmesartan and valsartan represent a class of drugs used for controlling blood pressure, although it was noticed that renin and angiotensin are expressed in cancer and TME (157). Specifically in the colon cancer mice model, ARB were able to significantly decrease the activity of immunosuppressive myeloid cells with decreased production of IL-6, IL-10, vascular endothelial growth factor (VEGF), and arginase (158). In clinical studies, ARB were associated with improved survival of gastro-oesophageal cancer patients (159) and patients undergoing resection of pancreatic cancer (160).

5-Nonyloxytryptamine

5-nonyloxytryptamine (5-NL) is a small compound designed in 1994 as a tryptamine derivative and a highly selective agonist of the HTR1D serotonin receptor for the treatment of migraine headaches (161). 5-NL was used in multiple studies attempting to uncover potential bioactivities of the compound. As the HTR1D receptor is mostly expressed on gamma motor neurons and proprioceptive sensory neurons (162), not surprisingly 5-NL was noticed to have neuro-regenerative properties in mice spinal cord injury models (163, 164). Additionally, 5-NL was reported to mimic polysialic acid and therefore improve neuritogenesis, myelination and Schwann cell migration, useful in the therapy of acute and chronic nervous system diseases (165, 166). Interestingly, 5-NL was also reported to have antiviral properties, inhibiting infection with reoviruses and coronavirus mouse hepatitis virus (167), but also chikungunya virus (168). 5-NL was proved to interfere with the Akt/mTOR pathway in triple-negative breast cancer cells and induce cell death (169). Our previous study showed the anti-cancer properties of tegaserod (170), an HTR4 agonist, hinting at a potential role of serotonin receptors in cancer treatment.

In our next study, to uncover novel agents capable of increasing the immune 'hotness' of tumors through potentiation of T cell activity, we screened 770 compounds. 5-NL a serotonin agonist was found to potentiate T cell activity against melanoma cells. The phenotype was recapitulated *in vivo* in a syngeneic melanoma tumor model. Through a combination of genetic knockouts and depletion antibodies, the phenotype was

confirmed to be dependent on the hosts' immune system, specifically $CD8^+$ T cells. 5-NL upregulated the antigen presenting machinery at the transcriptional and protein level in mouse and human melanoma as well as other solid tumor types. Mechanistically, we found that 5-NL increased the phosphorylation of cAMP response element-binding protein (CREB) without activating mitogenic pathways such as MAPK and independent of type-I interferon signaling. RNA-seq analysis additionally revealed early activation of the AMPK pathway, as regulating the expression of antigen presenting machinery. Results of this work are presented in the article "Unleashing T cell anti-tumor immunity: new potential for 5-Nonloxytryptamine as an agent mediating MHC-I upregulation in tumors" which is a part of this cumulative dissertation.

Role of the CREB pathway in cancer

The CREB pathway plays a significant role in cancer, acting through the cAMP-PKA-CREB signaling axis to regulate various cellular processes including growth, migration, invasion, and metabolism. This signaling pathway's role in cancer is complex, as it can exhibit both tumor-suppressive and tumor-promoting effects depending on the type of tumor and the context. Specifically, aberrant cAMP-PKA signaling has been implicated in various human tumors, emphasizing the importance of this pathway in tumorigenesis and its potential as a target for cancer therapy (171). The cAMP signaling, through PKA and EPAC, intricately modulates CREB activity, which in turn influences cancer cell behavior. For instance, CREB expression is regulated via multiple signal transduction pathways including PI3K/AKT and Ras/MEK/ERK pathways, which are activated by cellular growth factors (172). This regulation is crucial as it affects CREB phosphorylation at different serine sites, impacting cellular decisions between proliferation and apoptosis (172). Additionally, the interaction between the cAMP/PKA/CREB pathway and other signaling cascades, such as the TGFβ/SMAD4 pathway, plays a crucial role in determining the stemness and metastatic potential of colorectal cancer cells (173). This highlights the therapeutic potential of targeting CREB in metastatic colorectal cancer, suggesting that manipulating this pathway could influence cancer progression and metastasis (173). Moreover, CREB's activation and its link to cancer's hallmarks suggest its pivotal role in cancer progression and patient outcomes. Studies have explored CREB1 expression as a prognostic marker for

survival in various cancers, underscoring its significance across different cancer entities (174).

Importantly for cancer immunity, CREB as a transcription factor was found to bind to MHC I and II promotor regions, regulating their expression (175, 176). Inducing MHC expression in cancer is crucial for enhancing the immune system's ability to recognize and destroy cancer cells. MHC molecules present tumor antigens on the surface of cancer cells, making them visible to T cells. The importance of increased MHC expression was previously described in chapter 1.1. It is important to note that serotonin receptors, as G-copulated receptors can manipulate CREB activity through a cAMP level (177) and therefore can potentially influence the expression of the MHC complex.

Given the dual role of the CREB pathway in cancer progression—both as a promoter and a suppressor - it’s targeting for cancer therapy presents both opportunities and challenges. Future research and therapeutic strategies need to consider this complexity to effectively harness the potential of CREB pathway modulation in cancer treatment.

Role of the AMPK pathway in cancer

AMP-activated protein kinase (AMPK) is a universally conserved enzyme that plays a pivotal role in maintaining cellular energy balance. It operates as a critical metabolic controller, engaging in the regulation of energy metabolism and mitochondrial formation (178). Triggered by a drop in cellular energy levels due to factors like low oxygen and nutrient deficiency, AMPK activation boosts ATP production, ensuring energy equilibrium within the cell (179). The activation of AMPK occurs when a rise in the cellular AMP:ATP ratio signals a decrease in ATP generation, leading to high intracellular AMP concentrations. This stimulates AMPK through allosteric changes and phosphorylation of threonine 172 within the activation loop of AMPK's catalytic α-subunit (179). The potential of AMPK activation as a therapeutic approach to tackle various cancers has been thoroughly examined. Acting as a natural antagonist to cancerous growth, AMPK is recognized for its ability to hinder processes that promote tumor development and inhibit the proliferation cycle of cancer cells (180). An integral player in maintaining the core characteristics of cancer cells, Cyclooxygenase 2 (COX-

2), is effectively inhibited by AMPK, particularly in breast and colon cancers (180). This discovery highlights AMPK's dual role, not only as a guardian against malignant transformation by disrupting cancer cell division but also as a critical inhibitor of COX-2, thereby undermining a key factor in the perpetuation and resilience of cancer cells. Research into the specific AMPK activator MT 63–78 has highlighted its powerful role in targeting prostate cancer cells (181). This activator works by triggering a halt in cell division and promoting cell death in these cancer cells, acting through mechanisms that block mTORC1 signaling and inhibit lipogenesis (181). However, the role of AMPK in cancer is complex and multifaceted. While it has been praised for its capacity to suppress tumor growth, there are nuances in its protumorigenic effects. For instance, it has been observed that under conditions of metabolic stress, such as a shortage of glucose or oxygen, the activation of AMPK can enhance the survival capabilities of cancer cells (182). This is because AMPK-induced autophagy can serve a protective role for cancer cells, supplying them with essential nutrients through the recycling of cellular components, thereby supporting their growth and enabling them to resist the effects of chemotherapy (183). Studies suggest that the therapeutic potential of AMPK activators extends beyond their immediate effects on cell cycle and autophagy. For example, AMPK has been implicated in the modulation of the immune response within the tumor microenvironment, affecting both the efficacy of immunotherapies and the progression of the disease. Moreover, the ability of AMPK to influence systemic metabolism raises the possibility of using AMPK activators not only as direct anticancer agents but also as adjunct therapies to improve the overall metabolic health of cancer patients, potentially enhancing their response to conventional treatments.

2.3.3 Pharmacologically induced immunogenic cell death

Immunogenic cell death (ICD) in cancer represents a pivotal mechanism by which certain cancer therapies, such as chemotherapy, radiotherapy, and some targeted therapies, can not only kill cancer cells but also stimulate a potent anti-tumor immune responses. This phenomenon occurs through the release or presentation of damage-associated molecular patterns (DAMPs) by dying cancer cells, which then activate the immune system against the tumor (184). ICD is characterized by specific hallmarks, including the exposure of calreticulin on the cell surface, release of ATP, and secretion of high-mobility group box 1 (HMGB1) protein into the extracellular space. These events facilitate the uptake of cancer cells by dendritic cells, leading to the activation of T cells and the initiation of a targeted immune response against the tumor (184). Furthermore, the role of DAMPs in antigen cross-priming is critical. Upon release, these molecules bind to pattern recognition receptors (PRRs) on DCs, which is essential for the activation of T cells and the generation of a robust anti-tumor immune response (185). The cGAS-STING signaling pathway also plays a crucial role in ICD. The presence of cytosolic DNA, resulting from cellular damage, activates the cGAS enzyme, which then synthesizes cyclic GMP-AMP (cGAMP). cGAMP activates the STING pathway, leading to the production of type I interferons, critical mediators of the immune response to cancer (184). Recent studies identified a few compounds whose treatment leads to immunogenic cell death, namely doxorubicin, cyclophosphamide, and oxaliplatin lead to the exposure of DAMPs, such as calreticulin (CRT) and ATP (186). High doses of radiation can damage cancer cells in a way that leads to ICD. The process involves the release of HMGB1 and ATP, which signal immune cells to attack the tumor. This suggests that radiotherapy's effectiveness might partly derive from its ability to provoke an immune response against tumors (187).

A key trait shared among agents that trigger immunogenic cell death is their capability to initiate endoplasmic reticulum (ER) stress and the generation of reactive oxygen species (ROS) (188). The intensity of ER stress correlates with the immunogenic potential of the cell death induced. Accordingly, these inducers are categorized into two types: Type I inducers, like anthracyclines and radiotherapy, which cause indirect ER stress; and Type II inducers, such as the use of hypericin in photodynamic therapy, which leads to direct ROS-related ER stress (188). It has been observed that enhancing ER stress can augment the immunogenic qualities of certain

chemotherapeutics known for their weak induction of ICD, including drugs like cisplatin (189), etoposide, and mitomycin C (186). The role of ROS in this process is underscored by the observation that the presence of antioxidants can reduce the immunogenicity of ICD, highlighting the importance of oxidative stress in the effectiveness of ICD induction. Most anticancer therapies induce apoptosis, but only a few, like anthracyclines, and oxaliplatin do so in an immunogenic way (190). Immunogenic cell death also includes necroptosis, pyroptosis (184) and ferroptosis (191). In our study, we provide evidence on ferroptosis inducing abilities of volasertib in cancer treatment, with results included in the article ***"Deep transfer learning approach for automated cell death classification reveals novel ferroptosis-inducing agents in subsets of B-ALL"*** which is part of this cumulative dissertation.

Ferroptosis

Ferroptosis is a type of regulated cell death characterized by the accumulation of lipid peroxides to lethal levels. It is distinct from other forms of cell death such as apoptosis, necroptosis, and autophagy due to its unique iron-dependency and the way cells die by peroxidation of polyunsaturated fatty acids in the lipid bilayer (192). The discovery of ferroptosis has opened new avenues for cancer research, especially in understanding tumor suppression mechanisms and resistance to conventional therapies. Iron plays a pivotal role in ferroptosis by participating in the Fenton reaction, which produces free radicals leading to lipid peroxidation and cell death (193) and can be inhibited with iron chelating ferritin (FTH1) (Figure 4) (194). The glutathione (GSH)-dependent antioxidant enzyme glutathione peroxidase 4 (GPX4) is central to ferroptosis resistance, as it converts toxic lipid hydroperoxides into non-toxic lipid alcohols (193). When GPX4 activity is inhibited, either genetically or pharmacologically, cells are rendered susceptible to ferroptosis. The cystine/glutamate antiporter system Xc−, with main compartment SLC7A11, is another critical component, as it regulates the uptake of cystine for GSH synthesis, thus indirectly controlling GPX4 activity (193). Key regulatory pathways involve the tumor suppressor p53, which can promote ferroptosis by inhibiting the expression of SLC7A11, a component of the Xc− system, and Nrf2, a transcription factor that provides cellular resistance to ferroptosis by upregulating antioxidant response element (ARE)-driven

genes (195). Since ferroptosis execution depends on cell membrane lipid peroxidation, the lipid metabolism with acyl-CoA synthetase long-chain family member 4 (ACSL4) plays a crucial role in ferroptosis sensitivity (196). Importantly it was noticed that lipids composed of polyunsaturated fatty acids (PUFA) are highly sensitive to oxidation and their synthesis is controlled by ACSL4 (197).

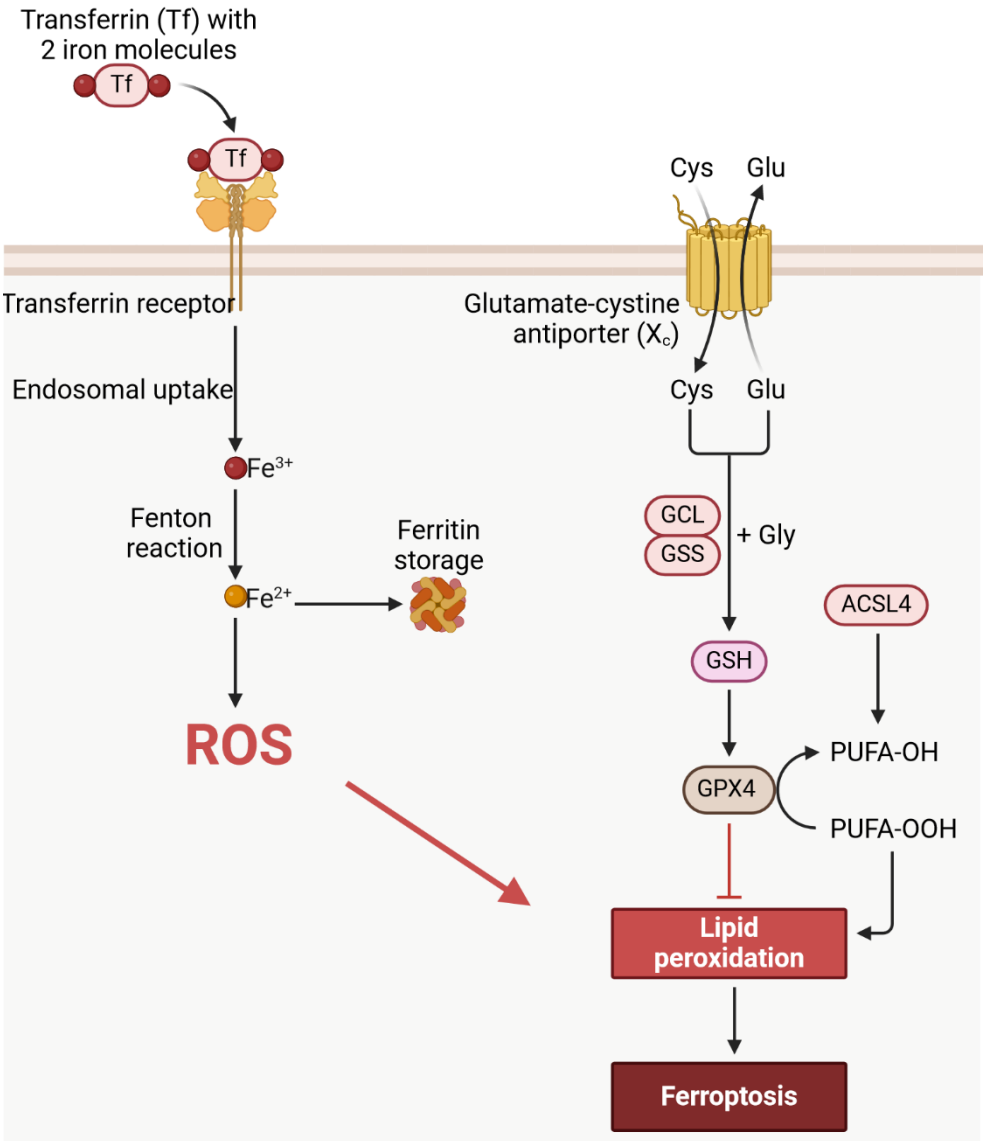

Figure 4. Schematic representation of pathways involved in ferroptosis induction. Iron ions are transferred to cell cytoplasm by transferrin receptor and induce ROS production in the Fenton reaction or are stored by ferritin. The main antioxidant GSH is used by GPX4, preventing lipid peroxidation and can be synthetized in cells from cysteine and glycine by GCL and GSS. Excessive lipid peroxidation leads to ferroptosis and cell death. ACSL4 is a regulator of lipid synthesis, preferentially producing PUFA that are sensitive to peroxidation. Figure created with Biorender, adapted from (198).

Cancer cells often exhibit altered iron metabolism and increased susceptibility to lipid peroxidation, making them particularly vulnerable to ferroptosis (199). However, resistance mechanisms, such as the upregulation of GPX4 or mutations affecting the Xc− system, can enable tumor survival and growth. The tumor microenvironment also significantly influences ferroptosis sensitivity, with factors such as hypoxia and nutrient availability playing critical roles (199). Exploiting ferroptosis for cancer therapy involves strategies to induce this form of cell death selectively in cancer cells. Small molecules like erastin, which inhibits the Xc−system, and sulfasalazine, have shown promise in preclinical studies (200).

Beyond inducing death in cancer cells, ferroptosis also influences systemic immunity by affecting both innate and adaptive immune cells, including macrophages and cytotoxic T cells (201). It is proposed that ferroptosis can alter cell immunogenicity through the emission of DAMPs, which are recognized by pattern recognition receptors (PRR) on immune cells like dendritic cells (191, 201).

The induction of ferroptosis offers a novel approach to cancer therapy by targeting the unique vulnerabilities of cancer cells related to iron metabolism and lipid peroxidation. While promising, the path from understanding to effectively targeting ferroptosis in clinical settings is full of challenges, including identifying biomarkers for sensitivity and resistance and developing safe and effective ferroptosis-inducing agents. In the article ***"Deep transfer learning approach for automated cell death classification reveals novel ferroptosis-inducing agents in subsets of B-ALL",*** which is part of this cumulative thesis, authors provide evidence of ferroptosis inducing ability of volasertib and evidence of potential immunostimulatory effects of the compound.

3. Publications

3.1. *PUBLICATION 1:* Senescent Tumor $CD8^+$ T Cells: Mechanisms of Induction and Challenges to Immunotherapy.

cancers

MDPI

Review

Senescent Tumor CD8$^+$ T Cells: Mechanisms of Induction and Challenges to Immunotherapy

Wei Liu [1,†], Paweł Stachura [1,†], Haifeng C. Xu [1], Sanil Bhatia [2], Arndt Borkhardt [2], Philipp A. Lang [1] and Aleksandra A. Pandyra [1,2,3,*]

1 Department of Molecular Medicine II, Medical Faculty, Heinrich-Heine-University, 40225 Düsseldorf, Germany; weliu100@uni-duesseldorf.de (W.L.); stachura@uni-duesseldorf.de (P.S.); xuh@uni-duesseldorf.de (H.C.X.); langp@uni-duesseldorf.de (P.A.L.)

2 Department of Pediatric Oncology, Hematology and Clinical Immunology, Medical Faculty, Center of Child and Adolescent Health, Heinrich-Heine-University, 40225 Düsseldorf, Germany; Sanil.Bhatia@uni-duesseldorf.de (S.B.); arndt.borkhardt@hhu.de (A.B.)

3 Department of Gastroenterology, Hepatology, and Infectious Diseases, Heinrich-Heine-University, 40225 Düsseldorf, Germany

* Correspondence: aleksandra.pandyra@uni-duesseldorf.de; Tel.: +49-211-81-17258

† These authors contributed equally to this work.

Received: 7 September 2020; Accepted: 29 September 2020; Published: 30 September 2020

Simple Summary: Immunotherapies harness the hosts' immune system to combat cancer and are currently used to treat many tumor types. Immunotherapies mainly target T cells, the major immune population responsible for tumor-cell killing. One of the reasons that T cells may not respond to immunotherapeutic treatment is that they are in a dysfunctional state termed senescence. This review seeks to describe the molecular mechanisms that characterize and induce T cell senescence within the context of the tumor microenvironment and how this might affect treatment responses.

Abstract: The inability of tumor-infiltrating T lymphocytes to eradicate tumor cells within the tumor microenvironment (TME) is a major obstacle to successful immunotherapeutic treatments. Understanding the immunosuppressive mechanisms within the TME is paramount to overcoming these obstacles. T cell senescence is a critical dysfunctional state present in the TME that differs from T cell exhaustion currently targeted by many immunotherapies. This review focuses on the physiological, molecular, metabolic and cellular processes that drive CD8$^+$ T cell senescence. Evidence showing that senescent T cells hinder immunotherapies is discussed, as are therapeutic options to reverse T cell senescence.

Keywords: CD8$^+$ T cells; senescence; immunotherapy; metabolism

1. Introduction

Harnessing the immune system to treat solid and hematological malignancies has ushered a novel therapeutic era. The tumor micro-environment (TME) is complex, with many targeting opportunities due to the signaling networks and cross-talk between immune, tumor and stromal cells. However, the modulation of cytotoxic antigen-activated CD8$^+$ T (T_c) cells has been at the forefront of the immunotherapy revolution [1]. The antigen-specific process requires the engagement of the T cell antigen receptor (TCR)-CD3 complex on T_c cells with a major histocompatibility complex (MHC) class I-bound tumor antigen-derived peptide as well as co-stimulatory signals. Responsible for the direct tumor cell killing through granule exocytosis [2], T_c cells are integral in eradicating tumors and are currently targeted by many approved immunotherapies. The monoclonal antibody checkpoint

inhibitors such as nivolumab [3] are currently used to treat solid tumors, and they target the inhibitory programmed cell death 1 (PD-1) [4] receptor expressed on T cells. In the adoptive T cell therapy field, a patient's T cells are expanded ex vivo, transduced with synthetic chimeric antigen receptors (CAR) targeting a tumor specific target antigen such as CD19, and transferred back to lymphodepleted patients. Currently approved CAR-T cell therapies include the second generation anti-CD19 CAR T-cell products axicabtagene ciloleucel and tisagenlecleucel for the treatment of B-cell malignancies [5,6]. Many more T cell based therapies are currently in the experimental phase of pre-clinical or clinical testing [7]. While immunotherapies have made remarkable progress in increasing the survival of some patients, low response rates, toxicities, as well as lack of available bio-markers in predicting response, make the successful implementation of these therapies challenging. A major obstacle is the inability to effectively target T_c cells. This can occur through T_c intrinsic or acquired resistance helped by dysfunctional states present within the immunosuppressive networks [8] of the TME: exhaustion and senescence. While T cell exhaustion has been extensively studied and targeted, T cell senescence, especially within the context of anti-tumor immunity, is an emerging concept in the field of T cell dysfunction. This review focuses on senescence in the $CD8^+$ T cell compartment. It aims to explore the different mechanisms that induce senescence in the context of TME, ways in which T cell senescence affects responses to immunotherapies and how T cell senescence can be therapeutically reversed.

2. Exhaustion and Senescence

Both exhausted and senescent T cells have been found to accumulate during chronic viral infections [9,10] and cancers [11,12]. Exhaustion and senescence are both considered dysfunctional states. They are characterized by dampened granzyme B (GzmB)—mediated effector function and impaired proliferation [13]. However, they are defined by distinct surface marker, cytokine, transcriptional and metabolic profiles (Table 1).

Table 1. Characteristics of senescent and exhausted T cells.

	Senescent T Cells	Exhausted T Cells
Stimulus	Repetitive Ag Stimulation, Stress	Continuous Ag Stimulation
Cytokine Secretion	↑ IFN–γ, IL-6, IL-8, IL-10, TNF, TGF-β	↓ IFN-γ, IL-2, TNF
Surface Markers	↑ CD57, Tim-3, TGIT, CD45RA, KLRG1, ↓ CD28, CD27	↑ PD-1, LAG-3, CD 160, 2B4, CTLA-4, Tim-3, TGIT
Metabolism	↑ Glycolysis, ↓ Mitochondrial Biogenesis	↓ Glycolysis, ↓ Mitochondrial Biogenesis
Transcriptional	T-bet	Eomes, NFAT, TOX, T-bet, Nr4a
Effector Functions	↓ Granzyme B, ↓Perforin	↓ Granzyme B
Phenotypic Characteristic	↓ Proliferative Capacity, ↑ DNA Damage Molecules, ↑ SA-β-gal activity	↓ Proliferative Capacity, Cell Cycle Arrest

↓ Decrease, ↑ Increase.

When T_c cells are exhausted through excessive and continuous stimulation, they upregulate inhibitory cell surface receptors such as PD-1 and LAG-3 and possess a decreased capacity to secrete interleukin 2 (IL-2) and interferon gamma (IFN-γ) [14] (Figure 1). The exhausted transcriptional T_c profile is very context dependent and is driven, during varying stages of exhaustion, by nuclear factor of activated T cell (NFAT), nuclear receptor Nr4a, thymocyte selection-associated HMG box (TOX), eomesodermin (Eomes) and T-Bet [15]. While exhausted and senescent T_c cells share characteristics such as the upregulation of surface markers Tim-3 and tyrosine-based inhibitory motif (ITIM) domain (TIGIT), senescent T_c cells also upregulate CD57 and CD45RA (Figure 1). The cytokine secretory profile of senescent T_c cells sharply contrasts that of exhausted T cells (Figure 1). Senescent T_c cells secrete high levels of inflammatory cytokines such as IL-2, IL-6, IL-8, TNF, IFN-γ and the immunosuppressive IL-10 and TGF-β (Figure 1), a program known as senescence-associated secretory phenotype (SASP). This in turn has critical consequences not only for T cell themselves, but for other immune cells within the TME milieu, including antigen presenting cells (APCs) such as dendritic cells (DCs), tumor-associated

macrophages (TAMs) and myeloid-derived suppressor cells (MDSC). Transcriptional programs in senescent T_cs have been shown to be mediated by T-bet [16] but otherwise are poorly characterized. Senescence-inducing stimuli include exposure to DNA damaging agents, stress signals and repetitive stimulation linked but not limited to the ageing process. It should be pointed out that dysfunctional T cell states other than exhaustion and senescence such as anergy have also been described. Anergic T cells are hypo-responsive, produce low levels of IL-2 and generally have little effector function. T cell anergy is caused by insufficient CD28 dependent co-stimulation of the TCR, but the surface markers of anergic T cells are poorly characterized [17]. Insufficient CD28 stimulation within the TME combined with tumor cell expressing factors, such as PD-L1 and CD95, is also closely linked to deletion of effector T cells through a process known as tolerance. Tolerance is exacerbated by TGF-β and IL-10 [18]. Taken together, senescent, anergic and exhausted T_c cells often co-exist in the TME or circulation and simultaneously exert immunosuppressive effects [11,19]. The current limitations of check-point inhibitors suggest that targeting multiple dysfunctional T_c cell states would be therapeutically beneficial. A deeper understanding of the mechanisms and functional consequences of T cell senescence are urgently needed.

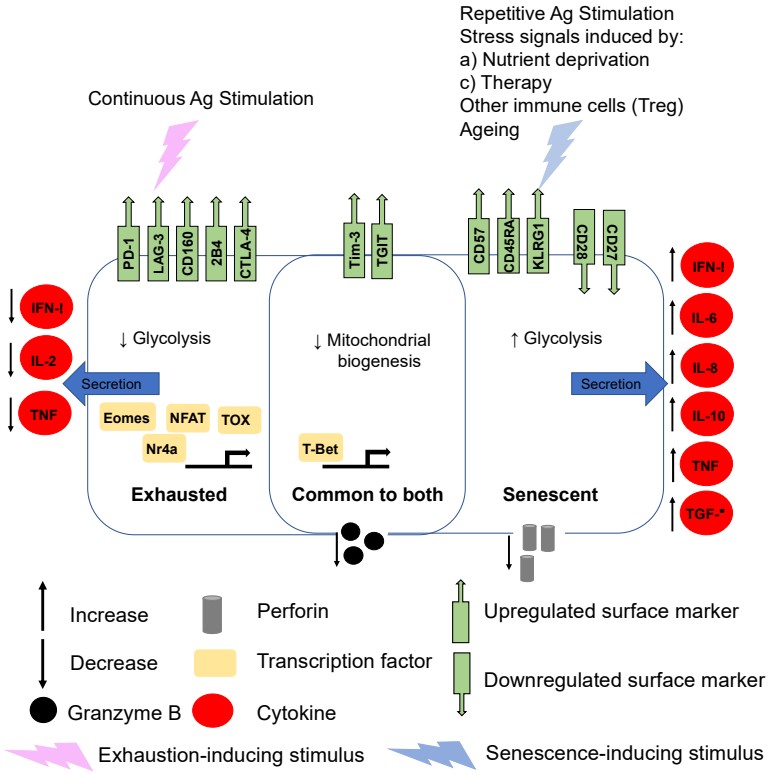

Figure 1. Surface phenotypic, metabolic and transcriptional differences between $CD8^+$ dysfunctional senescent and exhaustive states. Characteristics common to both dysfunctional states are shown the in the middle, purple overlapping section. While both T cell state exhibit decreased effector function, senescent T cells have a very distinct senescence-associated secretory phenotype (SASP) with increased cytokine production of IFN-γ, IL-6, IL-8, IL-10, TNF and TGF-β. In contrast. exhausted T cells are characterized by decreased IL-2, TNF and IFN-γ production. While some surface markers such as Tim-3 and TGIT are common to both dysfunctional T cell states, there is otherwise quite a distinct pattern of expression. Ag = antigen.

3. Mechanisms of T Cell Senescence Induction

Senescent T cells have been found in primary and metastatic solid tumor sites [19–23] as well as hematological malignancies [11,24]. T_c senescence can be classified into two major cellular mechanisms which are however not entirely separated from one another: premature and replicative senescence.

Premature senescence is caused by external factors such as stress within the TME incurred by (i) effects of immune and tumor cells, (ii) TME metabolic changes, (iii) and drug and radiation therapy, all of which are closely interlinked and not necessarily independently occurring events (Figure 2). Replicative senescence is linked to age-related changes and to telomeric shortening. T cell anergy on the other hand, is closely linked to peripheral tolerance.

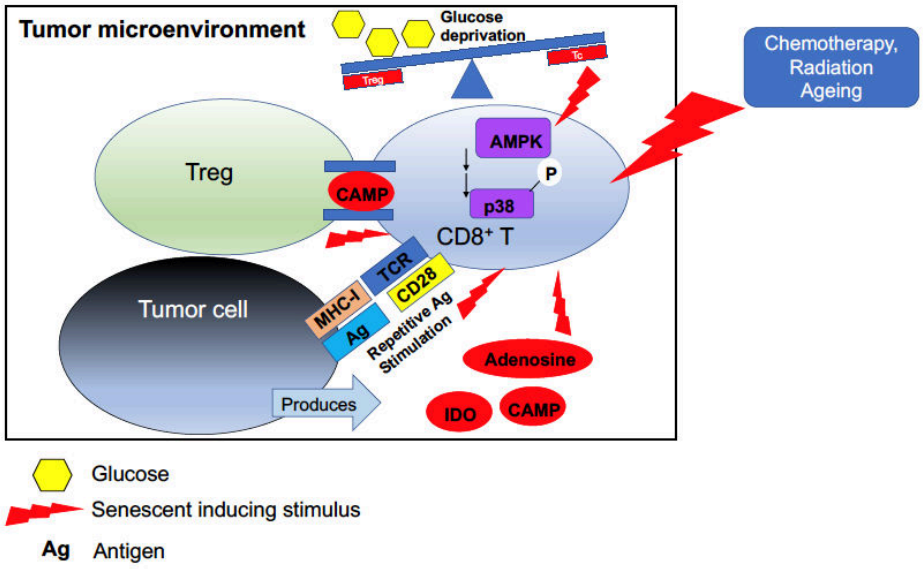

Figure 2. T cell senescence can occur via multiple mechanisms within the tumor microenvironment. Tregs, through glucose metabolic competition and transfer of cAMP produced by tumors, can induce $CD8^+$ T cell senescence, as can other metabolites produced by tumor cells, such as adenosine. Repeated antigen stimulation and external factors such as chemotherapeutic and radiation therapy also induce premature senescence. A key molecular pathway involved in $CD8^+$ T cell senescence induction is non-canonical signaling through p38-MAPK.

3.1. Signaling Pathways Involved in T_c Senescence

The intrinsic molecular pathways governing premature and replicative senescence are not completely defined but involve the MAPK pathway. The diverse and complex MAPK pathway with its three subgroups, Erk, Jnk and p38, is involved in many aspects of innate and acquired immune regulation. Classical engagement of the MAPK pathway downstream of the TCR does not occur in senescent T_c cells as they lack the costimulatory molecule CD28. p38-MAPK activation however, can also be mediated by environmental stressors such as low glucose, DNA damage and by proinflammatory cytokines which trigger AMPK to auto-phosphorylate p38. Henson et al. showed that p38 MAPK expression was elevated in human senescent $CD8^+$ T cells and that blocking p38 following inhibitor treatment resulted in increased mitochondrial mass, improved mitochondrial function and enhanced proliferation [25]. Human senescent $CD27^-CD28^-CD4^+$ T cells prompt AMPK-stimulated recruitment of p38, resulting in p38 autophosphorylation, facilitated by the protein scaffold TAB1, which inhibits telomerase activity and parts of the TCR signalosome [26]. In addition to p38, involvement of the other MAPK members Erk and Jnk have been found to impact T cell senescence in the context of a new immune inhibitory complex termed the sestrin—MAPK activation complex (sMAC). sMAC formation is increased with age [27]. In human and murine $CD4^+$ T cells, sestrins induced senescence through binding and simultaneous activation of Erk, Jnk and p38 to form sMAC. Silencing sestrin enhanced T cell activity. Although $CD4^+$ T cells were experimentally used in this study, the authors did show that sestrin deficiency increased vaccine responses in aged mice and increased the frequency of splenic $CD8^+$ T cells. A follow-up study specifically examining the effects of sestrin in $CD27^-CD28^-CD8^+$ T cells, showed that a divergent mechanism was responsible for sestrin-dependent senescence in

$CD27^{-}CD28^{-}CD8^{+}$ T cells linked to a natural killer group 2 member D (NKG2D)–DNAX Activating Protein of 12KDa (DAP12)–sestrin 2 complex. Disturbance of the NKG2D–DAP12–sestrin 2 complex through sestrin 2 genetic inhibition, restored TCR signaling [28]. T cell mitochondrial dysfunction also accelerates senescence. It was recently demonstrated that *Tfam*$^{fl/fl}$ *Cd4*^{Cre} mice (where mitochondrial transcription factor A (TFAM) is depleted in $CD4^{+}$ and $CD8^{+}$ lymphocytes) prematurely died due to multiple age-related changes [29]. Taken together, the full extent of the molecular pathways involved T_c senescence are not completely elucidated. The current knowledge, however, presents targetable opportunities to potentially reverse senescence and understand how senescent T_c cells might impact immunotherapies in the treatment of cancer.

3.2. The TME Drives Tc Premature Senescence

3.2.1. Immune and Tumor Cells

A tumor's ability to evade the immune system is dynamic, complex and partially dependent on the immunosuppressive activities of infiltrating immune cells. T_c effector function is similarly complicated and shaped by the spatiotemporal distribution of APCs in the tumor milieu and tumor-draining lymph nodes, cytokines and the presence of other immune cells such as regulatory $CD4^{+}CD25^{hi}FoxP3^{+}$ T (Treg) cells. Initial priming of naïve T cells occurs in the lymph node through direct interaction with antigen present on APCs such as DCs. DCs also co-express receptors such as CD80 necessary for binding to CD28 and inducing co-stimulatory signals. Upon migration of primed T_c cells into the TME, the tumor cells expressing the antigenic peptide become targets. The numbers of infiltrating $CD8^{+}$ T cells varies widely across tumor types. Some tumors, such as melanoma and non-small cell lung cancer (NSCLC), generally have a high degree T_c infiltration. Other tumors, such as pancreatic and neuroblastoma, typically have a low degree of T_c infiltrates, although of course within a specific tumor type, there is a lot of intra-tumoral heterogeneity [30]. Many factors during this process can impact the ability of T_c cells to target tumor cells.

Regulatory $CD4^{+}CD25^{hi}FoxP3^{+}$ T (Treg) cells are subsets of T cells which play a role in maintaining immune homeostasis and present a critical barrier for immunotherapies through their suppressive effects on T_c cells. Tregs have been found in lymph nodes where they impact DC function through CCL22. CCL22, a chemokine produced by dendritic cells, enables cell-to-cell contact between DCs and Treg through Treg-expressed CCR4 [31]. Tregs accumulate within the TME, and their ability to infiltrate into tumors has been linked to the expression of multiple chemokine receptors such as CCR4, CCR5, CCR8 and CCR10. Within the TME, Tregs usually express immunosuppressive molecules such as CTL-4, which binds to CD80 and CD86 on APCs thereby affecting T_c effector function [32]. Treg suppressive mediated-effects on APCs and T_c effector cells can also occur through inhibitory cytokine secretion of IL-10, TGF-β, and IL-35. These inhibitory cytokines suppress antigen presentation in APCs. IL-35 and IL-10 promote T cell exhaustion. Metabolic competition for the consumption of IL-2 through the expression of CD25 on Tregs also suppresses T_c effector functions [33]. Tregs are also found in peripheral circulation, but their precise role in facilitating immune evasion are not as well characterized as with the TME-associated Tregs [32].

Relating specifically to Treg-mediated T_c senescence induction, an important study demonstrated that co-transfer of Tregs and naïve $CD8^{+}$ T cells into *Rag1*$^{-/-}$ mice transformed naïve T cells into senescent T cells (as assessed by SA-β-Gal positivity). Furthermore, the senescent T cells acquired immunosuppressive functions both in vitro and in vivo. Involvement of the mitogen-activated protein kinase (MAPK) pathway was implicated, as pre-treatment with ERK and p38 inhibitors abrogated these immunosuppressive effects [34]. Another critical study by Liu at al. using ex vivo cultured primary human T cells demonstrated that human Tregs induced nuclear kinase ataxia–telangiectasia-mutated protein (ATM)-associated DNA damage responses in T_cs [35]. The majority of subsequent mechanistic experiments demonstrated that senescence was mediated by competition for glucose, which triggered phosphorylation of the energy sensor AMP-activated protein kinase (AMPK) in cooperation with

Stat1 and Stat3. These mechanistic studies were performed using naïve $CD4^+$ T cells. However, the authors did show that Treg-induced naïve $CD8^+$ T cell senescence was blocked by pre-treatment with ATM or STAT inhibitors in NOD SCID gamma (NSG) mice, indicating that similar mechanisms of senescence induction also occur in $CD8^+$ T cells. These studies did not directly explore the specific co-localized induction of Treg-induced T_c senescence within the TME. However, as Tregs and T_cs are often co-expressed within tumors [36,37] and tumor-draining lymph nodes [38], the clinical relevance of these in vivo and ex vivo studies is plausible. These interactions, however, would likely be mediated by APCs, which these studies did not address. APCs might guide the cellular interaction between Tregs and T_cs through costimulatory (CD28/CD80 and CD86, OXO/OXOL, CD95/CD95L) on $CD8^+$ T cells or co-inhibitory (PD-1/PD-L1 and CTLA-4/CD80) signals on $CD8^+$ and $CD4^+$ T cells, respectively. Other immune cells within the TME might also indirectly impact T_c senescence. Treg and MDSC populations often support each other's expansion through positive feedback loops involving TGF-β and other cytokines [33]. In turn, MDSCs can be expanded by many of the SASP cytokines secreted by T_c senescent cells such as TGF-β, IL-6 and IFN-γ [39].

Tumor cells are the targets of T_cs following priming in the lymph nodes. T_c-mediated tumor cell killing occurs through TCR-mediated T_c cell binding to MHC-I-restricted tumor antigens on tumor cells. This interaction releases cytolytic perforin and granzymes causing tumor cell killing. Tumor cell killing can also occur through the death receptor pathway mediated by the expression of CD95 on tumor cells and CD95L on T_c cells. Receptors present on tumor cells such as PD-L1 can diminish T_c cells responses through the PD-1–PD–L1 axis [2]. Tumor cells can also downregulate MHC-I and CD95 expression to dampen responses and evade apoptosis. Immunosuppressive cytokines produced by tumor cells such as TGF-β and IL-10 also influence T_c effector function. Metabolites produced by tumor cells, elaborated on in the section below, can also affect T_cs.

Tumor cells have been shown to induce T_c senescence in in vitro and in vivo models. Montes et al. showed that ex vivo incubation of human T cells isolated from healthy donors with a variety of human tumor cell lines triggered downregulation of CD28 expression. Activation of ATM, shortening of telomere length and an ability to suppress antigen nonspecific and allogeneic-induced proliferation of responder T cells were also observed [40]. Tumor-induced senescence was dependent on direct tumor-T cell contact [40]. Another pivotal investigation demonstrated that adoptive transfer of tumor-specific $CD8^+$ tumor-infiltrating lymphocytes (TIL) 586 cells into tumor-bearing (586 mel cells) NSG mice induced senescence, as assessed by SA-β-Gal^+ staining in TILs [41]. Activation of TLR8 signaling in tumor cells was able to reverse the tumor-induced senescence [42]. Taken together, tumor-infiltrating immune cells such as Tregs as well as tumor cells have been shown to be capable of inducing T cell senescence. As this evidence largely stems from ex vivo studies, the role of critical cells mediating T_c priming such as DCs in facilitating this process remains to be explored.

3.2.2. Metabolic Changes

Metabolic re-programming within the TME is critical to many pro-tumorigenic processes, including driving senescence [43,44]. Cancer cells have a high rate of glucose consumption through aerobic glycolysis, resulting in low glucose and high lactate concentrations in the TME [45]. Antigen-activated effector T cells, once they become primed and activated in the lymph nodes, begin their clonal expansion and rapid proliferation [43]. Therefore, they have metabolic requirements different to those of circulating naïve cells which rely on oxidative phosphorylation for their energy requirements. Rapidly proliferating T cells have higher glycolytic activity [46] and increased amino acid metabolism [47]. TCR-mediated T cell activation is followed by metabolic re-programming and biomass accumulation. Changes in metabolism include a switch to aerobic glycolysis despite there being enough oxygen present to generate glucose through the tricarboxylic acid (TCA) cycle [43]. Aerobic glycolysis provides important intermediates for cell growth, such as glucose-6-phosphate, 3-phosphoglycerate (3PG) and citrate. Molecularly, this metabolic transition is supported by mTOR, PI3K activity, the transcription factor Myc and hypoxia-inducible factor-1α (HIF-1α) [43,47]. As already described above in the study

by Liu et al., increased glucose consumption by Tregs reduced the glucose pool available for naïve T cells, initiating AMPK signaling cascades and DNA damage responses [35]. Effector T cell activity is sensitive towards intracellular NAD depletion, often occurring in the TME. Tregs, however, have developed re-programming strategies mediated by the transcription factor FOXP3 to maintain their proliferative capabilities and suppressive functions, despite low glucose and high lactate levels [48]. It remains to be elucidated whether within the TME Treg numbers would be high enough to deplete glucose pools. However, in addition to Treg competing for glucose consumption, other immune cells within the TME also have distinct metabolic requirements which can affect glucose pools. MDSCs have high glucose uptake rates and can contribute to the dysfunction of other immune cells by limiting pools of available glucose [39]. MDSCs can also affect the T cell activation through depletion of amino acids such as cystine and cysteine [49], but whether that eventually also contributes to T_c senescence induction is not known. Conditions of hypoxia within the TME compounded by increased tumor acidity can cause an accumulation of immunosuppressive M2 polarized TAMs, which are critical in maintaining a tolerogenic phenotype, expanding Tregs and suppressing T_c function [50].

Tumor cells also produce metabolites that are inducers of T_c cell senescence. For instance adenosine, whose production is catalyzed by the surface ectonucleotidases CD39 and CD73, accumulates in the TME through CD38 and CD73 expression on cancer exosomes [51]. Adenosine exposure triggered replicative senescence in human $CD8^+$ T cells, decreased proliferative capacity and reduced IL-2 production [52]. Furthermore, adenosine can impact APCs that are critical for T_c function. Tumor-produced adenosine has been shown to decrease DC maturation and immune function [53]. Another example is cyclic adenosine monophosphate (cAMP), produced by tumor cells and a suppressor of T cell function [54]. In ex vivo co-culturing experiments, cAMP was shown to be transferred from Tregs to T_cs through direct gap junction formation, thereby suppressing proliferation of T_cs and decreasing IL-2 production [55]. However, the in vivo relevance of these findings in the context of the TME has yet to be validated. Other TME-associated metabolites such as indoleamine 2,3-dioxygenase (IDO) [56], although not yet shown to directly induce T_c senescence, plausibly contribute to the induction of T_c dysfunction through activation of Tregs.

3.2.3. Chemotherapeutics and Radiation Therapy

DNA damage caused by commonly used chemotherapeutics can lead to senescence induction in both tumor and normal cells [57]. Most chemotherapeutic agents are genotoxic and cause DNA damage by triggering chromosomal breaks or double stranded DNA breaks. This is followed by induction of the DNA damage response (DDR) mediated by ATM and ATR kinases, whose downstream targets are cell cycle regulatory proteins checkpoint homologs 1 and 2 (Chk1 and Chk2). Chk1 and Chk2 trigger the activation of various cyclin-dependent kinase inhibitors causing cell cycle arrest [58]. It is not surprising that treatment with such agents can also lead to immuno-senescence, especially in rapidly proliferating populations such as T_c cells following antigen exposure. A six months longitudinal study tracked shifts in $CD8^+$ T cell populations in DNA-damaging chemotherapy-treated breast cancer patients. The study found that senescent-enriched $CD28^-CD57^+$ cells were more pre-dominant in cancer patients compared to the untreated healthy age-matched group. The study also found that immuno-senescence and immune risk parameters were more pronounced in the chemotherapy-treated group [22]. When peripheral $CD8^+$ T lymphocytes were assessed in metastatic breast cancer patients during the post-salvage taxane chemotherapy follow-up, it was found that $CD8^+CD28^-$ populations were increased in breast cancer patients compared to the control cohort [23]. In another longitudinal study, radiotherapy and chemotherapy in early-stage breast cancer patients increased senescent cytotoxic T lymphocytes [59]. Shortened telomere length was observed in peripheral blood mononuclear cells in non-Hodgkin's lymphoma patients undergoing chemotherapy [60]. These results are correlative, and the functional consequences of T_c cell senescence induction in these clinical settings should be mechanistically explored. Tumor senescence might be beneficial to the organism under some contexts, as it stops tumor-cell proliferation. However, the unintended potentially

detrimental consequences of T_c cell senescence should be considered during the course of therapy, especially if immunotherapy treatment such as CAR-T cell therapy is to be further applied.

3.3. Age-Related Replicative Senescence

Replicative senescence in normal somatic cells is telomere dependent and occurs as a result of telomere shortening or a classical DNA damage response triggered by a dysfunctional telomerase [61]. Telomerase dysfunction can be triggered by oxidative stress [62]. This is paralleled in T_c cells. The natural aging process is accompanied by blunted immune responses to anti-viral, bacterial and other stimuli as well as decreased responsiveness to vaccines [63,64]. Repeated antigen stimulation throughout an individual's life time is one potential cause of aging-induced T_c senescence. Others include physiological changes such as thymic shrinking which limits the naïve T cell pool, changes in the bone marrow, and obesity [62,65,66]. While ex vivo stimulated human $CD8^+$ T cells have been shown to have high initial telomerase activity, their telomere lengths shorten following several rounds of antigen stimulation, and their telomerase activity dramatically decreases [67]. A decrease in the number of naïve $CD8^+$ T cells and suppressed functionality in terms proliferation and decreased cytokine production accompany age-related dysfunction [63,68]. In aged mice, proliferative defects have also been demonstrated in anti-viral memory $CD8^+$ T cells [69]. Senescence has also been observed in $CD8^+$ T cells which have not undergone repetitive antigen stimulation. A recent study explored a specialized subset of semi-differentiated antigen naïve but semi-primed T cells expressing the activation marker CD44 termed "virtual memory" $CD8^+$ T cells ($CD44^{hi}CD49d^{lo}$; T_{VM}). The investigation found T_{VM} cells accumulated in aged mice and humans and acquired a dysfunctional senescent but not exhausted phenotype [70]. The presence of T_{VM} cells in aged individuals would be expected to diminish primary $CD8^+$ T cell responses while still maintaining a base effector function and the ability to secrete cytokines.

4. Tc Cell Senescence and Effects on Immunotherapy Response

4.1. Checkpoint Inhibitors

Given the increased accumulation of senescent T_c cells in older individuals, it would be reasonable to expect that age would dimmish response to immunotherapies. Curiously, however, some reports indicate that advanced age positively correlates with anti-PD-1 therapy response [71]. In this study, when a total of 538 metastatic melanoma patients treated with pembrolizumab were stratified according to age and response, a smaller percentage of patients aged over 62 years had progressive disease. The study, which controlled for prior MAPK inhibitor therapy, did not control for mutational burden but did corroborate the patient data with murine models. Genetically identical tumors experienced better, albeit minor, anti-PD-1 responses in aged mice. The study found that in younger patients, Tregs were increased and $CD8^+$ T cells decreased in the TME. The authors speculated that memory $CD8^+$ T cells, which accumulate with age and expand in response to immunotherapy, may be responsible for improved anti-PD-1 responses. However, accumulation of memory $CD8^+$ T cells in aged individuals is not absolute and is relative to a decrease in naïve T cells due to thymic shrinking. Other studies in various tumor types have found no correlation [72,73], or a negative correlation between age and checkpoint inhibitor response [74]. The study citing the negative correlation was carried out in patients with advanced renal cell carcinoma with a small sub-group of older patients. Furthermore, the study did not assess infiltrates in the TME. Age-induced senescence might affect other critical immune cells which could impact responses to checkpoint inhibitors, including the abovementioned T_{vM} cells [70]. The phagocytic function of macrophages/monocytes is decreased during aging and might impair release of antigens into the micro-environment. Aging also decreases numbers and antigen presenting functions of APCs, which would impact T cell effector function [75].

It is difficult to conclusively ascertain whether older patients fare better/worse following immunotherapy treatment given the usually low numbers of elderly patients included in clinical trials.

Immunotherapy response, particularly to checkpoint inhibitors, is complex, and no successful biomarker of response has been established. Several biomarkers have been suggested, including neo-antigen burden, PD-L1 expression, genomic and transcriptomic signatures and immune infiltration [76,77]. While age-induced T_c cell senescence might impact response to immunotherapy treatment, other more significant factors could over-ride these effects. For example, a recent study reported that tumors in younger female individuals accumulated more poorly presented driver mutations than those in older and male patients. Accordingly, these female patients had poorer immune checkpoint therapy responses [78]. Taken together, it remains to be proven whether age is a predictor of immunotherapy response

Irrespective of age, patients with accumulated senescent T_c cells within the TME might respond poorly to checkpoint inhibition, which seeks to de-repress the exhaustive T_c phenotype but does not target the senescent one. A small pilot study of melanoma patients was able to identify patients with primary resistance to checkpoint inhibitors by using lymphocyte phenotyping for senescence markers CD27, CD28, Tim-3 and CD57 [79]. The study tracked senescence markers in the peripheral blood for 12 weeks post diagnosis of metastatic melanoma. Another study found that in multiple myeloma, T-cell clones exhibited hypo-responsiveness and a telomere-independent senescent ($KLRG\text{-}1^+/CD57^+/CD160^+/CD28^-$) phenotype. These senescent T cells also expressed low levels of PD-1 and CTL-4 [24]. Although limited in the numbers of assessed patients, these studies suggest that senescent T_c impede responses to checkpoint inhibitors.

4.2. CAR-T Cell Therapy

CAR-T cell therapy has the potential to be curative in patients with hematological malignancies such as leukemia and lymphoma. However, CAR-T cell therapy application to solid tumors whose targetable antigen repertoire can be difficult to predict will be more challenging. CAR-T cell therapy depends on the isolation and expansion of a patient's T cells harvested from the periphery. It is plausible to speculate that functionally impaired senescent T cells in this context would provide an impediment to successful T cell expansion and/or CAR activity once in the TME. In vivo, murine studies have shown that PD-1 upregulation within the tumor microenvironment impeded the function of CD28-CAR-T cells, which was restored by concomitant treatment with anti-PD-1 antibodies [80]. Furthermore, introduction of a patient's expanded T cells into the TME might lead to terminal differentiation of the T cells caused by TME-induced T_c senescence or exhaustion [81]. Taken together, although this requires further exploration, there is reasonable correlative evidence to suggest that senescent T_c cells impact immunotherapy responses.

4.3. Targeting T Cell Senescence

As 40–85 percent of patients treated with checkpoint inhibitors fail to exhibit a sustained clinical response [82], combinatorial approaches that also reverse T_c cell senescence could be of therapeutic benefit. As induction of tumor cell senescence can be advantageous in the context of tumor clearance, strategies to reverse T cell senescence should be carefully considered. While induction of tumor cell senescence can initially stop uncontrolled proliferation, the SASP profile of senescent tumor cells can promote tumor relapse, inflammation and recruit immunosuppressive immune cells to the TME. Agents that induce apoptosis in senescent cells termed "senolytics" (e.g., dasatanib and quercetin), are currently being tested in pulmonary fibrosis and after radiotherapy to improve clinical symptoms [83,84]. Whether these agents can be used in neoplastic malignancies to clear senescent tumor cells and/or senescent T_c cells is an area warranting further exploration.

Agents such as ralimetinib that target p38 MAPK, which are safe and have already being used in clinical trials [85], are an attractive option as they could dually target T_c senescence signaling and tumor proliferation. In addition to their direct anti-tumoral effects, other inhibitors of the MAPK pathway already approved for the treatment of metastatic melanoma are also promising. These include the B-Raf-targeting inhibitor vemurafenib or MEK1/2 targeting inhibitor trametinib. These drugs have

already been shown to increase the number of $CD8^+$ TILs and enhance checkpoint inhibition in murine models [86,87]. During senescence, upregulation of BCL-2 family members (BCL-XL, BCL-W) have been reported in several studies, across various cell types [84]. Of note, inhibitors targeting the BCL-2 protein family, including novitoclax, are selectively senolytic in some cell types [88]. Moreover, several other pro-survival pathways have been implicated in eliminating senescence, including the p53/p21 axis, receptor tyrosine kinase, HIF-1α and serpine anti-apoptotic pathways [84,89]. HSP90, a member of the chaperone protein family, was identified as a new class of senolytics [90,91]. HSP90 is upregulated in several tumor types and promotes the stabilization of PI3K/Akt, ERK and other pro-survival signaling pathways upregulated during cellular senescence [92]. Therefore, downregulation of pro-survival signaling pathways upon HSP90 inhibition may be responsible for its senolytic activity [90]. Whether these inhibitors also reverse T_c senescence and enhance checkpoint inhibition in the clinical setting remains to be elucidated. However, combinatorial therapy is paramount in achieving clinical success. Therefore, these strategies might present good therapeutic opportunities. They also have the advantage of using already approved therapies.

Combining checkpoint inhibitors with other activators of the immune system such as TLR8 agonists could maximize the benefits of immunotherapy. TLR8 agonists have already been shown to reverse the T cell tumor-induced senescence in mouse models of cancer [41]. They have the added benefit of increasing immune infiltration and activating other anti-tumoral immune cells such as dendritic and NK cells. The TLR8 agonist motolimod (VTX-2337) has been evaluated in clinical trials, is well tolerated and shows promise activating the immune system in cancer patients [93,94]. Other approaches exist, such as the reprogramming of senescent T_c cells from pluripotent stem cells (T-IPSCs). However, this approach is complicated by the unpredictable re-arrangement of the TCR [81].

Taken together, as our molecular understanding of the pathways governing T_c cell senescence increases, so will the ability to effectively target this dysfunctional subset of T cells, reverse their immunosuppression and augment currently used immunotherapies. Furthermore, assessing senescent T cell accumulation following treatment with currently used therapies in cancer patients might help to optimize treatment strategies and uncover novel bio-markers of immunotherapy response.

5. Conclusions

Senescent T_c cells are phenotypically distinct from exhausted T_c cells. Their immunosuppressive function brings new obstacles to successful immunotherapy. Regardless of whether the tumor-specific T cell senescence is of replicative or premature origin, a deeper molecular understating of the molecular pathways driving this process is needed. This will open new therapeutic options to eradicate challenges imposed by a suppressive TME. Currently, MAPK pathway inhibitors and TLR8a agonists are amongst the most clinically promising candidates to reverse T cell senescence. They can potentially be used in combinatorial approaches with checkpoint inhibitors to target many levels of immune dysfunction and maximize anti-tumor immunity. Much progress has been made in defining T cell senescence as a distinct dysfunctional state. However, clinical evidence showing the functional importance of T cell senescence in solid tumors and hematological malignancies is largely correlative and needs to be further explored.

Author Contributions: W.L., P.S., S.B. and A.A.P. performed data research. A.A.P. wrote the manuscript. All authors edited the manuscript. H.C.X., S.B., A.B., P.A.L. and A.A.P. conceptualized the design of the study. All authors have read and agreed to the published version of the manuscript.

Funding: S.B. acknowledges the support by Forschungskommission (2018-04) and DSO-Netzwerkverbundes, HHU Düsseldorf. This work was supported by the funds from the Deutsche Forschungsgemeinschaft (DFG) SFB974, RTG1949 and the Düsseldorf School of Oncology (DSO).

Conflicts of Interest: The authors declare no conflict of interest.

References

1. Waldman, A.D.; Fritz, J.M.; Lenardo, M.J. A guide to cancer immunotherapy: From T cell basic science to clinical practice. *Nat. Rev. Immunol.* **2020**, 1–18. [CrossRef]
2. Martinez-Lostao, L.; Anel, A.; Pardo, J. How Do Cytotoxic Lymphocytes Kill Cancer Cells? *Clin. Cancer Res.* **2015**, *21*, 5047–5056. [CrossRef]
3. Larkin, J.; Chiarion-Sileni, V.; Gonzalez, R.; Grob, J.-J.; Cowey, C.L.; Lao, C.D.; Schadendorf, D.; Dummer, R.; Smylie, M.; Rutkowski, P.; et al. Combined Nivolumab and Ipilimumab or Monotherapy in Untreated Melanoma. *New Engl. J. Med.* **2015**, *373*, 23–34. [CrossRef]
4. Barber, D.L.; Wherry, E.J.; Masopust, D.; Zhu, B.; Allison, J.; Sharpe, A.H.; Freeman, G.J.; Ahmed, R. Restoring function in exhausted CD8 T cells during chronic viral infection. *Nature* **2006**, *439*, 682–687. [CrossRef]
5. Locke, F.L.; Neelapu, S.S.; Bartlett, N.L.; Siddiqi, T.; Chavez, J.C.; Hosing, C.M.; Ghobadi, A.; Budde, L.E.; Bot, A.; Rossi, J.M.; et al. Phase 1 Results of ZUMA-1: A Multicenter Study of KTE-C19 Anti-CD19 CAR T Cell Therapy in Refractory Aggressive Lymphoma. *Mol. Ther.* **2017**, *25*, 285–295. [CrossRef] [PubMed]
6. Neelapu, S.S.; Locke, F.L.; Bartlett, N.L.; Lekakis, L.J.; Miklos, D.B.; Jacobson, C.A.; Braunschweig, I.; Oluwole, O.O.; Siddiqi, T.; Lin, Y.; et al. Axicabtagene Ciloleucel CAR T-Cell Therapy in Refractory Large B-Cell Lymphoma. *N. Engl. J. Med.* **2017**, *377*, 2531–2544. [CrossRef] [PubMed]
7. Vitale, C.; Strati, P. CAR T-Cell Therapy for B-Cell non-Hodgkin Lymphoma and Chronic Lymphocytic Leukemia: Clinical Trials and Real-World Experiences. *Front. Oncol.* **2020**, *10*, 849. [CrossRef] [PubMed]
8. Zou, W. Immunosuppressive networks in the tumour environment and their therapeutic relevance. *Nat. Rev. Cancer* **2005**, *5*, 263–274. [CrossRef]
9. Appay, V.; Nixon, D.F.; Donahoe, S.M.; Gillespie, G.M.; Dong, T.; King, A.; Ogg, G.S.; Spiegel, H.M.; Conlon, C.; Spina, C.A.; et al. HIV-Specific Cd8+ T Cells Produce Antiviral Cytokines but Are Impaired in Cytolytic Function. *J. Exp. Med.* **2000**, *192*, 63–76. [CrossRef]
10. Wherry, E.J.; Ha, S.-J.; Kaech, S.M.; Haining, W.N.; Sarkar, S.; Kalia, V.; Subramaniam, S.; Blattman, J.N.; Barber, D.L.; Ahmed, R. Molecular Signature of CD8+ T Cell Exhaustion during Chronic Viral Infection. *Immunity* **2007**, *27*, 670–684. [CrossRef]
11. Zelle-Rieser, C.; Thangavadivel, S.; Biedermann, R.; Brunner, A.; Stoitzner, P.; Willenbacher, E.; Greil, R.; Jöhrer, K. T cells in multiple myeloma display features of exhaustion and senescence at the tumor site. *J. Hematol. Oncol.* **2016**, *9*, 116. [CrossRef]
12. Li, K.-K.; Adams, D.H. Antitumor CD8+ T cells in hepatocellular carcinoma: Present but exhausted. *Hepatology* **2014**, *59*, 1232–1234. [CrossRef] [PubMed]
13. Liu, X.; Hoft, D.F.; Peng, G. Senescent T cells within suppressive tumor microenvironments: Emerging target for tumor immunotherapy. *J. Clin. Investig.* **2020**, *130*, 1073–1083. [CrossRef] [PubMed]
14. Wherry, E.J.; Kurachi, M. Molecular and cellular insights into T cell exhaustion. *Nat. Rev. Immunol.* **2015**, *15*, 486–499. [CrossRef] [PubMed]
15. Zhao, Y.; Shao, Q.; Peng, G. Exhaustion and senescence: Two crucial dysfunctional states of T cells in the tumor microenvironment. *Cell. Mol. Immunol.* **2019**, *17*, 27–35. [CrossRef]
16. Dolfi, D.V.; Mansfield, K.D.; Polley, A.M.; Doyle, S.A.; Freeman, G.J.; Pircher, H.; Schmader, K.E.; Wherry, E.J. Increased T-bet is associated with senescence of influenza virus-specific CD8 T cells in aged humans. *J. Leukoc. Biol.* **2013**, *93*, 825–836. [CrossRef]
17. Crespo, J.; Sun, H.; Welling, T.H.; Tian, Z.; Zou, W. T cell anergy, exhaustion, senescence, and stemness in the tumor microenvironment. *Curr. Opin. Immunol.* **2013**, *25*, 214–221. [CrossRef]
18. Bour-Jordan, H.; Esensten, J.H.; Martínez-Llordella, M.; Penaranda, C.; Stumpf, M.; Bluestone, J.A. Intrinsic and extrinsic control of peripheral T-cell tolerance by costimulatory molecules of the CD28/B7 family. *Immunol. Rev.* **2011**, *241*, 180–205. [CrossRef]
19. Papalampros, A.; Vailas, M.; Ntostoglou, K.; Chiloeches, M.L.; Sakellariou, S.; Chouliari, N.V.; Samaras, M.G.; Veltsista, P.D.; Theodorou, S.D.P.; Margetis, A.T.; et al. Unique Spatial Immune Profiling in Pancreatic Ductal Adenocarcinoma with Enrichment of Exhausted and Senescent T Cells and Diffused CD47-SIRPα Expression. *Cancers* **2020**, *12*, 1825. [CrossRef]
20. Li, H.; Wu, K.; Tao, K.; Chen, L.; Zheng, Q.; Lu, X.; Liu, J.; Shi, L.; Liu, C.; Wang, G.; et al. Tim-3/galectin-9 signaling pathway mediates T-cell dysfunction and predicts poor prognosis in patients with hepatitis B virus-associated hepatocellular carcinoma. *Hepatology* **2012**, *56*, 1342–1351. [CrossRef]

21. Gruber, I.; El Yousfi, S.; Dürr-Störzer, S.; Wallwiener, D.; Solomayer, E.F.; Fehm, T. Down-regulation of CD28, TCR-zeta (zeta) and up-regulation of FAS in peripheral cytotoxic T-cells of primary breast cancer patients. *Anticancer Res.* **2008**, *28*, 779–784. [PubMed]
22. Onyema, O.O.; DeCoster, L.; Njemini, R.; Forti, L.N.; Bautmans, I.; De Waele, M.; Mets, T. Chemotherapy-induced changes and immunosenescence of CD8+ T-cells in patients with breast cancer. *Anticancer Res.* **2015**, *35*, 1481–1489. [PubMed]
23. Song, G.; Wang, X.; Jia, J.; Yuan, Y.; Wan, F.; Zhou, X.; Yang, H.; Ren, J.; Gu, J.; Lyerly, H.K. Elevated level of peripheral CD8+CD28− T lymphocytes are an independent predictor of progression-free survival in patients with metastatic breast cancer during the course of chemotherapy. *Cancer Immunol. Immunother.* **2013**, *62*, 1123–1130. [CrossRef] [PubMed]
24. Suen, H.; Brown, R.; Yang, S.; Weatherburn, C.; Ho, P.J.; Woodland, N.; Nassif, N.; Barbaro, P.; Bryant, C.; Hart, D.; et al. Multiple myeloma causes clonal T-cell immunosenescence: Identification of potential novel targets for promoting tumour immunity and implications for checkpoint blockade. *Leukemia* **2016**, *30*, 1716–1724. [CrossRef] [PubMed]
25. Henson, S.M.; Lanna, A.; Riddell, N.; Franzese, O.; Macaulay, R.; Griffiths, S.J.; Puleston, D.J.; Watson, A.S.; Simon, A.K.; Tooze, S.A.; et al. p38 signaling inhibits mTORC1-independent autophagy in senescent human CD8+ T cells. *J. Clin. Investig.* **2014**, *124*, 4004–4016. [CrossRef]
26. Lanna, A.; Henson, S.M.; Escors, D.; Akbar, A.N. The kinase p38 activated by the metabolic regulator AMPK and scaffold TAB1 drives the senescence of human T cells. *Nat. Immunol.* **2014**, *15*, 965–972. [CrossRef]
27. Lanna, A.; Gomes, D.C.; Müller-Durovic, B.; McDonnell, T.; Escors, D.; Gilroy, D.W.; Lee, J.H.; Karin, M.; Akbar, A.N. A sestrin-dependent Erk–Jnk–p38 MAPK activation complex inhibits immunity during aging. *Nat. Immunol.* **2017**, *18*, 354–363. [CrossRef]
28. Pereira, B.I.; De Maeyer, R.P.H.; Covre, L.P.; Nehar-Belaid, D.; Lanna, A.; Ward, S.; Marches, R.; Chambers, E.S.; Gomes, D.C.O.; Riddell, N.E.; et al. Sestrins induce natural killer function in senescent-like CD8+ T cells. *Nat. Immunol.* **2020**, *21*, 684–694. [CrossRef]
29. Desdín-Micó, G.; Soto-Heredero, G.; Aranda, J.F.; Oller, J.; Carrasco, E.; Gabandé-Rodríguez, E.; Blanco, E.M.; Alfranca, A.; Cussó, L.; Desco, M.; et al. T cells with dysfunctional mitochondria induce multimorbidity and premature senescence. *Science* **2020**, *368*, 1371–1376. [CrossRef]
30. Galon, J.; Bruni, D. Approaches to treat immune hot, altered and cold tumours with combination immunotherapies. *Nat. Rev. Drug Discov.* **2019**, *18*, 197–218. [CrossRef]
31. Rapp, M.; Wintergerst, M.W.M.; Kunz, W.G.; Vetter, V.K.; Knott, M.M.L.; Lisowski, D.; Haubner, S.; Moder, S.; Thaler, R.; Eiber, S.; et al. CCL22 controls immunity by promoting regulatory T cell communication with dendritic cells in lymph nodes. *J. Exp. Med.* **2019**, *216*, 1170–1181. [CrossRef] [PubMed]
32. Kim, J.-H.; Kim, B.S.; Lee, S.-K. Regulatory T Cells in Tumor Microenvironment and Approach for Anticancer Immunotherapy. *Immune Netw.* **2020**, *20*, e4. [CrossRef] [PubMed]
33. Li, C.; Jiang, P.; Wei, S.; Xu, X.; Wang, J. Regulatory T cells in tumor microenvironment: New mechanisms, potential therapeutic strategies and future prospects. *Mol. Cancer* **2020**, *19*, 1–23. [CrossRef] [PubMed]
34. Ye, J.; Huang, X.; Hsueh, E.C.; Zhang, Q.; Ma, C.; Zhang, Y.; Varvares, M.A.; Hoft, D.F.; Peng, G. Human regulatory T cells induce T-lymphocyte senescence. *Blood* **2012**, *120*, 2021–2031. [CrossRef]
35. Liu, X.; Mo, W.; Ye, J.; Li, L.; Zhang, Y.; Hsueh, E.C.; Hoft, D.F.; Peng, G. Regulatory T cells trigger effector T cell DNA damage and senescence caused by metabolic competition. *Nat. Commun.* **2018**, *9*, 249. [CrossRef]
36. Ji, A.L.; Rubin, A.J.; Thrane, K.; Jiang, S.; Reynolds, D.L.; Meyers, R.M.; Guo, M.G.; George, B.M.; Mollbrink, A.; Bergenstråhle, J.; et al. Multimodal Analysis of Composition and Spatial Architecture in Human Squamous Cell Carcinoma. *Cell* **2020**, *182*, 497–514.e22. [CrossRef]
37. Sakuishi, K.; Ngiow, S.F.; Sullivan, J.M.; Teng, M.W.L.; Kuchroo, V.K.; Smyth, M.J.; Anderson, A.C. TIM3+FOXP3+regulatory T cells are tissue-specific promoters of T-cell dysfunction in cancer. *OncoImmunology* **2013**, *2*, e23849. [CrossRef]
38. Zhou, X.; Zhao, S.; He, Y.; Geng, S.; Shi, Y.; Wang, B. Precise Spatiotemporal Interruption of Regulatory T-cell–Mediated CD8+ T-cell Suppression Leads to Tumor Immunity. *Cancer Res.* **2018**, *79*, 585–597. [CrossRef]
39. Hu, C.; Pang, B.; Lin, G.; Zhen, Y.; Yi, H. Energy metabolism manipulates the fate and function of tumour myeloid-derived suppressor cells. *Br. J. Cancer* **2020**, *122*, 23–29. [CrossRef]

40. Montes, C.L.; Chapoval, A.; Nelson, J.A.; Orhue, V.; Zhang, X.; Schulze, D.H.; Strome, S.E.; Gastman, B.R. Tumor-induced senescent T cells with suppressor function: A potential form of tumor immune evasion. *Cancer Res.* **2008**, *68*, 870–879. [CrossRef]
41. Ye, J.; Ma, C.; Hsueh, E.C.; Dou, J.; Mo, W.; Liu, S.; Han, B.; Huang, Y.; Zhang, Y.; Varvares, M.; et al. TLR 8 signaling enhances tumor immunity by preventing tumor-induced T-cell senescence. *EMBO Mol. Med.* **2014**, *6*, 1294–1311. [CrossRef] [PubMed]
42. Li, L.; Liu, X.; Sanders, K.L.; Edwards, J.L.; Ye, J.; Si, F.; Gao, A.; Huang, L.; Hsueh, E.C.; Ford, D.A.; et al. TLR8-Mediated Metabolic Control of Human Treg Function: A Mechanistic Target for Cancer Immunotherapy. *Cell Metab.* **2019**, *29*, 103–123.e5. [CrossRef] [PubMed]
43. Buck, M.D.; O'Sullivan, D.; Pearce, E.L. T cell metabolism drives immunity. *J. Exp. Med.* **2015**, *212*, 1345–1360. [CrossRef] [PubMed]
44. O'Neill, L.A.; Pearce, E.J. Immunometabolism governs dendritic cell and macrophage function. *J. Exp. Med.* **2015**, *213*, 15–23. [CrossRef] [PubMed]
45. Jiang, B. Aerobic glycolysis and high level of lactate in cancer metabolism and microenvironment. *Gene Funct. Dis.* **2017**, *4*, 25–27. [CrossRef]
46. Sukumar, M.; Liu, J.; Ji, Y.; Subramanian, M.; Crompton, J.G.; Yu, Z.; Roychoudhuri, R.; Palmer, D.C.; Muranski, P.; Karoly, E.D.; et al. Inhibiting glycolytic metabolism enhances CD8+ T cell memory and antitumor function. *J. Clin. Investig.* **2013**, *123*, 4479–4488. [CrossRef]
47. Wang, R.; Dillon, C.P.; Shi, L.Z.; Milasta, S.; Carter, R.; Finkelstein, D.; McCormick, L.L.; Fitzgerald, P.; Chi, H.; Munger, J.; et al. The Transcription Factor Myc Controls Metabolic Reprogramming upon T Lymphocyte Activation. *Immunity* **2011**, *35*, 871–882. [CrossRef]
48. Angelin, A.; Gil-de-Gómez, L.; Dahiya, S.; Jiao, J.; Guo, L.; Levine, M.H.; Wang, Z.; Quinn, W.J., III; Kopinski, P.K.; Wang, L.; et al. Foxp3 Reprograms T Cell Metabolism to Function in Low-Glucose, High-Lactate Environments. *Cell Metab.* **2017**, *25*, 1282–1293.e7. [CrossRef]
49. Srivastava, M.K.; Sinha, P.; Clements, V.K.; Rodriguez, P.; Ostrand-Rosenberg, S. Myeloid-derived suppressor cells inhibit T-cell activation by depleting cystine and cysteine. *Cancer Res.* **2010**, *70*, 68–77. [CrossRef]
50. Wu, K.; Lin, K.; Li, X.; Yuan, X.; Xu, P.; Ni, P.; Xu, D. Redefining Tumor-Associated Macrophage Subpopulations and Functions in the Tumor Microenvironment. *Front. Immunol.* **2020**, *11*, 1731. [CrossRef]
51. Clayton, A.; Al-Taei, S.; Webber, J.P.; Mason, M.D.; Tabi, Z. Cancer Exosomes Express CD39 and CD73, Which Suppress T Cells through Adenosine Production. *J. Immunol.* **2011**, *187*, 676–683. [CrossRef]
52. Parish, S.T.; Kim, S.; Sekhon, R.K.; Wu, J.E.; Kawakatsu, Y.; Effros, R.B. Adenosine Deaminase Modulation of Telomerase Activity and Replicative Senescence in Human CD8 T Lymphocytes. *J. Immunol.* **2010**, *184*, 2847–2854. [CrossRef]
53. Lee, J.-H.; Choi, S.-Y.; Jung, N.-C.; Song, J.-Y.; Seo, H.G.; Lee, H.S.; Lim, D.-S. The Effect of the Tumor Microenvironment and Tumor-Derived Metabolites on Dendritic Cell Function. *J. Cancer* **2020**, *11*, 769–775. [CrossRef]
54. Vang, T.; Torgersen, K.M.; Sundvold, V.; Saxena, M.; Levy, F.O.; Skålhegg, B.S.; Hansson, V.; Mustelin, T.; Taskén, K. Activation of the COOH-terminal Src Kinase (Csk) by cAMP-dependent Protein Kinase Inhibits Signaling through the T Cell Receptor. *J. Exp. Med.* **2001**, *193*, 497–508. [CrossRef]
55. Bopp, T.; Becker, C.; Klein, M.; Klein-Hessling, S.; Palmetshofer, A.; Serfling, E.; Heib, V.; Becker, M.; Kubach, J.; Schmitt, S.; et al. Cyclic adenosine monophosphate is a key component of regulatory T cell–mediated suppression. *J. Exp. Med.* **2007**, *204*, 1303–1310. [CrossRef]
56. Ustun, C.; Miller, J.S.; Munn, D.H.; Weisdorf, D.J.; Blazar, B.R. Regulatory T cells in acute myelogenous leukemia: Is it time for immunomodulation? *Blood* **2011**, *118*, 5084–5095. [CrossRef]
57. Campisi, J.; d'Adda di Fagagna, D. Cellular senescence: When bad things happen to good cells. *Nat. Rev. Mol. Cell Biol.* **2007**, *8*, 729–740. [CrossRef]
58. Faheem, M.M.; Seligson, N.D.; Ahmad, S.M.; Rasool, R.U.; Gandhi, S.G.; Bhagat, M.; Goswami, A. Convergence of therapy-induced senescence (TIS) and EMT in multistep carcinogenesis: Current opinions and emerging perspectives. *Cell Death Discov.* **2020**, *6*, 1–12. [CrossRef]
59. Sehl, M.E.; Carroll, J.E.; Horvath, S.; Bower, J.E. The acute effects of adjuvant radiation and chemotherapy on peripheral blood epigenetic age in early stage breast cancer patients. *NPJ Breast Cancer* **2020**, *6*, 23. [CrossRef]
60. Lee, J.-J.; Nam, C.-E.; Cho, S.-H.; Park, K.-S.; Chung, I.-J.; Kim, H.-J. Telomere length shortening in non-Hodgkin's lymphoma patients undergoing chemotherapy. *Ann. Hematol.* **2003**, *82*, 492–495. [CrossRef]

61. d'Adda di Fagagna, F.; Reaper, P.M.; Clay-Farrace, L.; Fiegler, H.; Carr, P.; Von Zglinicki, T.; Saretzki, G.; Carter, N.P.; Jackson, S.P. A DNA damage checkpoint response in telomere-initiated senescence. *Nature* **2003**, *426*, 194–198. [CrossRef] [PubMed]
62. Chou, J.P.; Effros, R.B. T Cell Replicative Senescence in Human Aging. *Curr. Pharm. Des.* **2013**, *19*, 1680–1698. [CrossRef]
63. Briceno, O.; Lissina, A.; Wanke, K.; Afonso, G.; Von Braun, A.; Ragon, K.; Miquel, T.; Gostick, E.; Papagno, L.; Stiasny, K.; et al. Reduced naïve CD8+ T-cell priming efficacy in elderly adults. *Aging Cell* **2016**, *15*, 14–21. [CrossRef] [PubMed]
64. Jiang, J.; Fisher, E.M.; Murasko, D.M. CD8 T cell responses to influenza virus infection in aged mice. *Ageing Res. Rev.* **2011**, *10*, 422–427. [CrossRef]
65. Brenchley, J.M.; Karandikar, N.J.; Betts, M.R.; Ambrozak, D.R.; Hill, B.J.; Crotty, L.E.; Casazza, J.P.; Kuruppu, J.; Migueles, S.A.; Connors, M.; et al. Expression of CD57 defines replicative senescence and antigen-induced apoptotic death of CD8+ T cells. *Blood* **2003**, *101*, 2711–2720. [CrossRef]
66. Wang, Z.; Aguilar, E.G.; Luna, J.I.; Dunai, C.; Khuat, L.T.; Le, C.T.; Mirsoian, A.; Minnar, C.M.; Stoffel, K.M.; Sturgill, I.R.; et al. Paradoxical effects of obesity on T cell function during tumor progression and PD-1 checkpoint blockade. *Nat. Med.* **2019**, *25*, 141–151. [CrossRef] [PubMed]
67. Valenzuela, H. Divergent Telomerase and CD28 Expression Patterns in Human CD4 and CD8 T Cells Following Repeated Encounters with the Same Antigenic Stimulus. *Clin. Immunol.* **2002**, *105*, 117–125. [CrossRef]
68. Renkema, K.R.; Li, G.; Wu, A.; Smithey, M.J.; Nikolich-Zugich, J. Two Separate Defects Affecting True Naive or Virtual Memory T Cell Precursors Combine To Reduce Naive T Cell Responses with Aging. *J. Immunol.* **2014**, *192*, 151–159. [CrossRef] [PubMed]
69. Decman, V.; Laidlaw, B.J.; DiMenna, L.J.; Abdulla, S.; Mozdzanowska, K.; Erikson, J.; Ertl, H.C.J.; Wherry, E.J. Cell-Intrinsic Defects in the Proliferative Response of Antiviral Memory CD8 T Cells in Aged Mice upon Secondary Infection. *J. Immunol.* **2010**, *184*, 5151–5159. [CrossRef]
70. Quinn, K.M.; Fox, A.; Harland, K.L.; Russ, B.E.; Li, J.; Nguyen, T.H.O.; Loh, L.; Olshanksy, M.; Naeem, H.; Tsyganov, K.; et al. Age-Related Decline in Primary CD8+ T Cell Responses Is Associated with the Development of Senescence in Virtual Memory CD8+ T Cells. *Cell Rep.* **2018**, *23*, 3512–3524. [CrossRef]
71. Kugel, C.H., III; Douglass, S.M.; Webster, M.R.; Kaur, A.; Liu, Q.; Yin, X.; Weiss, S.A.; Darvishian, F.; Al-Rohil, R.N.; Ndoye, A.; et al. Age Correlates with Response to Anti-PD1, Reflecting Age-Related Differences in Intratumoral Effector and Regulatory T-Cell Populations. *Clin. Cancer Res.* **2018**, *24*, 5347–5356. [CrossRef]
72. Hodi, F.S.; O'Day, S.J.; McDermott, D.F.; Weber, R.W.; Sosman, J.A.; Haanen, J.B.; Gonzalez, R.; Robert, C.; Schadendorf, D.; Hassel, J.C.; et al. Improved Survival with Ipilimumab in Patients with Metastatic Melanoma. *N. Engl. J. Med.* **2010**, *363*, 711–723. [CrossRef]
73. Chiarion-Sileni, V.; Pigozzo, J.; Ascierto, P.; Grimaldi, A.M.; Maio, M.; Di Guardo, L.; Marchetti, P.; de Rosa, F.; Nuzzo, C.; Testori, A.; et al. Efficacy and safety of ipilimumab in elderly patients with pretreated advanced melanoma treated at Italian centres through the expanded access programme. *J. Exp. Clin. Cancer Res.* **2014**, *33*, 30. [CrossRef]
74. Motzer, R.J.; Escudier, B.; George, S.; Hammers, H.J.; Srinivas, S.; Tykodi, S.S.; Sosman, J.A.; Plimack, E.R.; Procopio, G.; McDermott, D.F.; et al. Nivolumab versus everolimus in patients with advanced renal cell carcinoma: Updated results with long-term follow-up of the randomized, open-label, phase 3 CheckMate 025 trial. *Cancer* **2020**, *126*, 4156–4167. [CrossRef]
75. Daste, A.; Domblides, C.; Gross-Goupil, M.; Chakiba, C.; Quivy, A.; Cochin, V.; De Mones, E.; Larmonier, N.; Soubeyran, P.; Ravaud, A. Immune checkpoint inhibitors and elderly people: A review. *Eur. J. Cancer* **2017**, *82*, 155–166. [CrossRef]
76. McGranahan, N.; Furness, A.J.S.; Rosenthal, R.; Ramskov, S.; Lyngaa, R.; Saini, S.K.; Jamal-Hanjani, M.; Wilson, G.A.; Birkbak, N.J.; Hiley, C.; et al. Clonal neoantigens elicit T cell immunoreactivity and sensitivity to immune checkpoint blockade. *Science* **2016**, *351*, 1463–1469. [CrossRef]
77. Hugo, W.; Zaretsky, J.M.; Sun, L.; Song, C.; Moreno, B.H.; Hu-Lieskovan, S.; Berent-Maoz, B.; Pang, J.; Chmielowski, B.; Cherry, G.; et al. Genomic and Transcriptomic Features of Response to Anti-PD-1 Therapy in Metastatic Melanoma. *Cell* **2016**, *165*, 35–44. [CrossRef]

78. Castro, A.; Pyke, R.M.; Zhang, X.; Thompson, W.K.; Day, C.-P.; Alexandrov, L.B.; Zanetti, M.; Carter, H. Strength of immune selection in tumors varies with sex and age. *Nat. Commun.* **2020**, *11*, 1–9. [CrossRef]
79. Moreira, A.; Gross, S.; Kirchberger, M.C.; Erdmann, M.; Schuler, G.; Heinzerling, L.; Groß, S. Senescence markers: Predictive for response to checkpoint inhibitors. *Int. J. Cancer* **2019**, *144*, 1147–1150. [CrossRef]
80. Cherkassky, L.; Morello, A.; Villena-Vargas, J.; Feng, Y.; Dimitrov, D.S.; Jones, D.R.; Sadelain, M.; Adusumilli, P.S. Human CAR T cells with cell-intrinsic PD-1 checkpoint blockade resist tumor-mediated inhibition. *J. Clin. Investig.* **2016**, *126*, 3130–3144. [CrossRef]
81. Kasakovski, D.; Xu, L.; Li, Y. T cell senescence and CAR-T cell exhaustion in hematological malignancies. *J. Hematol. Oncol.* **2018**, *11*, 91. [CrossRef]
82. Das, S.; Johnson, D.B. Immune-related adverse events and anti-tumor efficacy of immune checkpoint inhibitors. *J. Immunother. Cancer* **2019**, *7*, 306–311. [CrossRef]
83. Battram, A.M.; Bachiller, M.; Martin-Antonio, B. Senescence in the Development and Response to Cancer with Immunotherapy: A Double-Edged Sword. *Int. J. Mol. Sci.* **2020**, *21*, 4346. [CrossRef]
84. Ovadya, Y.; Krizhanovsky, V. Strategies targeting cellular senescence. *J. Clin. Investig.* **2018**, *128*, 1247–1254. [CrossRef]
85. Patnaik, A.; Haluska, P.; Tolcher, A.W.; Erlichman, C.; Papadopoulos, K.P.; Lensing, J.L.; Beeram, M.; Molina, J.R.; Rasco, D.; Arcos, R.R.; et al. A First-in-Human Phase I Study of the Oral p38 MAPK Inhibitor, Ralimetinib (LY2228820 Dimesylate), in Patients with Advanced Cancer. *Clin. Cancer Res.* **2015**, *22*, 1095–1102. [CrossRef]
86. Ebert, P.J.; Cheung, J.; Yang, Y.; McNamara, E.; Hong, R.; Moskalenko, M.; Gould, S.E.; Maecker, H.; Irving, B.A.; Kim, J.M.; et al. MAP Kinase Inhibition Promotes T Cell and Anti-tumor Activity in Combination with PD-L1 Checkpoint Blockade. *Immunity* **2016**, *44*, 609–621. [CrossRef]
87. Loi, S.; Dushyanthen, S.; Beavis, P.A.; Salgado, R.; Denkert, C.; Savas, P.; Combs, S.; Rimm, D.L.; Giltnane, J.M.; Estrada, M.V.; et al. RAS/MAPK Activation Is Associated with Reduced Tumor-Infiltrating Lymphocytes in Triple-Negative Breast Cancer: Therapeutic Cooperation Between MEK and PD-1/PD-L1 Immune Checkpoint Inhibitors. *Clin. Cancer Res.* **2015**, *22*, 1499–1509. [CrossRef]
88. Chang, J.; Wang, Y.; Shao, L.; Laberge, R.-M.; Demaria, M.; Campisi, J.; Janakiraman, K.; Sharpless, N.E.; Ding, S.; Feng, W.; et al. Clearance of senescent cells by ABT263 rejuvenates aged hematopoietic stem cells in mice. *Nat. Med.* **2016**, *22*, 78–83. [CrossRef]
89. Zhu, Y.; Tchkonia, T.; Pirtskhalava, T.; Gower, A.C.; Ding, H.; Giorgadze, N.; Palmer, A.K.; Ikeno, Y.; Hubbard, G.B.; Lenburg, M.; et al. The Achilles' heel of senescent cells: From transcriptome to senolytic drugs. *Aging Cell* **2015**, *14*, 644–658. [CrossRef]
90. Fuhrmann-Stroissnigg, H.; Ling, Y.Y.; Zhao, J.; McGowan, S.J.; Zhu, Y.; Brooks, R.W.; Grassi, D.; Gregg, S.Q.; Stripay, J.L.; Dorronsoro, A.; et al. Identification of HSP90 inhibitors as a novel class of senolytics. *Nat. Commun.* **2017**, *8*, 422. [CrossRef]
91. Deschênes-Simard, X.; Gaumont-Leclerc, M.-F.; Bourdeau, V.; Lessard, F.; Moiseeva, O.; Forest, V.; Igelmann, S.; Mallette, F.A.; Saba-El-Leil, M.K.; Meloche, S.; et al. Tumor suppressor activity of the ERK/MAPK pathway by promoting selective protein degradation. *Genes Dev.* **2013**, *27*, 900–915. [CrossRef]
92. Astle, M.V.; Hannan, K.M.; Ng, P.Y.; Lee, R.S.; George, A.J.; Hsu, A.K.; Haupt, Y.; Hannan, R.D.; Pearson, R.B. AKT induces senescence in human cells via mTORC1 and p53 in the absence of DNA damage: Implications for targeting mTOR during malignancy. *Oncogene* **2011**, *31*, 1949–1962. [CrossRef]
93. Dietsch, G.N.; Randall, T.D.; Gottardo, R.; Northfelt, D.W.; Ramanathan, R.K.; Cohen, P.A.; Manjarrez, K.L.; Newkirk, M.; Bryan, J.K.; Hershberg, R.M. Late Stage Cancer Patients Remain Highly Responsive to Immune Activation by the Selective TLR8 Agonist Motolimod (VTX-2337). *Clin. Cancer Res.* **2015**, *21*, 5445–5452. [CrossRef]
94. Chow, L.Q.M.; Morishima, C.; Eaton, K.D.; Baik, C.S.; Goulart, B.H.; Anderson, L.N.; Manjarrez, K.L.; Dietsch, G.N.; Bryan, J.K.; Hershberg, R.M.; et al. Phase Ib Trial of the Toll-like Receptor 8 Agonist, Motolimod (VTX-2337), Combined with Cetuximab in Patients with Recurrent or Metastatic SCCHN. *Clin. Cancer Res.* **2017**, *23*, 2442–2450. [CrossRef]

3.2. *PUBLICATION 2:* Unleashing T cell anti-tumor immunity: new potential for 5-Nonloxytryptamine as an agent mediating MHC-I upregulation in tumors.

Molecular Cancer

RESEARCH

Open Access

Unleashing T cell anti-tumor immunity: new potential for 5-Nonloxytryptamine as an agent mediating MHC-I upregulation in tumors

Paweł Stachura[1,2†], Wei Liu[1†], Haifeng C. Xu[1], Agnès Wlodarczyk[2], Olivia Stencel[2], Piyush Pandey[1], Melina Vogt[2], Sanil Bhatia[2], Daniel Picard[2,3,4,5], Marc Remke[2,3,4,5], Karl S. Lang[6], Dieter Häussinger[7], Bernhard Homey[8], Philipp A. Lang[1], Arndt Borkhardt[2] and Aleksandra A. Pandyra[2,9,10*]

Abstract

Background New therapies are urgently needed in melanoma, particularly in late-stage patients not responsive to immunotherapies and kinase inhibitors. To uncover novel potentiators of T cell anti-tumor immunity, we carried out an ex vivo pharmacological screen and identified 5-Nonyloxytryptamine (5-NL), a serotonin agonist, as increasing the ability of T cells to target tumor cells.

Methods The pharmacological screen utilized lymphocytic choriomeningitis virus (LCMV)-primed splenic T cells and melanoma B16.F10 cells expressing the LCMV gp33 CTL epitope. In vivo tumor growth in C57BL/6 J and NSG mice, in vivo antibody depletion, flow cytometry, immunoblot, CRISPR/Cas9 knockout, histological and RNA-Seq analyses were used to decipher 5-NL's immunomodulatory effects in vitro and in vivo.

Results 5-NL delayed tumor growth in vivo and the phenotype was dependent on the hosts' immune system, specifically $CD8^+$ T cells. 5-NL's pro-immune effects were not directly consequential to T cells. Rather, 5-NL upregulated antigen presenting machinery in melanoma and other tumor cells in vitro and in vivo without increasing PD-L1 expression. Mechanistic studies indicated that 5-NL's induced MHC-I expression was inhibited by pharmacologically preventing cAMP Response Element-Binding Protein (CREB) phosphorylation. Importantly, 5-NL combined with anti-PD1 therapy showed significant improvement when compared to single anti-PD-1 treatment.

Conclusions This study demonstrates novel therapeutic opportunities for augmenting immune responses in poorly immunogenic tumors.

Keywords $CD8^+$ T cells, Immunotherapy, Antigen-presenting machinery, 5-Nonyloxytryptamine (5-NL), Cold tumors, cAMP response element-binding protein (CREB)

†Paweł Stachura and Wei Liu contributed equally to this work.

*Correspondence:
Aleksandra A. Pandyra
aleksandra.pandyra@uni-duesseldorf.de
Full list of author information is available at the end of the article

Introduction

The incidence of melanoma and mortality is on the rise and despite therapeutic advances, the 3-year survival low [1, 2]. Since the advent of immunotherapies such as ipilimumab [3], nivolumab and pembrolizumab [4, 5], the overall survival in patients with advanced melanoma has improved. Combining immunotherapeutic agents with each other when functionally non-redundant or tyrosine kinase targeting agents is a promising approach to overcome resistance associated with the application of single therapies [6]. However, due to toxicities as well as high costs [7, 8], it remains to be determined whether it's a feasible long-term strategy especially for patients receiving treatment in poorly funded health care settings. Taken together, there is a need to explore novel and more cost-effective treatment options that can enhance the activity of current immunotherapies.

Well characterized mediators of immune-directed tumor cell killing are cytotoxic T lymphocytes (CTLs). CTLs activation occurs through interaction of the T cell receptor-cluster of differentiation 3 (TCR-CD3) complex [9] present on the surface of T cells with peptides loaded onto the major histocompatibility complex class I (MHC-I) on antigen presenting cells (APCs) [10]. Effector CTLs can exert antigen-driven anti-tumor responses through granule exocytosis mediated by perforin and the granule-associated enzymes (granzymes), through Fas ligand (FasL) induced apoptosis, or indirectly through secreted cytokines such as interferon γ (IFNγ) [11, 12].

Therapeutic efforts to boost anti-tumor $CD8^+$ T cell immunity have focused on manipulating several aspects of CTL function including re-activation of exhausted CTLs (anti-PD1, LAG3 and TIM3 monoclonal antibodies) [6], expansion of highly reactive tumor infiltrating T cells (Adoptive Cell Transfer Immunotherapy) [13], boosting tumor antigen specific T cell responses (cancer vaccines employing neoantigens and tumor associated antigens) [14] and boosting CTL priming (CD27 agonists) [15]. Taken together, improving CTL function is a promising therapeutic approach with already apparent significant clinical benefits to late stage melanoma patients. Some major obstacles driving immune evasion and hampering immunotherapy responses include a poorly infiltrated 'cold' tumor microenvironment (TME), a heterogenous immunosuppressive TME, low mutational burden and silencing of MHC-I or other parts of the antigen-presenting machinery [16].

The lymphocytic choriomeningitis virus (LCMV) is a prototypic arenavirus that has been used for decades to study $CD8^+$ effector T cell responses. LCMV's experimental use has led to important discoveries such as programmed cell death protein 1 (PD1) and its role in T cell exhaustion [17]. Expression of LCMV-specific epitopes on tumor cells facilitates the study of various aspects of $CD8^+$ T cell mediated anti-tumor immunity [18, 19]. In our current study,we used B16.F10 cells expressing the H-2Db-restricted GP33 peptide (B16.GP33) CTL epitope [18] to uncover novel agents capable of augmenting T cell responses against tumor cells.

Results

Pharmacological screening identifies 5-Nonyloxytryptamine (5-NL) as potentiating anti-tumor immunity in vitro and in vivo

To identify novel drugs capable of modulating T cell anti-tumor immunity, we used the NIH Clinical Collection (NCC) composed of pharmacologically active small molecules. Splenic T cells were harvested from mice 14 days post infection with LCMV-Armstrong, a strain that causes robust effector $CD8^+$ T cells responses and is rapidly cleared in wild-type mice following infection (Fig. 1A) [20–22]. Specific anti-B16.GP33 activity of pan purified T cells and $CD8^+$ purified T cells was confirmed compared to B16.F10 parental controls (B16) by

(See figure on next page.)

Fig. 1 A pharmacological screen identifies the serotonin agonist 5-Nonyloxytryptamine (5-NL) as potentiating T cell mediated anti-tumor immunity. **A** Screen schematic is shown. **B**-**F** Mice were infected with 2×10^5 pfu of LCMV-Armstrong. 14 days post infection, splenic pan-T cells were purified. **B** Splenic T cells were analyzed using FACS to obtain the ratio of $CD8^+$, $CD4^+$ and $CD4^+CD25^+FoxP3^+$ T cells shown as percent composition ($n=3$). **C** $CD8^+$ T cells were evaluated for various surface markers using flow cytometry ($n=3$). **D** Co-cultured LCMV-primed splenic pan-T cells and B16.GP33 cells were treated with 770 pharmacological compounds at a concentration of 1 μM. T cells were removed from co-culture at 16 h. Tumor-cell viability was assessed using the MTT assay 48 h post-treatment. Viability for each compound was expressed as a fraction relative to control (B16.GP33 cells + T cells). Potential hit compounds below the cut-off of 0.7 are shown in red. (E, Left Panel) B16.GP33 and B16 cells were co-incubated with LCMV-primed splenic pan-T cells with and without 5-NL (1 μM) as described in D and tumor cell viability was assessed using the MTT assay ($n=3$–5). (E, Right Panel) B16.GP33 cells were co-incubated with LCMV-primed splenic pan-T cells with and without T-cells for 72 h and the IC50 was determined using the MTT assay ($n=4$). **F** B16.GP33 and B16 murine melanoma cells were co-incubated with LCMV-primed splenic pan-T cells and 5-NL for 16 h. Intracellular staining of $CD8^+$ T cells for TNFα, Granzyme B (GZMB) and IL-2 was measured using flow cytometry and normalized to its own respective cell line controls ($n=6$). **G** C57BL/6 J or (**H**) NSG mice were subcutaneously injected with 5×10^5 B16.GP33 cells. 7 days post-tumor injection, mice were randomized and into two groups and treated daily with 6.25 mg/kg of 5-NL or vehicle for five consecutive days and tumor volume was measured ($n=5$–12). Error bars indicate SEM; *$P<0.05$ as determined by a Student´s t-test (unpaired, 2 tailed), one or two-way ANOVA with a Dunnett's post-hoc test

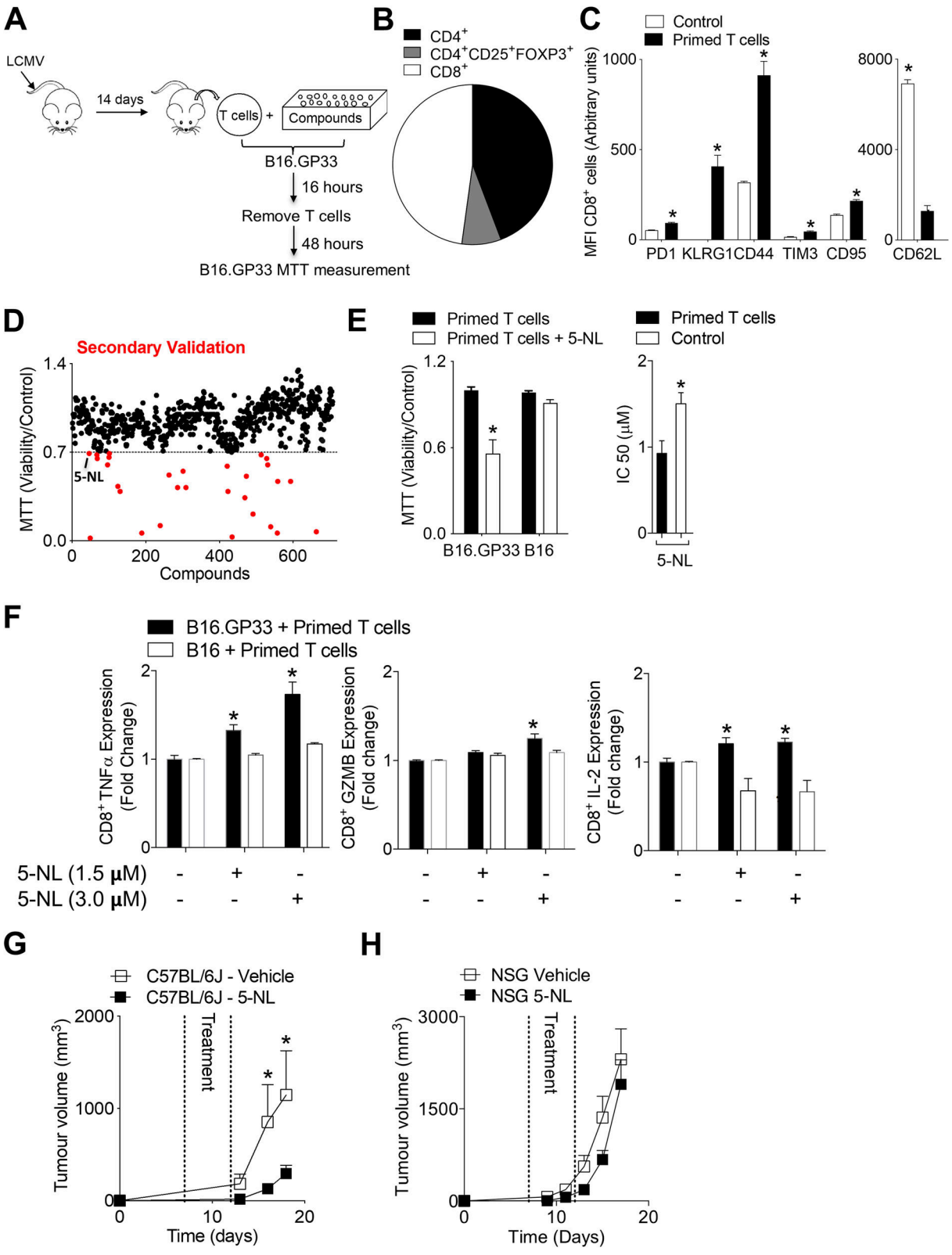

Fig. 1 (See legend on previous page.)

assessment of granzyme B (GZMB) and IL-2 production (Supplementary Fig. 1A). Since purified $CD8^+$ T cells have an increased intrinsic response towards tumor cells expressing gp33 when compared to pan-T cells, the challenge to stimulate pan-T cells against tumor cells is greater in this setting and likely better recapitulates the complexity of the TME. Splenic pan-T cells from LCMV infected mice are composed of several T cell subsets including regulatory and naïve $CD4^+$ T cells as well as $CD8^+$ T cells (Fig. 1B). As expected, splenic $CD8^+$ T cells were CD62L low compared to T cells from naïve mice and expressed killer cell lectin-like receptor subfamily G, member 1 (KLRG1) (Fig. 1C). Although residual levels of PD-1 and Tim-3 expression was detected in LCMV-primed T cells compared to naïve T cells, the low CD95 expression indicates that these T cells are mainly effector/effector memory T cells (Fig. 1C) [23]. To elicit anti-tumor activity, T cells were incubated with B16.GP33 cells (Fig. 1A). To uncover compounds capable of potentiating T cell activity, we titrated the T cell: target cell ratio to a T-cell sublethal anti-tumoral effect as assessed by the MTT assay (Supplementary Fig. 1B). Compounds were screened at a dose of 1 μM and those below a viability cut-off of 0.7 (70 percent viability relative to control cells + T cells) were considered potential hits (Fig. 1D and Supplementary Table 1). We reasoned that compounds affecting T cell immunity would result in decreased cancer cell viability in this setting and accordingly be identified as hits. As previously described, many compounds (mostly anti-chemotherapeutics or anti-metabolites) exhibited cytotoxic/anti-proliferative effects (IC50 < 250 nM, Supplementary Table 1) and these cytotoxic compounds were identified by comparing our results to a previous screen that used the same library to determine IC50 values in B16 melanoma cells [24]. Some potential hits (etoposide and docetaxel) are already known to modulate the immune system and T cells [25, 26]. A serotonin receptor (HTR) agonist 5-Nonyloxytryptamine (5-NL) was also a potential hit. Since another serotonin agonist, Tegaserod, modulated the tumor microenvironment (TME) by decreasing the infiltration of regulatory T cells (Tregs) [24], we opted to further validate 5-NL. Using the same ex vivo co-culture system as in the screen, 5-NL treatment resulted in significant decreased cancer cell viability of B16.GP33 but not B16 cells (Fig. 1E). Furthermore, addition of LCMV-primed effector T cells to a range of 5-NL doses resulted in a significantly lower half maximal inhibitory concentrations (IC50) values against B16.GP33 cells (Fig. 1E). When LCMV-primed T cells and tumor cells were co-incubated, 5-NL increased the expression of TNF alpha (TNFα), GZMB and IL-2 in $CD8^+$ T cells incubated with B16.GP33 but not B16 cells (Fig. 1F).

Next, we wondered whether 5-NL had anti-tumoral effects in vivo. Using a syngeneic immune-competent model, B16.GP33 cells were subcutaneously inoculated into C57BL/6 J mice. Treatment with 5-NL, commencing when tumors became palpable, delayed tumor growth (Fig. 1G). We wanted to separate any potential 5-NL induced immune anti-tumoral effects from direct effects on tumor cells especially as 5-NL induced apoptosis in vitro at 72 h post 5-NL treatment (Supplementary Fig. 1C and D). We therefore subcutaneously inoculated the immunocompromised NSG mice with B16.GP33 cells and treated the mice with 5-NL. Treatment with 5-NL did not significantly alter tumor growth indicating that the immune system was crucial in mediating 5-NL's anti-cancer effects in vivo (Fig. 1H). We next assessed tumors harvested from C57BL/6 J inoculated mice for markers of apoptosis using immunohistochemistry and images were scored using the IHC profiler [27]. At the early stage of tumor growth (day 13 post tumor inoculation), there were no significant differences of cleaved Caspase-3 and 8 between tumors harvested from 5-NL and vehicle treated mice (Supplementary Fig. 1E). Although active Caspase-9 was slightly increased in 5-NL tumors, differences were not apparent when assessed via immunoblot (Supplementary Fig. 1F). Taken together, we have uncovered a novel agent that has direct anti-tumor effects but is also capable of simultaneously boosting the immune system.

5-Nonyloxytryptamine (5-NL) improves T cell immunity in vivo but does not directly affect T cells

Next, we wanted to investigate how 5-NL mechanistically improved anti-tumor responses in vivo. To characterize the TME, we harvested tumors at day 13 post inoculation when there were no differences in tumor size between vehicle and 5-NL treated groups (Fig. 1G). Tumors from vehicle and 5-NL treated mice showed $CD8^+$ T cell infiltration (Fig. 2A). However, the number of $CD8^+$ T cells did not alter following 5-NL treatment (Fig. 2B). Tumoral infiltration of other immune subsets including $CD4^+$ T cells, monocytes ($CD11b^+Ly6C^{high}Ly6G^-$), granulocytes ($CD11b^+Ly6G^{high}Ly6C^{low}$), tumor-associated macrophages (TAMs, $CD11b^+F4/80^{high}Ly6C^{low}Ly6G^-$), dendritic cells (DCs, $CD11c^+$MHC-II^+) and regulatory T cells (Treg, $CD4^+CD25^+FOXP3^+$) was also not changed by 5-NL treatment (Fig. 2B and Supplementary Fig. 2A and B). Although the infiltration of Treg's was not different, the expression of the transcription factor GATA3 was lower in Treg's harvested from tumors of 5-NL treated mice (Supplementary Fig. 2C).

Next, we tested the functional significance of the $CD8^+$ T cell infiltrating subset in the context of 5-NL's anti-tumoral activity. Upon depletion of $CD8^+$ T cells

(Supplementary Fig. 3A) tumor growth was increased relative to undepleted controls (Fig. 2C). This highlights the importance of $CD8^+$ T cells in the tumor model (Fig. 2C). Notably, 5-NL's tumor-suppressive phenotype was abrogated in the absence of $CD8^+$ T cells indicating a dependency on $CD8^+$ T cells for 5-NL-mediated anti-tumoral effects (Fig. 2C). Gp33 antigen specific $CD8^+$ T cells were present in the tumor although there were no significant differences in tetramer-positive cell numbers between the 5-NL and vehicle treated groups (Fig. 2D). Another LCMV antigen, the H2-Db restricted np396 was used as a negative control (Fig. 2D). There was a higher percentage of GZMB producing $CD8^+$ T cells and higher expression of KLRG1 which is upregulated in highly cytotoxic effector $CD8^+$ T cells [28] in the tumor draining lymph node (LN) harvested from 5-NL treated mice at day 13 post tumor inoculation (Fig. 2E). When we assessed tumors and the tumor-draining lymph node from 5-NL and vehicle treated mice at day 20 post tumor inoculation, we observed higher cytotoxic $CD8^+$ T cell effector activity (higher percentage and expression of GZMB producing $CD8^+$ T cells) in the tumors of 5-NL treated mice (Fig. 2E).

Although 5-NL did not alter infiltration of various immune infiltrates including effector $CD8^+$ T cells (Fig. 2B), TCR downregulation in the TME might underestimate the infiltration of antigen specific T cells as assessed by tetramer staining. We therefore transferred purified and activated splenic $CD45.1^+$ $CD8^+$ T cells from transgenic TCR (P14) mice recognizing the LCMV gp33 peptide [29] into tumor-bearing mice followed by vehicle or 5-NL treatment (Supplementary Fig. 3B). Most of the $CD45.1^+CD8^+$ cells homed into the tumor but their numbers and percentages were not different between 5-NL and vehicle treated mice (Supplementary Fig. 3C) corroborating the earlier finding that 5-NL did not alter infiltration or expansion of effector $CD8^+$ T cells within the tumor.

Next we wondered whether 5-NL affected T cells intrinsically. 5-NL is a serotonin receptor (HTR) 1Dβ agonist (HTR1Dβ) that also has affinity for HTR1A-B, HTR2A and HTR2C [30]. There was a robust expression of HTRs in naïve T cells as well as tumor cells (Supplementary Fig. 4A and B respectively). Furthermore, members of Class 1 and 2 HTRs, including the ones targeted by 5-NL were upregulated in T cells following infection (Supplementary Fig. 4A). As serotonin signaling has been previously shown to be important for the activation of T cells [31–33], we reasoned that 5-NL might directly affect T cells through signaling of the HTRs to increase anti-tumor immunity. To test this, we treated LCMV-infected mice with 5-NL. We hypothesized that 5-NL might increase LCMV-triggered $CD8^+$ T cell effector responses. However, 5-NL did not increase the frequency of tetramer $gp33^+$ $CD8^+$ T cell frequencies in mice infected with LCMV in the blood, spleen as well as liver and there were no differences between IFNγ, GZMB and TNFα positive $CD8^+$ T cells in the blood, spleen and liver of LCMV infected mice following re-stimulation with gp33 (Fig. 2F and Supplementary Fig. 4C). Taken together, 5-NL does not improve T cell immunity in the context of acute viral infections. Therefore, its immunostimulatory effects are unlikely to occur through direct T-cell mediated effects. We confirmed this in our initial co-culture system by pre-treating the tumor cells with 5-NL, removing 5-NL, followed by incubation with LCMV-primed T cells. 5-NL pre-treatment increased the expression of Granzyme B (GZMB), TNF-α, IL-2 and surface activation marker KLRG1 in $CD8^+$ T cells co-incubated with B16.GP33 cells (Supplementary Fig. 4D).

5-Nonyloxytryptamine (5-NL) upregulates antigen presenting machinery in vitro and in vivo without upregulating PD-L1

As 5-NL did not improve T cell immunity in a tumor-free infection model, we postulated that 5-NL might affect the TME to promote anti-tumor immunity. B16

(See figure on next page.)

Fig. 2. 5-Nonyloxytryptamine (5-NL) improves T cell anti-tumor immunity in vivo. **A**-**E** C57BL/6 J mice were subcutaneously injected with 5×10^5 B16.GP33 cells. 7 days post-tumor injection, mice were randomized into two groups and treated daily with 6.25 mg/kg of 5-NL or with vehicle for five consecutive days. Mice were sacrificed on 13 days post tumor-inoculation. **A** Tumor sections were stained for $CD8^+$ T cells using immunofluorescence (a representative image of $n = 4$ is shown, scale bar indicates 50 µm). **B** Numbers of tumor infiltrating $CD8^+$ and $CD4^+$ T cells, Treg's ($CD4^+CD25^+FOXP3^+$), monocytes ($CD11b^+Ly6C^{high}Ly6G^-$), granulocytes ($CD11b^+Ly6G^{high}Ly6C^{low}$), tumor associated macrophages (TAMs, $CD11b^+F4/80^{high}Ly6C^{low}Ly6G^-$) and dendritic cells (DCs, $CD11c^+$MHC-II^+) were assessed using flow cytometry ($n = 6$–10). **C** In addition to the tumor inoculation and 5-NL treatment described in (A), C57BL/6 J mice were also treated with a $CD8^+$ T cell depleting antibody (anti-CD8) on days -2, -1 and 7 pre and post tumor cell inoculation. Tumor volume was measured ($n = 4$–8). **D**-**E** Tumor and tumor-draining lymph node infiltrating $CD8^+$ T cell markers, intracellular GZMB as well as tetramer were assessed by flow cytometry from mice sacrificed at day 13 (upper panel) or day 20 (bottom panel) post tumor inoculation ($n = 5$–11). **F** C57BL/6 J mice were infected with 2×10^5 pfu of LCMV Armstrong and treated daily with 6.25 mg/kg of 5-NL or vehicle for 5 consecutive days starting at day 1 post-infection. 10 days post-infection, cells from the blood, spleen and liver were re-stimulated with LCMV-specific gp33 epitope followed by staining for IFNγ using FACS analysis ($n = 5$). Tet-$gp33^+$ $CD8^+$ T cells in the blood, spleen and liver were measured 10 days post-infection ($n = 5$). Error bars indicate SEM; $^*P < 0.05$ as determined by a Student´s t-test (unpaired, 2 tailed), or a two-way ANOVA with a Tukey's post-hoc test

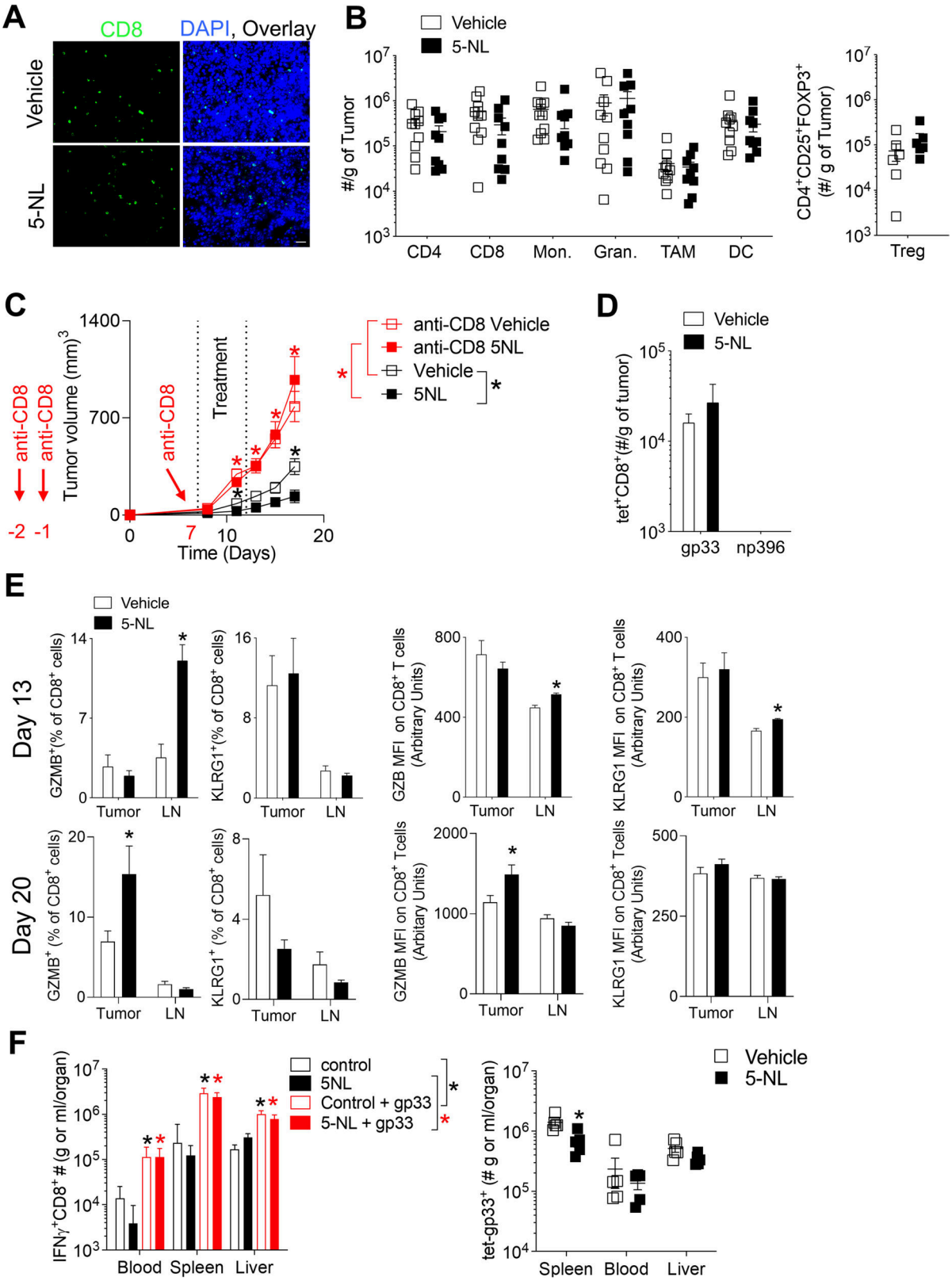

Fig. 2. (See legend on previous page.)

MHC-I expression (as assessed by measuring the H2-Db and H2-Kb isoforms comprising the MHC-I complex in C57BL/6 mice [34]) is low (though detectable as also previously reported [35]), relative to other murine and human cell lines including the immunogenic MC-38 cells (Fig. 3A). We therefore wondered whether 5-NL affected MHC-I expression in tumor cells.

When we stained for MHC-I whose relative low expression in part defines an immunologically ignorant phenotype [36, 37], we observed that tumors harvested from 5-NL treated mice had significantly higher expression of MHC-I (Fig. 3B). Next, we checked the expression of MHC-I molecules H2-Db and H2-Kb on tumor and tumor infiltrating immune cells using FACS analysis. To differentiate between tumor cells and immune infiltrating leukocytes, we used CD45.2 as a tumor infiltrating leukocyte (TIL) marker and found that both H2-Db and H2-Kb were significantly upregulated on CD45.2$^-$ cells harvested from 5-NL treated mice but not in tumor infiltrating lymphocytes (Fig. 3C-D and Supplementary Fig. 5A). As MHC-I shares some transcriptional elements with MHC-II such as the SXY regulatory module [38], we wondered whether 5-NL treatment also impacted MHC-II expression. However, MHC-II expression was not changed in immune infiltrates or CD45.2$^-$ cells in the tumors of 5-NL treated mice compared to controls (Supplementary Fig. 5B). MHC-I upregulation is often accompanied by PD-L1 upregulation [39] but 5-NL treatment did not result in concomitant increased PD-L1 expression in CD45.2$^-$ cells (Fig. 3C). Taken together, 5-NL upregulated MHC-I molecules H2-Db and H2-Kb in CD45.2$^-$ cells within the TME in vivo and we therefore hypothesized that 5-NL improved anti-tumor immunity through upregulation of H2-Db and H2-Kb in tumor cells. Indeed, 5-NL induced the expression of H2-Db and H2-Kb in B16 cells 18 h post 5-NL treatment without affecting PD-L1 (Fig. 3E and F). Expression of other members of the antigen presenting machinery including *B2M* were also increased in response to 5-NL treatment in melanoma cells (Supplementary Fig. 5C). To ensure that the upregulation of MHC-I antigen presenting machinery was not merely a consequence of apoptosis induction (evident at 72 h post 5-NL treatment, Supplementary Fig. 1 C-D), we treated melanoma cells with another serotonin agonist known to induce melanoma tumor cell apoptosis, Tegaserod (TM) [24]. Treatment with TM did not lead to upregulation of H2-Db and H2-Kb (Supplementary Fig. 5D).

Next, we wondered about the susceptibility of human cell lines to 5-NL induced MHC-I upregulation. Upon treatment with 5-NL, HLA A-C was upregulated in human melanoma RPMI-7591 (RPMI) and colon SW620 cells but not in human breast and lung adenocarcinoma cells (Fig. 3G). H2-Db and H2-Kb expression was increased in murine colon MC-38 cells and squamous oropharynx carcinoma MOPC cells (Fig. 3G). MHC-II was not upregulated in most cells following 5-NL treatment (Supplementary Fig. 5E). In the MC-38 as in B16.GP33 cells (Fig. 3B), there was also strong MHC-I upregulation in vivo (Supplementary Fig. 5F). B16 melanoma cells are poorly immunogenic and this has been attributed to relative low MHC-I expression [35]. Expression of HLA A-C also varied across the human cell lines but 5-NL was able to upregulate MHC-I/HLA A-C expression in cell lines of varying immunogenicity (Fig. 3G).

5-Nonyloxytryptamine (5-NL) and other inducers of CREB phosphorylation recapitulate MHC-I upregulation independent of IFNγ signaling

5-NL was designed to be an HTR1Dβ agonist. Although protein expression of HTR1D was confirmed in multiple cell lines (Fig. 4A), treatment with other HTR1Dβ agonists Sumatriptan and L694247 failed to recapitulate the H2-Db and H2-Kb upregulation (Fig. 4B). Consistently, dosing with the FDA approved Sumatriptan failed to delay tumor growth in vivo (Fig. 4C). Furthermore, knock-down with esiRNA's targeting HTR1D or knock-out of HTR1D using CRISPR-Cas9 did not alter 5-NL's ability to upregulate H2-Db (Supplementary Fig. 5G and H). Additionally, knock-down with an

(See figure on next page.)

Fig. 3 5-Nonyloxytryptamine (5-NL) upregulates antigen presenting machinery in human and murine tumors in vitro and in vivo. **A** Basal expression levels of H2-Db and H2-Kb in mouse cells and HLA A-C in human cells were assessed using flow cytometry ($n=5$). **B**-**D** C57BL/6 J mice were subcutaneously injected with 5×10^5 B16.GP33 cells. 7 days post-tumor injection mice were randomized into two groups and treated daily with 6.25 mg/kg of 5-NL or with vehicle for five consecutive days. Mice were sacrificed on day 13 post tumor-inoculation. **B** Tumor sections were stained for MHC-I using immunofluorescence (representative images of tumors harvested from 4 mice are shown; scale bar indicates 50 µm). **C** H2-Db/Kb and PD-L1 protein expression on CD45.2$^-$ and (**D**) H2-Db/Kb expression on tumor infiltrating CD8$^+$ and CD4$^+$ T cells, Treg's (CD4$^+$CD25$^+$FOXP3$^+$), monocytes (CD11b$^+$Ly6C^{high}Ly6G$^-$), granulocytes (CD11b$^+$Ly6G^{high}Ly6C^{low}), TAMs (CD11b$^+$F4/80^{high}Ly6C^{low}Ly6G$^-$) and DCs (CD11c$^+$MHC-II$^+$) was assessed using flow cytometry ($n=5$–16). **E** *H2DB* and *H2KB* mRNA expression in B16 cells treated with 5-NL for 18 h was assessed using RT-PCR. Expression was normalized to *β-Actin* ($n=4$). **F** H2-Db/Kb and PD-L1 protein expression was assessed by flow cytometry following treatment with 5-NL for 18 h in B16 cells (phenotype was recapitulated in B16.GP33 cells, data not shown) ($n=5$). **G** H2-Db/Kb (mouse cell lines) and HLA A-C (human cell lines) protein expression was assessed using flow cytometry following treatment with 5-NL (5 µM for RPMI-7591 and 3 µM for MC-38, SW620, A549, MDA-MB-231 and MOPC cells) for 24 h ($n=5$–9). Error bars indicate SEM; *$P<0.05$ as determined by a Student´s t-test (unpaired, 2 tailed) or a one-way ANOVA with a Tukey's post-hoc test

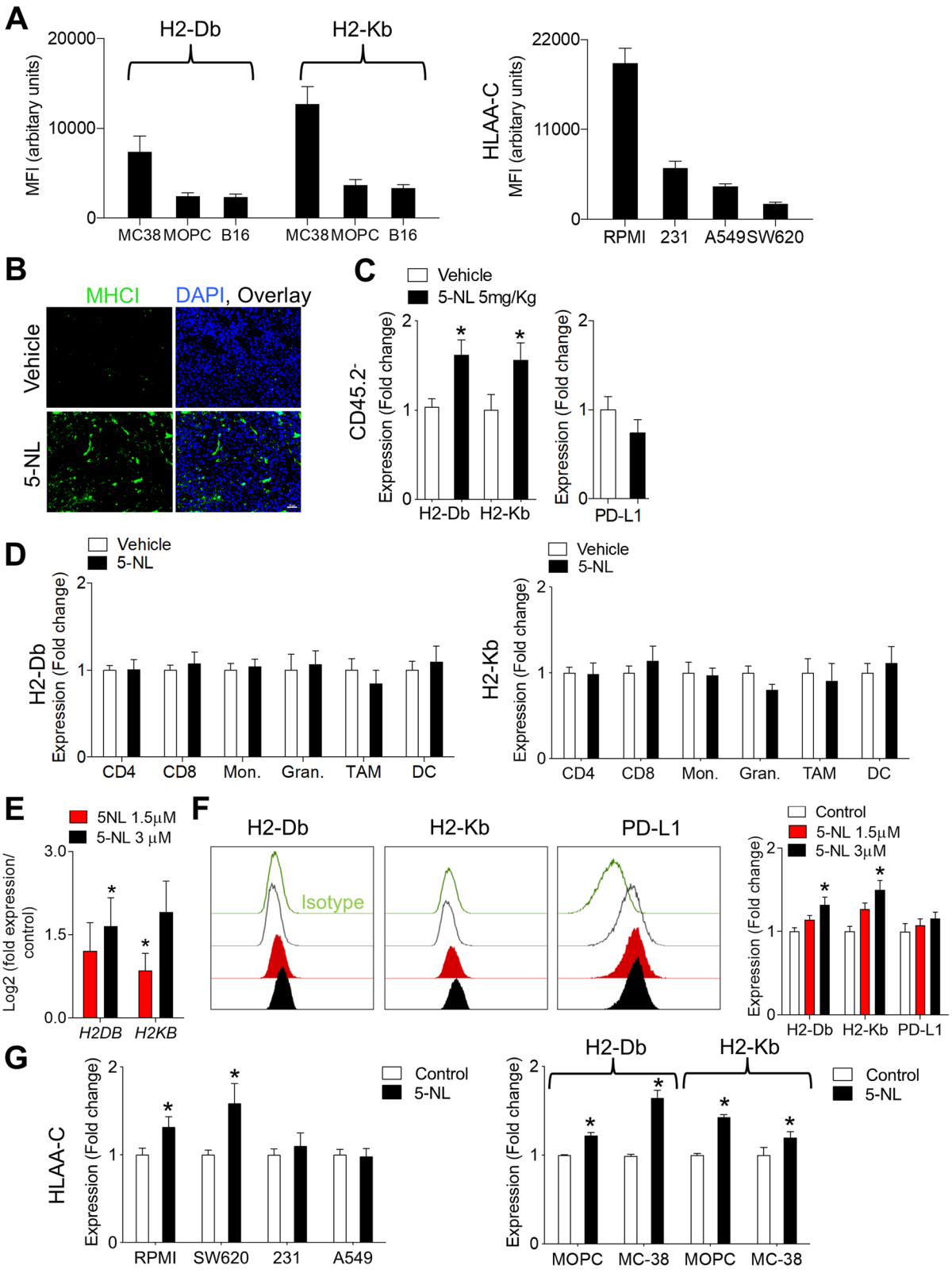

Fig. 3 (See legend on previous page.)

esiRNA targeting HTR2A, another putative 5-NL target, did not alter 5-NL's ability to upregulate H2-Db (Supplementary Fig. 5I). Treatment with serotonin did not impact H2-Db expression and co-treatment of 5-NL and the pan serotonin receptor inhibitor, Asenapine did not alter 5-NL's ability to upregulate H2-Db (Supplementary Fig. 5 J). Taken together, we surmise that 5-NL mediated improved anti-tumor immunity occurred irrespective of signaling through receptors HTR1Dβ and HTR2A. 5-NL's affinity for other receptors including HTR1A-B and HTR2C [30] broadens the range of targets since human melanoma cells do express other HTR's [24] as do murine B16 and MC-38 cells (Supplementary Fig. 4B). However, as treatment with serotonin and co-treatment of 5-NL and Asenapine did not recapitulate or block H2-Db upregulation respectively, this makes involvement of other HTRs less likely.

In order to uncover signaling pathways responsible for 5-NL's upregulation of antigen presenting machinery, we further immunoblotted transcription factors known to be involved in canonical serotonin signaling and in MHC-I gene transcription. Interferon γ (IFNγ) is a potent transcriptional inducer of MHC-I expression [40, 41]. However, there were no differences in IFNγ protein levels within the tumors of 5-NL or vehicle treated mice (Supplementary Fig. 6A) or mRNA levels of IFNγ and type I interferons (Supplementary Fig. 6B). Consistently, 5-NL treatment of B16 cells did not induce the expression of IFNγ and type I interferons (Supplementary Fig. 6C). Moreover, while exogenous treatment with IFNγ robustly increased STAT1 levels in B16 cells, treatment with 5-NL did not (Supplementary Fig. 6D). However, treatment with IFNγ upregulated MHC-I/HLAA-C in every cell line except the MOPC cells (Supplementary Fig. 6E). As expected, the upregulation was strongest in cells with low basal levels of MHC-I/HLAA-C such as B16 cells. This was accompanied by concomitant PD-L1 upregulation which again, 5-NL failed to upregulate in every cell line tested (Supplementary Fig. 6F and Supplementary Table 2). Taken together, we concluded that 5-NL-induced MHC-I upregulation independently from IFNγ.

NF-κB can regulate MHC-I genes through binding to their enhancers [41]. Phosphorylated NF-κB p100 was not detectable in B16 and MC-38 cells and treatment with 5-NL did not alter total and phosphorylated NF-κB p65 levels (Supplementary Fig. 7A and B). Mitogenic pathways potentially influenced by serotonin signaling such as MAPK were unaffected by 5-NL treatment, although a decrease in the activation of the PI3K/Akt/mTOR pathway (decreased p70 S6 phosphorylation) was observed in B16 cells (Supplementary Fig. 7C). cAMP response element binding protein (CREB) has been shown to bind to MHC-I promoters [40–42], and activation of $G\alpha_s$-coupled receptors (HTR4-7) occurs through protein kinase A (PKA) mediated phosphorylation of CREB (p-CREB) [43].

A robust increase in phosphorylation of CREB following treatment with 5-NL was observed in both B16 and MC-38 cells (Fig. 4D and Supplementary Fig. 8A and B). Notably, colorectal and melanoma cancer cells both expressed basal levels of p-CREB, which is consistent with what is reported in the literature [44]. Next, we investigated whether the changes in CREB phosphorylation were linked to the upregulation of antigen presenting machinery. Knockdown approaches of CREB are difficult in cancer cell lines as it often leads to cell death [45, 46]. Indeed, transient knockdown using esiRNA approaches in both cell lines led to an induction of apoptosis especially in B16 cells (Supplementary Fig. 8C). Using pharmacological inhibitors and activators to further dissect the mechanism of MHC-I upregulation in B16 and MC-38 cells, we observed a robust CREB

(See figure on next page.)

Fig. 4 5-Nonyloxytryptamine (5-NL) and other inducers of CREB activation upregulate antigen presenting machinery in vitro and in vivo. **A** Protein expression of HTR1D in cancer cell lines was assessed using immunoblot analysis (a representative immunoblot of $n = 3$ is shown, cropping is indicated by a black frame). Lysates harvested from the mouse brain were used as a positive control. **B** Treatment with other HTR1D agonists for 18 h (Sumatriptan and L694247, both 3 μM) did not increase H2-Db/Kb protein expression in B16 cells as assessed using FACS ($n = 3$). **C** C57BL/6 J mice were subcutaneously injected with 5×10^5 B16.GP33 cells. 7 days post-tumor injection mice were randomized into two groups and treated daily with 12.5 mg/kg of Sumatriptan or with vehicle for five consecutive days. Tumor volume was measured ($n = 6$–7). (**D**, left panel) Representative immunofluorescent images of B16 cells treated with 5-NL (3 μM) or forskolin (10 μM) for 18 h and stained for phosphorylated CREB (p-CREB Ser-133) and H2-Db are shown (representative images of $n = 3$–4 are shown; scale bar indicates 50 μm) and fluorescent signal is quantified in D, right panel. **E** The adenylyl cyclase activator forskolin (20 μM) increased H2-Db/Kb protein expression in B16 cells following 18 h of treatment ($n = 6$) as measured by FACS. **F** B16 cells were treated with 5-NL and forskolin at the indicated doses for 72 h. Apoptosis was assessed using Annexin V/7AAD staining ($n = 5$). Percent apoptosis was ascertained by summing up the Annexin $V^+/7AAD^-$ and Annexin $V^+/7AAD^+$ populations. **G** MC-38 cells were pre-treated for 30 min with the p-CREB inhibitor 3i (8 μM) followed by treatment with 3 μM of 5-NL for 24 h. Cells were analyzed using FACS for expression of H2-Db /Kb ($n = 3$–5). **H** C57BL/6 J mice were subcutaneously injected with 5×10^5 B16.GP33 or MC-38 cells. 7 days post-tumor injection mice were randomized into two groups and treated daily with 6.25 mg/kg of 5-NL or with vehicle for five consecutive days. Mice were sacrificed on 13 days post tumor-inoculation and tumor tissue was stained for p-CREB using immunofluorescence. Scale bars indicate 50 μm and 20 μm (region of interest outlined in red) (representative images of tumors harvested from 4–6 mice are shown). Fluorescent signal from p-CREB channel was quantified in the right panel. Error bars indicate SEM; $^*P < 0.05$ as determined by a Student´s t-test (unpaired, 2 tailed) or a one-way ANOVA with a with a with a Dunnett's post-hoc test

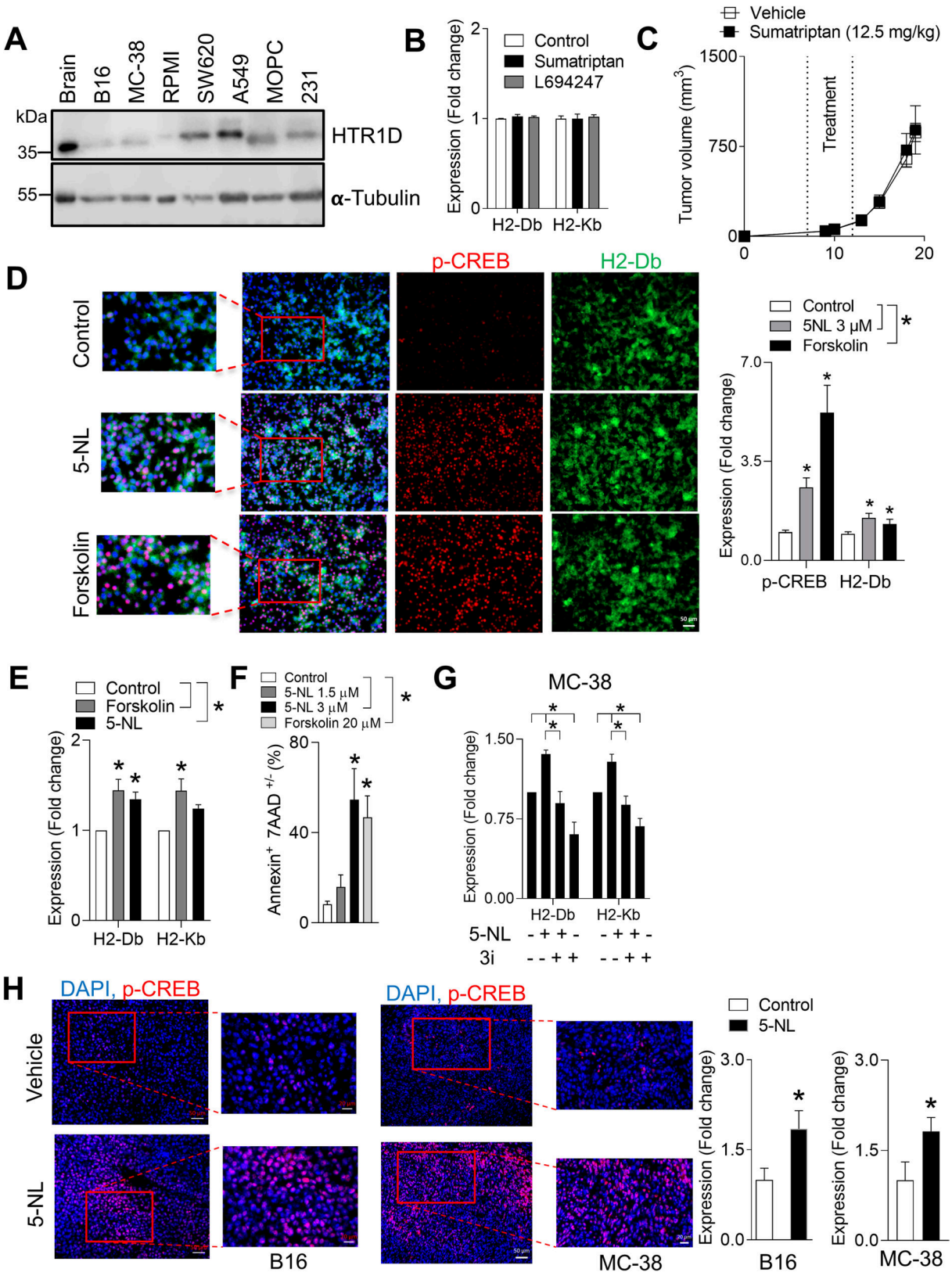

Fig. 4 (See legend on previous page.)

phosphorylation and upregulation of H2-Db and H2-Kb upon treatment with the adenylate cyclase (AC) activator forskolin which is upstream of p-CREB [43] (Fig. 4D, E and Supplementary Fig. 8A, E). Forskolin also induced apoptosis in B16 and MC-38 cells although to a lesser extent than 5-NL in MC-38 cells (Fig. 4F and Supplementary Fig. 8F). Co-treatment of forskolin with 3i, a CREB inhibitor [47], blunted the forskolin-mediated H2-Db/Kb upregulation in MC-38 cells (Supplementary Fig. 8D). Importantly, co-treatment of 5-NL and 3i abolished 5-NL mediated H2-Db and H2-Kb upregulation in MC-38 cells (Fig. 4G). The sensitivity of B16 cells to CREB inhibition resulted in significant induction of apoptosis following short-term treatment with the 3i inhibitor. This would confound any interpretation of MHC-I upregulation thereby precluding co-treatment of 5-NL and 3i (Supplementary Fig. 8G). Notably, treatment of MC-38 cells with the p-CREB 3i inhibitor alone resulted in slightly decreased H2-Db levels (Supplementary Fig. 8D,G). Consistent with the in vitro results, p-CREB was increased in tumors from 5-NL treated mice in both melanoma and colon cancer in vivo (Fig. 4H). Taken together, as shown by pharmacological manipulation, the 5-NL mediated upregulation of the antigen presenting machinery is linked to increases in CREB phosphorylation.

5-Nonyloxytryptamine (5-NL) induces differential gene expression in tumor cells and activates the AMPK pathway

To determine what other signalling pathways were perturbed by 5-NL, we performed RNA-seq analysis on B16.GP33 cells. As CREB phosphorylation occurred at or after 18 h post-treatment, the RNA-Seq was performed at 18 h to determine any potential earlier causative 5-NL-induced perturbations. There were 468 genes differentially expressed between the 5-NL and control groups (Supplementary Table 3). In addition to *B2M,* an MHC-I gene involved in antigen processing, binding and presentation *H2-T24* was highly upregulated following 5-NL treatment (Fig. 5A). *H2-T24* is an MHC-Ib gene that has been shown to be significantly expressed in adult spleen and thymus tissues of C57BL/6 mice [34]. Interestingly, High Mobility Group Box 1 pseudogene 2 (*Hmgb1-ps2)* was amongst the highly upregulated genes in 5-NL treated B16.GP33 cells. Hmgb1 and its pseudogenes are multifunctional redox sensitive proteins that play an important role in anti-tumoral immunity. Hmgb1 is a damage-associated molecular pattern (DAMP) and its release by tumor cells facilitates immunogenic cell death (ICD) [48]. GSEA on the differentially expressed genes was implemented to determine prominent pathways altered between control and 5-NL treated B16.GP33 cells (Fig. 5B and C). Notably, the AMPK pathway was activated in 5-NL treated B16.GP33 cells. We verified that AMPK was activated in both B16 and MC-38 cells following 5-NL treatment as early as 30 min post-treatment (Fig. 5D and Supplementary Fig. 9A). Taken together, using RNA-Seq analysis we have not only confirmed our previous findings involving upregulation of antigen presenting machinery but have identified that 5-NL affects AMPK activation.

5-Nonyloxytryptamine (5-NL) can be successfully combined with immunotherapy in vivo

We used two different studies to mine transcriptomic data from the Cancer Immunome Atlas (TCIA) [49]. Van Allen et al. correlated genomic and transcriptomic data with response to CTLA4 blockade [50] while Hugo et al. with response to anti-PD1 therapy [51], both using metastatic melanoma samples collected prior to immunotherapy treatment. As also reported by Van Allen et al., there was no correlation between expression of HLAA-C and clinical benefit with anti-CTLA4 therapy. Combined transcriptomic data from both studies showed that immunotherapy responders had significantly higher expression of *B2M* than immunotherapy non-responders (Fig. 6A). Furthermore, strong and significant correlations were observed between *CREB1* expression and *HLAA-C* as well as *B2M* (Fig. 6B). Although expression of *HLAA-C* as well as *B2M* did not correlate strongly with *IFNG,* there was also a strong correlation between the IFNγ responsive gene *IFIT3* suggesting that it is difficult to ascertain the specific causes of these correlations (Supplementary Fig. 9B). Accordingly, we wondered whether 5-NL would impact response to checkpoint inhibition. Not surprisingly, due to the low immunogenicity of the B16.GP33 melanoma cell line, treatment with the anti-PD1 antibody had little effect as a single agent. Although tumors grew slower in the 5-NL/Isotype group compared to Vehicle/Isotype, tumor growth in the 5-NL/anti-PD1 group was significantly delayed when compared to the Vehicle/anti-PD1 group and the Vehicle/Isotype group (Fig. 6C). Additionally, we wanted to assess whether 5-NL could be potentially used in combination therapy with the standard of care treatment for late-stage melanoma B-Raf inhibitor Vemurafenib [52]. We ascertained the combination index following treatment with 5-NL and Vemurafenib on human melanoma cell lines RPMI, A375 and the SK-MEL-24, harboring the $BRAF^{V600E}$ mutation and found a synergistic effect in A375 and SK-MEL-23 cell lines (Fig. 6D). Taken together, we therefore propose a model whereby 5-NL could increase the immunogenic profile of tumors and be combined with immunotherapies (Fig. 6E).

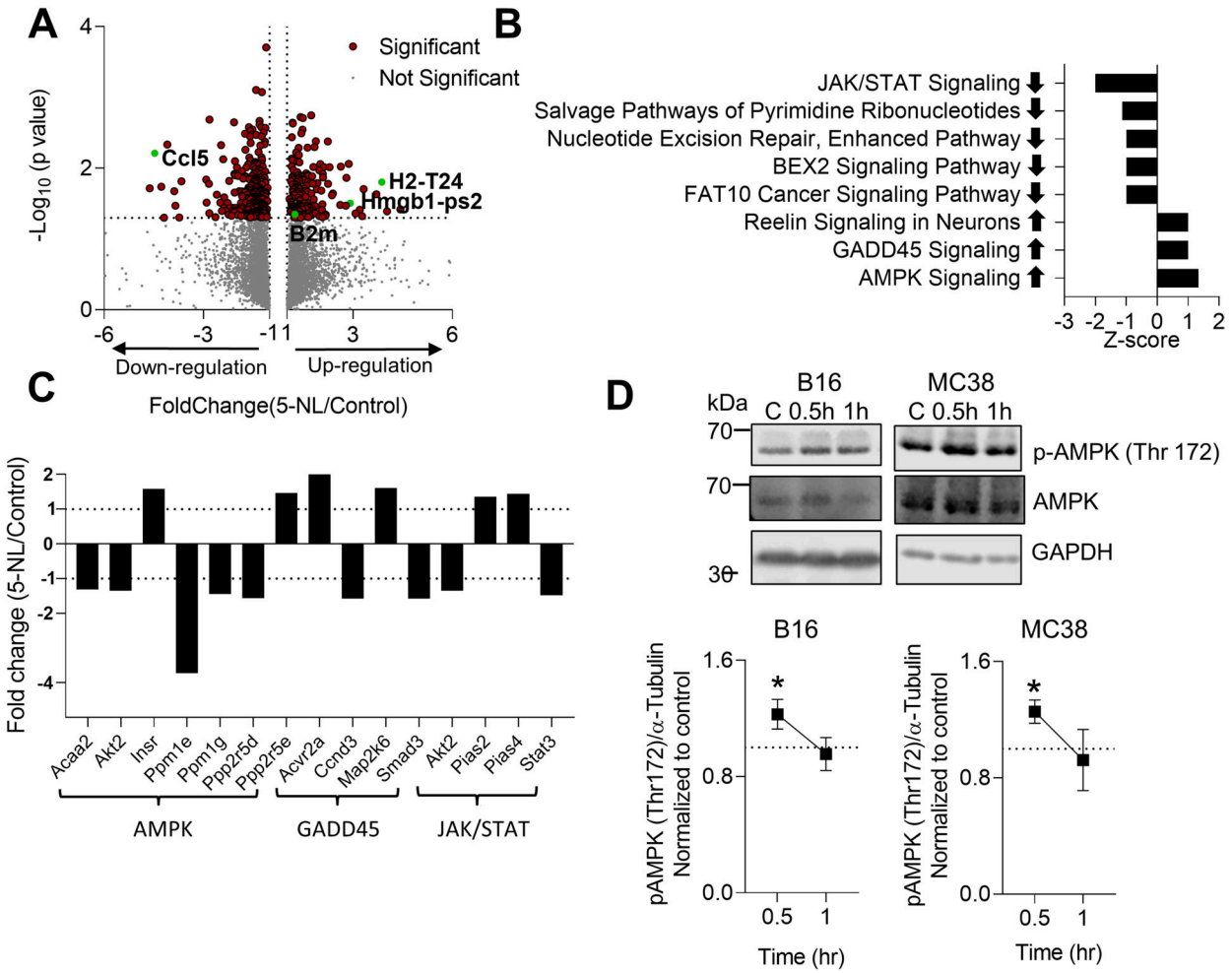

Fig. 5 5-Nonyloxytryptamine (5-NL) induces differential gene expression and activates the AMPK pathway in tumor cells. B16.GP33 cells were treated with 5-NL (3 μM) for 18 h and RNA was assessed using RNA-seq analysis. **A** A Volcano Plot of the fold change gene distribution is shown. **B**-**C** GSEA analysis of pathways altered in 5-NL treated B16.GP33 cells is shown with arrow pointing up indicating pathway activation and arrow pointing down indicating downregulation. Fold changes in individual genes in select pathways are shown in C ($n=4$). (D) Level of AMPK phosphorylation (Thr172) was assessed using immunoblot analysis in B16 and MC38 cells treated with 3 μM of 5-NL at the indicated time points quantified in the right panel (black frames indicate cropped immunoblot; $n=7$–9). Error bars indicate SEM; *$P<0.05$ as determined by a one-way ANOVA with a Dunnett's post-hoc test

(See figure on next page.)

Fig. 6 5-Nonyloxytryptamine (5-NL) can be successfully combined with immunotherapy in vivo. Transcriptomic data from melanoma samples of therapy naïve patients was mined from the Cancer Immunome Atlas. **A** Responders to checkpoint inhibitors (anti-PD1 and anti-CTL4) expressed higher mRNA levels of *B2M*. **B** Expression of *CREB1* positively correlated with *HLA A-C* and *B2M*. **C** C57BL/6 J mice were subcutaneously injected with 5×10^5 B16.GP33 cells. 7 days post-tumor injection mice were randomized and treated daily with 6.25 mg/kg of 5-NL or with vehicle for five consecutive days. Additionally, mice were intravenously injected with murine anti-PD1 antibody or isotype control on days -1, 1, 3, 5 and 7 pre and post tumor inoculation. Tumor volume was measured ($n=5$–9). Data is pooled from two independent in vivo experiments. **D** Combination index (CI) was calculated from dose response curves of human melanoma cell lines treated with 5-NL, Vemurafenib or in a combination in ratio 1:1. $CI<1$ indicates synergy, $CI=1$ indicates additivity, and $CI>1$ indicates antagonism. The EC50 (50% effective concentration) and EC75 (75% effective concentration) are shown ($n=3$). Error bars indicate SEM; *$P<0.05$ as determined by a Student´s t-test (unpaired, 2 tailed) or a two-way ANOVA with a Tukey's post-hoc test. **E** A schematic diagram summarizing 5-NL's anti-tumoral and pro-immune effects is shown. The diagram created with BioRender.com

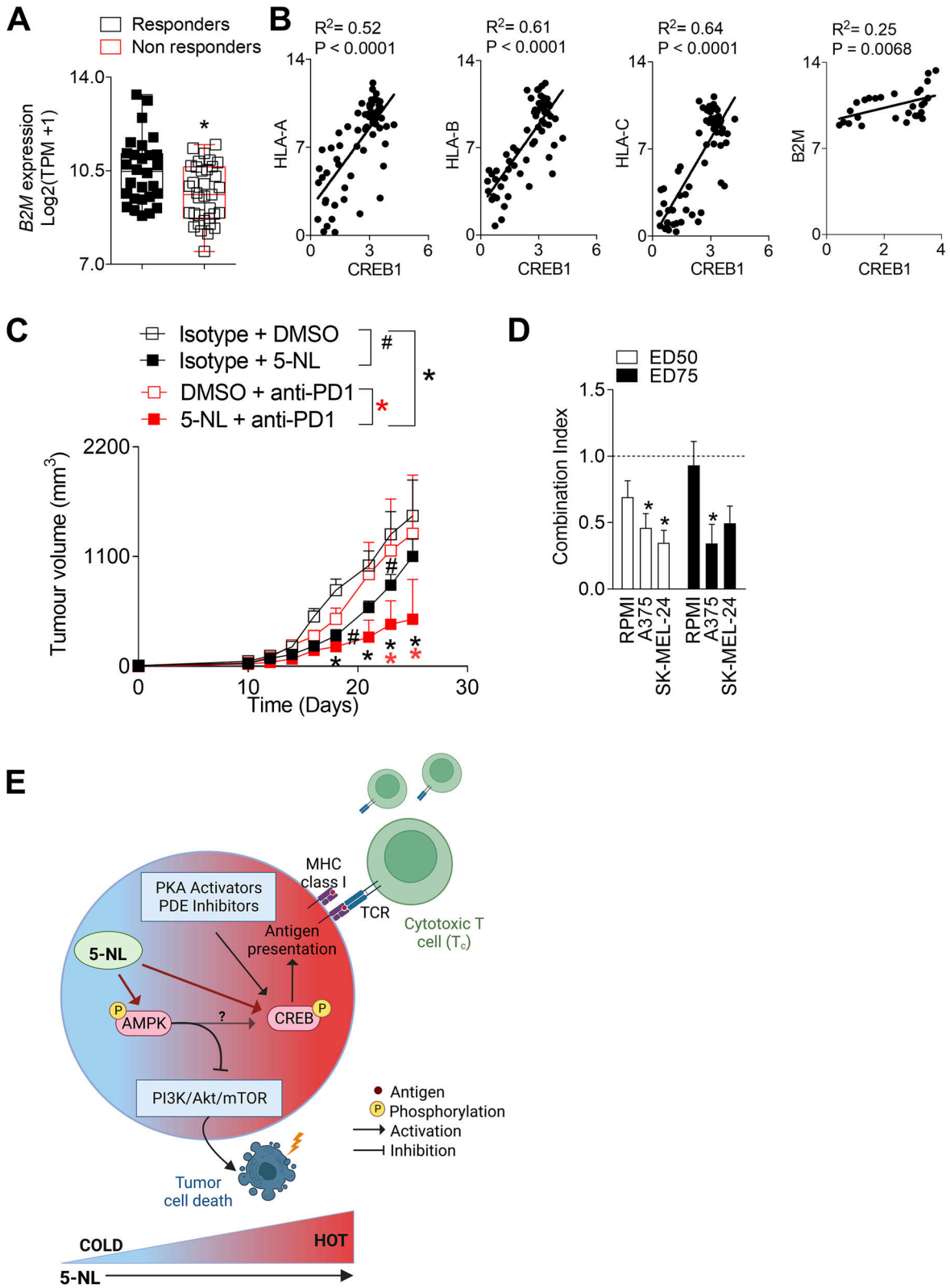

Fig. 6 (See legend on previous page.)

Discussion

5-NL increased T cell anti-tumor immunity through upregulation of the antigen presenting machinery in tumor cells while simultaneously inducing tumor cell apoptosis. 5-NL was developed as an HTR1Dβ agonist. However, 5-NL also has affinity for other HTR receptors also expressed by tumor cells in our system namely HTR1A-B, HTR2A and HTR2C [30]. HTR1A-F signaling occurs through G protein-coupled receptors (GPCRs) with inhibitory effects on adenylyl cyclase and corresponding decreased production of cAMP [43]. We observed increases in p-CREB following 5-NL treatment and other HTR1D agonists had no effects on MHC-I upregulation. This, combined with the fact that HTRID knockout and knockdown did not abrogate the phenotype, makes it is likely that 5-NL's effects are independent of HTR1 signaling. HTR2A-C signaling occurs through activation of $G\alpha_q$, PI3K/AKT, and ERK 1/2 pathways. There were no differences in ERK phosphorylation and the PI3K/AKT was blunted following 5-NL treatment. The mechanism of action could occur through canonical serotonin receptor signaling involving other HTR's [4, 6, 7] whose downstream signaling involves the cAMP/PKA/CREB pathway [53]. However, there is no reported binding activity of 5-NL to HTR4,6–7. Likely the observed effects are rather mediated by the earlier pathways perturbed by 5-NL particularly by the AMPK pathway which has been shown to activate CREB [54]. The activation of cAMP/PKA/CREB pathway in our system is plausibly responsible for the increases of antigen presenting machinery given that the MHC-I upregulation phenotype was recapitulated by the AC activator forskolin and 5-NL's action inhibited when combined with a p-CREB inhibitor. Recently, it was demonstrated that decreased AMPK activity in tumor cells led to attenuated antigen presentation and favoured an immunosuppressive TME [55]. Thus one can speculate that 5-NL-mediated early AMPK activation affects p-CREB and subsequently the antigen presenting machinery. However, AMPK activation has also been demonstrated to inhibit ribosomal protein p70 S6 kinase [56], which we also observe in our system following 5-NL treatment. As inhibition of PI3K/Akt/mTOR could be responsible for 5-NL's cell death-inducing effects as has been shown in similar systems [24, 57], it is not clear whether AMPK activation might be responsible for 5-NL induced MHC-I upregulation (upstream of p-CREB) or 5-NL induced cell death (upstream of PI3K/Akt/mTOR). The upregulation of MHC-I is probably uncoupled from the apoptosis inducing effects of 5-NL as evidenced by the modest increases in forskolin-mediated apoptosis at least in MC-38 cells. Consistently, our data indicate that inhibition of p-CREB can prevent upregulation of MHC-I following 5-NL treatment in tumor cells.

Clinically, tumors have variable MHC-I expression that tends to be suppressed in later stages of progression making tumors refractory to checkpoint inhibition [58–61]. Therefore, to elicit responsiveness to immunotherapies, the conversion of poorly inflamed cold tumors into hot tumors such as through MHC-I upregulation [16] is therapeutically attractive as it might stimulate anti-tumor T cell immunity not only in the tumor tissue but also in the LN as was observed in our system. Notably, we observed this in our study with the B16 cells that have a reversible MHC-I deficient phenotype and intrinsic resistance to immunotherapy [35]. Treatment with the anti-PD1 antibody alone had no effect on tumor growth but the combination of 5-NL and anti-PD1 was most effective. Current clinical efforts of administering systemic IFNγ to increase MHC-I expression [62] are fraught with challenges namely rate-limiting toxicity, PD-L1 upregulation and T cell dysfunction [63–65]. Furthermore, as a means of primary and acquired resistance, many tumors inactivate interferon signaling [66]. In our study, MHC-I/HLAA-C was upregulated following IFNγ treatment in tumor cells of varying basal MHC-I/HLAA-C expression. This was accompanied by strong PD-L1 upregulation. While the effects of 5-NL mediated MHC-I/HLAA-C upregulation were less dramatic than with IFNγ, there was also no PD-L1 upregulation observed in vitro and in vivo, precluding 5-NL involvement in IFNγ/STAT1 signaling. Furthermore, 5-NL upregulated MHC-I expression in MOPC cells which were refractive to IFNγ-mediated MHC-I upregulation. This broadens its applicability and demonstrates that it can be used to boost responses across a wide tumor immunogenicity range.

In vivo, 5-NL was well tolerated but the clinical applicability of 5-NL remains to be determined as it is not FDA approved. There is the possibility of using other already FDA-approved compounds that also increase MHC-I through cAMP/PKA/CREB mediated signaling. For example, phosphodiesterase (PDE) inhibitors are drugs that elevate cAMP/cGMP levels and often activate CREB. They are already being evaluated as re-purposed anti-cancer agents and may be of clinical benefit [67–69]. The possibility of exploring the combination of already FDA-approved PDE inhibitors with checkpoint inhibitors to augment their efficacy is subject to future investigations.

Conclusions

This study demonstrates novel therapeutic opportunities for the augmentation of immunotherapies. MHC-I upregulation in tumor cells using 5-Nonyloxytryptamine

was uncoupled from increases in PD-L1 expression and modulated through CREB signaling. Increased antigen expression converted poorly immunogenic 'cold' tumors into 'hot' and elicited responsiveness to anti-PD1 immunotherapies.

Materials and methods

Cell culture and compounds

B16.F10 and B16.gp33 (Kindly provided by Dr. H.P. Pircher), MC-38, A549, MDA-MB-231 cell lines were maintained Dulbecco Modified Eagle's Medium (DMEM). Human RPMI-7951 cells were maintained in Eagle's MEM. MOPC cells were cultured as previously described [70]. Media was supplemented with 10% FCS (15% for SK-MEL24) and penicillin/streptomycin. Cells were incubated at 37 °**C** in 5% CO2, and routinely confirmed to be mycoplasma-free (MycoAlert Mycoplasma Detection Kit, Lonza). For screening, the NIH Clinical Collection (NCC) composed of 770 small molecules was used in the screen. 5-Nonyloxytryptamine, Sumatriptan, Forskolin (all from Sigma), Asenapine and the p-CREB 3i inhibitor (SelleckChem) were dissolved in DMSO. Serotonin was dissolved in water (SelleckChem).

EsiRNA and CRISPR-Cas9

Cells were seeded and 24 h later, transfected with esiCREB (EMU067571, Sigma), esiHTR1D (EMU075541, Sigma), esiHTR2A (EMU023531, Sigma) or control esiFluc, (EHUFLUC, Sigma) using Lipofectamine 3000 (ThermoFisher) according to the manufacturer's instructions. Lentivirus carrying plasmid pGk1.2Cas9 overexpressing Cas-9 protein, plasmid LRGFP2.1 overexpressing GFP protein with cloned sgRNA (sgHTR1D1, sequence TGTACTGCCCACTGC TAGTT) or LRCherry2.1 plasmid overexpressing mCherry protein with cloned sgRNA2 (sgHTR1D2, sequence CTG GCTAACAATGGTACGGA) were produced using Lenti-X Packaging Single Shots (VSV-G) (Takara Bio) in Lenti-X 293 T cells according to the manufacturer's instructions. Cells were firstly transduced with pGk1.2Cas9 lentivirus and selected with puromycin for Cas-9 overexpressing clones. Next, cells were transduced with lentivirus carrying LRGFP2.1-sgHTR1D1 and LRCherry2.1-sgHTR1D2 simultaneously and sorted for double positive cells followed by clonal selection.

Viruses

LCMV Armstrong (kindly provided by Rolf Zinkernagel, University of Zurich, Zurich, Switzerland) was propagated in L929 cells as previously described [71].

T cell isolation

Splenic T cells were harvested from the spleens using the pan T cell or $CD8^+$ T cell MACS kit (Miltenyi Biotec) as per manufacturers' instructions.

MTT, Combination Index, Annexin V/7AAD apoptosis assays

For the MTT calorimetric assay, cells were seeded in 96 well plates and viability was assessed following addition of the MTT (Sigma) reagent. When assessing viability of tumor cells following co-culture experiments as done in the screen, T cells were removed prior to the MTT reagent addition. Half-maximal inhibitory concentrations (IC50) values were computed from dose–response curves using Prism (v5.0, GraphPad Software). Combination index was calculated from dose response curves of cells treated with 5-NL, Vemurafenib or in combination of two compounds at constant ratio. CompuSyn software was used to evaluate synergy using the median-effect model. For Annexin V/7AAD apoptosis assays, trypsinized cells were washed and stained in Annexin V binding buffer (BD Biosciences). Cells were analyzed for apoptosis using flow cytometry (FACS Fortessa, BD Biosciences).

Flow cytometric analysis

Tumors or lymph nodes were excised, weighed, crushed, strained through a 0.45 micron filter and re-suspended in FACS buffer (PBS, 1% FCS, 5 mM EDTA) and surface stained with anti-CD8, CD45.2, H2DB, H2KB, KLRG1, PD1, CD95, Tim3, CD62L or CD44 (eBioscience) A full list of all antibodies is provided in Supplementary Table 4. For tetramer staining, singly suspended cells were incubated with tetramer-gp33 or tetramer-np396 (CD8) for 15 min at 37 °C. After incubation, surface antibodies (anti-CD8, anti-PD1, anti-KLRG1) were added for 30 min at 4 °C. For intracellular cytokine re-stimulation following in vivo LCMV infection, singly suspended cells were stimulated with LCMV specific peptide gp33, for 1 h after which Brefeldin A (eBiocience) was added for another 5 h incubation at 37 °C followed by staining with anti-Granzyme B, anti-IFNγ and anti-TNF-α. Staining of $CD8^+$ T cells for Granzyme B and IFNγ within tumors, lymph nodes and for ex vivo co-culture systems was performed using the Foxp3 mouse Treg cell staining buffer kit (eBioscience). Experiments were performed with the BD Fortessa Cell Analyzer (BD Biosciences) or CytoFLEX (Beckman Coulter) and analyzed using FlowJo software.

ELISA

The IFNγ ELISA (eBioscience) was performed according to the manufacturers' instructions.

Immunoblotting

Cells were lysed using boiling hot SDS lysis buffer (1.1% SDS, 11% glycerol, 0.1 mol/L Tris, pH 6.8) with 10% β-mercaptoethanol. Blots were probed with anti-α-tubulin (Merck), anti-HTR1D (ThermoFischer, SantaCruz), anti-Akt, anti-p-Akt (Ser 473), anti-S6, anti-p-S6 (Ser235/236), anti-p70 S6, anti-p-p70 S6 (Thr421/Ser424), anti-p-ERK1/2, anti-ERK1/2, anti-NF-κB p65 anti-STAT-1, anti-Caspase-3, anti-Caspase-9, anti-Caspase-8, anti-AMPK and anti-p-AMPK (Thr172) (all from Cell Signaling) and detected using the Odyssey infrared imaging system (Odyssey Fc, LI-COR Biosciences). Immunoblots were quantified using ImageJ.

Histology

Histological analysis was performed on snap frozen tissue. Tissue sections were fixed in acetone or 10% neutral buffered formalin, blocked with 5% FCS/0.3% Triton-X in PBS and stained with anti-active Caspase 3 (BD Biosciences), cleaved Caspase 8, cleaved Caspase-9, p-CREB (Ser 133), p-AMPK (Thr172) (all from Cell Signaling), CD8 and MHC-I (both from BD Biosciences) followed by incubation with the appropriate secondary antibodies. Cy3-conjugated anti-rabbit secondary antibodies were used for immunofluorescence. HRP-linked anti-rabbit secondary antibodies were used for conventional staining, which were visualised with the Peroxidase Substrate (ImmPACT NovaRED). Images were taken with an Axio Observer Z1 fluorescence microscope or Axiocam 503 color microscope (ZEISS) and quantified using Image J using the fluorescence intensity (MFI) per area as previously described [72].

Quantitative RT-PCR

RNA was isolated using Trizol (Invitrogen). cDNA was synthetized with the Reverse Transcription System (Promega). RT-qPCR was performed using the GoTaq® qPCR mix (Promega) or the one step cDNA-qPCR (iTaq™ Universal Probes for fluorescent labeled primers or iTaq™ Universal SYBR® Green One-Step RT-qPCR Kit (Biorad)) according to the manufacturer's instructions. A full list of primers is provided in Supplementary Table 5. For analysis, expression levels were normalized to *β-Actin* and *GAPDH* for tumor cells *or TBP2* for T cells.

Mice and in vivo treatments

C57BL/6 J and NSG (the NOD.Cg-Prkdc^{scid} H2-K1^{tm1Bpe} H2-D1^{tm1Bpe} Il2rg$^{tm1Wjl/SzJ}$) mice were maintained under specific pathogen-free conditions. 7–9 week old C57BL/6 J mice were subcutaneously injected with 5×10^5 B16.GP33 or MC-38 cells. 7 days post injection, mice were randomized and treated daily for 5 consecutive days with 6.25 mg/kg 5-NL, Sumatriptan 12 mg/kg or vehicle control (2.5% DMSO in PBS). Tumors were measured using calipers and tumor volume was calculated using the following formula: (tumor length x width^2)/2. T cell transfer experiment was performed with isolated T cells from P14 mice expressing specific anti-LCMV TCR, as previously described [29]. For infection and T cell priming 7–9 week old C57BL/6 J mice were infected intravenously with 2×10^5 pfu of LCMV-Armstrong. Experiments were performed under the authorization of LANUV in accordance with German law for animal protection.

Data mining

CREB1, B2M, HLA A-C, IFNG and IFIT3 expression data was extracted directly from the Cancer Immunome Atlas [49].

RNA sequencing and gene set analysis

RNA was isolated using TRIzol (Thermo Fisher Scientific) and total RNA was checked for quality on tapestation. Next, RNA was processed using the QuantSeq 3′-mRNA Library Prep/Lexogen to prepare the barcoded libraries. Sequencing of samples were performed with standard: NovaSeq 6000 mode, covering: 10 M Raw Reads (on average) with standard reads: 1×100 bp. Fastq files were imported into Partek Flow (Partek Incorporated). Quality analysis and quality control were performed on all reads to assess read quality and to determine the amount of trimming required (both ends: 13 bases 5′ and 1 base 3′). Trimmed reads were aligned against the mm10 genome using the STAR v2.4.1d aligner. Unaligned reads were further processed using Bowtie 2 v2.2.5 aligner. Aligned reads were combined before quantifying the expression against the ENSEMBL (release 95) database by the Partek Expectation–Maximization algorithm using the counts per million normalization. Genes with missing values and with a mean expression less than one were filtered out. Finally, statistical gene set analysis was performed using a t test to determine differential expression at the gene level ($P<0.05$, fold change ± 1,3). Partek flow default settings were used in all analyses. Sequencing of samples was performed by NGS Core Facility—Institut for Human Genetics, Life & Brain Center, (Bonn, Germany).

Statistical analysis

Data are expressed as mean ± S.E.M. Statistically significant differences between two groups were determined using the student's t-test and between three or more groups, the one or two-way ANOVA was used with a post-hoc test. Values of $P<0.05$ were considered statistically significant.

Abbreviations

5-NL	5-Nonyloxytryptamine
CREB	CAMP Response Element-Binding Protein
AMPK	AMP-activated protein kinase
CTL	Cytotoxic T lymphocytes
MHC-I/II	major histocompatibility complex class I/II
IFNγ	Interferon γ
TME	Tumor microenvornment
Treg	Regulatory T cells
KLRG1	Killer cell lectin-like receptor subfamily G, member 1
TIL	Tumor infiltrating leukocyte
TM	Tegaserod
PKA	Protein kinase A
AC	Adenylate cyclase
Hmgb1-ps2	High Mobility Group Box 1 pseudogene 2
DAMP	Damage-associated molecular pattern
ICD	Immunogenic cell death
GPCR	G protein-coupled receptors
APC	Antigen presenting cells
DC	Dendritic cells
HTR	Serotonin receptor
TAM	Tumor associated macrophages
LCMV	Lymphocytic choriomeningitisvirus
GZMB	Granzyme B
FasL	Fas ligand

Supplementary Information

The online version contains supplementary material available at https://doi.org/10.1186/s12943-023-01833-8.

Additional file 1: Supplementary Figure 1. (A,B) C57BL/6J mice were infected with 2 x 10^5 pfu of LCMV-Armstrong. 14 days post infection, splenic LCMV-primed $CD8^+$ or pan T cells were isolated and co-incubated with B16 or B16.GP33 cells for 16 hours. $CD8^+$ T cells were assessed for surface KLRG1 and intracellular TNFα, Granzyme B (GZMB) and IL-2 expression by flow cytometry (*n* = 4). (B) B16.GP33 cell viability was assessed by the MTT assay following from incubation with different numbers of splenic LCMV-primed pan T cells for 24 hours (*n* = 3). The vertical dotted line indicates the concentration of T cells used in the screen (5 x 10^5). (C) Treatment with low micromolar doses of 5-NL induced apoptosis in a time and dose-dependent manner as assessed by Annexin V/7AAD staining (*n* = 3-4). Percent apoptosis was ascertained by summing up the Annexin V+/7AAD- and Annexin V+/7AAD+ populations. (D) Representative FACS blots from (C) are shown. (E, F) C57BL/6J mice were subcutaneously injected with 5 x 10^5 B16.GP33 cells. 7 days post-tumor injection mice were randomized into two groups and treated daily with 6.25 mg/kg of 5-NL or with vehicle for five consecutive days. Mice were sacrificed on 13 days post tumor-inoculation. Tumors were analyzed for cleaved Caspase-9, active Caspase-3 and cleaved Caspase-8 (E, top panel) using immunohistochemistry on tumor sections (representative images of tumors harvested from 4–5 mice are shown). Scale bar indicates 50 μm and slides were scored using the IHC profiler (bottom panel) (F). Cleaved Caspase-9, active Caspase-3 and pro-Caspase-8 expression from whole tumors was also analyzed using immunoblot analysis (representative images of *n* = 4 are shown, cropping is indicated by a black frame). Error bars indicate SEM; **P* < 0.05 as determined by a Student´s t-test (unpaired, 2 tailed) or one-way ANOVA with a Dunnett's post-hoc test, or a Fisher's exact test.

Additional file 2: Supplementary Figure 2. 5-NL does not affect infiltration of Treg's. (A-C) C57BL/6J mice were subcutaneously injected with 5 x 10^5 B16.GP33 cells and 13 days post-tumor inoculation tumor infiltrates were analyzed by flow cytometry. (A) The general gating strategy for identifying $CD45.2^+$ infiltrates is shown. (B) Gating strategy used for the identification of specific infiltrates from the $CD45.2^+$ population is shown. (C) 7 days post-tumor injection mice were randomized into two groups and treated daily with 6.25 mg/kg of 5-NL or with vehicle for five consecutive days. Expression of GATA3 and T-Bet in $CD4^+CD25^+FOXP3^+$ Treg cells was assessed using FACS analysis (n = 6). Error bars indicate SEM; *P < 0.05 as determined by a Student´s t-test (unpaired, 2 tailed).

Additional file 3: Supplementary Figure 3. 5-NL does not change the immune infiltration of transferred P14 CD45.1 $CD8^+$ T cells. (A) C57BL/6J mice were treated with $CD8^+$ T cell depleting antibody (anti-CD8) on days -2, -1 and 7 pre and post inoculation with 5 x 10^5 B16.GP33 cells. T cell depletion was confirmed in the blood on day 0 and day 15 post tumor-inoculation using flow cytometry (*n* = 3-4). (B) Schematic representation of T cells transfer experiment is shown. (B,C) C57BL/6J mice expressing CD45.2 isoform were inoculated with 5 x 10^5 B16.GP33 cells and 7 days later received 2 x 10^6 purified splenic $CD8^+$ T P14 cells expressing the CD45.1 congenic marker. 8 hours post T cell injection, mice were injected with GP33 peptide and poly(I:C) to stimulate and activate the T cells. Next day, mice were randomized into two groups and treated with 6.25 mg/kg of 5-NL or with vehicle for five consecutive days. Mice were sacrificed at day 15 post tumor inoculation and organs were FACS analyzed for number of $CD45.1^+$ $CD8^+$ T cells in blood, lymph nodes and tumors (*n* = 4-6). Error bars indicate SEM; **P* < 0.05 as determined by a Student´s t-test (unpaired, 2 tailed).

Additional file 4: Supplementary Figure 4. Infection upregulates serotonin receptors (HTR) in T cells. In vivo infection with LCMV Armstrong (A) resulted in an upregulation of several serotonin receptors (HTR's) in splenic T cells 8 days post-infection as assessed by RT-PCR (*n* = 3-4). For analysis, the expression levels of all genes were normalized to *TBP2* (ΔCt). Then gene expression values were calculated relative to naïve controls and Log2 transformed. (B) Basal levels of serotonin receptors in B16 and MC-38 cells were assessed using RT-PCR (n = 6). For analysis, the expression levels of all genes were normalized to *GAPDH* (ΔCt) and then Log2 transformed. (C) C57BL/6J mice were infected with 2 x 10^5 pfu of LCMV Armstrong and treated with 6.25 mg/kg of 5-NL or vehicle for 5 consecutive days starting at day 1 post-infection. Cells from the blood, spleen and liver were re-stimulated with LCMV-specific gp33 epitope followed by staining for IFNγ, TNFα and GZMB in the blood 8 days post-infection and TNFα and GZMB in the blood, spleen and liver 10 days post infection using FACS analysis (n = 4-5). Tet-$gp33^+$ $CD8^+$ T cells in the blood were measured 8 days post-infection (n = 5). (D) C57BL/6J mice were infected with 2 x 10^5 pfu of LCMV-Armstrong. 14 days post infection, splenic primed pan T cells were isolated and co-incubated with B16.GP33 cells pre-treated for 24 hours with 3 μM of 5-NL. KLRG1, TNFα, Granzyme B (GZMB) and IL-2 were measured on $CD8^+$ T cells using flow cytometry (n = 3). Error bars indicate SEM; *P < 0.05 as determined by a Student´s t-test (unpaired, 2 tailed) or a one-way ANOVA with a Dunnett's or a Tukey post-hoc test.

Additional file 5: Supplementary Figure 5. 5-Nonyloxytryptamine (5-NL) upregulates antigen presenting machinery and H2-Db and H2-Kb in vivo. (A, B) C57BL/6J mice were subcutaneously injected with 5 x 10^5 B16.GP33 cells. 7 days post-tumor injection mice were randomized into two groups and treated daily with 6.25 mg/kg of 5-NL or with vehicle for five consecutive days. (A) Mice were sacrificed on day 20 post tumor-inoculation and $CD45.2^-$ cells were analyzed for expression of H2-Db/Kb using flow cytometry (n = 6-8). (B) Mice were sacrificed on day 13 post tumor-inoculation and tumor infiltrates were FACS-analyzed for MHC-II expression (n = 6). (C) Treatment of B16 cells with 5-NL (3 μM) for 18 hours resulted in the upregulation of antigen presenting machinery genes *B2M* and *TAPBP* at the transcriptional level as assessed by RT-PCR. Expression was normalized to *GAPDH* (n = 4-5). (D) Treatment with the indicated concentrations of another HTR4 agonist, Tegaserod for 18 hours did not induce upregulation of H2-Db/Kb in B16 cells as analyzed with flow cytometry (n = 3). (E) MHC-II (mouse cell lines) and HLA- D (human cell lines) protein expression was assessed using flow cytometry following treatment with 5-NL (5 μM for RPMI-7591 and 3 μM for MC-38, SW620, A549, MDA-MB-231, B16 and MOPC cells) for 24 hours or 18 hours for B16 cells (*n* = 5). (F, left panel) C57BL/6J mice were subcutaneously injected with 5 x 10^5 MC-38 cells. 7 days post-tumor injection, mice were randomized into two groups and treated daily with 6.25 mg/kg of 5-NL or with vehicle for five consecutive days. Mice were sacrificed on day 13 post tumor-inoculation and tumor sections stained for MHC-I using immunofluorescence (representative images of n = 3-4 are shown, scale bar indicates 50 μm) and fluorescence signal is quantified in F, right panel. (G) B16 cells were transfected with control or HTRID targeting esiRNA. (G, left panel; immunoblot where cropped is indicated by black frame) Protein

levels of HTR1D were assessed using immunoblot analysis 48 hrs post transfection. (G, right panel) 48 hours post-transfection cells were treated with 3 μM of 5-NL after which H2-Db protein levels were assessed by FACS analysis 18 hrs post 5-NL treatment (n = 6). (H) sgRNA mediated HTR1D knockout clones 1 and 2 (HTR1D KO) and control clones (CTR) in B16 cells were validated using immunoblot analysis (left panel; immunoblot cropping is indicated by a black frame). H2-Db protein expression following treatment with 3 μM of 5-NL was assessed by FACS analysis (*n* = 5-6 right panel). (I) B16 cells were transfected with control or HTR2A targeting esiRNA and *HTR2A* expression was assessed using RT-PCR 24 hours post transfection in left panel (n = 4). Expression was normalized to *GAPDH*. 24 hours post esiRNA transfection, cells were treated with 3 μM of 5-NL for 18 hours and expression of H2-Db was analyzed by flow cytometry in the right panel (*n* = 3). (J) B16 cells were treated for 18 hours with 3 μM 5-NL, 10 μM Serotonin, 10 μM Asenapine or pre-treated for 30 min with Asenapine, followed by 5-NL treatment. The expression of H2-Db was measured using flow cytometry (*n* = 4). Error bars indicate SEM; $P < 0.05$ as determined by a Student´s t-test (unpaired, 2 tailed) or a 1-way ANOVA with a Tukey post-hoc test.

Additional file 6: Supplementary Figure 6. 5-Nonyloxytryptamine (5-NL) increases antigen presenting machinery independently of IFNγ. (A and B) C57BL/6J mice were subcutaneously injected with 5 x 10^5 B16. GP33 cells. 7 days post-tumor injection mice were randomized into two groups and treated daily with 6.25 mg/kg of 5-NL or with vehicle for five consecutive days. Mice were sacrificed on day 13 post tumor-inoculation. (A) Intra-tumoral levels of IFNγ were determined using ELISA (n = 3-4). (B) Tumoral mRNA levels of *IFNA1*, *IFNB1* and *IFNG* were assessed using RT-PCR. Expression was normalized to *GAPDH* (n = 8-11). (C) B16.GP33 cells were treated with 5-NL for 18 hours and expression of *IFNA1*, *IFNB1* and *IFNG* was assessed using RT-PCR and expression was normalized to *GAPDH* (*n* = 5). (D) Levels of STAT1 protein as assessed by immunoblot analysis are shown following treatment with 5-NL (3 μM) or murine IFNγ (5 ng/ml) at the indicated time-points and quantified in the right panel (representative immunoblot of *n* = 3 is shown; cropping is indicated by a black frame). (E) MHC-I (mouse cell lines) and HLA A-C (human cell lines) and (F) PD-L1 protein expression was assessed using flow cytometry following treatment with IFNγ or 5-NL for 24 hours (*n* = 5). Error bars indicate SEM; $P < 0.05$ as determined by a Student´s t-test (unpaired, 2 tailed) or a 1-way ANOVA with a Dunnett's post-hoc test.

Additional file 7: Supplementary Figure 7. 5-Nonyloxytryptamine (5-NL) does not affect NF-κB signaling. (A, left panel) Levels of NF-κB p65 protein were assessed in B16 cells using immunoblot analysis following treatment with 5-NL (1.5 μM and 3 μM) at the indicated time points and quantified in right panel (representative immunoblot of n = 5-6 is shown; immunoblot cropping is indicated by a black frame). (B, left panel) Representative immunofluorescent pictures of B16 or MC-38 cells treated with 5-NL (3 μM) or TNFα (40 ng/μl) for 18 hours or 24 hours respectively and stained for phosphorylated NF-κB p65 (p-NF-κB p65, Ser-536,) are shown (representative images of n = 3-4 are shown; scale bar indicates 50 μm). Single fluorescent signal from p-NF-κB p65 was quantified in the right panel. (C, top panel) Changes in protein levels of phosphorylated ERK (p-ERK), p-Akt (Ser473), p-p70 S6 (Thr421/Ser424) and p-S6 (Ser235/6)) following treatment with 5-NL (3 and 1.5 μM) at the indicated time-points were analyzed in B16 cells using immunoblot analysis (representative immunoblots of n = 3-8 are shown; immunoblot cropping is indicated by a black frame) and quantified in C, bottom panel). Error bars indicate SEM; $P < 0.05$ as determined by a one or two-way ANOVA with a Dunnett's post-hoc test.

Additional file 8: Supplementary Figure 8 (A, left panel) Representative immunofluorescent pictures of MC-38 cells treated with 5-NL (3 μM) or forskolin (10 μM) for 24 hours and stained for phosphorylated CREB (p-CREB, Ser-133) and H2-Db are shown (representative images of n = 3-4 are shown; scale bar indicates 50 μm) and fluorescent signal is quantified in A, right panel. (B, left panel). Changes in protein levels of phosphorylated CREB (ser 133) (following treatment with 5-NL (3 and 1.5 μM) in B16 cells at the indicated time-points are shown (representative immunoblots of n = 3-7 are shown; where immunoblots are cropped is indicated by a black frame) and signal quantified in B, right panel. (C, left panel) esiRNA mediated CREB knockdown using esiRNA in B16.GP33 and MC-38 cells 48 hrs post-transfection are shown using immunoblot (n = 3; where immunoblots are cropped is indicated by a black frame). (C, right panel) Levels of apoptosis using Annexin V/7AAD staining by FACS 48 hours post esiRNA transfection are shown (n = 3-7). (D) MC-38 cells were pre-treated for 30 min with the p-CREB inhibitor 3i at the indicated doses followed by treatment with 10 μM forskolin for 24 hours. Cells were FACS-analyzed for expression of H2-Db/Kb (n = 3). (E) H2-Db/Kb protein expression as measured by FACS in MC-38 cells following 24 hours of treatment with the adenylyl cyclase activator forskolin (10 μM) is shown (n = 5). (F) Levels of apoptosis as assessed by Annexin V/7AAD staining are shown following treatment of MC-38 with 5-NL and forskolin at the indicated doses for 72 hours (n = 4-6). Percent apoptosis was ascertained by summing up the Annexin $V^+/7AAD^-$ and Annexin $V^+/7AAD^+$ populations. (G) B16 and MC38 cells were treated with the CREB inhibitor 3i (8 μM) for 18 hours. Apoptosis was assessed using Annexin V/7AAD staining (n = 5). Error bars indicate SEM; $P < 0.05$ as determined by a Student's t-test (unpaired, 2 tailed), one or two-way ANOVA with a Dunnett's post-hoc test.

Additional file 9: Supplementary Figure 9. (A) Representative immunofluorescent pictures of B16 cells (left panel) stained for phosphorylated AMPK (p-AMPK, Thr 172, green) and DAPI (blue) detected 0.5 or 1 hour post-treatment with 3 μM of 5-NL. Scale bar indicates 50 μm. Green fluorescent signal (p-AMPK) was quantified in right panel (n = 3). Error bars indicate SEM; *$P < 0.05$ as determined by a one-way ANOVA with a Dunnett's post-hoc test. (B) Transcriptomic data from melanoma samples of therapy naïve patients was mined from the Cancer Immunome Atlas. Expression of *IFIT3* positively correlated with *HLA A-C* and *B2M*

Additional file 10.

Additional file 11.

Additional file 12.

Additional file 13.

Additional file 14.

Authors' contributions

PS, WL, AW, PP, OS, MV, HCX and AAP performed the experiments. DP analyzed RNA sequencing data. AAP directed the study and wrote the manuscript. HCX, SB, KSL, DH, MR, BH, PAL and AB discussed the project, provided suggestions and edited the manuscript.

Funding

Open Access funding enabled and organized by Projekt DEAL. A.A.P was supported by the Forschungskommission (2021-04) Medical faculty of Heinrich-Heine University Dusseldorf, Germany, the José Carreras Foundation, Munich, Germany (DJCLS 07 R/2019), the Ilsedore Luckow Stiftung, Dusseldorf, Germany, the German Federal Office for Radiation Protection, München-Neuherberg, Germany, the Düsseldorf School of Oncology and the NIH Tetramer Facility. Arndt Borkhardt was supported by the Katharina-Hardt Foundation, Bad Homburg, Germany and Löwenstern e.V. Erkrath, Germany. PAL was supported by the Deutsche Forschungsgemeinschaft (DFG, RTG1949, LA2558/8-1), the Jürgen Manchot Foundation (MOI), the Volkswagen Foundation, and the NIH Tetramer Facility.

Availability of data and materials

The dataset generated in this study are available on request from the corresponding author.

Declarations

Ethics approval and consent to participate

Experiments were performed under the authorization of LANUV in accordance with German law for animal protection.

Consent for publications

The authors declare no competing interests.

Competing interests
HCX, PP, KSL, and PAL declare that they are involved in the development of LCMV for clinical application in oncology in cooperation with or as advisors to Abalos Therapeutics GmbH. The other authors declare no competing interests.

Author details
[1]Department of Molecular Medicine II, Medical Faculty, Heinrich-Heine-University, Universitätsstraße 1, 40225 Düsseldorf, Germany. [2]Department of Pediatric Oncology, Hematology and Clinical Immunology, Medical Faculty, Center of Child and Adolescent Health, Heinrich-Heine-University, Moorenstrasse 5, 40225 Düsseldorf, Germany. [3]Division of Pediatric Neuro-Oncogenomics, German Cancer Research Center (DKFZ), Heidelberg, Germany. [4]Partner Site Essen/Düsseldorf, German Consortium for Translational Cancer Research (DKTK), Düsseldorf, Germany. [5]Department of Neuropathology, Medical Faculty, Heinrich-Heine University, Moorenstrasse 5, Düsseldorf 40225, Germany. [6]Institute of Immunology, Medical Faculty, University of Duisburg-Essen, Hufelandstrasse 55, 45147 Essen, Germany. [7]Department of Gastroenterology, Hepatology and Infectious Diseases, Medical Faculty, Heinrich-Heine-University, Moorenstrasse 5, Düsseldorf 40225, Germany. [8]Department of Dermatology, Medical Faculty, Heinrich-Heine-University, Moorenstrasse 5, Düsseldorf 40225, Germany. [9]Institute of Clinical Chemistry and Clinical Pharmacology, University Hospital Bonn, Venusberg-Campus 1, 53127 Bonn, Germany. [10]German Center for Infection Research (DZIF), Partner Site Bonn-Cologne, Bonn, Germany.

Received: 5 October 2022 Accepted: 27 July 2023
Published online: 15 August 2023

References

1. Shellenberger R, Nabhan M, Kakaraparthi S. Melanoma screening: A plan for improving early detection. Ann Med. 2016;48(3):142–8.
2. SEER Cancer Statistics Review, 1975–2014. 2017.
3. Eggermont AM, Chiarion-Sileni V, Grob JJ, Dummer R, Wolchok JD, Schmidt H, et al. Adjuvant ipilimumab versus placebo after complete resection of high-risk stage III melanoma (EORTC 18071): a randomised, double-blind, phase 3 trial. Lancet Oncol. 2015;16(5):522–30.
4. Larkin J, Chiarion-Sileni V, Gonzalez R, Grob JJ, Cowey CL, Lao CD, et al. Combined Nivolumab and Ipilimumab or Monotherapy in Untreated Melanoma. N Engl J Med. 2015;373(1):23–34.
5. Robert C, Schachter J, Long GV, Arance A, Grob JJ, Mortier L, et al. Pembrolizumab versus Ipilimumab in Advanced Melanoma. N Engl J Med. 2015;372(26):2521–32.
6. Khair DO, Bax HJ, Mele S, Crescioli S, Pellizzari G, Khiabany A, et al. Combining Immune Checkpoint Inhibitors: Established and Emerging Targets and Strategies to Improve Outcomes in Melanoma. Front Immunol. 2019;10:453.
7. Vermaelen K, Waeytens A, Kholmanskikh O, Van den Bulcke M, Van Valckenborgh E. Perspectives on the integration of Immuno-Oncology Biomarkers and drugs in a Health Care setting. Semin Cancer Biol. 2017.
8. Verma V. Economic sustainability of immune-checkpoint inhibitors: the looming threat. Nat Rev Clin Oncol. 2018;15(12):721–2.
9. Sun ZJ, Kim KS, Wagner G, Reinherz EL. Mechanisms contributing to T cell receptor signaling and assembly revealed by the solution structure of an ectodomain fragment of the CD3 epsilon gamma heterodimer. Cell. 2001;105(7):913–23.
10. Huang JF, Yang Y, Sepulveda H, Shi W, Hwang I, Peterson PA, et al. TCR-Mediated internalization of peptide-MHC complexes acquired by T cells. Science. 1999;286(5441):952–4.
11. Martinez-Lostao L, Anel A, Pardo J. How Do Cytotoxic Lymphocytes Kill Cancer Cells? Clin Cancer Res. 2015;21(22):5047–56.
12. Durgeau A, Virk Y, Corgnac S, Mami-Chouaib F. Recent Advances in Targeting CD8 T-Cell Immunity for More Effective Cancer Immunotherapy. Front Immunol. 2018;9:14.
13. Dudley ME, Wunderlich JR, Robbins PF, Yang JC, Hwu P, Schwartzentruber DJ, et al. Cancer regression and autoimmunity in patients after clonal repopulation with antitumor lymphocytes. Science. 2002;298(5594):850–4.
14. Doorduijn EM, Sluijter M, Querido BJ, Oliveira CC, Achour A, Ossendorp F, et al. TAP-independent self-peptides enhance T cell recognition of immune-escaped tumors. J Clin Invest. 2016;126(2):784–94.
15. Farhood B, Najafi M, Mortezaee K. CD8(+) cytotoxic T lymphocytes in cancer immunotherapy: A review. J Cell Physiol. 2019;234(6):8509–21.
16. Duan Q, Zhang H, Zheng J, Zhang L. Turning Cold into Hot: Firing up the Tumor Microenvironment. Trends Cancer. 2020;6(7):605–18.
17. Barber DL, Wherry EJ, Masopust D, Zhu B, Allison JP, Sharpe AH, et al. Restoring function in exhausted CD8 T cells during chronic viral infection. Nature. 2006;439(7077):682–7.
18. Prevost-Blondel A, Zimmermann C, Stemmer C, Kulmburg P, Rosenthal FM, Pircher H. Tumor-infiltrating lymphocytes exhibiting high ex vivo cytolytic activity fail to prevent murine melanoma tumor growth in vivo. J Immunol. 1998;161(5):2187–94.
19. Prevost-Blondel A, Neuenhahn M, Rawiel M, Pircher H. Differential requirement of perforin and IFN-gamma in CD8 T cell-mediated immune responses against B16.F10 melanoma cells expressing a viral antigen. Eur J Immunol. 2000;30(9):2507–15.
20. Peacock CD, Lin MY, Ortaldo JR, Welsh RM. The virus-specific and allospecific cytotoxic T-lymphocyte response to lymphocytic choriomeningitis virus is modified in a subpopulation of CD8(+) T cells coexpressing the inhibitory major histocompatibility complex class I receptor Ly49G2. J Virol. 2000;74(15):7032–8.
21. Ahmed R, Salmi A, Butler LD, Chiller JM, Oldstone MB. Selection of genetic variants of lymphocytic choriomeningitis virus in spleens of persistently infected mice. Role in suppression of cytotoxic T lymphocyte response and viral persistence. J Exp Med. 1984;160(2):521–40.
22. Suprunenko T, Hofer MJ. Complexities of Type I Interferon Biology: Lessons from LCMV. Viruses. 2019;11(2).
23. Reiser J, Banerjee A. Effector, Memory, and Dysfunctional CD8(+) T Cell Fates in the Antitumor Immune Response. J Immunol Res. 2016;2016:8941260.
24. Liu W, Stachura P, Xu HC, Umesh Ganesh N, Cox F, Wang R, et al. Repurposing the serotonin agonist Tegaserod as an anticancer agent in melanoma: molecular mechanisms and clinical implications. J Exp Clin Cancer Res. 2020;39(1):38.
25. Gao Q, Wang S, Chen X, Cheng S, Zhang Z, Li F, et al. Cancer-cell-secreted CXCL11 promoted CD8(+) T cells infiltration through docetaxel-induced-release of HMGB1 in NSCLC. J Immunother Cancer. 2019;7(1):42.
26. Sriram G, Milling LE, Chen JK, Kong YW, Joughin BA, Abraham W, et al. The injury response to DNA damage in live tumor cells promotes antitumor immunity. Sci Signal. 2021;14(705):eabc4764.
27. Varghese F, Bukhari AB, Malhotra R, De A. IHC Profiler: an open source plugin for the quantitative evaluation and automated scoring of immunohistochemistry images of human tissue samples. PLoS ONE. 2014;9(5):e96801.
28. Joshi NS, Cui W, Chandele A, Lee HK, Urso DR, Hagman J, et al. Inflammation directs memory precursor and short-lived effector CD8(+) T cell fates via the graded expression of T-bet transcription factor. Immunity. 2007;27(2):281–95.
29. Pircher H, Bürki K, Lang R, Hengartner H, Zinkernagel RM. Tolerance induction in double specific T-cell receptor transgenic mice varies with antigen. Nature. 1989;342(6249):559–61.
30. Glennon RA, Hong SS, Dukat M, Teitler M, Davis K. 5-(Nonyloxy) tryptamine: a novel high-affinity 5-HT1D beta serotonin receptor agonist. J Med Chem. 1994;37(18):2828–30.
31. Inoue M, Okazaki T, Kitazono T, Mizushima M, Omata M, Ozaki S. Regulation of antigen-specific CTL and Th1 cell activation through 5-Hydroxytryptamine 2A receptor. Int Immunopharmacol. 2011;11(1):67–73.
32. Abdouh M, Storring JM, Riad M, Paquette Y, Albert PR, Drobetsky E, et al. Transcriptional mechanisms for induction of 5-HT1A receptor mRNA and protein in activated B and T lymphocytes. J Biol Chem. 2001;276(6):4382–8.
33. Leon-Ponte M, Ahern GP, O'Connell PJ. Serotonin provides an accessory signal to enhance T-cell activation by signaling through the 5-HT7 receptor. Blood. 2007;109(8):3139–46.
34. Ohtsuka M, Inoko H, Kulski JK, Yoshimura S. Major histocompatibility complex (Mhc) class Ib gene duplications, organization and expression patterns in mouse strain C57BL/6. BMC Genomics. 2008;9:178.

35. Seliger B, Wollscheid U, Momburg F, Blankenstein T, Huber C. Characterization of the major histocompatibility complex class I deficiencies in B16 melanoma cells. Cancer Res. 2001;61(3):1095–9.
36. Hegde PS, Karanikas V, Evers S. The Where, the When, and the How of Immune Monitoring for Cancer Immunotherapies in the Era of Checkpoint Inhibition. Clin Cancer Res. 2016;22(8):1865–74.
37. Galon J, Bruni D. Approaches to treat immune hot, altered and cold tumours with combination immunotherapies. Nat Rev Drug Discov. 2019;18(3):197–218.
38. Saini V, Lutz D, Kataria H, Kaur G, Schachner M, Loers G. The polysialic acid mimetics 5-nonyloxytryptamine and vinorelbine facilitate nervous system repair. Sci Rep. 2016;6:26927.
39. Gu SS, Zhang W, Wang X, Jiang P, Traugh N, Li Z, et al. Therapeutically increasing MHC-I expression potentiates immune checkpoint blockade. Cancer Discov. 2021.
40. van den Elsen PJ, Gobin SJ, van Eggermond MC, Peijnenburg A. Regulation of MHC class I and II gene transcription: differences and similarities. Immunogenetics. 1998;48(3):208–21.
41. Jongsma MLM, Guarda G, Spaapen RM. The regulatory network behind MHC class I expression. Mol Immunol. 2019;113:16–21.
42. Carey BS, Poulton KV, Poles A. Factors affecting HLA expression: A review. Int J Immunogenet. 2019;46(5):307–20.
43. Nichols DE, Nichols CD. Serotonin receptors. Chem Rev. 2008;108(5):1614–41.
44. Sampurno S, Bijenhof A, Cheasley D, Xu H, Robine S, Hilton D, et al. The Myb-p300-CREB axis modulates intestine homeostasis, radiosensitivity and tumorigenesis. Cell Death Dis. 2013;4(4): e605.
45. van der Sligte NE, Kampen KR, ter Elst A, Scherpen FJ, Meeuwsen-de Boer TG, Guryev V, et al. Essential role for cyclic-AMP responsive element binding protein 1 (CREB) in the survival of acute lymphoblastic leukemia. Oncotarget. 2015;6(17):14970–81.
46. Wang Z, Zhang X, Tian X, Yang Y, Ma L, Wang J, et al. CREB stimulates GPX4 transcription to inhibit ferroptosis in lung adenocarcinoma. Oncol Rep. 2021;45(6).
47. Xie F, Li BX, Kassenbrock A, Xue C, Wang X, Qian DZ, et al. Identification of a Potent Inhibitor of CREB-Mediated Gene Transcription with Efficacious in Vivo Anticancer Activity. J Med Chem. 2015;58(12):5075–87.
48. Fucikova J, Kepp O, Kasikova L, Petroni G, Yamazaki T, Liu P, et al. Detection of immunogenic cell death and its relevance for cancer therapy. Cell Death Dis. 2020;11(11):1013.
49. Charoentong P, Finotello F, Angelova M, Mayer C, Efremova M, Rieder D, et al. Pan-cancer Immunogenomic Analyses Reveal Genotype-Immunophenotype Relationships and Predictors of Response to Checkpoint Blockade. Cell Rep. 2017;18(1):248–62.
50. Van Allen EM, Miao D, Schilling B, Shukla SA, Blank C, Zimmer L, et al. Genomic correlates of response to CTLA-4 blockade in metastatic melanoma. Science. 2015;350(6257):207–11.
51. Hugo W, Zaretsky JM, Sun L, Song C, Moreno BH, Hu-Lieskovan S, et al. Genomic and Transcriptomic Features of Response to Anti-PD-1 Therapy in Metastatic Melanoma. Cell. 2016;165(1):35–44.
52. Larkin J, Del Vecchio M, Ascierto PA, Krajsova I, Schachter J, Neyns B, et al. Vemurafenib in patients with BRAF(V600) mutated metastatic melanoma: an open-label, multicentre, safety study. Lancet Oncol. 2014;15(4):436–44.
53. Sarrouilhe D, Clarhaut J, Defamie N, Mesnil M. Serotonin and cancer: what is the link? Curr Mol Med. 2015;15(1):62–77.
54. Didier S, Sauve F, Domise M, Buee L, Marinangeli C, Vingtdeux V. AMP-activated Protein Kinase Controls Immediate Early Genes Expression Following Synaptic Activation Through the PKA/CREB Pathway. Int J Mol Sci. 2018;19(12).
55. Gao Y, Paivinen P, Tripathi S, Domenech-Moreno E, Wong IPL, Vaahtomeri K, et al. Inactivation of AMPK Leads to Attenuation of Antigen Presentation and Immune Evasion in Lung Adenocarcinoma. Clin Cancer Res. 2022;28(1):227–37.
56. Patel VA, Massenburg D, Vujicic S, Feng L, Tang M, Litbarg N, et al. Apoptotic cells activate AMP-activated protein kinase (AMPK) and inhibit epithelial cell growth without change in intracellular energy stores. J Biol Chem. 2015;290(37):22352–69.
57. Jose J, Tavares CDJ, Ebelt ND, Lodi A, Edupuganti R, Xie X, et al. Serotonin Analogues as Inhibitors of Breast Cancer Cell Growth. ACS Med Chem Lett. 2017;8(10):1072–6.
58. Garrido F, Ruiz-Cabello F, Aptsiauri N. Rejection versus escape: the tumor MHC dilemma. Cancer Immunol Immunother. 2017;66(2):259–71.
59. Yamamoto K, Venida A, Yano J, Biancur DE, Kakiuchi M, Gupta S, et al. Autophagy promotes immune evasion of pancreatic cancer by degrading MHC-I. Nature. 2020;581(7806):100–5.
60. McGranahan N, Rosenthal R, Hiley CT, Rowan AJ, Watkins TBK, Wilson GA, et al. Allele-Specific HLA Loss and Immune Escape in Lung Cancer Evolution. Cell. 2017;171(6):1259–71 e11.
61. Sade-Feldman M, Jiao YJ, Chen JH, Rooney MS, Barzily-Rokni M, Eliane JP, et al. Resistance to checkpoint blockade therapy through inactivation of antigen presentation. Nat Commun. 2017;8(1):1136.
62. Zhang S, Kohli K, Black RG, Yao L, Spadinger SM, He Q, et al. Systemic Interferon-gamma Increases MHC Class I Expression and T-cell Infiltration in Cold Tumors: Results of a Phase 0 Clinical Trial. Cancer Immunol Res. 2019;7(8):1237–43.
63. Benci JL, Xu B, Qiu Y, Wu TJ, Dada H, Twyman-Saint Victor C, et al. Tumor Interferon Signaling Regulates a Multigenic Resistance Program to Immune Checkpoint Blockade. Cell. 2016;167(6):1540–54 e12.
64. Benci JL, Johnson LR, Choa R, Xu Y, Qiu J, Zhou Z, et al. Opposing Functions of Interferon Coordinate Adaptive and Innate Immune Responses to Cancer Immune Checkpoint Blockade. Cell. 2019;178(4):933–48 e14.
65. Pai CS, Huang JT, Lu X, Simons DM, Park C, Chang A, et al. Clonal Deletion of Tumor-Specific T Cells by Interferon-gamma Confers Therapeutic Resistance to Combination Immune Checkpoint Blockade. Immunity. 2019;50(2):477–92 e8.
66. Gao J, Shi LZ, Zhao H, Chen J, Xiong L, He Q, et al. Loss of IFN-gamma Pathway Genes in Tumor Cells as a Mechanism of Resistance to Anti-CTLA-4 Therapy. Cell. 2016;167(2):397–404 e9.
67. Gong S, Chen Y, Meng F, Zhang Y, Wu H, Wu F. Roflumilast restores cAMP/PKA/CREB signaling axis for FtMt-mediated tumor inhibition of ovarian cancer. Oncotarget. 2017;8(68):112341–53.
68. Mehta A, Patel BM. Therapeutic opportunities in colon cancer: Focus on phosphodiesterase inhibitors. Life Sci. 2019;230:150–61.
69. Zhang L, Murray F, Zahno A, Kanter JR, Chou D, Suda R, et al. Cyclic nucleotide phosphodiesterase profiling reveals increased expression of phosphodiesterase 7B in chronic lymphocytic leukemia. Proc Natl Acad Sci U S A. 2008;105(49):19532–7.
70. Kalkavan H, Sharma P, Kasper S, Helfrich I, Pandyra AA, Gassa A, et al. Spatiotemporally restricted arenavirus replication induces immune surveillance and type I interferon-dependent tumour regression. Nat Commun. 2017;8:14447.
71. Battegay M, Cooper S, Althage A, Banziger J, Hengartner H, Zinkernagel RM. Quantification of lymphocytic choriomeningitis virus with an immunological focus assay in 24- or 96-well plates. J Virol Methods. 1991;33(1–2):191–8.
72. Shihan MH, Novo SG, Le Marchand SJ, Wang Y, Duncan MK. A simple method for quantitating confocal fluorescent images. Biochem Biophys Rep. 2021;25: 100916.

Publisher's Note

Additional file 1

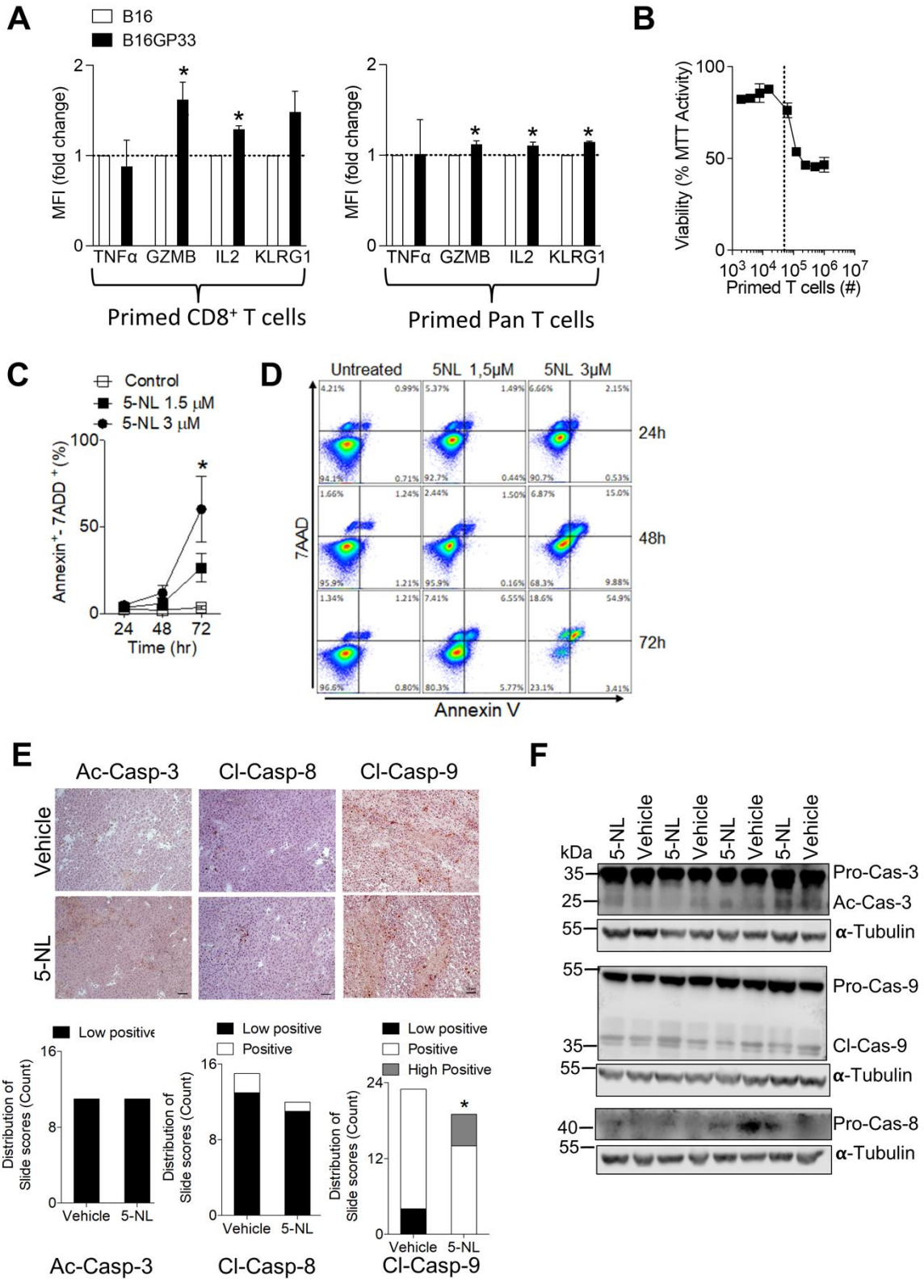

Supplementary file 2:

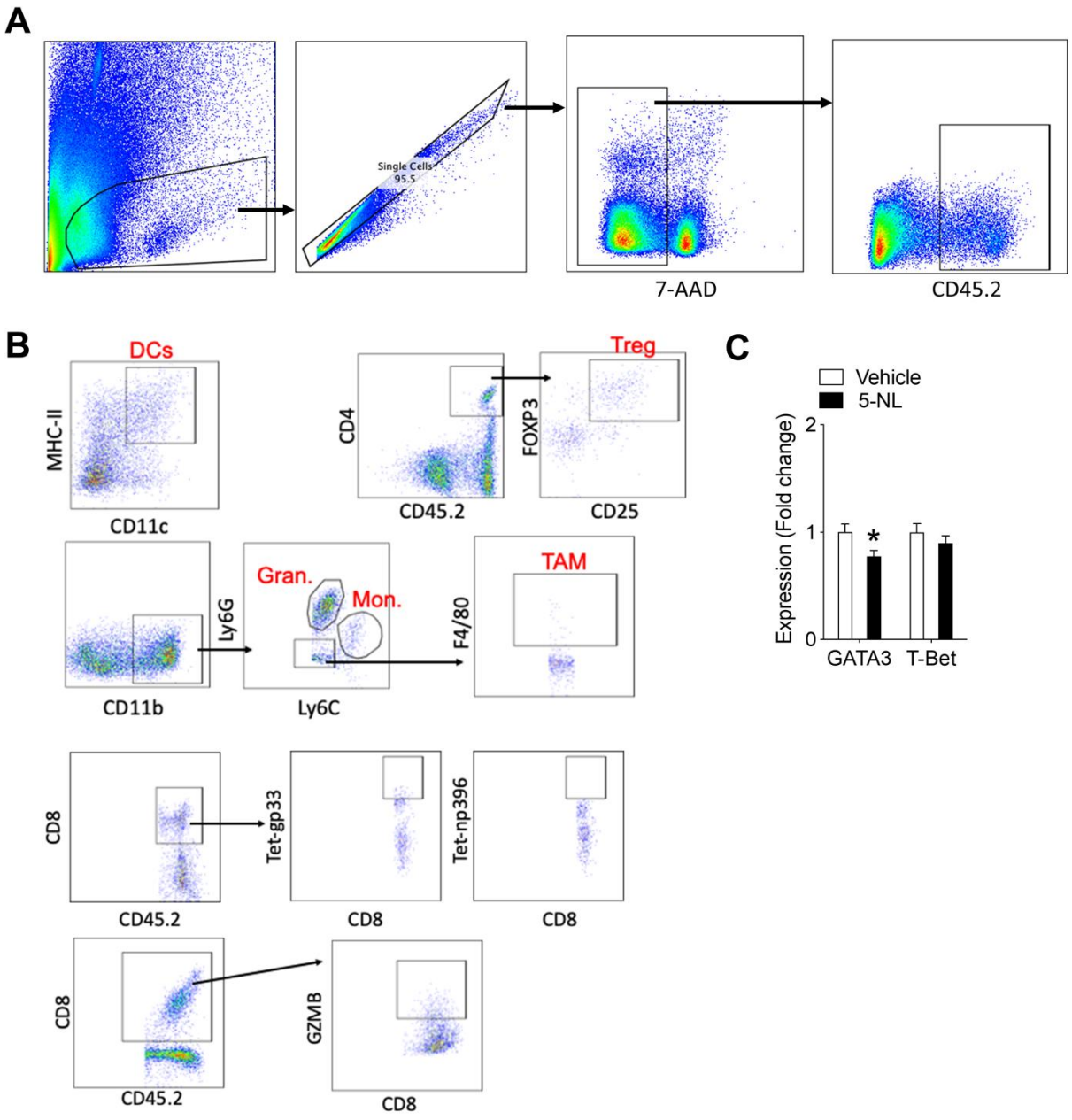

Supplementary file 3:

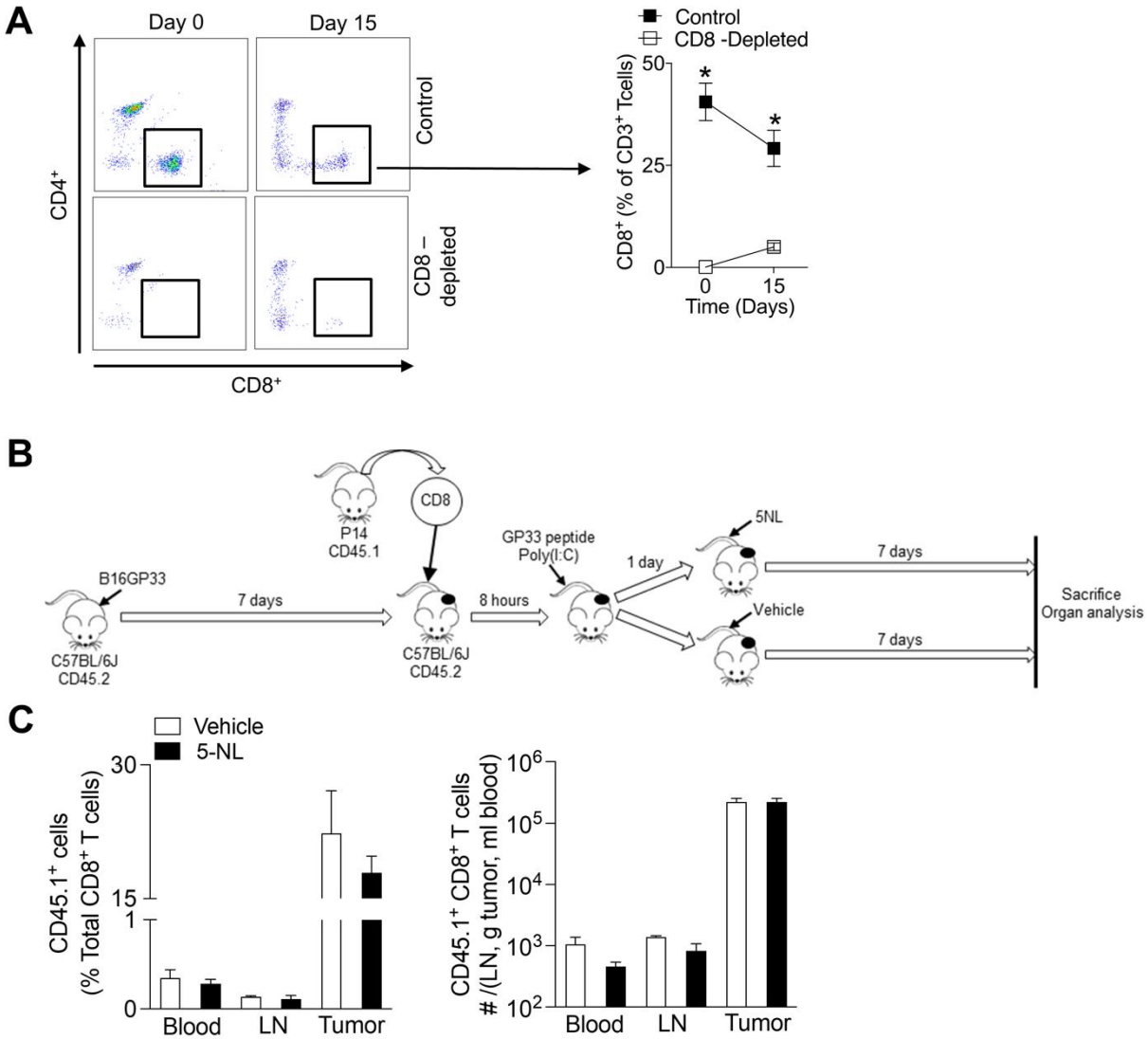

Supplementary file 4:

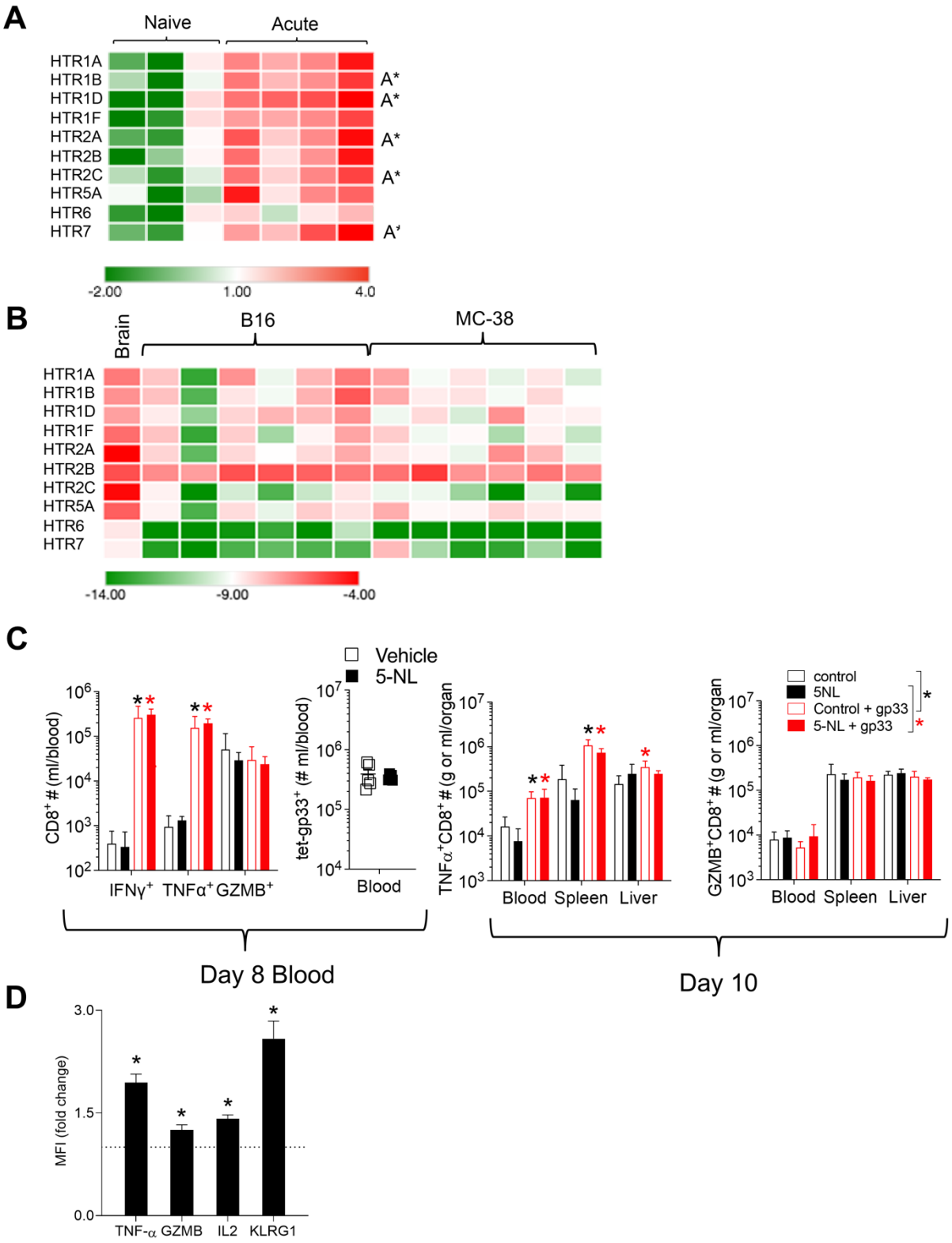

Supplementary file 5:

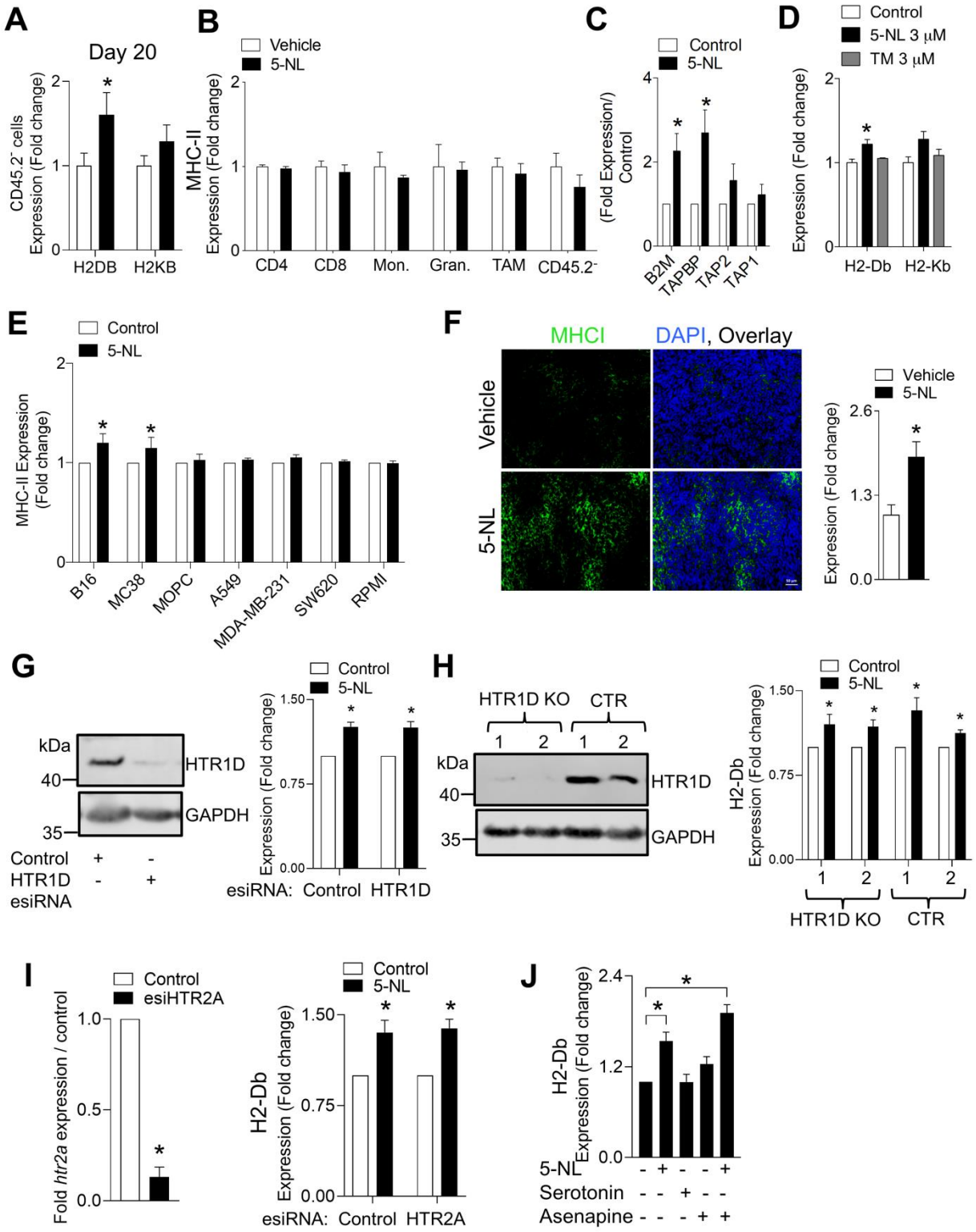

Supplementary file 6:

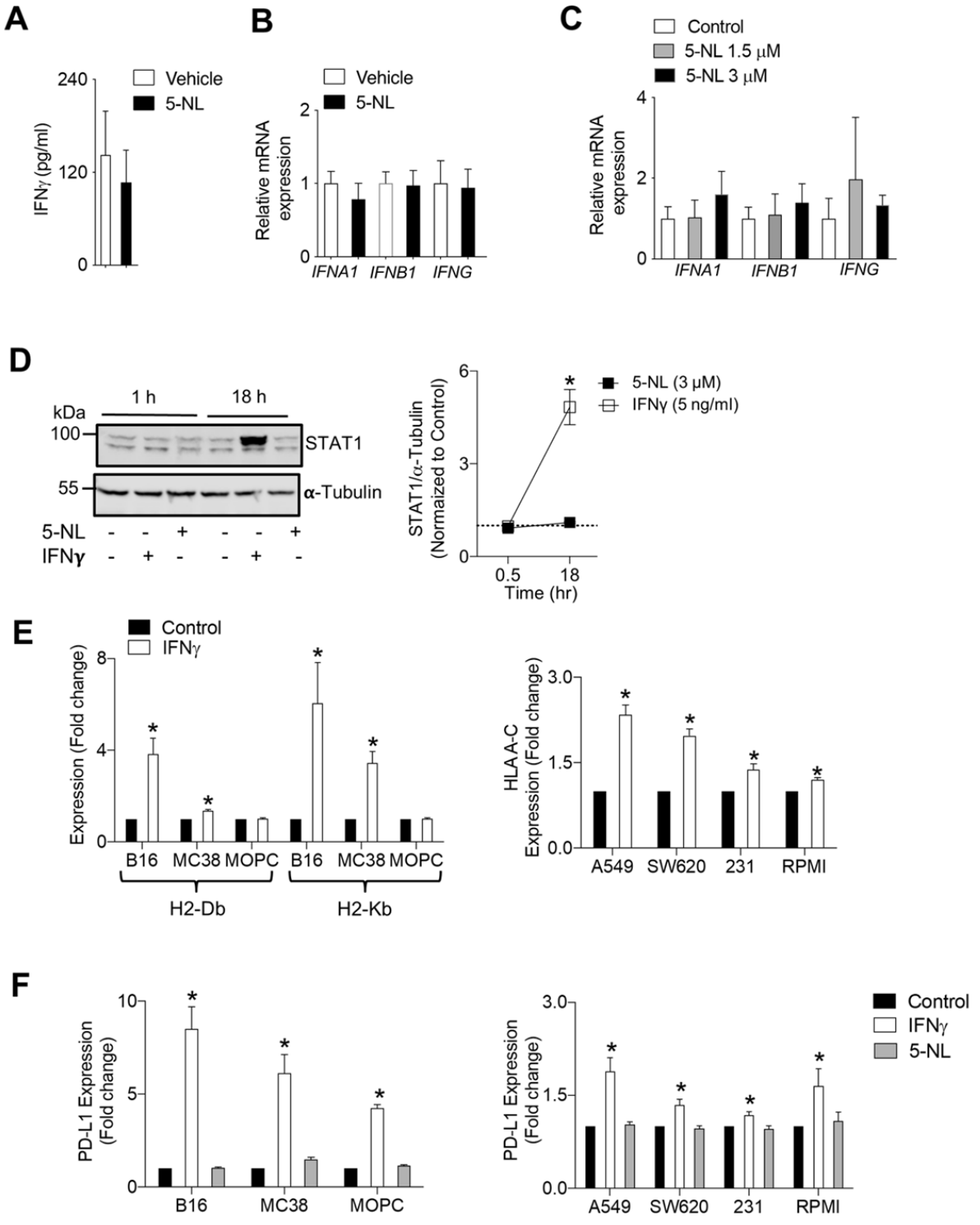

Supplementary file 7:

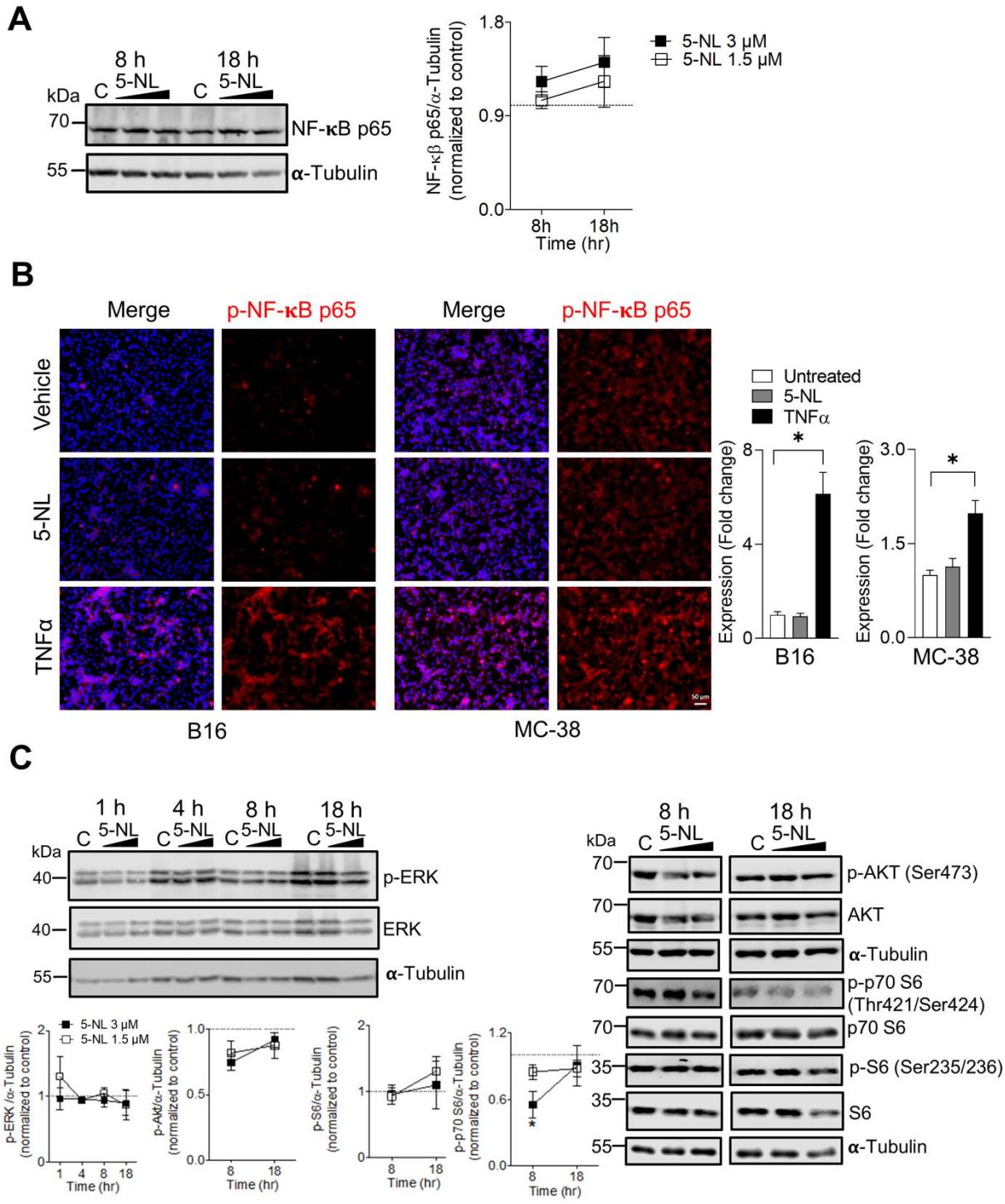

Supplementary file 8:

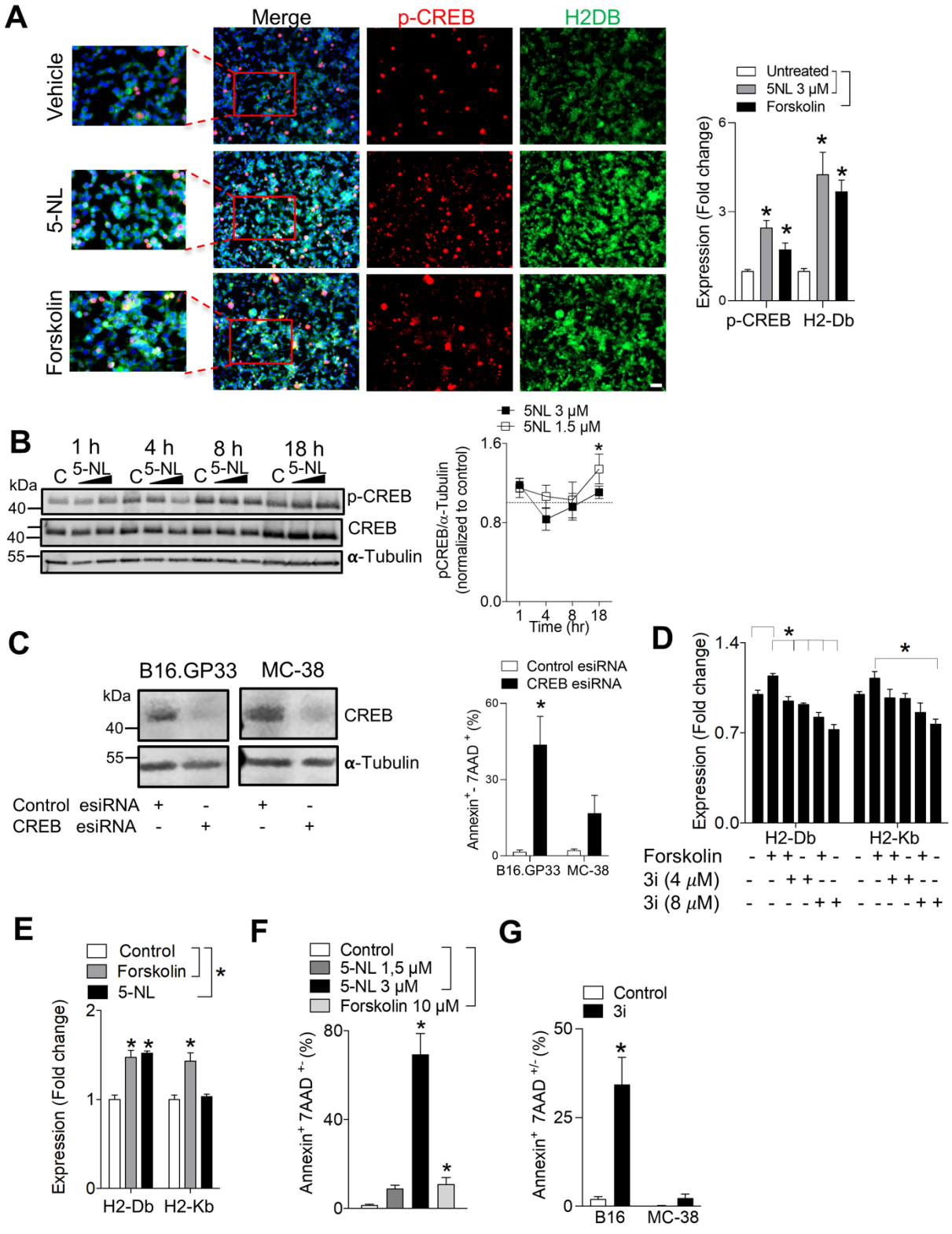

Supplementary file 9:

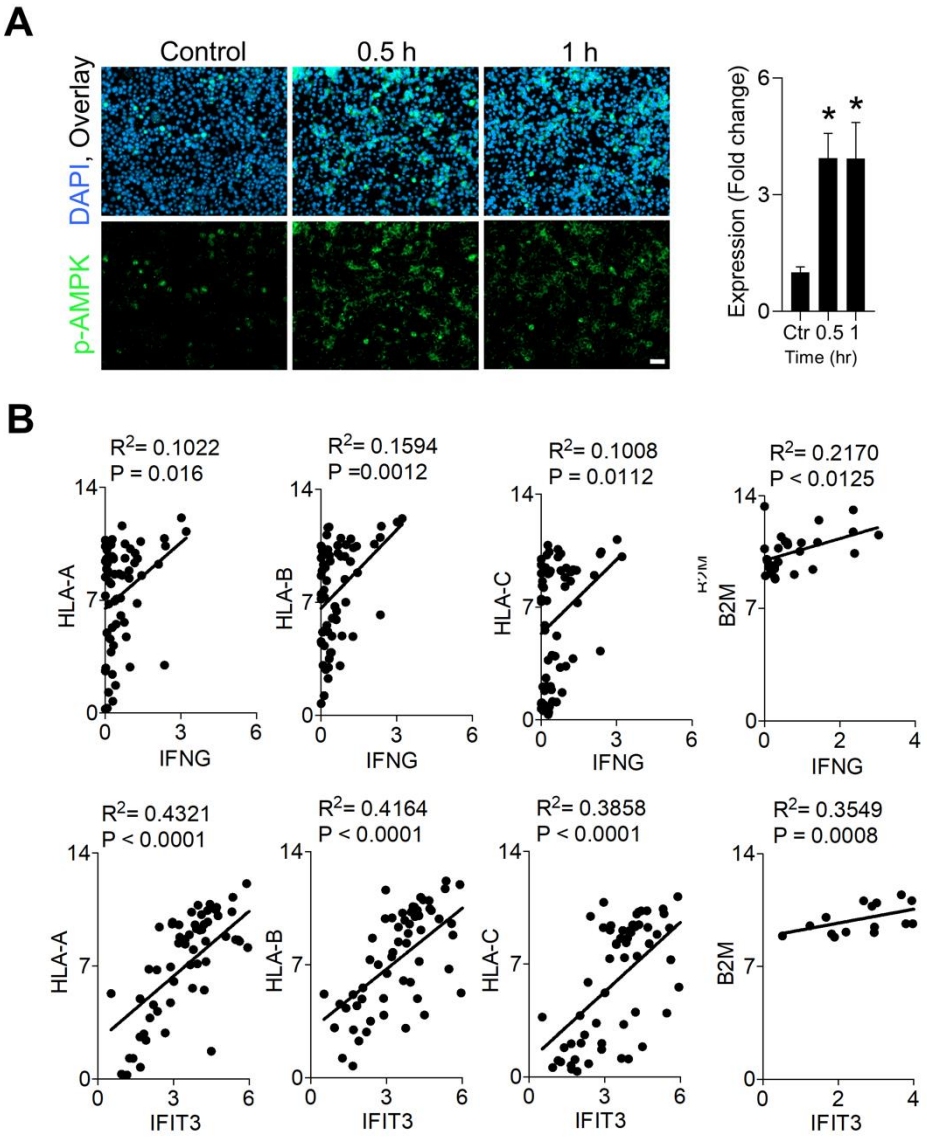

Supplementary Table 1: List of potenital T cell immunomdulatory hits

	Compound name	Toxic*	Imunomodulatory
1	5-Non-loxy tryptamine		
2	Disulfiram	yes	
3	Sotalol hydrochloride		
4	3,5,3'-Triiodothyronine		yes
5	Etoposide		Yes
6	Clomifene citrate		
7	Fluphenazine dihydrochloride		
8	Docetaxel		Yes
9	Vincristine sulfate	yes	
10	Daunorubicin hydrochloride	yes	
11	Fludarabine	yes	
12	Cerivastatin sodium	yes	
13	Raltitrexed		Yes
14	Itraconazole	yes	
15	Vindesine sulfate	yes	
16	Benazepril hydrochloride		
17	Topotecan hydrochloride		yes
18	Idarubicin hydrochloride	yes	
19	Podofilox	yes	
20	Albendazole		yes
21	Homoharringtonine	yes	
22	Mefloquine hydrochloride		
23	Mebendazole		yes
24	Flubendazole	yes	
25	Mitoxantrone hydrochloride	yes	
26	Dactinomycin	yes	
27	Methotrexate trihydrate	yes	
28	Vinorelbine tartrate	yes	
29	Doxorubicin hydrochloride	yes	

*** IC50 below 500 nM**

Supplementary Table 2: Summary of observed cell phenotype post 5-NL or IFNγ treatment.

		(H2-Db/H2-Kb)/HLAA-C		PD-L1	
		5-NL	IFNγ	5-NL	IFNγ
Murine	B16	↑	↑	no change	↑
	MOPC	↑	No change	no change	↑
	MC-38	↑	↑	no change	↑
Human	A549	No change	↑	no change	↑
	SW620	↑	↑	no change	↑
	MDA-MB.231	No change	↑	no change	↑
	RPMI	↑	↑	no change	↑

Supplementary Table 3: Differentially expressed genes evaluated by RNA sequencing of 18 hours treated B16 cells with 5-NL.

Probeset ID	p-value	FoldChange(5NL/Ctrl)
Gm15710	0,0145604	8,81E+13
Man2b2	0,0309053	7,63406
Gm6087	0,0380725	4,43028
Gm46496	0,0406018	4,02387
H2-T24	0,0156578	3,8677
Gm38009	0,0233591	3,70651
Shld2	0,0196615	3,31898
2510017J16Rik	0,0473638	3,2704
C130013H08Rik	0,0385481	3,19913
Zfp433	0,043561	3,07088
Hmgb1-ps2	0,0312081	2,91442
4930563E22Rik	0,00867791	2,86881
Gm37906	0,0136151	2,79881
Acvr2a	0,0338542	2,78003
Rpl21-ps6	0,00945331	2,62743
Zfp273	0,033019	2,61403
Mxd1	0,0227495	2,39024
Gm10136	0,023999	2,35792
Nek1	0,00967842	2,29219
Ttc16	0,0165932	2,2451
1700081N11Rik	0,0041725	2,23662
Gm4811	0,0450622	2,17462
Fam227a	0,0472784	2,15986
Eid3	0,00956978	2,11357
Gch1	0,0134666	2,09162
Atl1	0,0120313	2,08705
Armcx3	0,0322727	2,07464
Traf3ip1	0,048854	2,0743
Zfp566	0,0388652	2,06189
Ddx19b	0,0206287	2,03845
Kdm1b	0,00875406	2,01089
Gfra1	0,0475273	1,98813
Enpp5	0,0106991	1,98126
Pgm2	0,0161834	1,91921
Arhgef10	0,0197941	1,90221
Mau2	0,00417038	1,87162
Gm49708	0,0435499	1,86776
Cpeb2	0,0341672	1,85885
2210418O10Rik	0,00501104	1,83461
R3hdm2	0,0274429	1,80823
Gm20657	0,00956956	1,79683
Fzd5	0,0164759	1,78084
Unc13d	0,0379653	1,7738
Tnip2	0,0129932	1,76099
Chmp1b	0,0403186	1,74366
Srp54c	0,0226809	1,73914
Glce	0,00178932	1,73612
Cblb	0,0162079	1,73075
Gm47542	0,0422616	1,70903
Gm16072	0,0470455	1,69254
Mynn	0,0364533	1,68055
Tasor2	0,0441137	1,6602
Tenm4	0,0124757	1,65274
Sp3os	0,0488455	1,64752
Sec24d	0,0128482	1,63795
Cdkl2	0,0309455	1,63629
Ccdc82	0,0155525	1,63426
Apex2	0,0215869	1,63106
Hoxa10	0,00511289	1,62406

Probeset ID	p-value	FoldChange(5NL/Ctrl)
Map2k6	0,0432968	1,6133
Rbm4	0,0333568	1,60839
Inafm2	0,0176587	1,59017
Bbx	0,0344046	1,5868
Tubb2a	0,0346314	1,58487
Gm16153	0,0117983	1,58332
Insr	0,0431802	1,58201
Arl6ip6	0,0128449	1,57848
Uvssa	0,0348875	1,57393
Ddx19a	0,025454	1,56785
Jpx	0,0370819	1,56588
B930086L07Rik	0,0210356	1,56316
Tsen15	0,0476315	1,54998
Zyg11b	0,0194532	1,52271
Arvcf	0,0311247	1,51687
Aga	0,0148078	1,50496
Tmem64	0,0142732	1,50436
Zgrf1	0,0441117	1,49088
Ap1s2	0,0454315	1,48995
Lsm1	0,00194947	1,48179
Shox2	0,0352606	1,48141
Zkscan8	0,00284876	1,47144
Ppp2r5e	0,0452713	1,46861
Glcci1	0,0380796	1,46722
Arl6	0,0134011	1,4611
Akr1b10	0,0233161	1,4534
Mpv17	0,0126562	1,44341
Pias4	0,0337745	1,44214
Fmn1	0,00320716	1,43719
Ccpg1	0,0498282	1,41622
Trappc11	0,035199	1,41271
Synj1	0,0018882	1,41134
Nectin3	0,0467059	1,40707
Lpin2	0,0193249	1,40577
Gm1976	0,0488326	1,39927
Ccnh	0,0449334	1,39926
Senp8	0,0214416	1,39907
Gm43513	0,0286092	1,39875
Snx25	0,0240285	1,38917
Aifm2	0,0281198	1,38058
Il13ra1	0,00823997	1,37923
Btbd1	0,0319922	1,37858
Uap1	0,0152262	1,37557
Ints6	0,0194909	1,37511
Nudt2	0,0394865	1,36787
Gm37607	0,00648554	1,36093
Pias2	0,0331285	1,35581
Nfe2l1	0,0348258	1,3558
Rnf185	0,0402688	1,35332
Ostm1	0,040889	1,35234
Pcyox1	0,0406108	1,35196
Fkbp10	0,00514271	1,35187
Rbak	0,0488687	1,35079
Arl5b	0,0126	1,34986
Spopl	0,0260337	1,34212
Plekhh3	0,0138641	1,33363
Kif3b	0,0144693	1,33327
Daxx	0,0361885	1,33318
Pja2	0,0499924	1,32218

Probeset ID	p-value	FoldChange(5NL/Ctrl)
Usp34	0,0113678	1,3157
B3glct	0,049171	1,31414
Dnajb14	0,0348229	1,31367
Gm37939	0,00806299	1,31316
Steap1	0,021679	1,30423
4632427E13Rik	0,0497981	1,30251
Il18bp	0,0230503	1,29998
Lats1	0,0210661	1,29653
Fndc3b	0,0156856	1,29402
Tmem135	0,0156421	1,29269
D5Ertd579e	0,0374386	1,29171
Zfp113	0,0498577	1,28605
Tnrc6b	0,0183953	1,28421
Scaper	0,0492252	1,28319
Taok3	0,0172335	1,28284
Insig2	0,0387147	1,28198
Itsn2	0,0190015	1,27688
Aph1a	0,00598394	1,27568
Atad2b	0,0394865	1,27555
Spata7	0,0472627	1,27071
Mlx	0,0466143	1,26218
Tmco1	0,0226774	1,25964
Asph	0,0391383	1,25457
Dolk	0,0418653	1,2491
Ahdc1	0,0167368	1,24818
Ube2o	0,019945	1,2476
Fam220a	0,0385207	1,24668
B2m	0,0448774	1,24362
Nemf	0,0240394	1,23668
Sec22b	0,0385047	1,23487
Eif5a2	0,0457949	1,23376
Brca2	0,0492323	1,23013
Prpf6	0,049112	1,22695
Taf5	0,0106006	1,19364
Clk4	0,043049	1,19363
P2rx7	0,0238763	1,19079
Ppp2r3a	0,0145584	1,18119
Tnfaip8l1	0,0217851	1,17972
Srsf5	0,019865	1,17774
Spout1	0,00232469	1,17672
Flii	0,0371733	1,17578
Nktr	0,0353455	1,17544
Atrnl1	0,0170339	1,17058
Rab18	0,00227176	1,17019
Ubn2	0,00772546	1,1701
Faf2	0,0136604	1,16003
Stambp	0,0132675	1,1591
Nkapd1	0,0345414	1,15559
Gnptg	0,0394938	1,15525
Psma4	0,00365453	1,14898
Ylpm1	0,0265783	1,1465
Fkrp	0,00731389	1,14552
Gm16196	0,00941466	1,14534
Dnajc10	0,0264589	1,14456
BC005537	0,0411054	1,14147
Appl1	0,0326435	1,13522
Znfx1	0,0305114	1,13291
Yme1l1	0,0153305	1,12623
Rala	0,0296539	1,12484

Probeset ID	p-value	FoldChange(5NL/Ctrl)
Vcp	0,0414008	1,12089
Phospho2	0,0401498	1,10784
Zfp871	0,0271689	1,07983
Slc2a9	0,0188896	-1,06111
Pole4	0,0291082	-1,06909
Emsy	0,0379445	-1,07905
Arhgap42	0,0491044	-1,08667
Phax	0,000197144	-1,10094
Paqr4	0,0430086	-1,10379
Ndufs5-ps	0,0222956	-1,10542
Afg3l1	0,0486034	-1,11307
D10Wsu102e	0,021659	-1,12392
Uck1	0,0159919	-1,12562
Dnajc9	0,00269803	-1,12753
Pdp2	0,0251539	-1,12826
Ankrd40	0,0110689	-1,13161
Ahsa1	0,00421705	-1,13574
Pdhx	0,0229609	-1,13653
Racgap1	0,0390046	-1,13791
Nuf2	0,0431193	-1,1395
Ppp1cc	0,0392069	-1,14074
Lias	0,0136296	-1,14989
Ywhae	0,00457242	-1,1526
Prpf19	0,0327802	-1,15328
Tbc1d1	0,0359755	-1,15436
Ccdc93	0,0272978	-1,16752
Creb3	0,0326459	-1,17178
Tsn	0,0227809	-1,17319
Hmgn1	0,0155101	-1,17392
Marchf6	0,00314172	-1,17875
Haus8	0,0431707	-1,18111
Tanc1	0,0344845	-1,18661
Cux1	0,0391768	-1,18802
Chtop	0,0238381	-1,19319
Rarres2	0,0327853	-1,1967
Cep70	0,0390008	-1,19684
Cdkn2aipnl	0,0126395	-1,19819
Gpat4	0,0396627	-1,20124
Rps21	0,0321786	-1,20363
Slc12a4	0,00947733	-1,20665
S1pr2	0,0375934	-1,20688
Rps25-ps1	0,0375446	-1,21042
Pwp1	0,0145269	-1,21112
Mfsd10	0,0465125	-1,21116
Samm50	0,0380465	-1,21254
Pcif1	0,0240847	-1,21328
Elp3	0,027515	-1,21707
Tonsl	0,046485	-1,21834
Spc24	0,0490517	-1,21993
Glis3	0,0216717	-1,22178
Rpl7	0,0383455	-1,22311
Eef1d	0,0312549	-1,22327
Csnk1d	0,0170837	-1,22401
Thap11	0,0075948	-1,22419
Ehmt1	0,000840648	-1,22973
Zfp275	0,045812	-1,23259
Psmb5	0,00355043	-1,23666
Ess2	0,0268028	-1,23836
Dot1l	0,0363077	-1,24006

Probeset ID	p-value	FoldChange(5NL/Ctrl)
Dip2a	0,00870394	-1,24162
Tbl1x	0,00701919	-1,24245
Pprc1	0,0335876	-1,24333
Atp5a1	9,15E-06	-1,24496
Tubb5	0,0412224	-1,24661
Polr2a	0,0421077	-1,2485
Gnptab	0,00262442	-1,24866
Apip	0,0209834	-1,24933
Ppcs	0,0155763	-1,25201
Lsm2	0,0233051	-1,25208
Frmd8	0,0380879	-1,25552
Ttc9c	0,0197365	-1,25843
Gm10282	0,0170004	-1,26059
Noct	0,0211282	-1,26243
Gm9616	0,0403902	-1,26254
Map7d1	0,012016	-1,26333
Dlst	0,0482488	-1,26377
Usp39	0,0261724	-1,26386
Gins4	0,0359893	-1,2656
Tpm1	0,0488537	-1,26772
Gm11478	0,0109986	-1,26817
Crlf1	0,0135078	-1,27086
Calhm5	0,0418078	-1,27481
Rbx1-ps	0,00478961	-1,27489
Gm7536	0,0301865	-1,27643
Rex1bd	0,0400394	-1,28383
Tlnrd1	0,0201575	-1,29055
Phb	0,0414326	-1,29156
Foxd2os	0,0223617	-1,29301
Rangap1	0,0154289	-1,29577
Tgfbrap1	0,0151625	-1,29733
Eif1ad	0,00240664	-1,29866
Cipc	0,00215395	-1,30088
Cab39l	0,0105016	-1,30588
Tsen34	0,0186507	-1,30718
Cenpn	0,0190177	-1,31005
Akap11	0,0422667	-1,31032
St3gal5	0,0102954	-1,31305
Ogdh	0,0186716	-1,31382
Gart	0,0209734	-1,31441
Zfp869	0,0155017	-1,31656
Atp5md	0,016369	-1,31804
Gm20045	0,0442051	-1,31865
Mcm2	0,0402119	-1,32156
Dnph1	0,0248864	-1,32223
Serbp1	0,0266333	-1,32608
Banf1	0,00904682	-1,32878
Emc1	0,00591868	-1,32966
Tmem51	0,0350962	-1,33247
Snu13	0,0149773	-1,33288
6720475M21Rik	0,0263017	-1,33302
Pafah1b2	0,0408306	-1,33391
4933431E20Rik	0,0482495	-1,34016
Cdca5	0,0235095	-1,34382
Ssh1	0,0312152	-1,34656
Akt2	0,0193321	-1,35215
Zfp219	0,0475263	-1,35876
Polh	0,0287749	-1,36006
Arl6ip4	0,0209392	-1,36492
Epc1	0,0400556	-1,36657
Odf2	0,042616	-1,36927
Trmt12	0,0267325	-1,37067
Pdxk	0,0459625	-1,37258
Phb2	0,0436553	-1,37434
Acaca	0,0274335	-1,37501
Rilpl1	0,0145935	-1,37604
Gm11537	0,0255306	-1,37627
Snrpg	0,0182388	-1,38177
Rpsa-ps10	0,0278394	-1,38357
Gm13611	0,0138171	-1,38854
Rbbp5	0,0115514	-1,38864
Gm10288	0,0218544	-1,38993
Zfp955a	0,00877101	-1,39023
Eif4h	0,0423758	-1,39026
Alyref	0,0430384	-1,39229
Rps19-ps6	0,0362507	-1,39922
Vps9d1	0,00337868	-1,40316
Tyms	0,0444083	-1,4032
Mylk	0,000786923	-1,40686
Ddx39	0,0312161	-1,4099
Thg1l	0,0303484	-1,41042
Srgap2	0,0341426	-1,41087
Evl	0,0102327	-1,41525
Pwp2	0,0433884	-1,41638
Scap	0,0459366	-1,42302
Bcas3	0,00850511	-1,43171
Gpx1	0,0164416	-1,43325
Ppp1r8	0,0425918	-1,43375
Gm6204	0,0141938	-1,43438
Mrps7	0,00813879	-1,43469
Mrpl54	0,021947	-1,43619
Gm2614	0,029043	-1,43943
Ntmt1	0,0356242	-1,44134
Ppm1g	0,0322478	-1,44187
Cd151	0,044769	-1,44337
Trak1	0,0348698	-1,44383
Gm48226	0,0155712	-1,44427
Fam110a	0,0144278	-1,44884
Elf4	0,0360125	-1,44943
Tk1	0,0410688	-1,45167
Snhg1	0,02128	-1,47135
Coro7	0,0175729	-1,47214
Ptpn21	0,0323584	-1,47454
Rps16-ps2	0,0120156	-1,47723
Ccdc12	0,0466175	-1,47979
Gm6863	0,0152751	-1,47982
Stat3	0,0427004	-1,48064
Mast3	0,00965561	-1,48389
Plekhg3	0,0444276	-1,48575
Bop1	0,0232731	-1,48618
Unk	0,0485247	-1,48663
Tpm3	0,0491157	-1,48823
Osbpl5	0,0386659	-1,49026
Cdca4	0,0138753	-1,4949
Ndufaf5	0,0460437	-1,50106
Rpl28-ps1	0,025663	-1,50569
Zbtb18	0,00283511	-1,51606
2310061I04Rik	0,0226666	-1,5161

Probeset ID	p-value	FoldChange(5NL/Ctrl)
Trak2	0,0250092	-1,51714
Gcn1	0,0222636	-1,52307
Retreg3	0,0128132	-1,52667
Mon1a	0,0311952	-1,5279
Usp11	0,0449359	-1,52994
Rgl2	0,00335193	-1,53478
Rps15-ps3	0,0258871	-1,53514
Gm8186	0,0333898	-1,54273
Ypel1	0,0467162	-1,5454
Wars2	0,0369452	-1,54711
Rps10-ps2	0,0422659	-1,5482
Tuba1b	0,0176455	-1,55026
Ech1	0,0436995	-1,55214
Gm5963	0,0265527	-1,55307
Slc4a7	0,0454595	-1,55558
1810026B05Rik	0,0424853	-1,56091
Ppp2r5d	0,00440053	-1,56954
Enpp2	0,0492968	-1,57161
Prr12	0,0273057	-1,57436
Zfp653	0,00776143	-1,57562
Ccnd3	0,0207969	-1,57789
Neurl1a	0,00355491	-1,58557
Snrnp35	0,0318281	-1,58573
Smad3	0,0345891	-1,58661
Coro1c	0,00297468	-1,58858
Vps33a	0,0143214	-1,5988
Tsen2	0,0189087	-1,60743
Nsmf	0,0488702	-1,60787
Gm4799	0,00704461	-1,61014
Rabep2	0,0202159	-1,6117
Ncaph2	0,0230086	-1,61423
Gm5805	0,0139491	-1,61609
Psmb10	0,00262897	-1,62034
Eif3b	0,026572	-1,6244
Rpia	0,0186703	-1,63612
Wdr78	0,0201808	-1,64113
Cox5b-ps	0,0390568	-1,64128
Ppcdc	0,0262788	-1,6415
Urgcp	0,00885774	-1,64606
Cotl1	0,0237167	-1,66537
Wdr74	0,0477069	-1,6672
Rab26os	0,0387808	-1,69537
Gm42893	0,00972073	-1,69608
Gm9575	0,0437035	-1,69961
Cnst	0,0450214	-1,70014
Gm7434	0,0467545	-1,7044
Zfp866	0,0209443	-1,71119
Slc25a28	0,0133043	-1,71231
E330034L11Rik	0,0310005	-1,71714
Sirt6	0,0304698	-1,72038
Adssl1	0,00549624	-1,72917
Phf21b	0,0130187	-1,73059
Grk6	0,00325354	-1,74233
Polr1b	0,0215044	-1,74444
Cep89	0,0219261	-1,74585
Gm10639	0,0139674	-1,79074
Ccdc163	0,0374293	-1,81475
Rmi2	0,0251486	-1,82
Sigirr	0,010966	-1,83157

Probeset ID	p-value	FoldChange(5NL/Ctrl)
Rpl18-ps2	0,035356	-1,83283
Iba57	0,0243594	-1,83393
Gm5905	0,0211616	-1,83466
Shank2	0,0470892	-1,85934
Med12	0,0308945	-1,86258
Gm43848	0,0401862	-1,90652
Setmar	0,0210475	-1,91532
AC160336.1	0,0128525	-1,94848
Ass1	0,0457337	-1,95829
Samd11	0,00974627	-1,98556
Rpl10a-ps1	0,0395208	-1,99036
Gpd1	0,0390628	-2,01731
D130040H23Rik	0,0362209	-2,0341
Hunk	0,0125986	-2,04384
2700062C07Rik	0,00795361	-2,04545
Dennd6b	0,0220827	-2,05294
Arl11	0,0418997	-2,06293
9130008F23Rik	0,0120066	-2,06361
Hpse	0,00223984	-2,0709
E330034G19Rik	0,0403196	-2,10729
Gm4708	0,0362228	-2,1399
Med22	0,0360767	-2,14028
Pkn3	0,0468766	-2,14852
B3galt1	0,0150665	-2,22109
B130034C11Rik	0,0363556	-2,22259
Ccdc9	0,0365676	-2,23299
Thtpa	0,0451931	-2,23684
Eno3	0,0309331	-2,26875
Nme6	0,0396704	-2,32419
Pycrl	0,0258055	-2,3739
Sall4	0,0364243	-2,3776
Gm48887	0,00748452	-2,40074
Gm36988	0,0400854	-2,44246
Prag1	0,00470968	-2,46599
Gm15760	0,0305627	-2,49059
Trmt61a	0,0236186	-2,59574
Gm13268	0,0488578	-2,63404
A130012E19Rik	0,00205011	-2,81778
Cfap300	0,0430794	-2,82385
Ahr	0,0165882	-2,83188
Gm6206	0,030483	-2,9054
Chtf18	0,0144105	-2,91776
Gm16045	0,015272	-3,66244
Ppm1e	0,049591	-3,73081
Etv5	0,0337819	-3,84557
9330151L19Rik	0,021083	-3,87821
Rpusd2	0,00462367	-4,08923
Gm42898	0,049761	-4,19291
Amd-ps3	0,0182635	-4,27229
Ccl5	0,00612578	-4,46867
Masp1	0,0192024	-4,62262
Gm44758	0,0461341	-7,45622
A130050O07Rik	0,0307467	-7,96171
Gm5546	0,0111235	-9,03539

Supplementary Table 4: Antibodies used in this study

	Antibody	Fluorochrome	Source	Catalog number
	2B4	APC	eBioscience	17-2441-80
	2B4	PE-cy7	Invitrogen	25-2441-82
	7AAD	Percp-cy5.5	Invitrogen	00-6993-50
	Annexin V	APC	Immuno Tools	31490014
	Annexin V	PE	Immuno Tools	31490016
	CCR6	APC	eBioscience	17-1969-42
	CD11b	BV605	BD Biosciences	563015
	CD11c	PE-Cy7	Invitrogen	25-0114-82
	CD122	ef450	eBioscience	48-1222-82
	CD127	FITC	eBioscience	11-1271-82
	CD19	BV786	BD Bisociences	563333
	CD197	TexasRed	BD Biosciences	563596
	CD25	PE-Cy7	Invitrogen	25-0251-82
	CD3	APC780	Invitrogen	470031-82
	CD3	APC	BD Biosciences	553066
	CD3	PE-cy7	eBioscience	25-0031-82
	CD4	PE	eBioscience	553730
	CD4	ef450	Invitrogen	48-0041-82
	CD4	APC	Invitrogen	17-0042-82
	CD4	BV711	BD Bioscience	563050
	CD44	BV786	BD Bioscience	563736
	CD45.2	FITC	Invitrogen	11-0454-85
	CD45.2	APC-Cy7	BD Bioscience	560694
	CD45.2	BV711	BD Biosciences	563685
	CD45.2	Percp-cy5.5	eBioscience	45-0454-82
	CD45.2	ef450	eBioscience	48-0454-82
	CD62L	BV510	BD Biosciences	563117
	CD69	AlexaFluor 700	BD Biosciences	561238
	CD8	APC-Cy7	eBioscience	47-0081-82
	CD8	FITC	Invitrogen	11-0081-85
	CD8	Percp-cy5.5	Invitrogen	46-0081-82
	CD8	BV510	BD Biosciences	563068
	CD8	BV711	BD Biosciences	563046
	CXCR5	BV650	BD Biosciences	563981
	Eomes	PE-eFour610	eBioscience	61-4875-82
	F4/80	APC	eBioscience	17-4801-82
Anti-mouse	F4/80	Percp-cy5.5	Invitrogen	45-4801-82
	FOXP3	PerCP-Cy7	eBioscience	45-5773-82
	GATA3	FITC	eBioscience	53-9966-41
	Gp33 tetramer	APC	NIH tetramer facility	
	Granzyme B	PE	Invitrogen	12-8898-82
	IFNg	APC	Invitrogen	17-7311-82
	IgG2a kappa Isotype	FITC	eBioscience	11-4724-42
	IgG2b kappa Isotype	PE	eBioscience	12-4031-82
	IgG2b kappa Isotype	APC	eBioscience	17-4732-81
	IL2	Percp-cy5.5	Invitrogen	45-7021-82
	KLRG1	ef450	Invitrogen	48-5893-82
	KLRG1	BV650	Invitrogen	645893-82
	Lag3	BV711	BD Biosciences	563179
	Ly6C	APC-Cy7	Invitrogen	47-5932-82
	Ly6C	Percp-cy5.5	Invitrogen	45-5931-82
	Ly6G	APC-780	eBioscience	47593182
	Ly6G	FITC	eBioscience	11-5931-85
	MHC Class I	FITC	BioLegends	125507
	MHC Class I (H-2Db)	FITC	eBioscience	11-5999-85
	MHC Class I (H-2Db)	APC	eBioscience	17-5999-80
	MHC Class I (H-2Kb)	PE	Invitrogen	12-5958-82
	MHC Class I (H-2Kb)	FITC	eBioscience	11-5958-82
	MHCII	AlexaFluor 700	Invitrogen	56-5321-82
	MHCII	APC-780	eBioscience	47-5321-82
	NK1.1	PE-cy7	Invitrogen	25-5941-82
	Np396	APC	NIH tetramer facility	
	PD1	PE-CF594	BD Biosciences	562523
	PD1	FITC	eBioscience	11-998182
	PD-L1	PE	Invitrogen	12-5982-82
	PD-L1	APC	Invitrogen	17-5982-82
	Perforin	FITC	Invitrogen	11-9392-82
	RORyt	APC	eBioscience	17-6988-80
	SINGLEC-H	PE	Invitrogen	12-0333-82
	T-bet	PE-Cy7	Invitrogen	25-5825-82
	T-bet	PE	eBioscience	12-5825-80
	TIM3	PE	eBioscience	12-5870-82
	TNFa	ef450	Invitrogen	48-7321-82
	HLA A-C	PE	Invitrogen	12-9983-42
Anti-human	HLA DR	APC	Invitrogen	17-9956-42
	PD-L1	APC	Invitrogen	17-5983-42

Supplementary Table 5: List of used primers

Name	Forward	Reverse
HTR1A	GACAGGCGGCAACGATACT	CCAAGGAGCCGATGAGATAGTT
HTR1B	CGCCGACGGCTACATTTAC	TAGCTTCCGGGTCCGATACA
HTR1D	ATCACCGATGCCCTGGAGTA	GCCAGAAGAGTGGAGGGATG
HTR1F	ACACGTACAACAGATGATGTCG	ATCAACTCCCTCGTGATCGC
HTR2A	TAATGCAATTAGGTGACGACTCG	GCAGGAGAGGTTGGTTCTGTTT
HTR2B	CCGCGAGTATCAGGAGAGC	GAACAAAGCACAACTTCTGAGC
HTR2C	CTAATTGGCCTATTGGTTTGGCA	CGGGAATTGAAACAAGCGTCC
HTR4	CAGCAGGTTGCCCAAGATG	AGTTCCAACGAGGGTTTCAGG
HTR5A	CACTCGGAAAGCTGAGAGAAAA	ATGGATCTGCCTGTAAACTTGAC
HTR6	CATCAGGTCCGACGTGAAGAG	GCTGTGCGTGGTCATCGTA
HTR7	CCGACCTCTACGGCCATCT	TCTCGACTCTGCCATAGTTGAT
TAP1	GGACTTGCCTTGTTCCGAGAG	GCTGCCACATAACTGATAGCGA
TAP2	CTGGCGGACATGGCTTTACTT	CTCCCACTTTTAGCAGTCCCC
TAPBP	GGCCTGTCTAAGAAACCTGCC	CCACCTTGAAGTATAGCTTTGGG
GAPDH	TGCACCACCAACTGCTTAG	GGATGCAGGGATGATGTTC
ActB	GGCTGTATTCCCCTCCATCG	CCAGTTGGTAACAATGCCATGT
H-2Db	ACCCAGGACATGGAGCTTGT	GCTCCAAGGACACCCAGAAC
H-2Kb	TTGAATGGGGAGGAGCTGAT	GCCATGTTGGAGACAGTGGA
B2m	TaqMan Ref Mm00437762_m1	
Ifna1	TaqMan Ref Mm03030145_gH	
Ifnb1	TaqMan Ref Mm00439552_m1	
Ifng	TaqMan Ref Mm99999071_m1	
ActB	TaqMan Ref Mm00607939_s1	

3.3. *PUBLICATION 3:* Deep transfer learning approach for automated cell death classification reveals novel ferroptosis-inducing agents in subsets of B-ALL.

Deep transfer learning approach for automated cell death classification reveals novel ferroptosis-inducing agents in subsets of B-ALL.

Paweł Stachura[1,2], Zhe Lu[1], Raphael M. Kronberg[2,3], Haifeng C. Xu[2], Wei Liu[4,5], Jia-Wey Tu[1], Katerina Scharov[1], Ersen Kameri[1], Daniel Picard[1,6,7], Silvia von Karstedt[8,9, 10], Ute Fischer[1], Sanil Bhatia[1], Philipp A. Lang[2], Arndt Borkhardt[1] and Aleksandra A. Pandyra[1,,4, 5#]

[1]Department of Pediatric Oncology, Hematology and Clinical Immunology, Medical Faculty, Heinrich-Heine-University, Moorenstrasse 5, 40225 Düsseldorf, Germany. [2]Department of Molecular Medicine II, Medical Faculty, Heinrich-Heine-University, Universitätsstraße 1, 40225 Düsseldorf, Germany. [3]Mathematical Modelling of Biological Systems, Heinrich Heine University, Düsseldorf, North Rhine-Westphalia, Germany. [4]Institute of Clinical Chemistry and Clinical Pharmacology, University Hospital Bonn, Venusberg-Campus 1, 53127 Bonn, Germany. [5]German Center for Infection Research (DZIF), Partner Site Bonn-Cologne, Bonn, Germany. [6]German Consortium for Translational Cancer Research (DKTK), partner site Essen/Düsseldorf, Düsseldorf, Germany. [7]Division of Pediatric Neuro-Oncogenomics, German Cancer Research Center (DKFZ), Heidelberg, Germany. [8]Department of Translational Genomics, Medical Faculty, University of Cologne, Weyertal 115b, Cologne 50931, Germany. [9]CECAD Cluster of Excellence, University of Cologne, Joseph-Stelzmann-Strasse 26, Cologne 50931, Germany. [10]Center for Molecular Medicine Cologne, Medical Faculty, University Hospital of Cologne, Robert-Koch-Straße 21, Cologne 50931, Germany.

[#]Address correspondence to: apandyr1@uni-bonn.de

Abstract

Ferroptosis is a recently described type of regulated necrotic cell death whose induction has anti-cancer therapeutic potential, especially in hematological malignancies although efforts to uncover novel ferroptosis-inducing therapeutics have so far been largely unsuccessful. In the current investigation, we classified brightfield microscopy images of tumor cells undergoing defined modes of cell death using deep transfer learning (DTL). The trained DTL network was subsequently combined with high-throughput pharmacological screening approaches using automated live cell imaging to identify novel ferroptosis-inducing functions of the polo-like kinase Inhibitor volasertib. Validation indicated that subsets of B-cell acute lymphoblastic leukemia (B-ALL) cell lines, namely 697, NALM6, HAL01, REH and primary patient B-ALL samples were sensitive to ferroptosis induction by volasertib and accompanied by an upregulation of ferroptosis-related genes post-volasertib treatment. Importantly, using a syngeneic leukemia model, we determined that volasertib induced ferroptosis *in vivo* and upregulated the ferroptosis mediator Acyl-CoA synthetase long-chain family member 4 (ACSL4). Taken together, we have applied DTL to automated live-cell imaging in pharmacological screening to identify novel ferroptosis-inducing functions of a clinically relevant anticancer therapeutic.

Introduction

Cell death is central to homeostatic physiological processes and its dysregulation is linked to several human diseases. The ability to effectively assess cell death is crucial to many assays used in drug development, particularly for the purpose of uncovering novel anti-cancer therapies. There exists a wide plethora of assays scoring cell death parameters and this is accompanied by increasingly specific and novel classifications(202). Amongst the most expansively-characterized and to some extent interconnected modes of regulated cell death (RCD) that rely on a specific molecular machinery are apoptosis, necroptosis, ferroptosis and autophagy. Both intrinsic and extrinsic apoptotic stimuli eventually converge on the executioner protease caspase 3 (CASP3)(203-206) but otherwise follow different biochemical and molecular upstream sequence of events. Following perturbations such as endoplasmic reticulum stress, intrinsic apoptosis is driven by mitochondrial outer membrane permeabilization (MOMP)(202) mediated by members of the BCL2 apoptosis regulator (BCL2) protein family(207). Extrinsic apoptosis is triggered by binding of ligands (ie. FAS ligand or TRAIL) to death receptors such as those of the TNF receptor superfamily members and downstream caspase-8 activation(208) following its binding to the adapter Fas associated via death domain (FADD) at the death-inducing signalling complex (DISC)(209, 210). Necroptosis, at the molecular level is dependent on RIPK1 and/or 3 activation and mixed lineage kinase domain like pseudokinase (MLKL) following engagement of death receptors or toll-like receptors (TLR)(211, 212). Ferroptosis is caspase-independent(213) and occurs as a result of excess accumulation of iron-dependent lipid reactive oxygen species (lipid ROS) and ensuing lipid peroxidation controlled by the glutathione (GSH)-dependent enzyme glutathione peroxidase 4 (GPX4)(214). Autophagy is a cellular degradation pathway that clears damaged proteins and organelles. Autophagy does not directly cause cell death, rather RCD might occur when autophagy is blocked as autophagic responses mediate adaptive stress responses and are often cytoprotective. Perturbations that block or stimulate autophagy have an impact on RCD especially in pathophysiological settings(215). Notably, various modes of regulated cell death differ in their capacity to elicit an inflammatory response which will ultimately impact their

therapeutic efficacy. While the cell death types described above are thought to be an important feature of tissue homeostasis, manipulating these modes of cell death in tumor cells where RCD is dysregulated, will likely have therapeutic implication for tumor clearance as well as immune system stimulation.

The number of assays evaluating cell death is vast and based on several different technique modalities(216, 217). Microscopic (fluorescent cyto/histo chemistry, electron, light), fluorescence activated cell sorting (FACS)-based, luminometric, immunoblotting, spectrophotometric (calorimetry/fluorescence reader based mainly metabolic assays) methods are available with varying degrees of discernibility for the different modes of cell death. Recently, the application of artificial intelligence (machine and deep learning inclusive) has expanded into the medical field. In radiology, for instance, CT, MRI and X-Rays images are analyzed using deep learning approaches to segment brain tumors (218, 219) or to identify pneumonia in chest X-rays(220). An automated deep learning method was used to quantitatively evaluate lung burden changes in patients with coronavirus disease using serial CT scans(221). An image-based environment for capturing, managing, and interpreting pathological information is emerging(222-226). In experimental models, deep learning was able to predict cell death after one hour of exposure to camptothecin(227). Others have developed an algorithm to predict neuronal cell death using a robotic microscopy pipeline(228). We have recently implemented a fast deep learning-based method for classification of patched brightfield images of SARS-CoV-2 infected Vero cells(229). Here we apply this methodology and trained a neuronal network to classify several modes of cell deaths using brightfield microscopy images. Following validation of our neural network, we applied this methodology to a drug screening platform to identify novel death-inducing functions of several drugs which we validated in additional tumor types. Specifically, we found that the polo-like kinase inhibitor volasertib induced ferroptosis in subsets of B-cell acute lymphoblastic leukemia (B-ALL) cell lines, primary patient samples and in an *in vivo* model of leukemia.

Results

Several modes of cell death are induced in L929 cells. To have a cellular system capable of undergoing multiple forms of cell death, we made use of the mammalian adherent L929 cell line derived from murine subcutaneous areolar and adipose tissue(230). Firstly, we treated L929 cells with staurosporine, a phospholipid/calcium-dependent protein kinase inhibitor and common inducer of caspase dependent and independent apoptosis(231) in L929 cells(232). As expected, there was a robust induction of apoptosis as ascertained by Annexin V staining (Annexin $V^+/7AAD^-$ population, early apoptosis + Annexin $V^+/7AAD^+$ population, late apoptosis) 24 hours post-treatment (Figure 1A). Next, when we treated L929 cells with the GPX4 inhibitor RSL3, a known inducer of ferroptotic cell death, we observed an increase in cell death which was entirely reversible by the addition of the ferroptosis inhibitor ferrostatin-1 (Fer-1)(233) (Figure 1B). We corroborated the induction of ferroptosis and its reversibility in L929 cells by also measuring lipid ROS accumulation using BODIPY C11 staining (Figure 1C)(233, 234). Next, we treated L929 cells with TNF-α and the pan-caspase inhibitor zVAD to induce necroptosis. Indeed, we observed the induction of cell death which was reversed by the addition of Necrostatin-1s (Nec-1s), a RIP1 kinase inhibitor and necroptosis blocker (Figure 1D). Furthermore, we also induced autophagy using the mTORC1/2 inhibitor Torin1 and confirmed this through LC3 increases using immunofluorescence (Figure 1E). In our study, we aimed to create a rapid system for cell death classification using morphological differences. Apoptosis is characterized with caspase-dependent cytoskeleton reorganization, which leads to membrane blebbing and finally membrane vesicle generation, called apoptotic bodies(235, 236). Characteristic apoptotic body accumulation was visible in L929 cells induced by staurosporine (Figure 1F). A critical step during ferroptosis execution depends on lipid ROS accumulation that specifically leads to membrane lipid peroxidation(237). Induction of ferroptosis results in damaged membrane integrity likely due to sterical causes within peroxidized polyunsaturated fatty acid (PUFA) tails and cell “ballooning”(238). This was indeed observed upon RSL3 treatment (Figure 1F). TNF-α-induced necroptosis through RIP kinase 1 and 3 interaction consequently leads to MLKL phosphorylation and its oligomerization,

creating a cell membrane pores(239). Additionally, MLKL complex in cell membrane mediates recruitment of Na^+ and Ca^{2+} ion channels(239). Changes in a cell membrane composition, but also cytoskeletal integration leads to cell membrane blebbing, without apoptotic body formation, and finally cell membrane rupture(240) (Figure 1F). Although ferroptosis and necroptosis finally converge on the necrotic morphotype(202), the neural network will likely be able to discern distinguishing subtle and early occurring morphological changes. Autophagy, on the other hand, is a primarily cytoprotective process induced under stress or starvation conditions, however prolonged and pharmacologically activated can lead to cell death(241). Morphologically, autophagy is characterized with cytoplasmic accumulation of double membrane vesicles, autophagosomes, complexes that deliver cellular components to lysosome(241, 242). Also in case of autophagy induction upon the treatment with Torin 1, L929 cells became spindle-shaped with visible vacuoles accumulated in cells, distinct from healthy cells morphotype (Figure 1F).

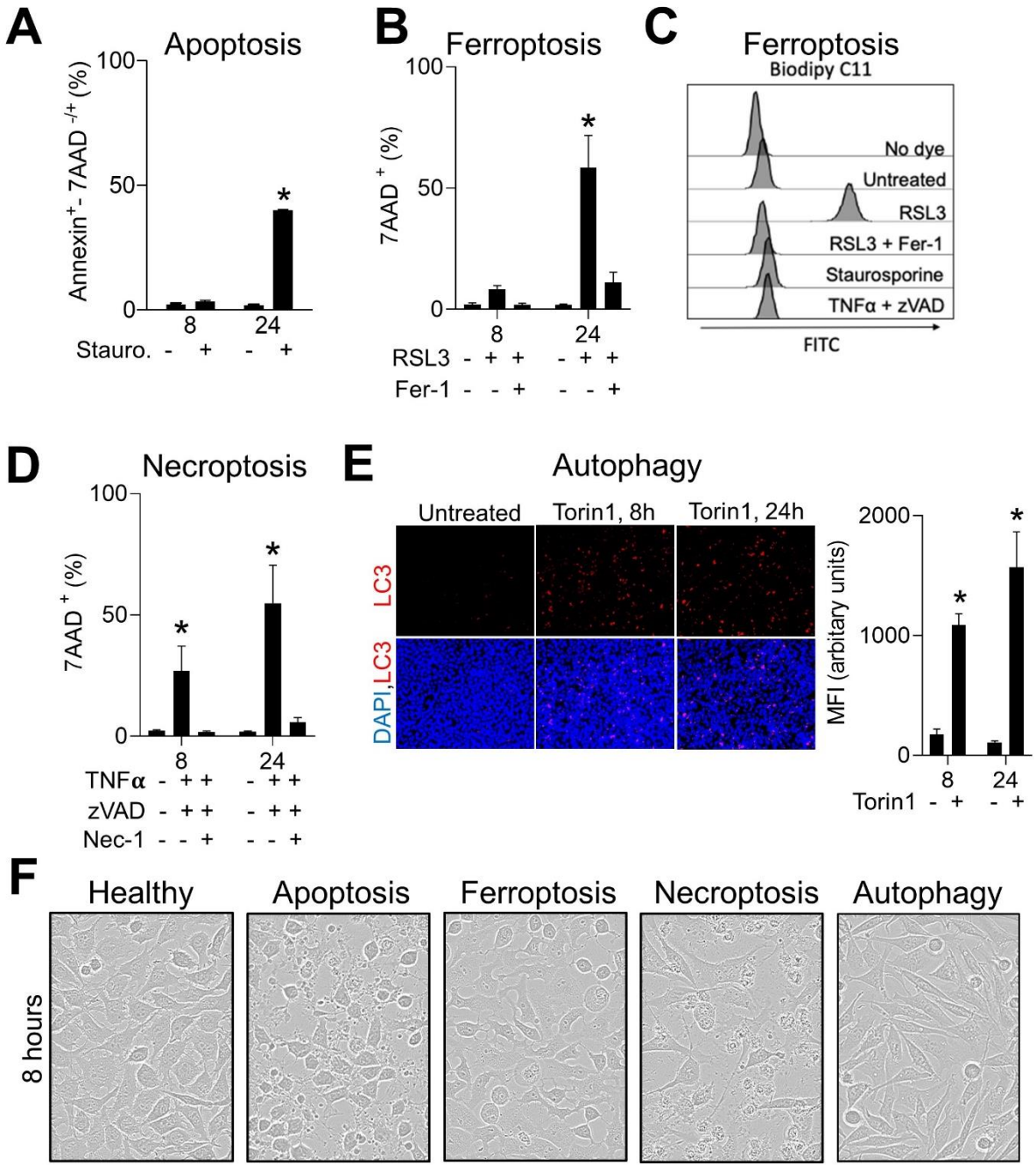

Figure 1. Different modes of cell death can be induced in L929 cells. (A,B) L929 cells were analyzed for 7AAD and/or Annexin V (A) positivity using FACS analysis after 8 or 24 hour treatment with (A) staurosporine (n = 4), (B) RSL3 and Fer1 (n = 4). (C) L929 cells were treated as indicated with the same concentrations as in A,B,D, stained with BODIPY C11 and FACS analyzed in the FITC channel for ferroptosis induction (n = 4, representative histogram shown). (D) L929 cells were analyzed for 7AAD and Annexin V positive cells using FACS after 8 and 24 hour treatment with zVAD, TNFα and Nec-1s (n = 4),. (E,Left panel) L929 cells were treated with Torin1 for 8 or 24 hours and evaluated for LC3 and DAPI staining using immunofluorescence (Representative image of n of 4 is shown). LC3 fluorescent signal was quantified in the right panel (F) Representative brightfield images of L929 cells after 8 hour treatment with staurosporine for apoptosis induction, RSL3 for ferroptosis induction, zVAD and TNFα for necroptosis induction and Torin1 for autophagy induction are shown (Representative image of n of 3 are shown). In every experiment the following concentrations were used: staurosporine (1 μM), zVAD (40 μM), TNFα (40 ng/ml), RSL3 (1 μM), Torin1 (5 μM), Nec-1s (10 μM) and Fer1 (5 μM). Error bars in all experiments indicate SEM; *P < 0.05 as determined by a Student´s t-test (unpaired, 2-tailed) or a 1-way ANOVA with a Dunnett's post-hoc test.

Retraining of a convolutional neural network predicts different models of cell death for brightfield images. Next, we set up the Incucyte® Live-Cell Analysis imagining system microscope to acquire brightfield images of L929 cells taken every hour following treatment with the apoptosis, ferroptosis, necroptosis and autophagy inducers. One picture of each well of a 384 well plate was taken every hour for 24 hours (Figure 2A) and this was repeated three independent times. In order to discern subtle morphological changes before any convergence on common morphotypes and before measurable cell death using biochemical, and/or other microscopic methods, the 8 hour time point was selected to train the Resnet50 neural network (223, 243). Accordingly, to retrain 'Resnet50′ to distinguish ferroptosis, apoptosis, necroptosis and autophagy from each other and healthy L929 cells, larger images (1408 x 1040) from the first two independent experiments were dissected into the required input image size (224 × 224) for 'Resnet50′ using Adam as the optimizer (Figure 2B). The third experiment was used for independent evaluation. In total, 108 images of each condition (healthy, apoptotic, ferroptotic, autophagic and necroptotic cells) were split into 64 images for training, 22 for validation and 22 for testing. The network could accurately predict all modes of cell death with almost 100% accuracy for the 8 hour time point (Figure 2C, D). An f1 score of 1.00 for apoptosis ferroptosis and necroptosis was achieved and 0.97 and 099 for autophagy and healthy cells respectively (Table 1). The network could predict the mode of cell death for the duration of the 24 hours for apoptosis and autophagy but at the later time points (past 14 hours) ferroptosis was classified as necroptosis which is expected as they eventually converge on the necrotic morphotype(202) (Supplementary Figure 1A). Taken together, we have successfully applied a neural network to train bright field images to identify four different modes of cell death.

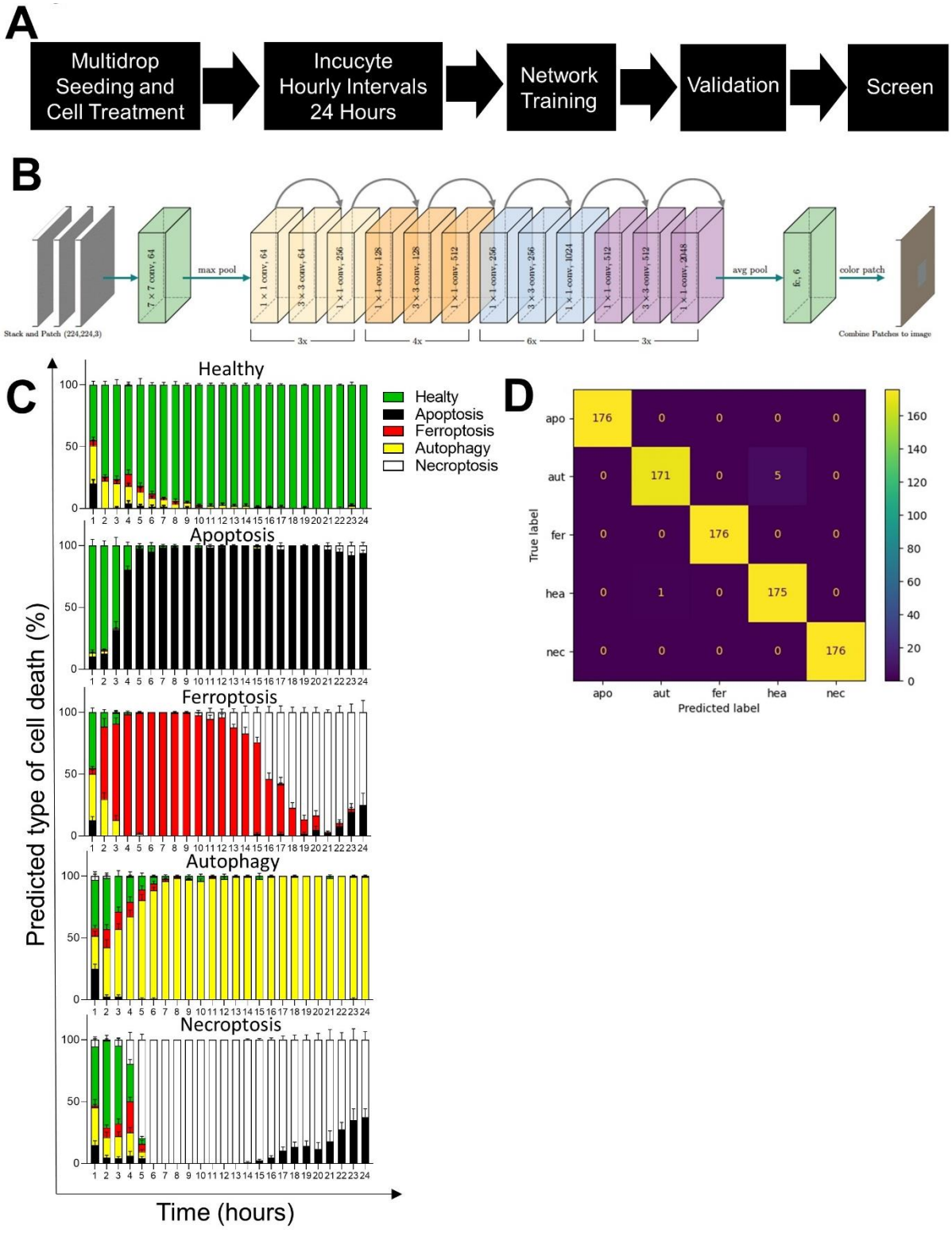

Figure 2. Deep transfer learning is used for automated recognition of different types of cell death. (A) Schematic representations of the workflow in training / fine-tunning CNN and drug screening and (B) CNN architecture and example of image classification are shown. (C) Deep learning images classification from L929 cells induced with the corresponding type of cell death stimuli during a 24 hour time course are shown. (D) Confusion matrix of cell death modes predicted by DTL ResNet50 versus final categorization by a biologist is shown. The y-axis represents the evaluated labels and the x-axis the predicted labels of cell death. The color gradient indicates the number of images.

Retraining of a convolutional neural network can be applied to a high throughput screen. L929 cells were screened using a library of clinically active chemotherapeutic and targeted-therapy anti-leukemia drugs at a wide concentration range (5nM - 25μM)(244). Again, images were acquired every hour and fed into the convolutional neural network (CNN). As most of the drugs constituting the library have been in the clinic for years, their mode of action can be classically attributed to inducing apoptotic or anti-proliferative effects. As expected, many of these drugs were identified by the CNN as pro-apoptotic or having no effects in L929 cells (Table 2). Bortezomib is clinically effective in treatment of T-cell acute lymphoblastic leukemia and lymphoma(245) and has mainly been reported to induce apoptosis in leukemia and solid tumor cell lines(246). Indeed, bortezomib-inducing modes cell death include immunogenic cell death(247), necroptosis as a single agent(248, 249) and in combination with toll-like receptor (TLR). Strikingly, this capacity of bortezomib to also induce necroptosis under certain contexts was corroborated by our deep learning approach and screening strategy (Figure 3). In addition, the known autophagy inducer 6-Thioguanine(250) was successfully identified by our screening approach and interestingly, the HSP90 inhibitor PUH71 also induced autophagy in L929 cells. Moreover, known apoptosis inducing FLT3 inhibitors (midostaurin, lestaurib), AT9283 (Aurora Kinase) and others were correctly classified (Figure 3 and Table 2) altogether verifying the validity of our novel screening approach. Interestingly, several novel ferroptosis-inducing activities were identified amongst the molecules screened (Figure 3 and Table 2). Notably, this includes volasertib, designed to function as a polo-like kinase (PLK) inhibitor with a high potency against mitosis-controlling PLK1, PLK2 and PLK3 (122). Inhibition of PLK with volasertib has been shown to induce mitotic arrest, inhibit proliferation and induce apoptosis(122, 251). The only report, to our knowledge, connecting volasertib with ferroptosis is a bioinformatics study in which primary breast cancer expression data with a ferroptosis-related gene signature was predicted to be responsive to volasertib treatment(252). Therefore, we decided to further validate the ferroptosis-inducing functions of volasertib.

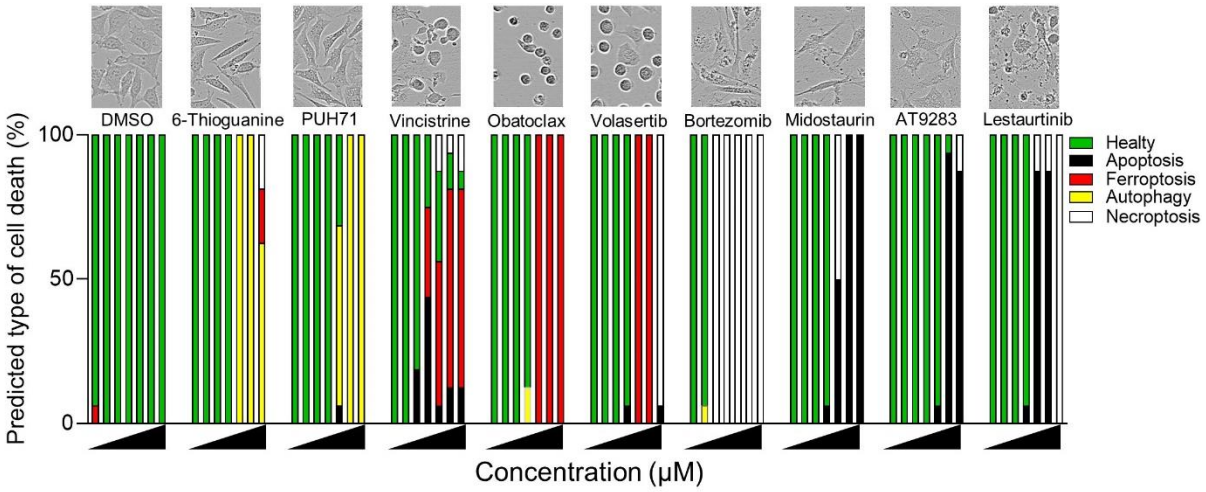

Figure 3. Deep transfer learning combined with drug screen successfully classifies 4 different modes of cell death. Brightfield images were acquired of L929 cells treated with increasing concentrations of drugs from a library of 84 compounds. Images were classified using the DLT learning program to identify different modes of cell death. Several examples of drugs and their classification at the 8-hour time-point are shown with the accompanying representative brightfield image.

Subsets of precursor B-cell lymphoblastic leukemia (B-ALL) are sensitive to RSL3 and volasertib-mediated ferroptosis. It has been suggested that cells that are resistant to other forms of cell death may be sensitive to ferroptosis(253). Furthermore, the link between ferroptosis induction and sensitization to immunotherapies is an exciting approach to uncover novel tumor vulnerabilities(254, 255). Notably, some hematological malignancies including leukemias have been suggested to be ferroptosis-sensitive in part due to an elevated steady-state oxidative stress potential (256, 257). To understand if ferroptosis might impact leukemia patient survival we mined data from the large gene expression collection of leukemia patient database (MILE study)(258) for patients' survival according to an expression of genes known to be involved in ferroptosis. Lower expression of major ferroptosis protective genes namely *GPX4, FTH1 and SLC7A11* correlated with significantly better survival (Figure 4A). Although the functional consequences of this stratification are not clear in the context of actual ferroptosis induction, we reasoned that decreased *GPX4, FTH1 and SLC7A11* levels might facilitate ferroptosis induction in leukemia cells. We therefore firstly assessed whether cell

death was induced in leukemia cells following treatment with a known-ferroptosis inducer and GPX4 inhibitor RSL3(259) in parallel to volasertib. We observed that some B-ALL subtypes namely 697 (*TCF3::PBX1*+), NALM6 (*DUX4*-rearanged), SUPB15 (*BCR::ABL1*+), HAL01 (*TCF3::HLF*+) and the *ETV6::RUNX1* positive REH's presented with significantly reduced viability after RSL3 and volasertib treatment (Figure 4B). To further validate whether volasertib and RSL3 induced ferroptosis, we quantified lipid ROS accumulation using BODIPY C11 post-treatment(234). Both RSL3 and volasertib were able to significantly induce lipid ROS accumulation in several subtypes of B-ALL including 697, NALM6, HAL01, SUPB15 and REH. Importantly, lipid ROS accumulation was specifically reversed upon co-treatment with Fer-1, a lipophilic radical scavenger and inhibitor of ferroptosis(213) (Figure 4C). Strikingly, treatment of NSG mice-transplanted primary patient B-ALL (primary B-ALL) but not healthy $CD19^+$ cells purified from the blood of healthy donors resulted in significant BODIPY C11 accumulation following volasertib treatment (Figure 4D).

Next, we wondered how the ability to induce ferroptosis translates into anti-cancer drug sensitivity in the context of a therapeutic index. We used a navigable drug sensitivity profile tool recently provided by the interactive online Functional Omics Resource of ALL (FORALL)(260) which includes both RSL3 and volasertib in its drug repertoire. FORALL assigns a selective drug sensitivity score (sDSS, using the CellTiter Glo cell viability assay) against 43 leukemia cells lines (25 BCP-ALL, 16 T-ALL, and 2 B-ALL) by normalizing to the response of normal bone marrow, a high sDSS thereby implying a high therapeutic index with low toxicity in healthy cells. The top twenty sDSS scores were plotted for each cell line (Figure 4E). Only B-ALL cell lines has a discernible RSL3 sDSS score including the REH, HAL01 and NALM6 cells that we uncovered as being sensitive to ferroptosis induction using our deep-learning screening approach (Figure 4E). Many hematological malignancies are exquisitely sensitive to the anti-proliferative/pro-apoptotic functions of volasertib(261-263) and this is reflected in the high sDSS scores for the drug across B/T-ALL cell lines. Sensitivity to volasertib does not necessarily correlate to ferroptosis induction and it is clear that volasertib selectively induces ferroptosis in specific B-ALL cell lines and primary leukemia patient samples.

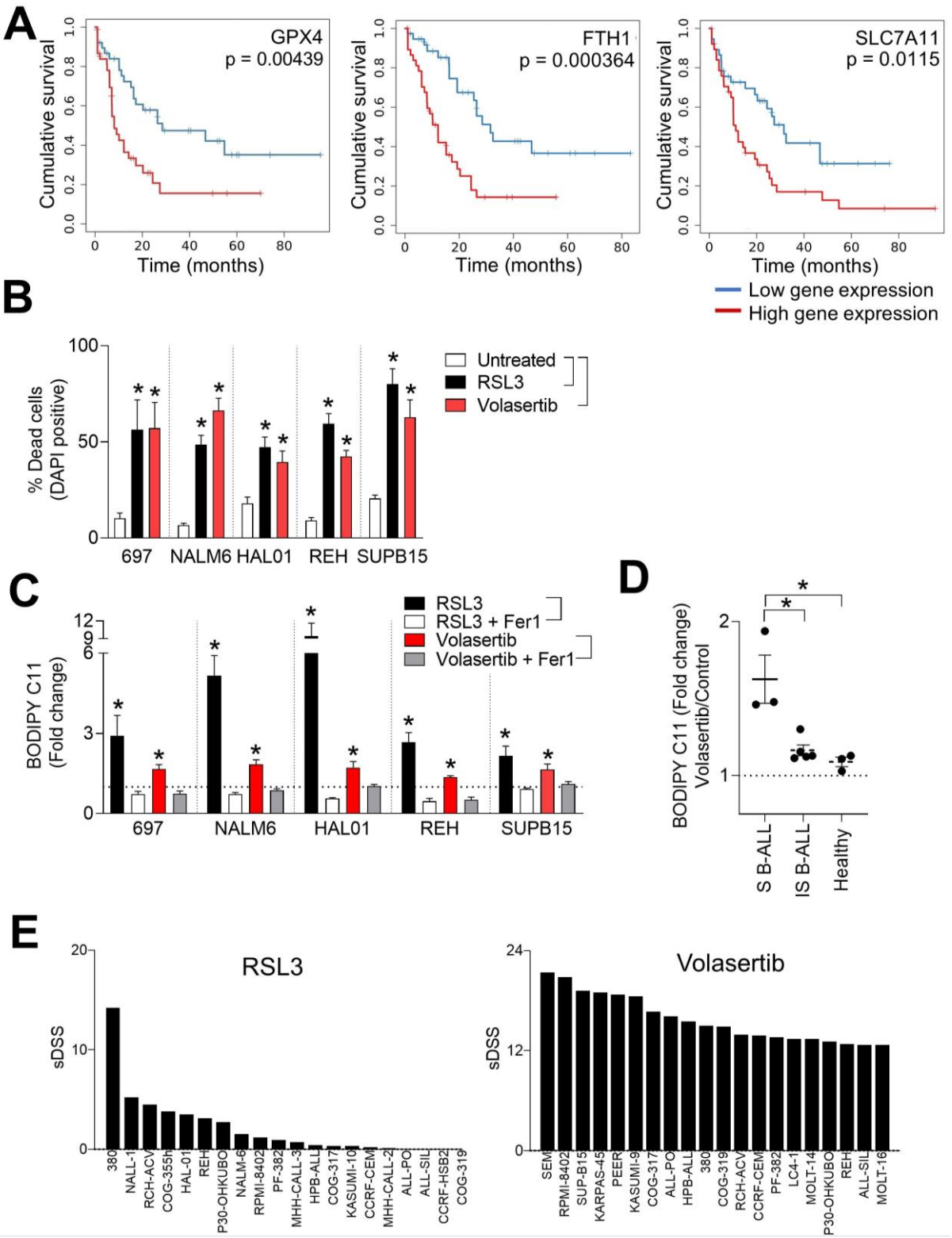

Figure 4. B-ALL cells are sensitive to ferroptosis induction. (A) Kaplan–Meier survival curves for patients with leukemia (n = 173, from the TCGA LAML cohort) were stratified according to *GPX4, FTH1 and SLC7A11* transcript expression. (B) Cell death was measured by evaluating the percentage of DAPI positive cells using FACS after 72 hours treatment with 1 μM RSL3 or 6 μM volasertib (n = 4-8). (C) Ferroptosis induction in several human B-ALL cell lines and (D) primary patient samples was assessed by measuring BODIPY C11 green fluorescent influx following treatment with RSL3 (1 μM) or volasertib (6 μM) alone and in combination with Fer1 (5 μM) for 24 hours (n = 3-9). Primary patient samples were stratified as ferroptosis sensitive (S B-ALL) and ferroptosis insensitive (IS B-ALL). (E) Top 20 cell line

selective drug sensitivity (sDSS) RSL3 and volasertib scores from the online FORALL resource are shown. Error bars in all experiments indicate SEM; *P < 0.05 as determined by a Student´s t-test (unpaired, 2-tailed) or a 1-way ANOVA with a Dunnett's post-hoc test.

Volasertib induces a ferroptosis gene signature in B-ALL. In contrast to other types of regulated cell death, the currently known molecular machinery for ferroptosis hinges upon the collapse of the lipid ROS-specific antioxidant defenses. Mechanisms involved in ferroptosis are dependent on the interplay between the antioxidant pathway, control of cellular iron levels and metabolism of lipids(194, 198). The antioxidant pathway depends on the cysteine transporter SLC7A11 and glutathione peroxidase 4 (GPX4)(264). A main source of ROS during ferroptosis is through iron catalyzed in the Fenton reaction and to counteract this cells regulate levels of free iron by upregulating iron chelating ferritin (FTH1)(264, 265). A distinct hallmark of ferroptosis is increased peroxidation of membrane phospholipids(266) where acyl-CoA synthetase long-chain family member 4 (ACSL4) plays a crucial role through the incorporation of polyunsaturated fatty acids (PUFAs) into membrane lipids(196). Increased transcript levels of prostaglandin-endoperoxide synthase 2 (PTGS2) is also characteristic of ferroptosis marker(266). We, therefore, analyzed changes in cell lines and patient-derived B-ALL samples 24 hours post volasertib treatment. We observed an upregulation of antioxidant pathway genes NFE2L2, AIFM2, ACSL4 and GPX4 which was the most pronounced in the NALM6, 697 and REH's (Figure 5A). Similar to other studies(267), we also noticed increased mRNA levels of ferritin (FTH1) suggesting an accumulation of iron. To test this, we stained cells with FerroOrange, a dye that labels ferrous (Fe^{2+}) ions serving as a substrate for the ROS-producing Fenton reaction. Indeed, 24 hours post volasertib treatment, there was a robust accumulation of iron ions in B-ALL cell lines suggesting induction of ferroptosis (Figure 5B). Volasertib treatment downregulated expression of *SLC7A11* (Figure 5A) suggesting lower levels of cellular glutathione (GSH), a main antioxidant and a substrate of GPX4, that can sensitize cells for ferroptosis(268). When we supplemented volasertib treated cells with GSH, we observed a reversal of lipid peroxidation in NALM6 and SUPB15 cells (Figure 5C), but also increased viability (Figure 5D). Interestingly, when we re-analyzed available online

(GSE103068) RNA sequencing data of a volasertib-treated human AML cell line MV-4-11B(269), there was an activation of synthesis and metabolism of ROS (Supplementary Figure 2A). Furthermore, as confirmed by our results in B-ALL cells, when ferroptosis related genes were identified on a volcano plot, it was evident that volasertib induced expression of *NFE2L2, GPX4* and *ABCC1* (Supplementary Figure 2B). Furthermore, when we evaluated ferroptosis gene related changes in primary patient samples, the samples termed ferroptosis-sensitive according to their BODIPY C11 accumulation (Figure 4D) responded to volasertib treatment by significantly upregulating *CHAC1, NFE2L2, SLC7A11* and *NFS1* (Figure 5E). Taken together, we demonstrate that volasertib treatment induced the accumulation of ROS, iron ions and upregulated antioxidant pathway across leukemia cell lines and volasertib-responsive patient-derived B-ALL samples.

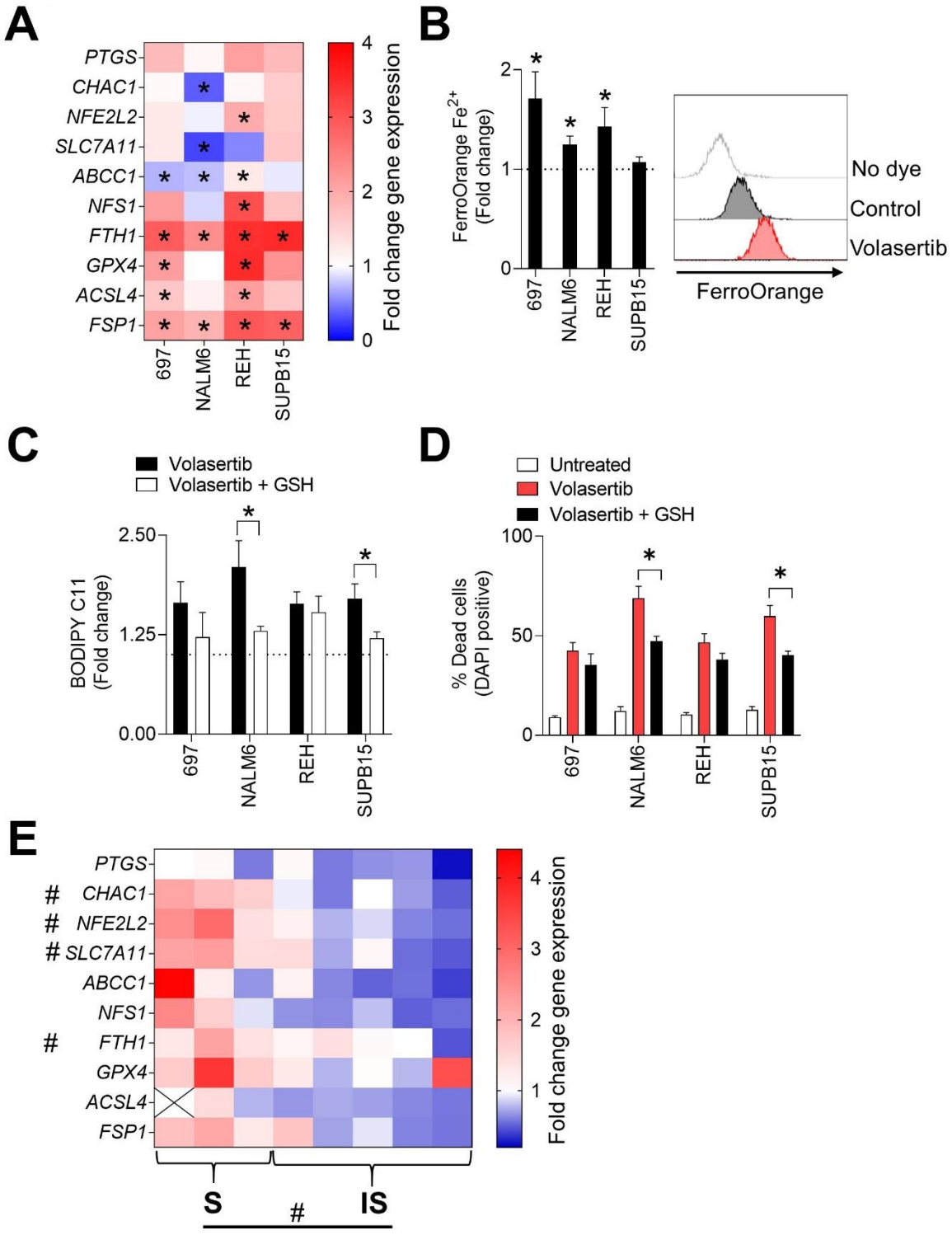

Figure 5. Sensitive B-ALL cells upregulate ferroptosis related genes post volasertib treatment (A, E) Heat maps representing fold change of ferroptosis-related genes expression after 24 hours of treatment with 6 µM volasertib relative to untreated (B) B-ALL cell lines and (E) primary patient samples are shown (n = 4-8). (B, left panel) B-ALL cells were treated with 6 µM volasertib for 24 hours and levels of Fe^{2+} were measured using FerroOrange dye by FACS. Relative levels, compared to untreated cells are shown (n = 4-6). Representative shift of the signal is illustrated using the histogram on the right pane (Representative histogram of n of 4-6 is shown). (C,D) B-ALL cells, treated with 6 µM volasertib with supplementation of 5 mM GSH, were FACS-analyzed after 24 hours for lipid peroxidation using BODIPY C11 in C (n = 3-5) or analyzed after 72 hours for DAPI positive cells in D (n = 4). Error bars in all experiments indicate SEM; *P < 0.05 as determined by a Student´s t-test (unpaired, 2-tailed).

Volasertib induces ferroptosis *in vivo.* Next, we wondered about the effects of volasertib in a syngeneic leukemia immuno-competent *in vivo* model. We utilized the C1498 murine leukemia cell line engineered to express GFP and luciferase (C1498-GFP-luc)(270, 271). First, we confirmed ferroptosis induction by assessing ROS dependent lipid peroxidation using BODIPY C11. C1498 cells had a significantly increased level of BODIPY C11 upon RSL3 and volasertib treatment, which was reversed by pre-treatment with Fer1 (Figure 6A). Additionally, viability was decreased with RSL3 and volasertib treatment (Figure 6B), suggesting induction of ferroptosis. Similar to human B-ALL we noticed iron accumulation in C1498 upon volasertib treatment (Figure 6C). Next, we inoculated C57BL/6J mice with C1498-GFP-luc, and, after 7 days, we randomized mice and treated them with 20 mg/kg volasertib or vehicle on day 7, 9, 11 and 13, as previously described (251),(261). The Kaplan-Meier curve shows prolonged survival of volasertib treated mice (Figure 6D).

Next, we addressed whether volasertib induces similar changes in gene expression *in vivo* as observed in in the ferroptosis-sensitive BCP-ALL cells *in vitro*. Previous studies have shown that T cell-derived interferon gamma (IFNγ) can promote ferroptosis *in vivo(254)*. To exclude any potential confounding effects of immune infiltrating cells, we inoculated the immunocompromised NSG mice with C1498-GFP-luc cells. After 10 days, mice were IVIS scanned for tumor engraftment, randomized and treated with volasertib (Figure 6E). To further eliminate confounding effects of differing tumor sizes, we chose a time point where there were no differences in tumor burden (Supplementary Figure 3). We sacrificed mice and isolated GFP positive cells from engrafted organs, stained for 1 hour with BODIPY C11 and analyzed level of peroxided lipids. To account for constitutive GFP expression and baseline level of fluorescence, we included a BODIPY C11-unstained group. Only C1498-GFP-luc cells isolated from volasertib treated mice had elevated BODIPY C11, suggesting ongoing ferroptosis with increased level of ROS and membrane lipid peroxidation (Figure 6F). Additionally, C1498-GFP-luc cells isolated from volasertib treated mice had increased AIFM2 and ACSL4 expression (Figure 6G) suggesting compensatory mechanism during induced ferroptosis similar to the *in vitro* system. Taken together, we demonstrated that volasertib induced

ferroptosis in murine leukemic C1498 cells *in vivo*, *in vitro* and also prolongs survival in C1498 inoculated mice.

Figure 6

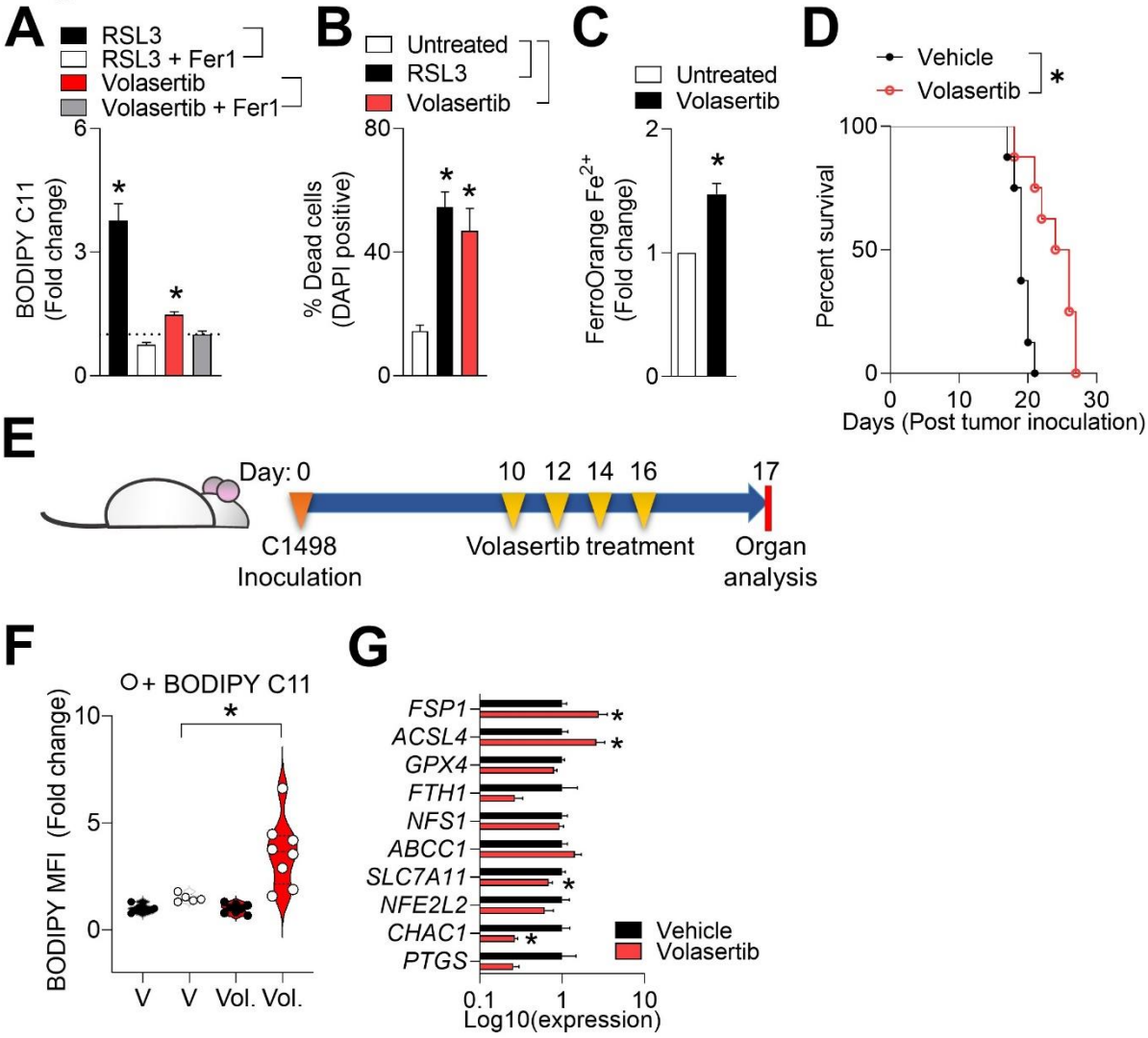

Figure 6. Volasertib induces ferroptosis and increases ACSL4 expression *in vivo*. (A) Lipids peroxidation was measured with BODIPY C11 in C1498 cells following treatment volasertib (6 μM) or RSL3 (1μM) with or without fer-1 (5 μM) for 24 hours (n = 5). (B) Viability of C1498 cells was measured by FACS and analyzed for the percentage of DAPI positive cells after 72 hours of treatment with volasertib (6 μM) or RSL3 (1 μM, n = 8). (C) Level of Fe^{2+} in C1498 cells after 24 hours treatment with 6 μM volasertib was measured by staining with FerroOrange dye and assessed using FACS (n = 6). (D) C57BL/6J mice were intravenously inoculated with 500,000 C1498-luc-GFP cells. After 7 days, mice were randomized by luminescent signal as assessed by IVIS and treated with 20 mg/kg volasertib or vehicle on day 7, 9, 11 and 13 post-inoculation. Survival was monitored (n = 8). (E-G) Schematic representation of the treatment and endpoint regimen is shown in E. NSG mice were inoculated intravenously with 500,000 C1498-luc-GFP cells. Mice were randomized and treated with 20 mg/kg volasertib or vehicle on the indicated days. (F) Leukemia-engrafted spleens of volasertib or vehicle treated mice were stained with BODIPY C11 (n = 6). (G) Expression of genes related to ferroptosis from leukemia-engrafted spleens of volasertib or vehicle treated mice is shown (n = 6). Error bars in all experiments indicate SEM; *P < 0.05 as determined by a Student´s t-test (unpaired, 2-tailed) or a 1-way ANOVA with a Dunnett's post-hoc test. For the Kaplan–Meier survival curve, the log-rank test was used.

Discussion

Artificial intelligence-based deep learning approaches have become indispensable in various applications used to for example classify organisms into specific taxa(272) or in medical imaging (273) (274). In case of pre-clinical research in the field of drug development, there is a need for rapid automated prediction of cell death, especially with the discovery of new modes of cell death. While others have used digital holographic microscopy to classify apoptosis and necroptosis(275), we created a pipeline that can be rapidly implemented, uses easily accessible brightfield images and can differentiate not only between apoptosis and necroptosis, but also autophagy and ferroptosis. Ferroptosis-induction is increasingly recognized as being a vulnerability in many types of cancers and its induction was recently demonstrated to circumvent drug resistance to apoptosis(198),(276). Ferroptosis induction has been shown to be subtype and mutation specific(234, 277). Studies have reported a connection between RAS mutations and sensitivity to ferroptosis induction, which led to the discovery of RSL3 (RAS-selective lethal 3) compound(259). More recent literature supports a concept wherein RAS mutations render cells more resistant to ferroptosis via activation of NRF2 and ensuing FSP1 upregulation(278). It was observed that cancers carrying the NRAS mutation differ in their Peroxisomal Biogenesis Factor 1 (PEX1) expression(279) that was reported to be crucial for generation of lipids with polyunsaturated acids making them sensitive to oxidation(280). The 697, Nalm6 and Hal01 BCP-ALL cells also carry NRAS mutation and whether this property makes them sensitive to ferroptosis induction remains to be further explored. Others have shown that low levels of FSP1 also determine B-ALL sensitivity and upregulation of ferritin represents the major compensatory mechanism for ferroptosis-induction in leukemia(256). Taken together, ferroptosis-induction is increasingly recognized as being a tumor vulnerability in hematological malignancies, particularly leukemia.

Interestingly, evidence of apoptosis induction following volasertib treatment has generally been limited to flow cytometric annexin V/PI cell assays which do not necessarily preclude ferroptosis induction(251, 269, 281, 282). Thus, it is not clear if volasertib-induced

apoptosis requires alternative cancer-type specific classifications as was recently demonstrated for sorafenib, which was found to induce ferroptosis and not apoptosis in some cancers(267, 283, 284). Correct classification of cell death is especially important when it comes to immune activation, since ferroptosis, necroptosis and pyroptosis are considered immunogenic forms of cell death(285) known to induce “eat me” signals on their surface and release high levels of antigens and DAMPs(286). In our system, increased expression of ACSL4 *in vitro* and *in vivo* is particularly important as others have recently shown that elevated ACSL4 modulates cancer cell membrane lipid composition *in vivo* and makes them susceptible to T cell-derived IFNγ induced ferroptosis(254) . Taken together, ferroptosis induction has clinical implications especially in the context of immunotherapeutic combinatorial approaches (287).

Although RSL3 is very effective at inducing ferroptosis *in vitro*, its general toxicity(214) and poor pharmacokinetic precludes it from being utilized as a clinical compound. To potentially identify ferroptosis inducers which meet clinical criteria we specifically chose a clinically relevant small molecular library for the screen. PLK is overexpressed in many cancers and especially leukemia(288, 289), creating a therapeutic vulnerability. As such, volasertib entered phase II clinical trials for elderly patients with relapsed or refractory AML as a monotherapy or in combination with cytarabine resulting in increased complete response and prolonged survival(290, 291). However, as this was not recapitulated in subsequent phase III clinical trials in chemotherapy-naive patients (292), it appears that responders are composed of relapsed or refractory patients as evidenced by currently open new phase II clinical trials designed at identifying further biomarkers of efficacy(293). Notably, another PLK inhibitor used in our screen, BI2536 also induced ferroptosis (Table 2), suggesting connection between polo like kinase and ferroptosis pathway. This should be further explored, taking in consideration recent study on cell cycle arrest sensitizing cancer cells to ferroptosis(294) and PLK properties in cell cycle.

In our study, we observed an upregulation of ferroptosis-related genes in B-ALL cell lines and the ferroptosis-sensitive primary B-ALL patient samples upon volasertib treatment. Several studies have also observed such changes(267),(295). The upregulation of antioxidant pathway upon ferroptosis-induction may represent a compensatory mechanism that cells employ to counteract the effects of ferroptosis and this may have potential clinical implications in deriving a ferroptosis-responsive expression signature and identify predictors of response sensitivity. It's conceivable that cancer cells with dysregulated oxidative pathways are ferroptosis insensitive. Importantly, ferroptosis inducing agents are associated with overcoming chemoresistance as recent studies suggest that cancer cells resistant to typical apoptosis inducing molecules are highly dependent on GPX4(198, 253), which could also potentially explain the successful outcome of volasertib in phase II of clinical trial on relapsed or refractory AML, but not on therapy-naive patients.

Material and methods

Deep learning

For Comparison and Evaluation of our models we used the following five metrics, we show the metrics for the binary case.

The scores of the metrics are in the Interval [0, 1] and so greater the score so better.

$$Precision = \frac{TP}{TP + FP}$$

$$Recall = \frac{TP}{TP + FN}$$

$$F1 - Score = \frac{2TP}{2TP + FP + FN}$$

$$Jaccard - Score = \frac{TP}{TP + FP + FN}$$

$$Accuracy = \frac{TP + TN}{TP + FP + TN + FN}$$

For the multiclass (not-binary) case the positive is the target class and the other classes are the negative class. With this definition, we get separate true positive (TP), false positive (FP), true negative (TN), false negative (FN) for each class and therefore separate metrics.

Classification score vector

We defined classification score vector that sums up the classification labels of each patch of an image and point the perceptual portion of this class from the image.

$$c := (c_1, \dots, c_i, \dots, c_N),$$

where i ∈ 1, …, N and N is the number of classes.

With the definition

$$p := (p_1, \dots, p_j, \dots, p_M),$$

where j ∈ 1, … , M and M is the number of patches for this image.

Then we defined

$$c_i := \frac{\sum_{i=1}^{M} 1_{f(p_i = c_i\})}{\sum_{i=1}^{M} 1},$$

where f is the prediction function of the neural network. The dominator guarantees that the sum of the vector entries is equal to one.

Architecture. We used a deep transfer learning approach for our architecture (296) and chose to fine-tune (num_train_layers=3) the convolutional neural network Resnet50 (243) and adapted it for our experiments. To fit the single color channel images (224,224,1) into the input format (three color channel (224,224,3)) of the ResNet50, we stack the same image three times. We used a square image patch size of 224 pixels.

Training. We trained the network with the batch size of 100 and 50 epochs, Early Stopping of 25 on the images of the samples from the data set (n_{train} = 1024 patches for each class) using the expert annotations data set as ground truth. The predicted probability for each image patch to contain each of the labels ('apo', 'aut', 'fer', 'hea', 'nec') was used as the objective/loss function (Cross Entropy Loss) in the training. We used Adam as the optimizer for this deep transfer learning approach and initial learning rate of 0.0001 and a decrease it by 5% each five epochs. Training and validation was performed on a Nvidia A100 of the high performance cluster (HPC, Hilbert) of the HHU, and on Quadro T2000 with Max-Q Design (Nvidia Corp., Santa Clara, CA, USA), depending on the computational power needed.

Evaluation. Evaluation was carried out by applying the previously trained model to the remaining, previously unseen data set (n_{val} = 352, n_{test} = 352 patches for each class) for each sequence set separately and comparing the results with the expert annotations as supplied by the biologist. In addition to the accuracy, we calculated the confusion matrix, the precision, recall, Jaccard index and the F1-score for each class. For Visualization we color each image patch in the color of the predicted class.

Software

We used the Python VERSION:3.8.8 [MSC v.1916 64 bit (AMD64)] software (pyTorch VERSION:1.9.0.dev20210423, CUDNN VERSION:8005). On the high-performance cluster we used the following software: Python VERSION:3.6.5 [GCC Intel(R)\\ C++ gcc 4.8.5 mode] (including pyTorch VERSION:1.8.0.dev20201102+cu110, CUDNN VERSION:8004).

Cell culture. 697 (*TCF3::PBX1*+) , REH (*ETV6::RUNX1*+), NALM6 (*DUX4*-rearanged) and HAL01 (*TCF3::HLF*+) cells were maintained in RPMI 1640 medium supplemented with 10% fetal calf serum (FCS) and glutamine. SUPB15 (*BCR::ABL1*+) cells were cultivated in McCoy's modified medium supplemented with 20% FCS. L929, C1498 (ATCC) and modified C1498-luc-GFP (stably expressing luciferase and GFP) were maintained in Dulbecco's Modified Eagle's medium with 10% FCS. All media were additionally supplemented with penicillin and streptomycin. Cells were incubated at 37 °C in 5% CO2. Human B-ALL cell lines were purchased from (DSMZ) and were additionally identified using short tandem repeats (STR) profiling. Cell cultures were regularly controlled for Mycoplasma negativity using the MycoAlert Detection Kit (Lonza). Staurosporin, Torin1, Nec-1s, zVAD, RSL3, Fer-1, GSH were purchased from Selleckchem and dissolved in DMSO or GSH in PBS. Recombinant murine TNF-α was purchased from R&D Systems and dissolved in PBS.

Flow Cytometry. Cells were washed twice with FACS buffer (PBS with 1% FCS and 5 mM EDTA) or Annexin buffer (ThermoFisher) followed by Annexin V staining. Next, cells were incubated with 7AAD or DAPI and analyzed using FACS (CytoFLEX, BeckmanCoulter). For lipid peroxidation measurements, cells were additionally incubated for the last hour of treatment with 2.5 µM BODIPY C11 (ThermoFisher). FerroOrange (Cell Signaling) staining was performed according to the manufacturer's instructions. Experiments were analyzed using FlowJo software.

Drug screening and Incucyte measurements. L929 cells were seeded on a flat bottom 96-well plate using Multidrop (Thermo Fisher). The next day cells were treated with the indicated compounds and incubated in the Incucyte machine (Sartorius). Leukemia-relevant drugs were dispensed onto a 384-well plate using the Digital Dispenser D300e (Tecan) in randomized well positions for drug screening(297). Next, L929 cells were seeded using Multidrop and incubated in the Incucyte. Brightfield pictures using the Incucyte were taken at an interval of one hour for 24 hours.

Real-time qPCR. Cells were lysed with QIAzol Lysis Reagent (QIAGEN) and RNA was isolated according to the manufacturer's instructions. RNA was transcribed to cDNA (GoScript, Promega) and real-time qPCR analysis was performed according to manufacturer's instructions (GoTaq, Promega).

Mice and *in vivo* treatments. Wildtype C57BL/6J and immunocompromised NSG (NOD.Cg-Prkdcscid H2-K1tm1Bpe H2-D1tm1Bpe Il2rgtm1Wjl/SzJ) mice were maintained in pathogen-free conditions and in the duration of the experiment transferred to standard-barrier conditions. Mice were injected intravenously with 0.5 x 10^6 C1498-luc-GFP cells. IVIS scans were performed on the indicated days, 10 minutes after I.P. injection of 10 µl/g of D-Luciferin (at a

concentration of 15 mg/ml). Scans were performed with the IVIS In Vivo Imaging System (Perkin Elmer) and luminescence signal was analyzed. On day 10 mice were randomized according to engraftment signal and treated with vehicle or volasertib (20 mg/kg) on the indicated days. Experiments were performed under the authorization of LANUV in accordance with the German law for animal protection.

Patient derived cells.

Primary patient leukemia blasts were obtained from BioBank, University Clinic Duesseldorf, after obtaining informed consent in accordance with the Declaration of Helsinki. The experiments were approved by the ethics committee of the Heinrich Heine University medical faculty (Study Nr.: 2019-566). The patient cells were injected intravenously into 6-week-old NSG mice (The Jackson Laboratory)(244). Engraftment of the leukemia cells was verified regularly through examination of the human $CD45^+$ population in peripheral blood four weeks post-inoculation by flow cytometry. Mice were sacrificed at predefined endpoints, where more than 90% of human $CD45^+$ cells were isolated from the BM and spleen of the mice with mouse cell depletion kit (Miltenyi Biotec). The isolated cells were short-term cultivated in RPMI 1640 Glutamax medium (Gibco) supplemented with 15% FCS, 1mM Sodium Pyruvate (Gibco), 0.1 mM 2-Mercaptoethanol (Gibco) and 0.5 µg/ ml Gentamicin (Invitrogen).

Data mining. Kaplan–Meier survival curve data was generated with TIMER2.0 database. Expression of GPX4, SLC7A11 and FHC1 in patients and healthy bone marrow samples were extracted from Microarray Innovations in Leukemia (MILE) database. RNA-sequencing data was taken from open-source NCBI Gene Expression Omnibus (GEO) with accession number GSE103068. Gene expression data were analyzed in-house with Partek flow default settings.

Declarations

Ethics approval and consent to participate. Experiments were performed under the authorization of LANUV in accordance with German law for animal protection.

Patient consent for publication. This study involves human participants with ethical approval.

Competing interests. Authors declare no competing interests.

Funding. AAP receives funding from the José Carreras Foundation (DJCLS 18R/2021) and the German Federal Office for Radiation Protection (BfS). S.v.K. receives funding from a collaborative research center grant on B-cell lymphomas (CRC1530, project ID 455784452), cell death (CRC1403, project ID 414786233), predictability in evolution (CRC1310, project ID 325931972), small cell lung cancer (CRC1399, project ID 413326622), through a priority program on ferroptosis (SPP2306, project ID 461704389) all funded by the German Research Foundation (Deutsche Forschungsgesellschaft, DFG), an eMed consortium grant by the BMBF (InCa-01ZX1901A), via CANTAR which is funded through the program " Netzwerke 2021", an initiative of the Ministry of Culture and Science of the State of Northrhine Westphalia, Germany and a project grant (A06) funded by the center for molecular medicine cologne (CMMC). A.B. and U.F. (FKZ: 3618S32275 and 3618S32274) are supported by the German Federal Office for Radiation Protection (BfS). A.B. (DJCLS 07/19) and U.F. are funded by the German Carreras Foundation (DJCLS 18R/2021, DJCLS 21 R/2019). U.F. is funded by the Deutsche Forschungsgemeinschaft (DFG, German Research Foundation—Projektnummer 495318549) and the German Cancer Aid (Priority Program Cancer Prevention—Graduate School). S.B. acknowledges the financial support by the Elterninitiative Kinderkrebsklinik e.V. and Deutsche Forschungsgemeinschaft (DFG, German Research Foundation) – 270650915 (Research Training Group GRK2158, TP2d) and BH 162/4-1 (528968169).

Authors' contributions. PS, ZL, WL, JWT, KS and EK performed experiments. JWT, KS, SB and AB provided patient samples. RMK wrote the deep learning program and with PS analyzed images. DP analyzed RNA sequencing data. PS, AAP and PAL were responsible for the conceptualization and methodology. PS and AAP analyzed data. AAP and PS wrote the manuscript. HCX, SvK, UF, SB, PAL and AB discussed the project and provided suggestions.

Supplementary Figure 1

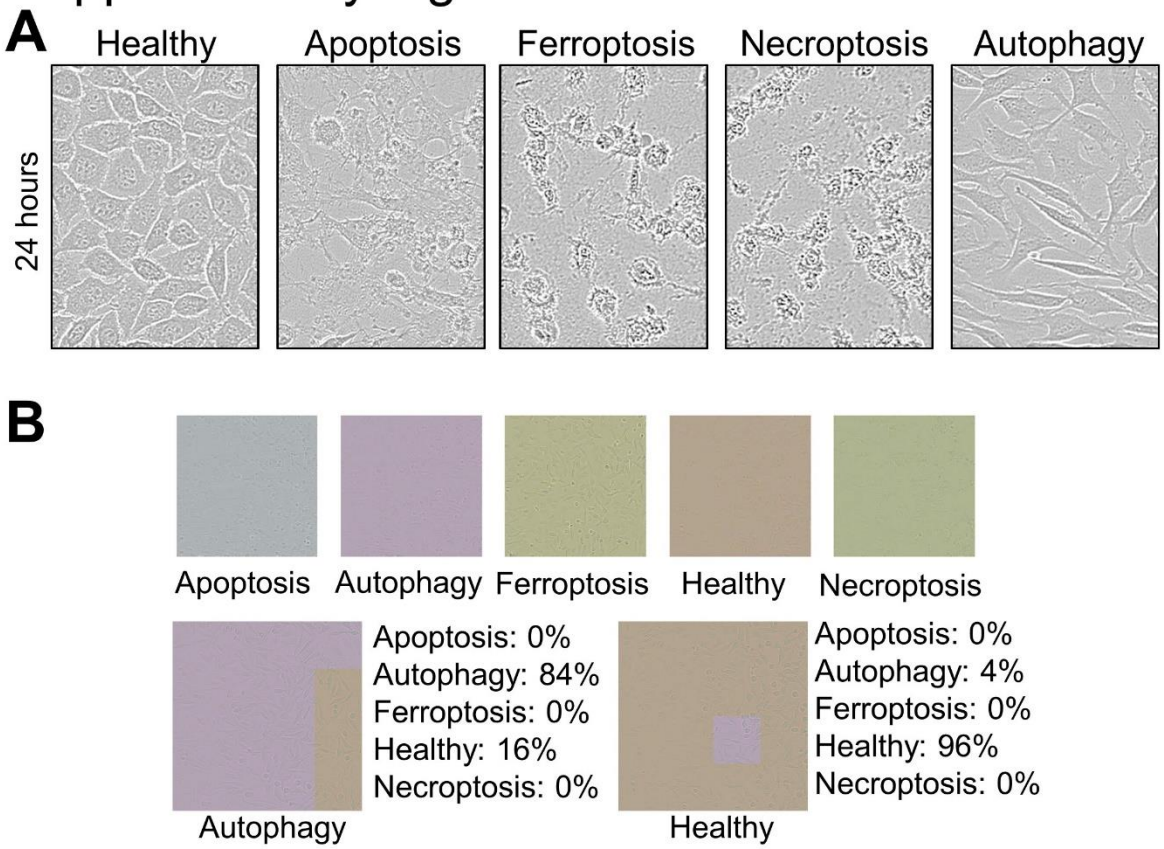

Supplementary Figure 1. **Deep learning algorithm correctly classifies different modes of cell death.** (A) Representative brightfield images of L929 cells treated with staurosporine for apoptosis induction, RSL3 for ferroptosis induction, zVAD and TNFα for necroptosis induction and Torin1 for autophagy induction are shown 24 hours post-treatment. Cells were treated with 1 μM staurosporine, 40 μM of zVAD, 40ng/ml of TNFα, 1μM of RSL3, 5 μM of Torin1, 10 μM of nec-1 and 5 μM Fer1. (B) Color coded classification type of cell death in panel above and representative validation of images deep learning classification from L929 cells induced with the corresponding type of cell death in bottom panel are shown.

Supplementary Figure 2

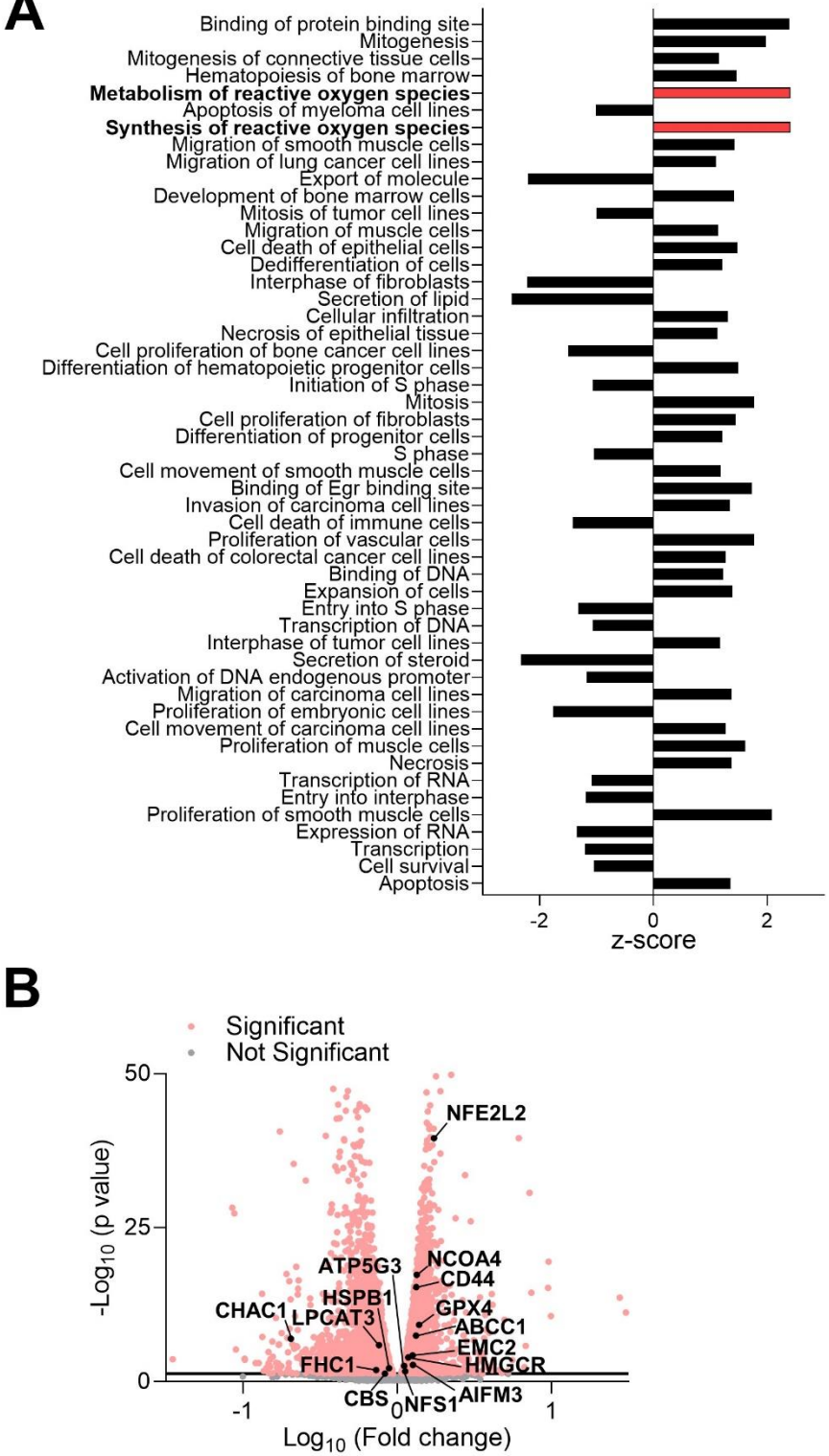

Supplementary Figure 2. **Volasertib induces a ferroptosis gene signature.** RNA sequencing data (GSE103068) of the human AML cell line MV-4-11B treated with volasertib were reanalyzed for (A) pathways activation, (B) volcano plot of fold change gene expression with highlighted genes involved in ferroptosis pathway.

Supplementary Figure 3

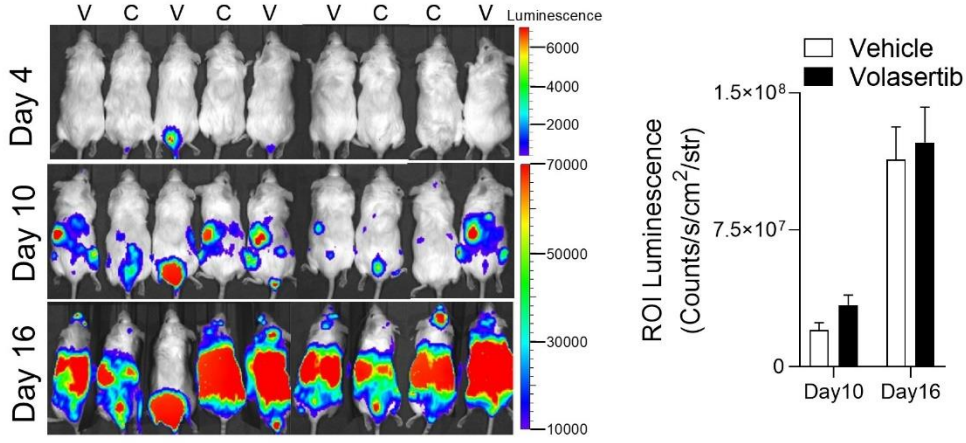

Supplementary Figure 3. Volasertib treatment *in vivo*. NSG mice were inoculated intravenously with 500,000 C1498-luc-GFP cells. Mice were randomized and treated with 20 mg/kg volasertib or vehicle at day 10, 12, 14 and 16 post-inoculation. Representative IVIS scan images of mice treated with volasertib (indicated as V) or vehicle were taken and ROI signal was quantified in the right panel.

References

1. Galluzzi, L. *et al.* Molecular mechanisms of cell death: recommendations of the Nomenclature Committee on Cell Death 2018. *Cell Death Differ* **25**, 486-541 (2018).

2. Zheng, T.S. *et al.* Caspase-3 controls both cytoplasmic and nuclear events associated with Fas-mediated apoptosis in vivo. *Proc Natl Acad Sci U S A* **95**, 13618-13623 (1998).

3. Inoue, S., Browne, G., Melino, G. & Cohen, G.M. Ordering of caspases in cells undergoing apoptosis by the intrinsic pathway. *Cell Death Differ* **16**, 1053-1061 (2009).

4. Walsh, J.G. *et al.* Executioner caspase-3 and caspase-7 are functionally distinct proteases. *Proc Natl Acad Sci U S A* **105**, 12815-12819 (2008).

5. Vitale, I. *et al.* Apoptotic cell death in disease-Current understanding of the NCCD 2023. *Cell Death Differ* **30**, 1097-1154 (2023).

6. Delbridge, A.R., Grabow, S., Strasser, A. & Vaux, D.L. Thirty years of BCL-2: translating cell death discoveries into novel cancer therapies. *Nat Rev Cancer* **16**, 99-109 (2016).

7. Dickens, L.S. *et al.* A death effector domain chain DISC model reveals a crucial role for caspase-8 chain assembly in mediating apoptotic cell death. *Mol Cell* **47**, 291-305 (2012).

8. Muzio, M. *et al.* FLICE, a novel FADD-homologous ICE/CED-3-like protease, is recruited to the CD95 (Fas/APO-1) death--inducing signaling complex. *Cell* **85**, 817-827 (1996).

9. Seidel, E. & von Karstedt, S. Extrinsic cell death pathway plasticity: a driver of clonal evolution in cancer? *Cell Death Discov* **8**, 465 (2022).

10. Linkermann, A. & Green, D.R. Necroptosis. *N Engl J Med* **370**, 455-465 (2014).

11. Murphy, J.M. *et al.* The pseudokinase MLKL mediates necroptosis via a molecular switch mechanism. *Immunity* **39**, 443-453 (2013).

12. Dixon, S.J. *et al.* Ferroptosis: an iron-dependent form of nonapoptotic cell death. *Cell* **149**, 1060-1072 (2012).

13. Yang, W.S. *et al.* Regulation of ferroptotic cancer cell death by GPX4. *Cell* **156**, 317-331 (2014).

14. Klionsky, D.J. *et al.* Autophagy in major human diseases. *EMBO J* **40**, e108863 (2021).

15. Galluzzi, L. *et al.* Guidelines for the use and interpretation of assays for monitoring cell death in higher eukaryotes. *Cell Death Differ* **16**, 1093-1107 (2009).

16. Kepp, O., Galluzzi, L., Lipinski, M., Yuan, J. & Kroemer, G. Cell death assays for drug discovery. *Nat Rev Drug Discov* **10**, 221-237 (2011).

17. Havaei, M. *et al.* Brain tumor segmentation with deep neural networks. *Medical image analysis* **35**, 18-31 (2017).

18. Kronberg, R.M. *et al.* Optimal acquisition sequence for AI-assisted brain tumor segmentation under the constraint of largest information gain per additional MRI sequence. *Neuroscience Informatics* **2**, 100053 (2022).

19. Jaiswal, A.K. *et al.* Identifying pneumonia in chest X-rays: a deep learning approach. *Measurement* **145**, 511-518 (2019).

20. Huang, L. *et al.* Serial quantitative chest CT assessment of COVID-19: a deep learning approach. *Radiology: Cardiothoracic Imaging* **2**, e200075 (2020).

21. Pan, J. *et al.* An artificial intelligence model for the pathological diagnosis of invasion depth and histologic grade in bladder cancer. *J Transl Med* **21**, 42 (2023).

22. Kronberg, R.M. *et al.* Communicator-Driven Data Preprocessing Improves Deep Transfer Learning of Histopathological Prediction of Pancreatic Ductal Adenocarcinoma. *Cancers (Basel)* **14** (2022).

23. Sun, T. *et al.* Deep learning based on preoperative MR images improves the predictive power of survival models in primary spinal cord astrocytomas. *Neuro Oncol* (2022).

24. Shamai, G. *et al.* Deep learning-based image analysis predicts PD-L1 status from H&E-stained histopathology images in breast cancer. *Nat Commun* **13**, 6753 (2022).

25. Esteva, A. *et al.* Dermatologist-level classification of skin cancer with deep neural networks. *Nature* **542**, 115-118 (2017).

26. La Greca, A.D. *et al.* celldeath: A tool for detection of cell death in transmitted light microscopy images by deep learning-based visual recognition. *PLoS One* **16**, e0253666 (2021).

27. Linsley, J.W. *et al.* Superhuman cell death detection with biomarker-optimized neural networks. *Sci Adv* **7**, eabf8142 (2021).

28. Werner, J. *et al.* Deep Transfer Learning Approach for Automatic Recognition of Drug Toxicity and Inhibition of SARS-CoV-2. *Viruses* **13** (2021).

29. Sanford, K.K., Earle, W.R. & Likely, G.D. The growth in vitro of single isolated tissue cells. *J Natl Cancer Inst* **9**, 229-246 (1948).

30. Belmokhtar, C.A., Hillion, J. & Segal-Bendirdjian, E. Staurosporine induces apoptosis through both caspase-dependent and caspase-independent mechanisms. *Oncogene* **20**, 3354-3362 (2001).

31. Humphreys, D.T. & Wilson, M.R. Modes of L929 cell death induced by TNF-alpha and other cytotoxic agents. *Cytokine* **11**, 773-782 (1999).

32. Alborzinia, H. *et al.* MYCN mediates cysteine addiction and sensitizes neuroblastoma to ferroptosis. *Nat Cancer* **3**, 471-485 (2022).

33. Bebber, C.M. *et al.* Ferroptosis response segregates small cell lung cancer (SCLC) neuroendocrine subtypes. *Nat Commun* **12**, 2048 (2021).

34. Battistelli, M. & Falcieri, E. Apoptotic Bodies: Particular Extracellular Vesicles Involved in Intercellular Communication. *Biology* **9** (2020).

35. Oropesa-Ávila, M. *et al.* Apoptotic microtubules delimit an active caspase free area in the cellular cortex during the execution phase of apoptosis. *Cell Death Dis* **4**, e527 (2013).

36. Agmon, E., Solon, J., Bassereau, P. & Stockwell, B.R. Modeling the effects of lipid peroxidation during ferroptosis on membrane properties. *Scientific reports* **8**, 5155 (2018).

37. Dodson, M., Castro-Portuguez, R. & Zhang, D.D. NRF2 plays a critical role in mitigating lipid peroxidation and ferroptosis. *Redox biology* **23**, 101107 (2019).

38. Dhuriya, Y.K. & Sharma, D. Necroptosis: a regulated inflammatory mode of cell death. *Journal of neuroinflammation* **15**, 199 (2018).

39. Shkarina, K. *et al.* Optogenetic activators of apoptosis, necroptosis, and pyroptosis. *The Journal of cell biology* **221** (2022).

40. Wirawan, E., Vanden Berghe, T., Lippens, S., Agostinis, P. & Vandenabeele, P. Autophagy: for better or for worse. *Cell research* **22**, 43-61 (2012).

41. Parzych, K.R. & Klionsky, D.J. An overview of autophagy: morphology, mechanism, and regulation. *Antioxidants & redox signaling* **20**, 460-473 (2014).

42. He, K., Zhang, X., Ren, S. & Sun, J. Deep residual learning for image recognition. Proceedings of the IEEE conference on computer vision and pattern recognition; 2016; 2016. p. 770-778.

43. Vogt, M. *et al.* Co-targeting HSP90 alpha and CDK7 overcomes resistance against HSP90 inhibitors in BCR-ABL1+ leukemia cells. *Cell Death Dis* **14**, 799 (2023).

44. Teachey, D.T. *et al.* Children's Oncology Group Trial AALL1231: A Phase III Clinical Trial Testing Bortezomib in Newly Diagnosed T-Cell Acute Lymphoblastic Leukemia and Lymphoma. *J Clin Oncol* **40**, 2106-2118 (2022).

45. Chu, Y.Y. *et al.* Bortezomib-induced miRNAs direct epigenetic silencing of locus genes and trigger apoptosis in leukemia. *Cell Death Dis* **8**, e3167 (2017).

46. Gulla, A. *et al.* Bortezomib induces anti-multiple myeloma immune response mediated by cGAS/STING pathway activation. *Blood Cancer Discov* **2**, 468-483 (2021).

47. Wang, Y.C. *et al.* Severe cellular stress drives apoptosis through a dual control mechanism independently of p53. *Cell Death Discov* **8**, 282 (2022).

48. Moriwaki, K. & Chan, F.K. Regulation of RIPK3- and RHIM-dependent Necroptosis by the Proteasome. *The Journal of biological chemistry* **291**, 5948-5959 (2016).

49. Zeng, X. & Kinsella, T.J. Mammalian target of rapamycin and S6 kinase 1 positively regulate 6-thioguanine-induced autophagy. *Cancer Res* **68**, 2384-2390 (2008).

50. Rudolph, D. *et al.* BI 6727, a Polo-like kinase inhibitor with improved pharmacokinetic profile and broad antitumor activity. *Clinical cancer research : an official journal of the American Association for Cancer Research* **15**, 3094-3102 (2009).

51. Gjertsen, B.T. & Schöffski, P. Discovery and development of the Polo-like kinase inhibitor volasertib in cancer therapy. *Leukemia* **29**, 11-19 (2015).

52. Peng, Y. *et al.* A ferroptosis-associated gene signature for the prediction of prognosis and therapeutic response in luminal-type breast carcinoma. *Scientific reports* **11**, 17610 (2021).

53. Hangauer, M.J. *et al.* Drug-tolerant persister cancer cells are vulnerable to GPX4 inhibition. *Nature* **551**, 247-250 (2017).

54. Liao, P. *et al.* CD8(+) T cells and fatty acids orchestrate tumor ferroptosis and immunity via ACSL4. *Cancer Cell* **40**, 365-378 e366 (2022).

55. Gong, D., Chen, M., Wang, Y., Shi, J. & Hou, Y. Role of ferroptosis on tumor progression and immunotherapy. *Cell Death Discov* **8**, 427 (2022).

56. Lalonde, M.E. *et al.* Genome-wide CRISPR screens identify ferroptosis as a novel therapeutic vulnerability in acute lymphoblastic leukemia. *Haematologica* (2022).

57. Zhao, Y., Huang, Z. & Peng, H. Molecular Mechanisms of Ferroptosis and Its Roles in Hematologic Malignancies. *Front Oncol* **11**, 743006 (2021).

58. Haferlach, T. *et al.* Clinical utility of microarray-based gene expression profiling in the diagnosis and subclassification of leukemia: report from the International Microarray Innovations in Leukemia Study Group. *J Clin Oncol* **28**, 2529-2537 (2010).

59. Yang, W.S. & Stockwell, B.R. Synthetic lethal screening identifies compounds activating iron-dependent, nonapoptotic cell death in oncogenic-RAS-harboring cancer cells. *Chemistry & biology* **15**, 234-245 (2008).

60. Leo, I.R. *et al.* Integrative multi-omics and drug response profiling of childhood acute lymphoblastic leukemia cell lines. *Nat Commun* **13**, 1691 (2022).

61. Rudolph, D. *et al.* Efficacy and mechanism of action of volasertib, a potent and selective inhibitor of Polo-like kinases, in preclinical models of acute myeloid leukemia. *The Journal of pharmacology and experimental therapeutics* **352**, 579-589 (2015).

62. Adachi, Y., Ishikawa, Y. & Kiyoi, H. Identification of volasertib-resistant mechanism and evaluation of combination effects with volasertib and other agents on acute myeloid leukemia. *Oncotarget* **8**, 78452-78465 (2017).

63. Shah, K. *et al.* PLK1 as a cooperating partner for BCL2-mediated antiapoptotic program in leukemia. *Blood cancer journal* **13**, 139 (2023).

64. Zhang, C., Liu, X., Jin, S., Chen, Y. & Guo, R. Ferroptosis in cancer therapy: a novel approach to reversing drug resistance. *Mol Cancer* **21**, 47 (2022).

65. Dixon, S.J. & Olzmann, J.A. The cell biology of ferroptosis. *Nature reviews. Molecular cell biology* (2024).

66. Gao, M., Monian, P., Quadri, N., Ramasamy, R. & Jiang, X. Glutaminolysis and Transferrin Regulate Ferroptosis. *Mol Cell* **59**, 298-308 (2015).

67. Dixon, S.J. & Stockwell, B.R. The role of iron and reactive oxygen species in cell death. *Nature chemical biology* **10**, 9-17 (2014).

68. Tang, D., Chen, X., Kang, R. & Kroemer, G. Ferroptosis: molecular mechanisms and health implications. *Cell research* **31**, 107-125 (2021).

69. Doll, S. *et al.* ACSL4 dictates ferroptosis sensitivity by shaping cellular lipid composition. *Nature chemical biology* **13**, 91-98 (2017).

70. Sun, X. *et al.* Activation of the p62-Keap1-NRF2 pathway protects against ferroptosis in hepatocellular carcinoma cells. *Hepatology (Baltimore, Md.)* **63**, 173-184 (2016).

71. von Mässenhausen, A. *et al.* Dexamethasone sensitizes to ferroptosis by glucocorticoid receptor-induced dipeptidase-1 expression and glutathione depletion. *Sci Adv* **8**, eabl8920 (2022).

72. Tontsch-Grunt, U. *et al.* Synergistic activity of BET inhibitor BI 894999 with PLK inhibitor volasertib in AML in vitro and in vivo. *Cancer letters* **421**, 112-120 (2018).

73. Boyer, M.W. *et al.* Dependency on intercellular adhesion molecule recognition and local interleukin-2 provision in generation of an in vivo CD8+ T-cell immune response to murine myeloid leukemia. *Blood* **85**, 2498-2506 (1995).

74. Zhang, L., Gajewski, T.F. & Kline, J. PD-1/PD-L1 interactions inhibit antitumor immune responses in a murine acute myeloid leukemia model. *Blood* **114**, 1545-1552 (2009).

75. Oldenburg, E., Kronberg, R.M., Niehoff, B., Ebenhöh, O. & Popa, O. DeepLOKI-a deep learning based approach to identify zooplankton taxa on high-resolution images from the optical plankton recorder LOKI. *Frontiers in Marine Science* (2023).

76. Kleesiek, J. *et al.* Deep MRI brain extraction: A 3D convolutional neural network for skull stripping. *NeuroImage* **129**, 460-469 (2016).

77. Cicero, M. *et al.* Training and Validating a Deep Convolutional Neural Network for Computer-Aided Detection and Classification of Abnormalities on Frontal Chest Radiographs. *Investigative radiology* **52**, 281-287 (2017).

78. Verduijn, J., Van der Meeren, L., Krysko, D.V. & Skirtach, A.G. Deep learning with digital holographic microscopy discriminates apoptosis and necroptosis. *Cell Death Discov* **7**, 229 (2021).

79. Sun, Y. *et al.* ent-Kaurane diterpenoids induce apoptosis and ferroptosis through targeting redox resetting to overcome cisplatin resistance. *Redox biology* **43**, 101977 (2021).

80. Lim, J.K.M. *et al.* Cystine/glutamate antiporter xCT (SLC7A11) facilitates oncogenic RAS transformation by preserving intracellular redox balance. *Proc Natl Acad Sci U S A* **116**, 9433-9442 (2019).

81. Müller, F. *et al.* Elevated FSP1 protects KRAS-mutated cells from ferroptosis during tumor initiation. *Cell Death Differ* **30**, 442-456 (2023).

82. Andreani, C., Bartolacci, C. & Scaglioni, P.P. Ferroptosis: A Specific Vulnerability of RAS-Driven Cancers? *Front Oncol* **12**, 923915 (2022).

83. Luo, M. *et al.* miR-137 regulates ferroptosis by targeting glutamine transporter SLC1A5 in melanoma. *Cell Death Differ* **25**, 1457-1472 (2018).

84. Al Mamun Bhuyan, A. *et al.* Inhibition of Suicidal Erythrocyte Death by Volasertib. *Cellular physiology and biochemistry : international journal of experimental cellular physiology, biochemistry, and pharmacology* **43**, 1472-1486 (2017).

85. Van den Bossche, J. *et al.* In vitro study of the Polo-like kinase 1 inhibitor volasertib in non-small-cell lung cancer reveals a role for the tumor suppressor p53. *Molecular oncology* **13**, 1196-1213 (2019).

86. Zhang, L. *et al.* Sorafenib triggers ferroptosis via inhibition of HBXIP/SCD axis in hepatocellular carcinoma. *Acta pharmacologica Sinica* **44**, 622-634 (2023).

87. Lachaier, E. *et al.* Sorafenib induces ferroptosis in human cancer cell lines originating from different solid tumors. *Anticancer research* **34**, 6417-6422 (2014).

88. Gao, W., Wang, X., Zhou, Y., Wang, X. & Yu, Y. Autophagy, ferroptosis, pyroptosis, and necroptosis in tumor immunotherapy. *Signal transduction and targeted therapy* **7**, 196 (2022).

89. Friedmann Angeli, J.P., Krysko, D.V. & Conrad, M. Ferroptosis at the crossroads of cancer-acquired drug resistance and immune evasion. *Nat Rev Cancer* **19**, 405-414 (2019).

90. Reda, M. *et al.* Development of a nanoparticle-based immunotherapy targeting PD-L1 and PLK1 for lung cancer treatment. *Nat Commun* **13**, 4261 (2022).

91. Renner, A.G. *et al.* Polo-like kinase 1 is overexpressed in acute myeloid leukemia and its inhibition preferentially targets the proliferation of leukemic cells. *Blood* **114**, 659-662 (2009).

92. Tsykunova, G. *et al.* Targeting of polo-like kinases and their cross talk with Aurora kinases--possible therapeutic strategies in human acute myeloid leukemia? *Expert opinion on investigational drugs* **21**, 587-603 (2012).

93. Döhner, H. *et al.* Randomized, phase 2 trial of low-dose cytarabine with or without volasertib in AML patients not suitable for induction therapy. *Blood* **124**, 1426-1433 (2014).

94. Ottmann, O.G. *et al.* Phase I dose-escalation trial investigating volasertib as monotherapy or in combination with cytarabine in patients with relapsed/refractory acute myeloid leukaemia. *British journal of haematology* **184**, 1018-1021 (2019).

95. Döhner, H. *et al.* Adjunctive Volasertib in Patients With Acute Myeloid Leukemia not Eligible for Standard Induction Therapy: A Randomized, Phase 3 Trial. *HemaSphere* **5**, e617 (2021).

96. Wagner, J., Lacher, M.D., Gu, C.J., Leonardi, C. & Mannis, G. A Phase 2 Study with Volasertib for Ven-HMA Relapsed/Refractory Acute Myeloid Leukemia Patients Guided By a Predictive Precision Medicine Platform. *Blood* **142**, 5952-5952 (2023).

97. Rodencal, J. *et al.* Sensitization of cancer cells to ferroptosis coincident with cell cycle arrest. *Cell chemical biology* **31**, 234-248.e213 (2024).

98. Gagliardi, M. *et al.* Aldo-keto reductases protect metastatic melanoma from ER stress-independent ferroptosis. *Cell Death Dis* **10**, 902 (2019).

99. Tan, C. *et al.* A survey on deep transfer learning. International conference on artificial neural networks; 2018: Springer; 2018. p. 270-279.

100. Oikonomou, A. *et al.* High-throughput screening as a drug repurposing strategy for poor outcome subgroups of pediatric B-cell precursor Acute Lymphoblastic Leukemia. *Biochemical pharmacology* **217**, 115809 (2023).

4. Discussion

Recent research has shown that cancer development is not only intrinsic to malignant cells but is also driven by interactions with surrounding stromal cells as well as with innate and adaptive immune cell infiltrates. Cancer outgrowth is influenced by a shifting balance towards an immunosuppressive tumor micro-environment (TME) leading to immune escape. The concept of tumor hotness which generally describes an intra-tumoral T cell signature is a useful therapeutic measure in predicting immunotherapy responsiveness. A "hot" tumor is characterized by high levels of immune cell infiltration and presents a more favorable prognosis in the context of immunotherapy responses compared to "cold" tumors, which exhibit minimal immune cell penetration. One promising approach in increasing tumor hotness is the modulation of the TME to enhance antigen presentation and T cell activation. This strategy depends on the ability to manipulate immune checkpoints, cytokine production, and immunogenic cell death pathways to promote anti-tumoral immunity within the TME. Many clinically approved chemotherapeutics are recognized to not only be cytotoxic directly towards cancer cells but are increasingly recognized to also have immunomodulatory effects. It is crucial to re-evaluate chemotherapeutics for their potential influence on the TME to improve outcomes in the context of combinatorial therapy, boosting anti-cancer immunity and tumor hotness. Additionally, many non-cancer related therapeutics that are currently approved for clinical use might have immunomodulatory effects that could be potentially explored in anti-cancer therapy. This doctoral thesis focuses on anti-cancer therapies encompassing several above-mentioned aspects (Figure 5). Publication 1 covers current challenges related to T cell senescence and exhaustion in cancer therapy. Both original article research publications are based on pharmacological screens with the intent of identifying drugs with novel immunomodulatory effects. While the second published body of work focuses on drug-repurposing, Publication 3 offers insight into using deep learning approaches to decode different types of cell death induced by known chemotherapeutics.

Senescent CD8$^+$ T cells in cancer treatment

Immunotherapies exploit the host's immune system to fight cancer and are currently utilized for various tumor types. These therapies primarily focus on effector T cells, the main immune cells responsible for tumor-cell killing. A significant reason why T cells may not respond effectively to immunotherapies is that the T cells may be in a dysfunctional state that is phenotypically distinct from exhausted T cells. Publication 1 reviews the molecular mechanisms that define and trigger T cell senescence in the tumor microenvironment and examines its impact on treatment efficacy. Both exhausted and senescent T cells are known to accumulate during various stages of tumor progression (298). T cell senescence, a state of irreversible cell cycle arrest, is triggered by stress signals such as DNA damage, oxidative stress, and chronic inflammation within the TME. This senescence is marked by altered cell surface markers, such as increased CD57 and KLRG1 expression, and a changed secretory cytokine profile, including elevated levels of pro-inflammatory cytokines such as IL-6 and TNF-α (299). Senescent T cells have been detected in primary and metastatic solid tumors as well as hematological malignancies and the molecular pathways regulating premature and replicative senescence are not completely understood but involve the MAPK pathway. The MAPK pathway, particularly the p38 MAPK and ERK pathways, are crucial in regulating cellular senescence (300). Activation of p38 MAPK results in the phosphorylation of downstream targets that mediate cell cycle arrest and the senescence-associated secretory phenotype (SASP), contributing to an immunosuppressive environment (301). Additionally, numerous studies have shown that Tregs and tumor cells can induce T cell senescence through direct cell-cell contact and secretion of immunosuppressive cytokines like TGF-β and IL-10 (302). These interactions inhibit T cell proliferation and function, promoting a senescent state.

Whether tumor-specific T cell senescence arises from replicative or premature origins, a deeper understanding of the molecular pathways driving this process is essential. This understanding will lead to new therapeutic strategies to overcome the suppressive TME. Targeting senescent T cells within the TME is a promising therapeutic strategy. MAPK pathway inhibitors, such as selumetinib and trametinib, have shown potential in preclinical models to reduce senescence markers and restore T cell function (303). Additionally, TLR8 agonists including motolimod can activate innate immune responses and potentially reverse senescence-induced immunosuppression (304,

305). Combining these agents with checkpoint inhibitors like anti-PD-1 or anti-CTLA-4 antibodies could enhance overall anti-tumor efficacy.

Significant progress has been made in defining T cell senescence as a distinct dysfunctional state. Further research is needed to identify specific biomarkers of T cell senescence and develop targeted therapies that can selectively eliminate or rejuvenate senescent T cells. Clinical trials assessing the combination of senolytic drugs with existing immunotherapies are crucial to evaluate the translational potential of these approaches in solid tumors and hematological malignancies.

Immunomodulatory effects of 5-Nonyloxytryptamine in cancer treatment

The drug screening described in Publication 2 resulted in the identification of 5-Nonyloxytryptamine (5-NL), initially developed as a serotonin receptor 1D (HTR1D) agonist, as an immunostimulant. The family of serotonin receptors consists of thirteen G protein-coupled receptors, including HTR1D and one ligand-gated cation channel (306). Within the intricate network of the human central nervous system, diverse serotonin receptor subtypes have different roles, from regulating sleep-wake cycles to influencing appetite, mood, and even memory (307). However, serotonin's influence extends beyond the functions of the nervous system. A significant portion of this neurotransmitter resides in the gastrointestinal tract, where it orchestrates the rhythmic contractions essential for peristalsis (308). Serotonin also courses through the bloodstream, primarily housed within platelets, contributing to crucial functions like blood coagulation and regulating blood vessel diameter through vasoconstriction (309). The influence of the HTR1D receptor in cancer was previously investigated. Research has highlighted the role of HTR1D in the progression of gastric cancer serving as an independent risk factor for reduced overall survival (310). Recent studies showed that knockdown and inhibition of HTR1D, using the inhibitor GR127935, impair the proliferation and migration of gastric cancer cells. Mechanistically, depletion of HTR1D inhibited tumor progression, making HTR1D a potential therapeutic target (310). In pancreatic cancer, HTR1D functions as a key target in the malignant progression of the disease. It has been shown to promote malignant outcomes via the PI3K-AKT signaling pathway, influencing cell proliferation, migration, and apoptosis (311). Nevertheless, despite suggestions of HTR1D involvement in cancer, the study

presented in Publication 2 demonstrated that 5-NL's action encompasses mechanisms beyond its intended HTR1D target. 5-NL enhanced MHC class I expression on tumor cells, which is crucial for T cell recognition and subsequent tumor cell elimination. The effectiveness of 5-NL lies in its ability to modulate several signaling pathways independently from classical serotonin signaling. HTR1D canonical activation leads to ERK 1/2 pathway modulation which was not apparent in our study. Experiments knocking down and knocking out HTR1D did not abrogate the phenotype upon 5-NL treatment. 5-NL treatment led to CREB phosphorylation potentially linked to modulation of the AMPK pathway. Recent studies have revealed that reduced AMPK activity in tumor cells led to decreased antigen presentation, thereby promoting an immunosuppressive tumor microenvironment. Consequently, it is plausible that early activation of AMPK by 5-NL affects phospho-CREB, which subsequently influences the antigen-presenting machinery. Additionally, AMPK activation has been shown to inhibit ribosomal protein p70 S6 kinase, a phenomenon we also observed following 5-NL treatment. Inhibition of the PI3K/Akt/mTOR pathway, which has been implicated in cell death-inducing effects in similar systems, might be responsible for the apoptotic effects of 5-NL. Thus, it remains to be determined whether the upregulation of MHC-I (mediated by phospho-CREB) or cell death (mediated by PI3K/Akt/mTOR) is primarily driven by AMPK activation in response to 5-NL.

This alternative pathway suggests a novel mechanism by which 5-NL enhances the immune presentation of tumor cells, independent of its initial pharmacological target. In clinical settings, tumors display variable MHC-I expression that is generally suppressed during advanced stages of progression, rendering them resistant to checkpoint inhibition therapies. Therefore, converting poorly inflamed "cold" tumors into "hot" tumors by upregulating MHC-I is an attractive therapeutic strategy. This approach could enhance anti-tumor T cell immunity not only in the tumor tissue but also in the lymph nodes, as observed in our study. Notably, our study demonstrated that B16 cells with a reversible MHC-I low phenotype and intrinsic resistance to immunotherapy showed no response to anti-PD1 antibody treatment alone. However, the combination of 5-NL and anti-PD1 was highly effective. This synergy suggests that 5-NL can potentiate the efficacy of existing immunotherapies, providing a foundation for combination therapies in clinical settings. The study, however, did not identify the direct target of 5-NL. Another agonist, Sumatriptan did not recapitulate the described phenotype *upon in* vivo *and in vitro* treatment, which again supports that pleiotropic

effects are responsible for the immunomodulatory and anti-tumoral effects of 5-NL. Further studies on identifying the biochemical target of 5-NL are needed, which would be potentially beneficial for further clinical development as 5-NL is not currently approved for treatment. For example, tag-labeled 5-NL pull-down assays combined with mass spectrometry could potentially uncover proteins interacting with 5-NL. However, using this approach, there is a possibility of a changed compound structure due to tag labeling and cell penetration and therefore missing the protein target.

In vivo, 5-NL was well tolerated, although its clinical applicability remains to be determined as it is not yet FDA-approved. However, there is potential for using other FDA-approved compounds that also enhance MHC-I expression through cAMP/PKA/CREB-mediated signaling such as phosphodiesterase (PDE) inhibitors (Dipyridamole, Pentoxifylline, Theophylline, and others).

Successful drug screening in Publication 2 provides evidence that parallel to novel drug development, the repurposing of existing compounds presents a strategic advantage in cancer therapy. Repurposing non-oncological drugs that exhibit immunomodulatory effects opens new therapeutic avenues with reduced development costs and time for clinical application.

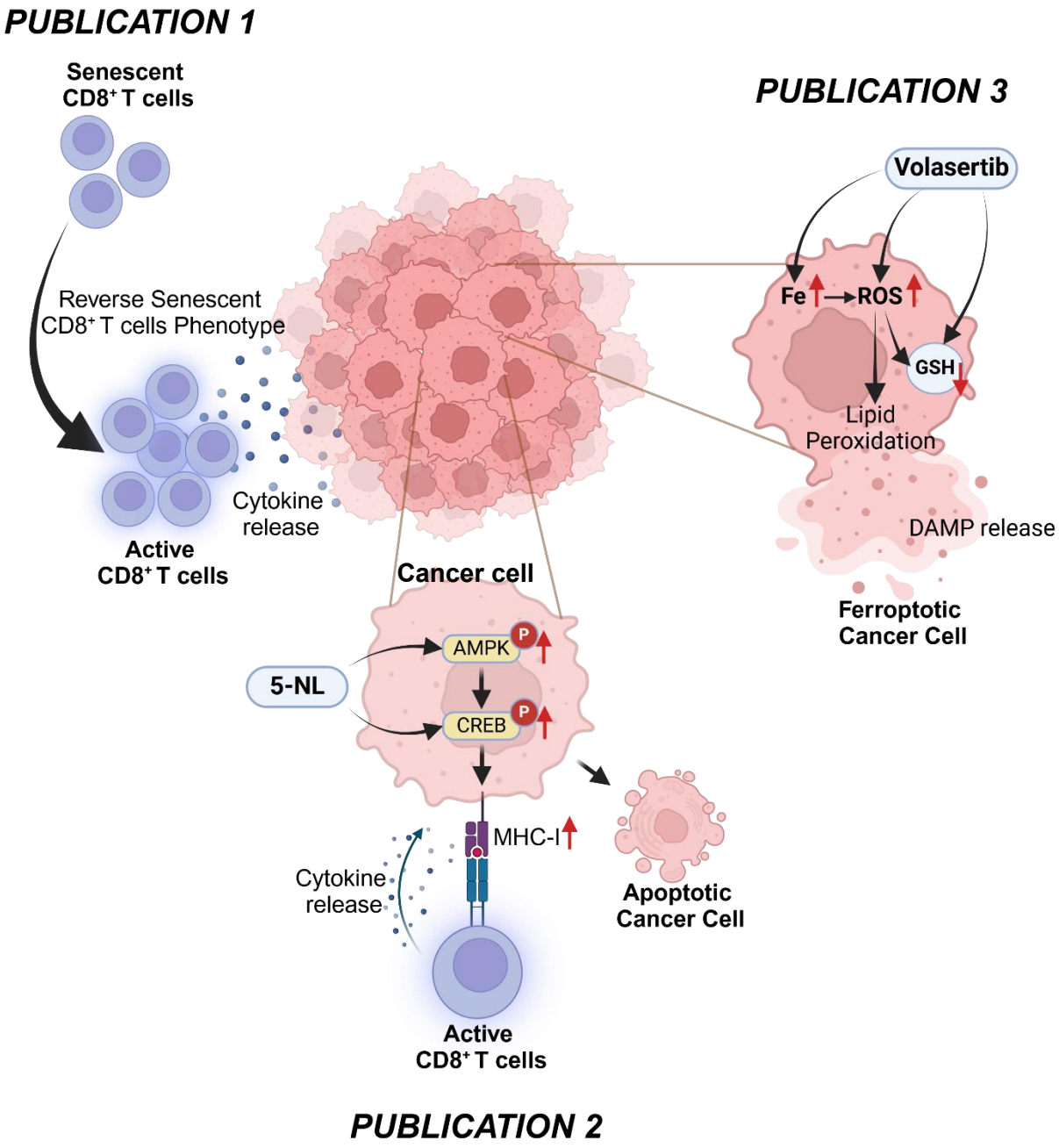

Figure 5. Schematic summary of Publication 1, 2 and 3 which are part of this cumulative dissertation. ***Publication 1*** highlights the importance of reversing senescent CD8⁺ T cells in anti-cancer therapy. ***Publication 2*** provides evidence of novel immunomodulatory functions of 5-NL, that, through increased CREB phosphorylation upregulate MHC-I expression. Increased surface antigen presentation on cancer cell leads to increased T cell stimulation. The study described in ***Publication 3*** demonstrates that volasertib, through an accumulation of iron in cancer cells leads to increased ROS production, depletion of GSH and ferroptosis induction.

Ferroptosis induction with Volasertib

In the evolving landscape of cancer therapy, the induction of immunogenic cell death (ICD) has emerged as a potent strategy to enhance the efficacy of treatments through not only cytotoxic effects but also by turning the tumor itself into a vaccine. ICD involves the death of cancer cells with the release of danger signals that alert and activate the immune system, thereby transforming the TME from immunosuppressive to immune activating. This reprogramming is facilitated by the recruitment and activation of various immune cells including dendritic cells, T cells and NK cells. By contributing to the conversion of the TME from a "cold" to a "hot" phenotype, ICD not only helps in the direct elimination of tumor cells, but also sets the stage for more effective immunotherapy strategies. Ferroptosis is a form of regulated cell death distinguished by the accumulation of lipid peroxides to lethal levels, which is distinct from other forms of cell death such as apoptosis, necrosis, and autophagy. Unlike other non-immunogenic death pathways, ferroptosis has been identified as potentially immunogenic by releasing DAMPs, making it a promising target in cancer therapy. The immunogenicity of ferroptosis may be attributed to the release of ATP, HMGB1 and other cellular contents that can act as adjuvants, stimulating dendritic cells and other components of the immune system (Figure 6) (312). In the study presented in Publication 3, a machine learning program was used for rapid and off-label analysis type of cell death and utilized for evaluation of commonly studied chemotherapeutics in the treatment of B-ALL. From several potentially interesting compounds, volasertib was further evaluated due to novel ferroptosis-inducing effects. Initially, volasertib-induced ferroptosis was detected in the screen's murine L929 cell line and later confirmed in human B-ALL cell lines, patient derived samples, and *in vivo* murine models. Most interestingly, volasertib not only led to cellular iron accumulation and lethal generation of ROS, but also upregulated expression of ACSL4 in cancer cells. ACSL4 has been shown to increase PUFA biosynthesis and to shape lipid membrane composition therefore making cancer cells susceptible to ferroptosis induction (313). When murine C1498 leukemia cells were injected into wildtype mice, survival was improved. This effect was not as pronounced in immunocompromised NSG mice suggesting an immune component of the volasertib-induced ferroptosis. However, these results require additional experiments to confirm the stimulation of the immune system. Immunogenic features of ferroptosis include HMGB1 release that has been reported to contribute to macrophage activation. CXCL1, TNFα and IFN-β release

contribute to activation of DCs and T cells (314). Further evaluation of HMGB1, CXCL1, TNFα and IFN-β in serum samples, but also flow cytometry evaluation of dendritic cells and T cell activation could provide additional evidence of ICD induction. Ferroptosis was reported to play a crucial role in suppressing carcinogenesis (315) and tumor growth (214), also in overcoming cancer chemoresistance (253) and sensitizing cancer cells to radiotherapy (316). Several studies show that ferroptosis induction is especially of interest in the case of apoptosis resistance in cancer treatment (198). Volasertib advanced to Phase II clinical trials for elderly patients with relapsed or refractory acute myeloid leukemia, both as a single treatment and in combination with cytarabine, yielding higher complete response rates and extended survival (290, 291). However, these promising results were not replicated in subsequent phase III clinical trials involving chemotherapy-naive patients, indicating that the positive outcomes were primarily observed in relapsed or refractory patients (292). This conclusion is supported by ongoing Phase II clinical trials focused on identifying additional biomarkers to better understand and predict patient responses focused on on relapsed and refractory patients (293).

Furthermore, these findings highlight the challenges in translating clinical trial successes across different patient populations. The disparity in outcomes between Phase II and Phase III trials underscores the need for more targeted approaches in treatment protocols and emphasizes the importance of precision medicine. By identifying specific biomarkers of efficacy, researchers aim to adjust treatments more effectively to individual patient profiles, potentially improving outcomes and offering more personalized therapeutic options.

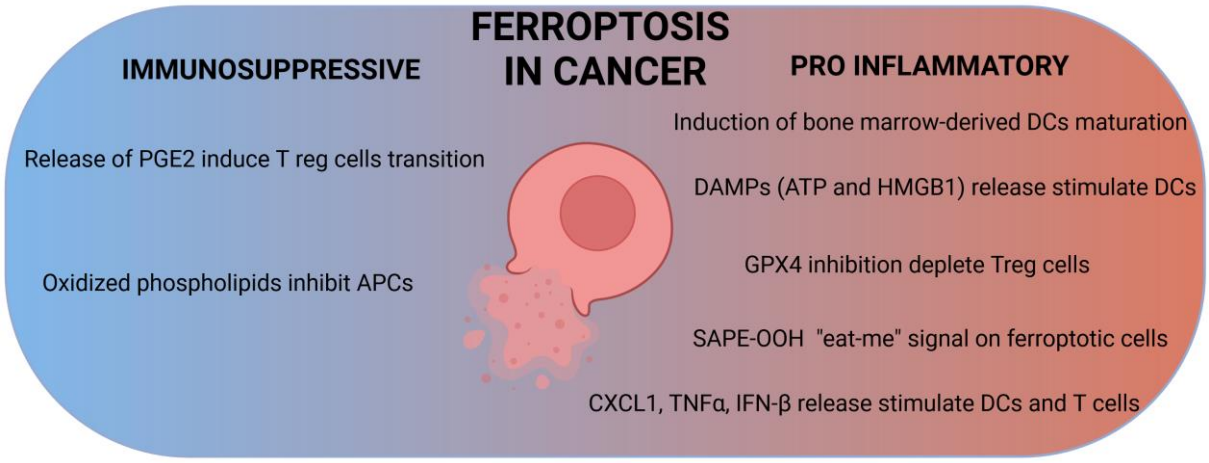

Figure 6. Schematic summary of the immunosuppressive and pro-inflammatory conditions induced by ferroptosis in cancer cells.

Although ferroptosis can lead to the release of DAMPs required for immunogenic cell death, it does not necessarily guarantee the induction of immunogenicity (Figure 6). Lipid metabolism-related mechanisms, which may also occur during ferroptosis, can negatively impact immunogenicity. A notable characteristic of ferroptosis is the increased expression of cyclooxygenase 2 (COX-2), an enzyme that produces prostaglandin E2 (PGE2) (214). PGE2 has been found to suppress immune activation and promote the FOXP3 transcription factor in T lymphocytes, indicating its role in fostering a regulatory phenotype (317). Furthermore, ferroptosis results in the overproduction of oxidized phospholipids, which exhibit strong immunosuppressive effects on antigen-presenting cells (318). Therefore, the immunosuppressive conditions induced by ferroptosis could potentially undermine the success of immunotherapies. On the other hand, induction of ferroptosis promoted anti-tumor immunity by the phenotypic maturation of bone marrow-derived dendritic cells (312). Additionally, Luo et al. identified an eat-me signal on the ferroptotic cancer cell surface, 1-steaoryl-2-15-HpETE-sn-glycero-3-phosphatidylethanolamine (SAPE-OOH). The enrichment of SAPE-OOH facilitated phagocytosis by targeting toll-like receptor 2 on macrophages (319). Additionally, cancer cells are under higher oxidative stress than healthy cells, and to facilitate production of antioxidant GSH, depending on cysteine uptake (320). Cramer et al. reported that depletion of L-cysteine with cysteinase not only induced ferroptosis in multiple tumor models, but also prolonged the survival of tumor baring mice (320). Additionally, induction of ferroptosis in tumors by treatment with cysteinase improved $CD8^+$ T cells activity that synergized in combination with anti-

PDL1 checkpoint blockade for maximal tumor inhibition (321). The development of nanoparticles with encapsulated GPX4 inhibitor, RSL3 showed to not only induce ferroptosis in melanoma and lung cancer, but also increase T cells infiltration of tumors, synergizing with blockade of programmed death ligand 1 (322). Another study investigating immunosuppressive Tregs demonstrated that these cells have a high expression of GPX4, making them more resistant to oxidative stress, but also increasing their susceptibility to GPX4 inhibition (323). The above reports underscore the complexity of immune responses in relation to cell death and the importance of understanding how various types of cell death affect immune activation. Further studies should asses implementing ferroptosis induction not only in combination with immune checkpoint blockade inhibitors but also with CAR-T cell therapies or precise delivery of ferroptosis inducers conjugated with specific anti-cancer antibodies, especially in apoptosis resistant cancers. Therefore, while targeting ferroptosis might offer therapeutic advantages, it is crucial to also develop strategies to reduce its immunosuppressive impact to improve the overall effectiveness of cancer immunotherapies.

References corresponding to chapters 1, 2, 4 and Discussion:

1. KOCARNIK J. M., COMPTON K., DEAN F. E., FU W., GAW B. L., HARVEY J. D. et al. Cancer Incidence, Mortality, Years of Life Lost, Years Lived With Disability, and Disability-Adjusted Life Years for 29 Cancer Groups From 2010 to 2019: A Systematic Analysis for the Global Burden of Disease Study 2019, JAMA oncology 2022: 8: 420-444.
2. LACONI E., MARONGIU F., DEGREGORI J. Cancer as a disease of old age: changing mutational and microenvironmental landscapes, British journal of cancer 2020: 122: 943-952.
3. SMITH M. A., SEIBEL N. L., ALTEKRUSE S. F., RIES L. A., MELBERT D. L., O'LEARY M. et al. Outcomes for children and adolescents with cancer: challenges for the twenty-first century, J Clin Oncol 2010: 28: 2625-2634.
4. ARNOLD M., RUTHERFORD M. J., BARDOT A., FERLAY J., ANDERSSON T. M., MYKLEBUST T. et al. Progress in cancer survival, mortality, and incidence in seven high-income countries 1995-2014 (ICBP SURVMARK-2): a population-based study, The Lancet Oncology 2019: 20: 1493-1505.
5. Cancer in 2022, Cancer discovery 2022: 12: 2733-2738.
6. OCRAN MATTILA P., AHMAD R., HASAN S. S., BABAR Z. U. Availability, Affordability, Access, and Pricing of Anti-cancer Medicines in Low- and Middle-Income Countries: A Systematic Review of Literature, Frontiers in public health 2021: 9: 628744.
7. HANAHAN D., WEINBERG R. A. Hallmarks of cancer: the next generation, Cell 2011: 144: 646-674.
8. ZHANG J., HUANG D., SAW P. E., SONG E. Turning cold tumors hot: from molecular mechanisms to clinical applications, Trends in immunology 2022: 43: 523-545.
9. GALON J., BRUNI D. Approaches to treat immune hot, altered and cold tumours with combination immunotherapies, Nat Rev Drug Discov 2019: 18: 197-218.
10. CAMUS M., TOSOLINI M., MLECNIK B., PAGÈS F., KIRILOVSKY A., BERGER A. et al. Coordination of intratumoral immune reaction and human colorectal cancer recurrence, Cancer Res 2009: 69: 2685-2693.
11. MLECNIK B., BINDEA G., ANGELL H. K., SASSO M. S., OBENAUF A. C., FREDRIKSEN T. et al. Functional network pipeline reveals genetic determinants associated with in situ lymphocyte proliferation and survival of cancer patients, Sci Transl Med 2014: 6: 3007240.
12. MALEKI VAREKI S. High and low mutational burden tumors versus immunologically hot and cold tumors and response to immune checkpoint inhibitors, Journal for immunotherapy of cancer 2018: 6: 157.
13. PAGÈS F., MLECNIK B., MARLIOT F., BINDEA G., OU F. S., BIFULCO C. et al. International validation of the consensus Immunoscore for the classification of colon cancer: a prognostic and accuracy study, Lancet 2018: 391: 2128-2139.
14. REN X., GUO S., GUAN X., KANG Y., LIU J., YANG X. Immunological Classification of Tumor Types and Advances in Precision Combination Immunotherapy, Frontiers in immunology 2022: 13: 790113.
15. MAIMELA N. R., LIU S., ZHANG Y. Fates of CD8+ T cells in Tumor Microenvironment, Computational and structural biotechnology journal 2019: 17: 1-13.
16. VAN DER LEUN A. M., THOMMEN D. S., SCHUMACHER T. N. CD8(+) T cell states in human cancer: insights from single-cell analysis, Nature reviews Cancer 2020: 20: 218-232.
17. WIECZOREK M., ABUALROUS E. T., STICHT J., ÁLVARO-BENITO M., STOLZENBERG S., NOÉ F. et al. Major Histocompatibility Complex (MHC) Class I and MHC Class II Proteins: Conformational Plasticity in Antigen Presentation, Frontiers in immunology 2017: 8: 292.
18. ABELE R., TAMPÉ R. Function of the transport complex TAP in cellular immune recognition, Biochim Biophys Acta 1999: 6: 405-419.
19. HEWITT E. W. The MHC class I antigen presentation pathway: strategies for viral immune evasion, Immunology 2003: 110: 163-169.

20. KELDERMAN S., KVISTBORG P. Tumor antigens in human cancer control, Biochim Biophys Acta 2016: 1: 83-89.
21. COULIE P. G., BRICHARD V., VAN PEL A., WÖLFEL T., SCHNEIDER J., TRAVERSARI C. et al. A new gene coding for a differentiation antigen recognized by autologous cytolytic T lymphocytes on HLA-A2 melanomas, J Exp Med 1994: 180: 35-42.
22. FISK B., BLEVINS T. L., WHARTON J. T., IOANNIDES C. G. Identification of an immunodominant peptide of HER-2/neu protooncogene recognized by ovarian tumor-specific cytotoxic T lymphocyte lines, J Exp Med 1995: 181: 2109-2117.
23. CHOMEZ P., DE BACKER O., BERTRAND M., DE PLAEN E., BOON T., LUCAS S. An overview of the MAGE gene family with the identification of all human members of the family, Cancer Res 2001: 61: 5544-5551.
24. GERMANO G., LAMBA S., ROSPO G., BARAULT L., MAGRÌ A., MAIONE F. et al. Inactivation of DNA repair triggers neoantigen generation and impairs tumour growth, Nature 2017: 552: 116-120.
25. SADELAIN M., RIVIÈRE I., RIDDELL S. Therapeutic T cell engineering, Nature 2017: 545: 423-431.
26. MCGRANAHAN N., FURNESS A. J., ROSENTHAL R., RAMSKOV S., LYNGAA R., SAINI S. K. et al. Clonal neoantigens elicit T cell immunoreactivity and sensitivity to immune checkpoint blockade, Science (New York, NY) 2016: 351: 1463-1469.
27. KROEMER G., GALLUZZI L., KEPP O., ZITVOGEL L. Immunogenic cell death in cancer therapy, Annu Rev Immunol 2013: 31: 51-72.
28. JANEWAY C. A., JR., MEDZHITOV R. Innate immune recognition, Annu Rev Immunol 2002: 20: 197-216.
29. HILDNER K., EDELSON B. T., PURTHA W. E., DIAMOND M., MATSUSHITA H., KOHYAMA M. et al. Batf3 deficiency reveals a critical role for CD8alpha+ dendritic cells in cytotoxic T cell immunity, Science (New York, NY) 2008: 322: 1097-1100.
30. SPRANGER S., LUKE J. J., BAO R., ZHA Y., HERNANDEZ K. M., LI Y. et al. Density of immunogenic antigens does not explain the presence or absence of the T-cell-inflamed tumor microenvironment in melanoma, Proc Natl Acad Sci U S A 2016: 113: E7759-E7768.
31. SPRANGER S., DAI D., HORTON B., GAJEWSKI T. F. Tumor-Residing Batf3 Dendritic Cells Are Required for Effector T Cell Trafficking and Adoptive T Cell Therapy, Cancer Cell 2017: 31: 711-723.
32. XIAO Z., WANG R., WANG X., YANG H., DONG J., HE X. et al. Impaired function of dendritic cells within the tumor microenvironment, Frontiers in immunology 2023: 14: 1213629.
33. FAIA K., WHITE K., MURPHY E., PROCTOR J., PINK M., KOSMIDER N. et al. The phosphoinositide-3 kinase (PI3K)-δ,γ inhibitor, duvelisib shows preclinical synergy with multiple targeted therapies in hematologic malignancies, PLoS One 2018: 13.
34. RASKOV H., ORHAN A., CHRISTENSEN J. P., GÖGENUR I. Cytotoxic CD8(+) T cells in cancer and cancer immunotherapy, British journal of cancer 2021: 124: 359-367.
35. BASU R., WHITLOCK B. M., HUSSON J., LE FLOC'H A., JIN W., OYLER-YANIV A. et al. Cytotoxic T Cells Use Mechanical Force to Potentiate Target Cell Killing, Cell 2016: 165: 100-110.
36. GORDY C., HE Y. W. Endocytosis by target cells: an essential means for perforin- and granzyme-mediated killing, Cell Mol Immunol 2012: 9: 5-6.
37. FU Q., FU T. M., CRUZ A. C., SENGUPTA P., THOMAS S. K., WANG S. et al. Structural Basis and Functional Role of Intramembrane Trimerization of the Fas/CD95 Death Receptor, Mol Cell 2016: 61: 602-613.
38. PHILIP M., SCHIETINGER A. CD8(+) T cell differentiation and dysfunction in cancer, Nature reviews Immunology 2022: 22: 209-223.
39. LIU W., STACHURA P., XU H. C., BHATIA S., BORKHARDT A., LANG P. A. et al. Senescent Tumor CD8(+) T Cells: Mechanisms of Induction and Challenges to Immunotherapy, Cancers 2020: 12.
40. HAREL-BELLAN A., QUILLET A., MARCHIOL C., DEMARS R., TURSZ T., FRADELIZI D. Natural killer susceptibility of human cells may be regulated by genes in the HLA region on chromosome 6, Proc Natl Acad Sci U S A 1986: 83: 5688-5692.

41. NI J., MILLER M., STOJANOVIC A., GARBI N., CERWENKA A. Sustained effector function of IL-12/15/18-preactivated NK cells against established tumors, J Exp Med 2012: 209: 2351-2365.
42. BÖTTCHER J. P., BONAVITA E., CHAKRAVARTY P., BLEES H., CABEZA-CABRERIZO M., SAMMICHELI S. et al. NK Cells Stimulate Recruitment of cDC1 into the Tumor Microenvironment Promoting Cancer Immune Control, Cell 2018: 172: 1022-1037.
43. ALSPACH E., LUSSIER D. M., MICELI A. P., KIZHVATOV I., DUPAGE M., LUOMA A. M. et al. MHC-II neoantigens shape tumour immunity and response to immunotherapy, Nature 2019: 574: 696-701.
44. ZHANG B., KRACKER S., YASUDA T., CASOLA S., VANNEMAN M., HÖMIG-HÖLZEL C. et al. Immune surveillance and therapy of lymphomas driven by Epstein-Barr virus protein LMP1 in a mouse model, Cell 2012: 148: 739-751.
45. QUEZADA S. A., SIMPSON T. R., PEGGS K. S., MERGHOUB T., VIDER J., FAN X. et al. Tumor-reactive CD4(+) T cells develop cytotoxic activity and eradicate large established melanoma after transfer into lymphopenic hosts, J Exp Med 2010: 207: 637-650.
46. PONCETTE L., BLUHM J., BLANKENSTEIN T. The role of CD4 T cells in rejection of solid tumors, Curr Opin Immunol 2022: 74: 18-24.
47. LI C., JIANG P., WEI S., XU X., WANG J. Regulatory T cells in tumor microenvironment: new mechanisms, potential therapeutic strategies and future prospects, Mol Cancer 2020: 19: 020-01234.
48. TOOMER K. H., MALEK T. R. Cytokine Signaling in the Development and Homeostasis of Regulatory T cells, Cold Spring Harb Perspect Biol 2018: 10.
49. SARHAN D., HIPPEN K. L., LEMIRE A., HYING S., LUO X., LENVIK T. et al. Adaptive NK Cells Resist Regulatory T-cell Suppression Driven by IL37, Cancer Immunol Res 2018: 6: 766-775.
50. CARMENATE T., ORTÍZ Y., ENAMORADO M., GARCÍA-MARTÍNEZ K., AVELLANET J., MORENO E. et al. Blocking IL-2 Signal In Vivo with an IL-2 Antagonist Reduces Tumor Growth through the Control of Regulatory T Cells, J Immunol 2018: 200: 3475-3484.
51. OHTA A., KINI R., SUBRAMANIAN M., MADASU M., SITKOVSKY M. The development and immunosuppressive functions of CD4(+) CD25(+) FoxP3(+) regulatory T cells are under influence of the adenosine-A2A adenosine receptor pathway, Frontiers in immunology 2012: 3.
52. HEDRICK C. C., MALANCHI I. Neutrophils in cancer: heterogeneous and multifaceted, Nature reviews Immunology 2022: 22: 173-187.
53. CANLI Ö., NICOLAS A. M., GUPTA J., FINKELMEIER F., GONCHAROVA O., PESIC M. et al. Myeloid Cell-Derived Reactive Oxygen Species Induce Epithelial Mutagenesis, Cancer Cell 2017: 32: 869-883.
54. WCULEK S. K., BRIDGEMAN V. L., PEAKMAN F., MALANCHI I. Early Neutrophil Responses to Chemical Carcinogenesis Shape Long-Term Lung Cancer Susceptibility, iScience 2020: 23: 17.
55. BAYIK D., ZHOU Y., PARK C., HONG C., VAIL D., SILVER D. J. et al. Myeloid-Derived Suppressor Cell Subsets Drive Glioblastoma Growth in a Sex-Specific Manner, Cancer discovery 2020: 10: 1210-1225.
56. ANTONIO N., BØNNELYKKE-BEHRNDTZ M. L., WARD L. C., COLLIN J., CHRISTENSEN I. J., STEINICHE T. et al. The wound inflammatory response exacerbates growth of pre-neoplastic cells and progression to cancer, Embo J 2015: 34: 2219-2236.
57. HE G., ZHANG H., ZHOU J., WANG B., CHEN Y., KONG Y. et al. Peritumoural neutrophils negatively regulate adaptive immunity via the PD-L1/PD-1 signalling pathway in hepatocellular carcinoma, Journal of experimental & clinical cancer research : CR 2015: 34: 015-0256.
58. JAMIESON T., CLARKE M., STEELE C. W., SAMUEL M. S., NEUMANN J., JUNG A. et al. Inhibition of CXCR2 profoundly suppresses inflammation-driven and spontaneous tumorigenesis, J Clin Invest 2012: 122: 3127-3144.
59. KATOH H., WANG D., DAIKOKU T., SUN H., DEY S. K., DUBOIS R. N. CXCR2-expressing myeloid-derived suppressor cells are essential to promote colitis-associated tumorigenesis, Cancer Cell 2013: 24: 631-644.

60. TRINER D., DEVENPORT S. N., RAMAKRISHNAN S. K., MA X., FRIELER R. A., GREENSON J. K. et al. Neutrophils Restrict Tumor-Associated Microbiota to Reduce Growth and Invasion of Colon Tumors in Mice, Gastroenterology 2019: 156: 1467-1482.
61. KOGA Y., MATSUZAKI A., SUMINOE A., HATTORI H., HARA T. Neutrophil-derived TNF-related apoptosis-inducing ligand (TRAIL): a novel mechanism of antitumor effect by neutrophils, Cancer Res 2004: 64: 1037-1043.
62. FINISGUERRA V., DI CONZA G., DI MATTEO M., SERNEELS J., COSTA S., THOMPSON A. A. et al. MET is required for the recruitment of anti-tumoural neutrophils, Nature 2015: 522: 349-353.
63. CHEN X., LI Y., XIA H., CHEN Y. H. Monocytes in Tumorigenesis and Tumor Immunotherapy, Cells 2023: 12.
64. GRIFFITH T. S., WILEY S. R., KUBIN M. Z., SEDGER L. M., MALISZEWSKI C. R., FANGER N. A. Monocyte-mediated tumoricidal activity via the tumor necrosis factor-related cytokine, TRAIL, J Exp Med 1999: 189: 1343-1354.
65. HORZUM U., YOYEN-ERMIS D., TASKIRAN E. Z., YILMAZ K. B., HAMALOGLU E., KARAKOC D. et al. CD66b(+) monocytes represent a proinflammatory myeloid subpopulation in cancer, Cancer Immunol Immunother 2021: 70: 75-87.
66. QU Y., WEN J., THOMAS G., YANG W., PRIOR W., HE W. et al. Baseline Frequency of Inflammatory Cxcl9-Expressing Tumor-Associated Macrophages Predicts Response to Avelumab Treatment, Cell Rep 2020: 32: 107873.
67. CASSETTA L., FRAGKOGIANNI S., SIMS A. H., SWIERCZAK A., FORRESTER L. M., ZHANG H. et al. Human Tumor-Associated Macrophage and Monocyte Transcriptional Landscapes Reveal Cancer-Specific Reprogramming, Biomarkers, and Therapeutic Targets, Cancer Cell 2019: 35: 588-602.
68. LI T., BOU-DARGHAM M. J., FULTANG N., LI X., PEAR W. S., SUN H. et al. c-Rel-dependent monocytes are potent immune suppressor cells in cancer, J Leukoc Biol 2022: 112: 845-859.
69. SCHLECKER E., STOJANOVIC A., EISEN C., QUACK C., FALK C. S., UMANSKY V. et al. Tumor-infiltrating monocytic myeloid-derived suppressor cells mediate CCR5-dependent recruitment of regulatory T cells favoring tumor growth, J Immunol 2012: 189: 5602-5611.
70. JAKUBZICK C. V., RANDOLPH G. J., HENSON P. M. Monocyte differentiation and antigen-presenting functions, Nature reviews Immunology 2017: 17: 349-362.
71. KUHN S., YANG J., RONCHESE F. Monocyte-Derived Dendritic Cells Are Essential for CD8(+) T Cell Activation and Antitumor Responses After Local Immunotherapy, Frontiers in immunology 2015: 6.
72. FRANKLIN R. A., LIAO W., SARKAR A., KIM M. V., BIVONA M. R., LIU K. et al. The cellular and molecular origin of tumor-associated macrophages, Science (New York, NY) 2014: 344: 921-925.
73. MOSSER D. M., EDWARDS J. P. Exploring the full spectrum of macrophage activation, Nature reviews Immunology 2008: 8: 958-969.
74. LECOULTRE M., DUTOIT V., WALKER P. R. Phagocytic function of tumor-associated macrophages as a key determinant of tumor progression control: a review, Journal for immunotherapy of cancer 2020: 8: 2020-001408.
75. MANTOVANI A., ALLAVENA P., MARCHESI F., GARLANDA C. Macrophages as tools and targets in cancer therapy, Nat Rev Drug Discov 2022: 21: 799-820.
76. DEBELA D. T., MUZAZU S. G., HERARO K. D., NDALAMA M. T., MESELE B. W., HAILE D. C. et al. New approaches and procedures for cancer treatment: Current perspectives, SAGE Open Med 2021: 9.
77. ZAIGHAM A., SAKINA R. An Overview of Cancer Treatment Modalities. In: Hafiz Naveed S., editor. Neoplasm, Rijeka: IntechOpen; 2018, p. Ch. 6.
78. PHILIP P. A., LACY J., PORTALES F., SOBRERO A., PAZO-CID R., MANZANO MOZO J. L. et al. Nab-paclitaxel plus gemcitabine in patients with locally advanced pancreatic cancer (LAPACT): a multicentre, open-label phase 2 study, Lancet Gastroenterol Hepatol 2020: 5: 285-294.

79. NAJAFI M., MAJIDPOOR J., TOOLEE H., MORTEZAEE K. The current knowledge concerning solid cancer and therapy, J Biochem Mol Toxicol 2021: 35: 31.
80. LEE S. Y., JEONG E. K., JU M. K., JEON H. M., KIM M. Y., KIM C. H. et al. Induction of metastasis, cancer stem cell phenotype, and oncogenic metabolism in cancer cells by ionizing radiation, Mol Cancer 2017: 16: 016-0577.
81. BENOIT A., VOGIN G., DUHEM C., BERCHEM G., JANJI B. Lighting Up the Fire in the Microenvironment of Cold Tumors: A Major Challenge to Improve Cancer Immunotherapy, Cells 2023: 12.
82. STERNER R. C., STERNER R. M. CAR-T cell therapy: current limitations and potential strategies, Blood Cancer J 2021: 11: 021-00459.
83. BUKOWSKI K., KCIUK M., KONTEK R. Mechanisms of Multidrug Resistance in Cancer Chemotherapy, Int J Mol Sci 2020: 21.
84. YARBRO J. W. Mechanism of action of hydroxyurea, Semin Oncol 1992: 19: 1-10.
85. SINGH R., MALHOTRA A., BANSAL R. Chapter 15 - Synthetic cytotoxic drugs as cancer chemotherapeutic agents. In: Acharya P. C. & Kurosu M., editors. Medicinal Chemistry of Chemotherapeutic Agents: Academic Press; 2023, p. 499-537.
86. FU D., CALVO J. A., SAMSON L. D. Balancing repair and tolerance of DNA damage caused by alkylating agents, Nature reviews Cancer 2012: 12: 104-120.
87. NUSSBAUMER S., BONNABRY P., VEUTHEY J. L., FLEURY-SOUVERAIN S. Analysis of anticancer drugs: a review, Talanta 2011: 85: 2265-2289.
88. MIN H. Y., LEE H. Y. Molecular targeted therapy for anticancer treatment, Exp Mol Med 2022: 54: 1670-1694.
89. ABRAHAM J., OCEN J., STAFFURTH J. Hormonal therapy for cancer, Medicine 2023: 51: 28-31.
90. ZHONG L., LI Y., XIONG L., WANG W., WU M., YUAN T. et al. Small molecules in targeted cancer therapy: advances, challenges, and future perspectives, Signal transduction and targeted therapy 2021: 6: 201.
91. ROSKOSKI R., JR. The ErbB/HER family of protein-tyrosine kinases and cancer, Pharmacological research 2014: 79: 34-74.
92. DEAN-COLOMB W., ESTEVA F. J. Her2-positive breast cancer: herceptin and beyond, European journal of cancer (Oxford, England : 1990) 2008: 44: 2806-2812.
93. HA S. Y., CHOI S. J., CHO J. H., CHOI H. J., LEE J., JUNG K. et al. Lung cancer in never-smoker Asian females is driven by oncogenic mutations, most often involving EGFR, Oncotarget 2015: 6: 5465-5474.
94. THOMAS R., WEIHUA Z. Rethink of EGFR in Cancer With Its Kinase Independent Function on Board, Frontiers in oncology 2019: 9: 800.
95. SUDA K., ONOZATO R., YATABE Y., MITSUDOMI T. EGFR T790M mutation: a double role in lung cancer cell survival?, Journal of thoracic oncology : official publication of the International Association for the Study of Lung Cancer 2009: 4: 1-4.
96. DHILLON S. Lazertinib: First Approval, Drugs 2021: 81: 1107-1113.
97. GALIZIA G., LIETO E., DE VITA F., ORDITURA M., CASTELLANO P., TROIANI T. et al. Cetuximab, a chimeric human mouse anti-epidermal growth factor receptor monoclonal antibody, in the treatment of human colorectal cancer, Oncogene 2007: 26: 3654-3660.
98. KEATING G. M. Panitumumab: a review of its use in metastatic colorectal cancer, Drugs 2010: 70: 1059-1078.
99. NAMI B., MAADI H., WANG Z. Mechanisms Underlying the Action and Synergism of Trastuzumab and Pertuzumab in Targeting HER2-Positive Breast Cancer, Cancers (Basel) 2018: 10.
100. DELLA CORTE C. M., VISCARDI G., DI LIELLO R., FASANO M., MARTINELLI E., TROIANI T. et al. Role and targeting of anaplastic lymphoma kinase in cancer, Molecular Cancer 2018: 17: 30.
101. GOLDING B., LUU A., JONES R., VILORIA-PETIT A. M. The function and therapeutic targeting of anaplastic lymphoma kinase (ALK) in non-small cell lung cancer (NSCLC), Mol Cancer 2018: 17: 52.

102. YAMAOKA T., KUSUMOTO S., ANDO K., OHBA M., OHMORI T. Receptor Tyrosine Kinase-Targeted Cancer Therapy, Int J Mol Sci 2018: 19.
103. GREUBER E. K., SMITH-PEARSON P., WANG J., PENDERGAST A. M. Role of ABL family kinases in cancer: from leukaemia to solid tumours, Nature reviews Cancer 2013: 13: 559-571.
104. WEN T., WANG J., SHI Y., QIAN H., LIU P. Inhibitors targeting Bruton's tyrosine kinase in cancers: drug development advances, Leukemia 2021: 35: 312-332.
105. HENDRIKS R. W., YUVARAJ S., KIL L. P. Targeting Bruton's tyrosine kinase in B cell malignancies, Nature reviews Cancer 2014: 14: 219-232.
106. ROZKIEWICZ D., HERMANOWICZ J. M., KWIATKOWSKA I., KRUPA A., PAWLAK D. Bruton's Tyrosine Kinase Inhibitors (BTKIs): Review of Preclinical Studies and Evaluation of Clinical Trials, Molecules (Basel, Switzerland) 2023: 28.
107. SEAVEY M. M., DOBRZANSKI P. The many faces of Janus kinase, Biochemical pharmacology 2012: 83: 1136-1145.
108. CHO K. N., LEE K. I. Chemistry and biology of Ras farnesyltransferase, Archives of pharmacal research 2002: 25: 759-769.
109. PRIOR I. A., HOOD F. E., HARTLEY J. L. The Frequency of Ras Mutations in Cancer, Cancer Res 2020: 80: 2969-2974.
110. ZHANG S. S., NAGASAKA M. Spotlight on Sotorasib (AMG 510) for KRAS (G12C) Positive Non-Small Cell Lung Cancer, Lung Cancer (Auckland, NZ) 2021: 12: 115-122.
111. YAEGER R., CORCORAN R. B. Targeting Alterations in the RAF-MEK Pathway, Cancer discovery 2019: 9: 329-341.
112. KOELBLINGER P., THUERIGEN O., DUMMER R. Development of encorafenib for BRAF-mutated advanced melanoma, Current opinion in oncology 2018: 30: 125-133.
113. YANG J., NIE J., MA X., WEI Y., PENG Y., WEI X. Targeting PI3K in cancer: mechanisms and advances in clinical trials, Mol Cancer 2019: 18: 26.
114. SIMIONI C., MARTELLI A. M., ZAULI G., MELLONI E., NERI L. M. Targeting mTOR in Acute Lymphoblastic Leukemia, Cells 2019: 8.
115. LEE S. Y., JANG C., LEE K. A. Polo-like kinases (plks), a key regulator of cell cycle and new potential target for cancer therapy, Development & reproduction 2014: 18: 65-71.
116. LIM S., KALDIS P. Cdks, cyclins and CKIs: roles beyond cell cycle regulation, Development (Cambridge, England) 2013: 140: 3079-3093.
117. LU J. Palbociclib: a first-in-class CDK4/CDK6 inhibitor for the treatment of hormone-receptor positive advanced breast cancer, Journal of hematology & oncology 2015: 8: 98.
118. WATT A. C., GOEL S. Cellular mechanisms underlying response and resistance to CDK4/6 inhibitors in the treatment of hormone receptor-positive breast cancer, Breast cancer research : BCR 2022: 24: 17.
119. GOROSHCHUK O., KOLOSENKO I., VIDARSDOTTIR L., AZIMI A., PALM-APERGI C. Polo-like kinases and acute leukemia, Oncogene 2019: 38: 1-16.
120. HOLTRICH U., WOLF G., BRÄUNINGER A., KARN T., BÖHME B., RÜBSAMEN-WAIGMANN H. et al. Induction and down-regulation of PLK, a human serine/threonine kinase expressed in proliferating cells and tumors, Proc Natl Acad Sci U S A 1994: 91: 1736-1740.
121. LIU Z., SUN Q., WANG X. PLK1, A Potential Target for Cancer Therapy, Translational oncology 2017: 10: 22-32.
122. RUDOLPH D., STEEGMAIER M., HOFFMANN M., GRAUERT M., BAUM A., QUANT J. et al. BI 6727, a Polo-like kinase inhibitor with improved pharmacokinetic profile and broad antitumor activity, Clinical cancer research : an official journal of the American Association for Cancer Research 2009: 15: 3094-3102.
123. NGUYEN T., PARKER R., HAWKINS E., HOLKOVA B., YAZBECK V., KOLLURI A. et al. Synergistic interactions between PLK1 and HDAC inhibitors in non-Hodgkin's lymphoma cells occur in vitro and in vivo and proceed through multiple mechanisms, Oncotarget 2017: 8: 31478-31493.

124. JAYANTHAN A., COOPER T., DUNN S. E., LEWIS V. A., NARENDRAN A. Cooperative Lethality of Polo-Like Kinases (PLK) and Aurora Kinases (AK) in Refractory Pediatric Leukemia, Blood 2012: 120: 3573.
125. STACHURA P., STENCEL O., LU Z., BORKHARDT A., PANDYRA A. A. Arenaviruses: Old viruses present new solutions for cancer therapy, Frontiers in immunology 2023: 14: 1110522.
126. HODGE J. W., GARNETT C. T., FARSACI B., PALENA C., TSANG K. Y., FERRONE S. et al. Chemotherapy-induced immunogenic modulation of tumor cells enhances killing by cytotoxic T lymphocytes and is distinct from immunogenic cell death, Int J Cancer 2013: 133: 624-636.
127. LIU L., CHEN J. Therapeutic antibodies for precise cancer immunotherapy: current and future perspectives, Medical Review 2022: 2: 555-569.
128. ZAHAVI D., ALDEGHAITHER D., O'CONNELL A., WEINER L. M. Enhancing antibody-dependent cell-mediated cytotoxicity: a strategy for improving antibody-based immunotherapy, Antibody therapeutics 2018: 1: 7-12.
129. NIMMERJAHN F., RAVETCH J. V. Fcgamma receptors as regulators of immune responses, Nature reviews Immunology 2008: 8: 34-47.
130. LABRIJN A. F., JANMAAT M. L., REICHERT J. M., PARREN P. Bispecific antibodies: a mechanistic review of the pipeline, Nat Rev Drug Discov 2019: 18: 585-608.
131. FENIS A., DEMARIA O., GAUTHIER L., VIVIER E., NARNI-MANCINELLI E. New immune cell engagers for cancer immunotherapy, Nature reviews Immunology 2024: 24: 471-486.
132. CARTER P. J., RAJPAL A. Designing antibodies as therapeutics, Cell 2022: 185: 2789-2805.
133. DEAN A. Q., LUO S., TWOMEY J. D., ZHANG B. Targeting cancer with antibody-drug conjugates: Promises and challenges, mAbs 2021: 13: 1951427.
134. RILEY J. L. PD-1 signaling in primary T cells, Immunological reviews 2009: 229: 114-125.
135. YOKOSUKA T., KOBAYASHI W., TAKAMATSU M., SAKATA-SOGAWA K., ZENG H., HASHIMOTO-TANE A. et al. Spatiotemporal basis of CTLA-4 costimulatory molecule-mediated negative regulation of T cell activation, Immunity 2010: 33: 326-339.
136. WEI S. C., DUFFY C. R., ALLISON J. P. Fundamental Mechanisms of Immune Checkpoint Blockade Therapy, Cancer discovery 2018: 8: 1069-1086.
137. QIN S., XU L., YI M., YU S., WU K., LUO S. Novel immune checkpoint targets: moving beyond PD-1 and CTLA-4, Mol Cancer 2019: 18: 155.
138. CONROY M., NAIDOO J. Immune-related adverse events and the balancing act of immunotherapy, Nat Commun 2022: 13: 392.
139. HUANG R. Y., FRANCOIS A., MCGRAY A. R., MILIOTTO A., ODUNSI K. Compensatory upregulation of PD-1, LAG-3, and CTLA-4 limits the efficacy of single-agent checkpoint blockade in metastatic ovarian cancer, Oncoimmunology 2017: 6: e1249561.
140. MILLER B. C., SEN D. R., AL ABOSY R., BI K., VIRKUD Y. V., LAFLEUR M. W. et al. Subsets of exhausted CD8(+) T cells differentially mediate tumor control and respond to checkpoint blockade, Nature immunology 2019: 20: 326-336.
141. CHIM C. S., KUMAR S. K., ORLOWSKI R. Z., COOK G., RICHARDSON P. G., GERTZ M. A. et al. Management of relapsed and refractory multiple myeloma: novel agents, antibodies, immunotherapies and beyond, Leukemia 2018: 32: 252-262.
142. LUPTAKOVA K., ROSENBLATT J., GLOTZBECKER B., MILLS H., STROOPINSKY D., KUFE T. et al. Lenalidomide enhances anti-myeloma cellular immunity, Cancer Immunol Immunother 2013: 62: 39-49.
143. DERISSEN E. J., BEIJNEN J. H., SCHELLENS J. H. Concise drug review: azacitidine and decitabine, Oncologist 2013: 18: 619-624.
144. LUO N., NIXON M. J., GONZALEZ-ERICSSON P. I., SANCHEZ V., OPALENIK S. R., LI H. et al. DNA methyltransferase inhibition upregulates MHC-I to potentiate cytotoxic T lymphocyte responses in breast cancer, Nat Commun 2018: 9: 017-02630.
145. BANACH M., SERBAN C., SAHEBKAR A., MIKHAILIDIS D. P., URSONIU S., RAY K. K. et al. Impact of statin therapy on coronary plaque composition: a systematic review and meta-analysis of virtual histology intravascular ultrasound studies, BMC Med 2015: 13: 015-0459.

146. LONGO J., PANDYRA A. A., STACHURA P., MINDEN M. D., SCHIMMER A. D., PENN L. Z. Cyclic AMP-hydrolyzing phosphodiesterase inhibitors potentiate statin-induced cancer cell death, Molecular oncology 2020: 14: 2533-2545.
147. SARRABAYROUSE G., PICH C., TEITI I., TILKIN-MARIAME A. F. Regulatory properties of statins and rho gtpases prenylation inhibitiors to stimulate melanoma immunogenicity and promote anti-melanoma immune response, Int J Cancer 2017: 140: 747-755.
148. ZIEGLER V., HENNINGER C., SIMIANTONAKIS I., BUCHHOLZER M., AHMADIAN M. R., BUDACH W. et al. Rho inhibition by lovastatin affects apoptosis and DSB repair of primary human lung cells in vitro and lung tissue in vivo following fractionated irradiation, Cell death & disease 2017: 8: 372.
149. PALOMINO-MORALES R., PERALES S., TORRES C., LINARES A., ALEJANDRE M. J. Effect of HMG-CoA Reductase Inhibition on Vascular Smooth Muscle Cells Extracellular Matrix Production: Role of RhoA, Curr Vasc Pharmacol 2016: 14: 345-352.
150. ISLAM M., SHARMA S., KUMAR B., TEKNOS T. N. Atorvastatin inhibits RhoC function and limits head and neck cancer metastasis, Oral Oncol 2013: 49: 778-786.
151. SARRABAYROUSE G., PICH C., MORIEZ R., ARMAND-LABIT V., ROCHAIX P., FAVRE G. et al. Melanoma cells treated with GGTI and IFN-gamma allow murine vaccination and enhance cytotoxic response against human melanoma cells, PLoS One 2010: 5: 0009043.
152. VOGEL T. J., GOODMAN M. T., LI A. J., JEON C. Y. Statin treatment is associated with survival in a nationally representative population of elderly women with epithelial ovarian cancer, Gynecol Oncol 2017: 146: 340-345.
153. WANG A., WAKELEE H. A., ARAGAKI A. K., TANG J. Y., KURIAN A. W., MANSON J. E. et al. Protective Effects of Statins in Cancer: Should They Be Prescribed for High-Risk Patients?, Curr Atheroscler Rep 2016: 18: 016-0625.
154. SHAW R. J., LAMIA K. A., VASQUEZ D., KOO S. H., BARDEESY N., DEPINHO R. A. et al. The kinase LKB1 mediates glucose homeostasis in liver and therapeutic effects of metformin, Science (New York, NY) 2005: 310: 1642-1646.
155. PEREIRA F. V., MELO A. C. L., LOW J. S., DE CASTRO Í A., BRAGA T. T., ALMEIDA D. C. et al. Metformin exerts antitumor activity via induction of multiple death pathways in tumor cells and activation of a protective immune response, Oncotarget 2018: 9: 25808-25825.
156. CHA J. H., YANG W. H., XIA W., WEI Y., CHAN L. C., LIM S. O. et al. Metformin Promotes Antitumor Immunity via Endoplasmic-Reticulum-Associated Degradation of PD-L1, Mol Cell 2018: 71: 606-620.
157. GEORGE A. J., THOMAS W. G., HANNAN R. D. The renin-angiotensin system and cancer: old dog, new tricks, Nature reviews Cancer 2010: 10: 745-759.
158. NAKAMURA K., YAGUCHI T., OHMURA G., KOBAYASHI A., KAWAMURA N., IWATA T. et al. Involvement of local renin-angiotensin system in immunosuppression of tumor microenvironment, Cancer Sci 2018: 109: 54-64.
159. BUSBY J., MCMENAMIN Ú., SPENCE A., JOHNSTON B. T., HUGHES C., CARDWELL C. R. Angiotensin receptor blocker use and gastro-oesophageal cancer survival: a population-based cohort study, Aliment Pharmacol Ther 2018: 47: 279-288.
160. CERULLO M., GANI F., CHEN S. Y., CANNER J. K., PAWLIK T. M. Impact of Angiotensin Receptor Blocker Use on Overall Survival Among Patients Undergoing Resection for Pancreatic Cancer, World J Surg 2017: 41: 2361-2370.
161. GLENNON R. A., HONG S. S., DUKAT M., TEITLER M., DAVIS K. 5-(Nonyloxy)tryptamine: a novel high-affinity 5-HT1D beta serotonin receptor agonist, Journal of medicinal chemistry 1994: 37: 2828-2830.
162. ENJIN A., LEÃO K. E., MIKULOVIC S., LE MERRE P., TOURTELLOTTE W. G., KULLANDER K. Sensorimotor function is modulated by the serotonin receptor 1d, a novel marker for gamma motor neurons, Molecular and cellular neurosciences 2012: 49: 322-332.
163. SAINI V., LUTZ D., KATARIA H., KAUR G., SCHACHNER M., LOERS G. The polysialic acid mimetics 5-nonyloxytryptamine and vinorelbine facilitate nervous system repair, Scientific reports 2016: 6: 26927.

164. KALOTRA S., SAINI V., SINGH H., SHARMA A., KAUR G. 5-Nonyloxytryptamine oxalate-embedded collagen-laminin scaffolds augment functional recovery after spinal cord injury in mice, Annals of the New York Academy of Sciences 2020: 1465: 99-116.
165. LOERS G., SAINI V., MISHRA B., PAPASTEFANAKI F., LUTZ D., CHAUDHURY S. et al. Nonyloxytryptamine mimics polysialic acid and modulates neuronal and glial functions in cell culture, Journal of neurochemistry 2014: 128: 88-100.
166. KALOTRA S., KAUR G. PSA mimetic 5-nonyloxytryptamine protects cerebellar neurons against glutamate induced excitotoxicity: An in vitro perspective, Neurotoxicology 2021: 82: 69-81.
167. MAINOU B. A., ASHBROOK A. W., SMITH E. C., DORSET D. C., DENISON M. R., DERMODY T. S. Serotonin Receptor Agonist 5-Nonyloxytryptamine Alters the Kinetics of Reovirus Cell Entry, Journal of virology 2015: 89: 8701-8712.
168. BOUMA E. M., VAN DE POL D. P. I., SANDERS I. D., RODENHUIS-ZYBERT I. A., SMIT J. M. Serotonergic Drugs Inhibit Chikungunya Virus Infection at Different Stages of the Cell Entry Pathway, Journal of virology 2020: 94.
169. JOSE J., TAVARES C. D. J., EBELT N. D., LODI A., EDUPUGANTI R., XIE X. et al. Serotonin Analogues as Inhibitors of Breast Cancer Cell Growth, ACS medicinal chemistry letters 2017: 8: 1072-1076.
170. LIU W., STACHURA P., XU H. C., UMESH GANESH N., COX F., WANG R. et al. Repurposing the serotonin agonist Tegaserod as an anticancer agent in melanoma: molecular mechanisms and clinical implications, Journal of experimental & clinical cancer research : CR 2020: 39: 38.
171. ZHANG H., KONG Q., WANG J., JIANG Y., HUA H. Complex roles of cAMP-PKA-CREB signaling in cancer, Experimental hematology & oncology 2020: 9: 32.
172. AHMED M. B., ALGHAMDI A. A. A., ISLAM S. U., LEE J. S., LEE Y. S. cAMP Signaling in Cancer: A PKA-CREB and EPAC-Centric Approach, Cells 2022: 11.
173. FUJISHITA T., KOJIMA Y., KAJINO-SAKAMOTO R., MISHIRO-SATO E., SHIMIZU Y., HOSODA W. et al. The cAMP/PKA/CREB and TGFβ/SMAD4 Pathways Regulate Stemness and Metastatic Potential in Colorectal Cancer Cells, Cancer Res 2022: 82: 4179-4190.
174. STEVEN A., FRIEDRICH M., JANK P., HEIMER N., BUDCZIES J., DENKERT C. et al. What turns CREB on? And off? And why does it matter?, Cellular and molecular life sciences : CMLS 2020: 77: 4049-4067.
175. JONGSMA M. L. M., GUARDA G., SPAAPEN R. M. The regulatory network behind MHC class I expression, Molecular immunology 2019: 113: 16-21.
176. MORENO C. S., BERESFORD G. W., LOUIS-PLENCE P., MORRIS A. C., BOSS J. M. CREB regulates MHC class II expression in a CIITA-dependent manner, Immunity 1999: 10: 143-151.
177. BALLOU Y., RIVAS A., BELMONT A., PATEL L., AMAYA C. N., LIPSON S. et al. 5-HT serotonin receptors modulate mitogenic signaling and impact tumor cell viability, Molecular and clinical oncology 2018: 9: 243-254.
178. KEMP B. E., OAKHILL J. S., SCOTT J. W. AMPK structure and regulation from three angles, Structure (London, England : 1993) 2007: 15: 1161-1163.
179. HARDIE D. G., ROSS F. A., HAWLEY S. A. AMPK: a nutrient and energy sensor that maintains energy homeostasis, Nature reviews Molecular cell biology 2012: 13: 251-262.
180. PARK C. E., YUN H., LEE E. B., MIN B. I., BAE H., CHOE W. et al. The antioxidant effects of genistein are associated with AMP-activated protein kinase activation and PTEN induction in prostate cancer cells, Journal of medicinal food 2010: 13: 815-820.
181. ZADRA G., PHOTOPOULOS C., TYEKUCHEVA S., HEIDARI P., WENG Q. P., FEDELE G. et al. A novel direct activator of AMPK inhibits prostate cancer growth by blocking lipogenesis, EMBO molecular medicine 2014: 6: 519-538.
182. JEON S. M., HAY N. The dark face of AMPK as an essential tumor promoter, Cellular logistics 2012: 2: 197-202.
183. BUNGARD D., FUERTH B. J., ZENG P. Y., FAUBERT B., MAAS N. L., VIOLLET B. et al. Signaling kinase AMPK activates stress-promoted transcription via histone H2B phosphorylation, Science (New York, NY) 2010: 329: 1201-1205.

184. AHMED A., TAIT S. W. G. Targeting immunogenic cell death in cancer, Molecular oncology 2020: 14: 2994-3006.
185. GALLUZZI L., KEPP O., HETT E., KROEMER G., MARINCOLA F. M. Immunogenic cell death in cancer: concept and therapeutic implications, Journal of translational medicine 2023: 21: 162.
186. OBEID M., TESNIERE A., GHIRINGHELLI F., FIMIA G. M., APETOH L., PERFETTINI J. L. et al. Calreticulin exposure dictates the immunogenicity of cancer cell death, Nature medicine 2007: 13: 54-61.
187. APETOH L., GHIRINGHELLI F., TESNIERE A., OBEID M., ORTIZ C., CRIOLLO A. et al. Toll-like receptor 4-dependent contribution of the immune system to anticancer chemotherapy and radiotherapy, Nature medicine 2007: 13: 1050-1059.
188. GARG A. D., GALLUZZI L., APETOH L., BAERT T., BIRGE R. B., BRAVO-SAN PEDRO J. M. et al. Molecular and Translational Classifications of DAMPs in Immunogenic Cell Death, Frontiers in immunology 2015: 6: 588.
189. MARTINS I., KEPP O., SCHLEMMER F., ADJEMIAN S., TAILLER M., SHEN S. et al. Restoration of the immunogenicity of cisplatin-induced cancer cell death by endoplasmic reticulum stress, Oncogene 2011: 30: 1147-1158.
190. MESSMER M. N., SNYDER A. G., OBERST A. Comparing the effects of different cell death programs in tumor progression and immunotherapy, Cell death and differentiation 2019: 26: 115-129.
191. TANG D., KEPP O., KROEMER G. Ferroptosis becomes immunogenic: implications for anticancer treatments, Oncoimmunology 2020: 10: 1862949.
192. CHEN Z., WANG W., ABDUL RAZAK S. R., HAN T., AHMAD N. H., LI X. Ferroptosis as a potential target for cancer therapy, Cell death & disease 2023: 14: 460.
193. LEI P., BAI T., SUN Y. Mechanisms of Ferroptosis and Relations With Regulated Cell Death: A Review, Frontiers in physiology 2019: 10: 139.
194. DIXON S. J., OLZMANN J. A. The cell biology of ferroptosis, Nature reviews Molecular cell biology 2024.
195. LIU Y., GU W. p53 in ferroptosis regulation: the new weapon for the old guardian, Cell Death & Differentiation 2022: 29: 895-910.
196. DOLL S., PRONETH B., TYURINA Y. Y., PANZILIUS E., KOBAYASHI S., INGOLD I. et al. ACSL4 dictates ferroptosis sensitivity by shaping cellular lipid composition, Nature chemical biology 2017: 13: 91-98.
197. GAN B. ACSL4, PUFA, and ferroptosis: new arsenal in anti-tumor immunity, Signal transduction and targeted therapy 2022: 7: 128.
198. ZHANG C., LIU X., JIN S., CHEN Y., GUO R. Ferroptosis in cancer therapy: a novel approach to reversing drug resistance, Mol Cancer 2022: 21: 47.
199. ZHANG X., LI X., XIA R., ZHANG H.-S. Ferroptosis resistance in cancer: recent advances and future perspectives, Biochemical pharmacology 2024: 219: 115933.
200. ZHAO Y., LI Y., ZHANG R., WANG F., WANG T., JIAO Y. The Role of Erastin in Ferroptosis and Its Prospects in Cancer Therapy, OncoTargets and therapy 2020: 13: 5429-5441.
201. KEPP O., KROEMER G. Is ferroptosis immunogenic? The devil is in the details!, Oncoimmunology 2022: 11: 2127273.
202. GALLUZZI L., VITALE I., AARONSON S. A., ABRAMS J. M., ADAM D., AGOSTINIS P. et al. Molecular mechanisms of cell death: recommendations of the Nomenclature Committee on Cell Death 2018, Cell Death Differ 2018: 25: 486-541.
203. ZHENG T. S., SCHLOSSER S. F., DAO T., HINGORANI R., CRISPE I. N., BOYER J. L. et al. Caspase-3 controls both cytoplasmic and nuclear events associated with Fas-mediated apoptosis in vivo, Proc Natl Acad Sci U S A 1998: 95: 13618-13623.
204. INOUE S., BROWNE G., MELINO G., COHEN G. M. Ordering of caspases in cells undergoing apoptosis by the intrinsic pathway, Cell Death Differ 2009: 16: 1053-1061.
205. WALSH J. G., CULLEN S. P., SHERIDAN C., LUTHI A. U., GERNER C., MARTIN S. J. Executioner caspase-3 and caspase-7 are functionally distinct proteases, Proc Natl Acad Sci U S A 2008: 105: 12815-12819.

206. VITALE I., PIETROCOLA F., GUILBAUD E., AARONSON S. A., ABRAMS J. M., ADAM D. et al. Apoptotic cell death in disease-Current understanding of the NCCD 2023, Cell Death Differ 2023: 30: 1097-1154.
207. DELBRIDGE A. R., GRABOW S., STRASSER A., VAUX D. L. Thirty years of BCL-2: translating cell death discoveries into novel cancer therapies, Nat Rev Cancer 2016: 16: 99-109.
208. DICKENS L. S., BOYD R. S., JUKES-JONES R., HUGHES M. A., ROBINSON G. L., FAIRALL L. et al. A death effector domain chain DISC model reveals a crucial role for caspase-8 chain assembly in mediating apoptotic cell death, Mol Cell 2012: 47: 291-305.
209. MUZIO M., CHINNAIYAN A. M., KISCHKEL F. C., O'ROURKE K., SHEVCHENKO A., NI J. et al. FLICE, a novel FADD-homologous ICE/CED-3-like protease, is recruited to the CD95 (Fas/APO-1) death--inducing signaling complex, Cell 1996: 85: 817-827.
210. SEIDEL E., VON KARSTEDT S. Extrinsic cell death pathway plasticity: a driver of clonal evolution in cancer?, Cell Death Discov 2022: 8: 465.
211. LINKERMANN A., GREEN D. R. Necroptosis, N Engl J Med 2014: 370: 455-465.
212. MURPHY J. M., CZABOTAR P. E., HILDEBRAND J. M., LUCET I. S., ZHANG J. G., ALVAREZ-DIAZ S. et al. The pseudokinase MLKL mediates necroptosis via a molecular switch mechanism, Immunity 2013: 39: 443-453.
213. DIXON S. J., LEMBERG K. M., LAMPRECHT M. R., SKOUTA R., ZAITSEV E. M., GLEASON C. E. et al. Ferroptosis: an iron-dependent form of nonapoptotic cell death, Cell 2012: 149: 1060-1072.
214. YANG W. S., SRIRAMARATNAM R., WELSCH M. E., SHIMADA K., SKOUTA R., VISWANATHAN V. S. et al. Regulation of ferroptotic cancer cell death by GPX4, Cell 2014: 156: 317-331.
215. KLIONSKY D. J., PETRONI G., AMARAVADI R. K., BAEHRECKE E. H., BALLABIO A., BOYA P. et al. Autophagy in major human diseases, EMBO J 2021: 40: e108863.
216. GALLUZZI L., AARONSON S. A., ABRAMS J., ALNEMRI E. S., ANDREWS D. W., BAEHRECKE E. H. et al. Guidelines for the use and interpretation of assays for monitoring cell death in higher eukaryotes, Cell Death Differ 2009: 16: 1093-1107.
217. KEPP O., GALLUZZI L., LIPINSKI M., YUAN J., KROEMER G. Cell death assays for drug discovery, Nat Rev Drug Discov 2011: 10: 221-237.
218. HAVAEI M., DAVY A., WARDE-FARLEY D., BIARD A., COURVILLE A., BENGIO Y. et al. Brain tumor segmentation with deep neural networks, Medical image analysis 2017: 35: 18-31.
219. KRONBERG R. M., MESKELEVICIUS D., SABEL M., KOLLMANN M., RUBBERT C., FISCHER I. Optimal acquisition sequence for AI-assisted brain tumor segmentation under the constraint of largest information gain per additional MRI sequence, Neuroscience Informatics 2022: 2: 100053.
220. JAISWAL A. K., TIWARI P., KUMAR S., GUPTA D., KHANNA A., RODRIGUES J. J. Identifying pneumonia in chest X-rays: a deep learning approach, Measurement 2019: 145: 511-518.
221. HUANG L., HAN R., AI T., YU P., KANG H., TAO Q. et al. Serial quantitative chest CT assessment of COVID-19: a deep learning approach, Radiology: Cardiothoracic Imaging 2020: 2: e200075.
222. PAN J., HONG G., ZENG H., LIAO C., LI H., YAO Y. et al. An artificial intelligence model for the pathological diagnosis of invasion depth and histologic grade in bladder cancer, J Transl Med 2023: 21: 42.
223. KRONBERG R. M., HAEBERLE L., PFAUS M., XU H. C., KRINGS K. S., SCHLENSOG M. et al. Communicator-Driven Data Preprocessing Improves Deep Transfer Learning of Histopathological Prediction of Pancreatic Ductal Adenocarcinoma, Cancers (Basel) 2022: 14.
224. SUN T., WANG Y., LIU X., LI Z., ZHANG J., LU J. et al. Deep learning based on preoperative MR images improves the predictive power of survival models in primary spinal cord astrocytomas, Neuro Oncol 2022.
225. SHAMAI G., LIVNE A., POLONIA A., SABO E., CRETU A., BAR-SELA G. et al. Deep learning-based image analysis predicts PD-L1 status from H&E-stained histopathology images in breast cancer, Nat Commun 2022: 13: 6753.
226. ESTEVA A., KUPREL B., NOVOA R. A., KO J., SWETTER S. M., BLAU H. M. et al. Dermatologist-level classification of skin cancer with deep neural networks, Nature 2017: 542: 115-118.

227. La Greca A. D., Perez N., Castaneda S., Milone P. M., Scarafia M. A., Mobbs A. M. et al. celldeath: A tool for detection of cell death in transmitted light microscopy images by deep learning-based visual recognition, PLoS One 2021: 16: e0253666.
228. Linsley J. W., Linsley D. A., Lamstein J., Ryan G., Shah K., Castello N. A. et al. Superhuman cell death detection with biomarker-optimized neural networks, Sci Adv 2021: 7: eabf8142.
229. Werner J., Kronberg R. M., Stachura P., Ostermann P. N., Muller L., Schaal H. et al. Deep Transfer Learning Approach for Automatic Recognition of Drug Toxicity and Inhibition of SARS-CoV-2, Viruses 2021: 13.
230. Sanford K. K., Earle W. R., Likely G. D. The growth in vitro of single isolated tissue cells, J Natl Cancer Inst 1948: 9: 229-246.
231. Belmokhtar C. A., Hillion J., Segal-Bendirdjian E. Staurosporine induces apoptosis through both caspase-dependent and caspase-independent mechanisms, Oncogene 2001: 20: 3354-3362.
232. Humphreys D. T., Wilson M. R. Modes of L929 cell death induced by TNF-alpha and other cytotoxic agents, Cytokine 1999: 11: 773-782.
233. Alborzinia H., Florez A. F., Kreth S., Bruckner L. M., Yildiz U., Gartlgruber M. et al. MYCN mediates cysteine addiction and sensitizes neuroblastoma to ferroptosis, Nat Cancer 2022: 3: 471-485.
234. Bebber C. M., Thomas E. S., Stroh J., Chen Z., Androulidaki A., Schmitt A. et al. Ferroptosis response segregates small cell lung cancer (SCLC) neuroendocrine subtypes, Nat Commun 2021: 12: 2048.
235. Battistelli M., Falcieri E. Apoptotic Bodies: Particular Extracellular Vesicles Involved in Intercellular Communication, Biology 2020: 9.
236. Oropesa-Ávila M., Fernández-Vega A., de la Mata M., Maraver J. G., Cordero M. D., Cotán D. et al. Apoptotic microtubules delimit an active caspase free area in the cellular cortex during the execution phase of apoptosis, Cell Death Dis 2013: 4: e527.
237. Agmon E., Solon J., Bassereau P., Stockwell B. R. Modeling the effects of lipid peroxidation during ferroptosis on membrane properties, Scientific reports 2018: 8: 5155.
238. Dodson M., Castro-Portuguez R., Zhang D. D. NRF2 plays a critical role in mitigating lipid peroxidation and ferroptosis, Redox biology 2019: 23: 101107.
239. Dhuriya Y. K., Sharma D. Necroptosis: a regulated inflammatory mode of cell death, Journal of neuroinflammation 2018: 15: 199.
240. Shkarina K., Hasel de Carvalho E., Santos J. C., Ramos S., Leptin M., Broz P. Optogenetic activators of apoptosis, necroptosis, and pyroptosis, The Journal of cell biology 2022: 221.
241. Wirawan E., Vanden Berghe T., Lippens S., Agostinis P., Vandenabeele P. Autophagy: for better or for worse, Cell research 2012: 22: 43-61.
242. Parzych K. R., Klionsky D. J. An overview of autophagy: morphology, mechanism, and regulation, Antioxidants & redox signaling 2014: 20: 460-473.
243. He K., Zhang X., Ren S., Sun J. Deep residual learning for image recognition. Proceedings of the IEEE conference on computer vision and pattern recognition; 2016, p. 770-778.
244. Vogt M., Dienstbier N., Schliehe-Diecks J., Scharov K., Tu J. W., Gebing P. et al. Co-targeting HSP90 alpha and CDK7 overcomes resistance against HSP90 inhibitors in BCR-ABL1+ leukemia cells, Cell Death Dis 2023: 14: 799.
245. Teachey D. T., Devidas M., Wood B. L., Chen Z., Hayashi R. J., Hermiston M. L. et al. Children's Oncology Group Trial AALL1231: A Phase III Clinical Trial Testing Bortezomib in Newly Diagnosed T-Cell Acute Lymphoblastic Leukemia and Lymphoma, J Clin Oncol 2022: 40: 2106-2118.
246. Chu Y. Y., Ko C. Y., Wang S. M., Lin P. I., Wang H. Y., Lin W. C. et al. Bortezomib-induced miRNAs direct epigenetic silencing of locus genes and trigger apoptosis in leukemia, Cell Death Dis 2017: 8: e3167.

247. GULLA A., MORELLI E., SAMUR M. K., BOTTA C., HIDESHIMA T., BIANCHI G. et al. Bortezomib induces anti-multiple myeloma immune response mediated by cGAS/STING pathway activation, Blood Cancer Discov 2021: 2: 468-483.
248. WANG Y. C., WANG L. T., HUNG T. I., HONG Y. R., CHEN C. H., HO C. J. et al. Severe cellular stress drives apoptosis through a dual control mechanism independently of p53, Cell Death Discov 2022: 8: 282.
249. MORIWAKI K., CHAN F. K. Regulation of RIPK3- and RHIM-dependent Necroptosis by the Proteasome, The Journal of biological chemistry 2016: 291: 5948-5959.
250. ZENG X., KINSELLA T. J. Mammalian target of rapamycin and S6 kinase 1 positively regulate 6-thioguanine-induced autophagy, Cancer Res 2008: 68: 2384-2390.
251. GJERTSEN B. T., SCHÖFFSKI P. Discovery and development of the Polo-like kinase inhibitor volasertib in cancer therapy, Leukemia 2015: 29: 11-19.
252. PENG Y., YU H., ZHANG Y., QU F., TANG Z., QU C. et al. A ferroptosis-associated gene signature for the prediction of prognosis and therapeutic response in luminal-type breast carcinoma, Scientific reports 2021: 11: 17610.
253. HANGAUER M. J., VISWANATHAN V. S., RYAN M. J., BOLE D., EATON J. K., MATOV A. et al. Drug-tolerant persister cancer cells are vulnerable to GPX4 inhibition, Nature 2017: 551: 247-250.
254. LIAO P., WANG W., WANG W., KRYCZEK I., LI X., BIAN Y. et al. CD8(+) T cells and fatty acids orchestrate tumor ferroptosis and immunity via ACSL4, Cancer Cell 2022: 40: 365-378 e366.
255. GONG D., CHEN M., WANG Y., SHI J., HOU Y. Role of ferroptosis on tumor progression and immunotherapy, Cell Death Discov 2022: 8: 427.
256. LALONDE M. E., SASSEVILLE M., GELINAS A. M., MILANESE J. S., BELAND K., DROUIN S. et al. Genome-wide CRISPR screens identify ferroptosis as a novel therapeutic vulnerability in acute lymphoblastic leukemia, Haematologica 2022.
257. ZHAO Y., HUANG Z., PENG H. Molecular Mechanisms of Ferroptosis and Its Roles in Hematologic Malignancies, Front Oncol 2021: 11: 743006.
258. HAFERLACH T., KOHLMANN A., WIECZOREK L., BASSO G., KRONNIE G. T., BENE M. C. et al. Clinical utility of microarray-based gene expression profiling in the diagnosis and subclassification of leukemia: report from the International Microarray Innovations in Leukemia Study Group, J Clin Oncol 2010: 28: 2529-2537.
259. YANG W. S., STOCKWELL B. R. Synthetic lethal screening identifies compounds activating iron-dependent, nonapoptotic cell death in oncogenic-RAS-harboring cancer cells, Chemistry & biology 2008: 15: 234-245.
260. LEO I. R., ASWAD L., STAHL M., KUNOLD E., POST F., ERKERS T. et al. Integrative multi-omics and drug response profiling of childhood acute lymphoblastic leukemia cell lines, Nat Commun 2022: 13: 1691.
261. RUDOLPH D., IMPAGNATIELLO M. A., BLAUKOPF C., SOMMER C., GERLICH D. W., ROTH M. et al. Efficacy and mechanism of action of volasertib, a potent and selective inhibitor of Polo-like kinases, in preclinical models of acute myeloid leukemia, The Journal of pharmacology and experimental therapeutics 2015: 352: 579-589.
262. ADACHI Y., ISHIKAWA Y., KIYOI H. Identification of volasertib-resistant mechanism and evaluation of combination effects with volasertib and other agents on acute myeloid leukemia, Oncotarget 2017: 8: 78452-78465.
263. SHAH K., NASIMIAN A., AHMED M., AL ASHIRI L., DENISON L., SIME W. et al. PLK1 as a cooperating partner for BCL2-mediated antiapoptotic program in leukemia, Blood cancer journal 2023: 13: 139.
264. GAO M., MONIAN P., QUADRI N., RAMASAMY R., JIANG X. Glutaminolysis and Transferrin Regulate Ferroptosis, Mol Cell 2015: 59: 298-308.
265. DIXON S. J., STOCKWELL B. R. The role of iron and reactive oxygen species in cell death, Nature chemical biology 2014: 10: 9-17.
266. TANG D., CHEN X., KANG R., KROEMER G. Ferroptosis: molecular mechanisms and health implications, Cell research 2021: 31: 107-125.

267. SUN X., OU Z., CHEN R., NIU X., CHEN D., KANG R. et al. Activation of the p62-Keap1-NRF2 pathway protects against ferroptosis in hepatocellular carcinoma cells, Hepatology (Baltimore, Md) 2016: 63: 173-184.
268. VON MÄSSENHAUSEN A., ZAMORA GONZALEZ N., MAREMONTI F., BELAVGENI A., TONNUS W., MEYER C. et al. Dexamethasone sensitizes to ferroptosis by glucocorticoid receptor-induced dipeptidase-1 expression and glutathione depletion, Sci Adv 2022: 8: eabl8920.
269. TONTSCH-GRUNT U., RUDOLPH D., WAIZENEGGER I., BAUM A., GERLACH D., ENGELHARDT H. et al. Synergistic activity of BET inhibitor BI 894999 with PLK inhibitor volasertib in AML in vitro and in vivo, Cancer letters 2018: 421: 112-120.
270. BOYER M. W., ORCHARD P. J., GORDEN K. B., ANDERSON P. M., MCLVOR R. S., BLAZAR B. R. Dependency on intercellular adhesion molecule recognition and local interleukin-2 provision in generation of an in vivo CD8+ T-cell immune response to murine myeloid leukemia, Blood 1995: 85: 2498-2506.
271. ZHANG L., GAJEWSKI T. F., KLINE J. PD-1/PD-L1 interactions inhibit antitumor immune responses in a murine acute myeloid leukemia model, Blood 2009: 114: 1545-1552.
272. OLDENBURG E., KRONBERG R. M., NIEHOFF B., EBENHÖH O., POPA O. DeepLOKI-a deep learning based approach to identify zooplankton taxa on high-resolution images from the optical plankton recorder LOKI, Frontiers in Marine Science 2023.
273. KLEESIEK J., URBAN G., HUBERT A., SCHWARZ D., MAIER-HEIN K., BENDSZUS M. et al. Deep MRI brain extraction: A 3D convolutional neural network for skull stripping, NeuroImage 2016: 129: 460-469.
274. CICERO M., BILBILY A., COLAK E., DOWDELL T., GRAY B., PERAMPALADAS K. et al. Training and Validating a Deep Convolutional Neural Network for Computer-Aided Detection and Classification of Abnormalities on Frontal Chest Radiographs, Investigative radiology 2017: 52: 281-287.
275. VERDUIJN J., VAN DER MEEREN L., KRYSKO D. V., SKIRTACH A. G. Deep learning with digital holographic microscopy discriminates apoptosis and necroptosis, Cell Death Discov 2021: 7: 229.
276. SUN Y., QIAO Y., LIU Y., ZHOU J., WANG X., ZHENG H. et al. ent-Kaurane diterpenoids induce apoptosis and ferroptosis through targeting redox resetting to overcome cisplatin resistance, Redox biology 2021: 43: 101977.
277. LIM J. K. M., DELAIDELLI A., MINAKER S. W., ZHANG H. F., COLOVIC M., YANG H. et al. Cystine/glutamate antiporter xCT (SLC7A11) facilitates oncogenic RAS transformation by preserving intracellular redox balance, Proc Natl Acad Sci U S A 2019: 116: 9433-9442.
278. MÜLLER F., LIM J. K. M., BEBBER C. M., SEIDEL E., TISHINA S., DAHLHAUS A. et al. Elevated FSP1 protects KRAS-mutated cells from ferroptosis during tumor initiation, Cell Death Differ 2023: 30: 442-456.
279. ANDREANI C., BARTOLACCI C., SCAGLIONI P. P. Ferroptosis: A Specific Vulnerability of RAS-Driven Cancers?, Front Oncol 2022: 12: 923915.
280. LUO M., WU L., ZHANG K., WANG H., ZHANG T., GUTIERREZ L. et al. miR-137 regulates ferroptosis by targeting glutamine transporter SLC1A5 in melanoma, Cell Death Differ 2018: 25: 1457-1472.
281. AL MAMUN BHUYAN A., ASHIQUL HAQUE A. K. M., SAHU I., CAO H., KORMANN M. S. D., LANG F. Inhibition of Suicidal Erythrocyte Death by Volasertib, Cellular physiology and biochemistry : international journal of experimental cellular physiology, biochemistry, and pharmacology 2017: 43: 1472-1486.
282. VAN DEN BOSSCHE J., DEBEN C., DE PAUW I., LAMBRECHTS H., HERMANS C., DESCHOOLMEESTER V. et al. In vitro study of the Polo-like kinase 1 inhibitor volasertib in non-small-cell lung cancer reveals a role for the tumor suppressor p53, Molecular oncology 2019: 13: 1196-1213.
283. ZHANG L., LI X. M., SHI X. H., YE K., FU X. L., WANG X. et al. Sorafenib triggers ferroptosis via inhibition of HBXIP/SCD axis in hepatocellular carcinoma, Acta pharmacologica Sinica 2023: 44: 622-634.

284. LACHAIER E., LOUANDRE C., GODIN C., SAIDAK Z., BAERT M., DIOUF M. et al. Sorafenib induces ferroptosis in human cancer cell lines originating from different solid tumors, Anticancer research 2014: 34: 6417-6422.
285. GAO W., WANG X., ZHOU Y., WANG X., YU Y. Autophagy, ferroptosis, pyroptosis, and necroptosis in tumor immunotherapy, Signal transduction and targeted therapy 2022: 7: 196.
286. FRIEDMANN ANGELI J. P., KRYSKO D. V., CONRAD M. Ferroptosis at the crossroads of cancer-acquired drug resistance and immune evasion, Nat Rev Cancer 2019: 19: 405-414.
287. REDA M., NGAMCHERDTRAKUL W., NELSON M. A., SIRIWON N., WANG R., ZAIDAN H. Y. et al. Development of a nanoparticle-based immunotherapy targeting PD-L1 and PLK1 for lung cancer treatment, Nat Commun 2022: 13: 4261.
288. RENNER A. G., DOS SANTOS C., RECHER C., BAILLY C., CRÉANCIER L., KRUCZYNSKI A. et al. Polo-like kinase 1 is overexpressed in acute myeloid leukemia and its inhibition preferentially targets the proliferation of leukemic cells, Blood 2009: 114: 659-662.
289. TSYKUNOVA G., REIKVAM H., AHMED A. B., NEPSTAD I., GJERTSEN B. T., BRUSERUD Ø. Targeting of polo-like kinases and their cross talk with Aurora kinases--possible therapeutic strategies in human acute myeloid leukemia?, Expert opinion on investigational drugs 2012: 21: 587-603.
290. DÖHNER H., LÜBBERT M., FIEDLER W., FOUILLARD L., HAALAND A., BRANDWEIN J. M. et al. Randomized, phase 2 trial of low-dose cytarabine with or without volasertib in AML patients not suitable for induction therapy, Blood 2014: 124: 1426-1433.
291. OTTMANN O. G., MÜLLER-TIDOW C., KRÄMER A., SCHLENK R. F., LÜBBERT M., BUG G. et al. Phase I dose-escalation trial investigating volasertib as monotherapy or in combination with cytarabine in patients with relapsed/refractory acute myeloid leukaemia, British journal of haematology 2019: 184: 1018-1021.
292. DÖHNER H., SYMEONIDIS A., DEEREN D., DEMETER J., SANZ M. A., ANAGNOSTOPOULOS A. et al. Adjunctive Volasertib in Patients With Acute Myeloid Leukemia not Eligible for Standard Induction Therapy: A Randomized, Phase 3 Trial, HemaSphere 2021: 5: e617.
293. WAGNER J., LACHER M. D., GU C. J., LEONARDI C., MANNIS G. A Phase 2 Study with Volasertib for Ven-HMA Relapsed/Refractory Acute Myeloid Leukemia Patients Guided By a Predictive Precision Medicine Platform, Blood 2023: 142: 5952-5952.
294. RODENCAL J., KIM N., HE A., LI V. L., LANGE M., HE J. et al. Sensitization of cancer cells to ferroptosis coincident with cell cycle arrest, Cell chemical biology 2024: 31: 234-248.e213.
295. GAGLIARDI M., COTELLA D., SANTORO C., CORÀ D., BARLEV N. A., PIACENTINI M. et al. Aldo-keto reductases protect metastatic melanoma from ER stress-independent ferroptosis, Cell Death Dis 2019: 10: 902.
296. TAN C., SUN F., KONG T., ZHANG W., YANG C., LIU C. A survey on deep transfer learning. International conference on artificial neural networks: Springer; 2018, p. 270-279.
297. OIKONOMOU A., VALSECCHI L., QUADRI M., WATRIN T., SCHAROV K., PROCOPIO S. et al. High-throughput screening as a drug repurposing strategy for poor outcome subgroups of pediatric B-cell precursor Acute Lymphoblastic Leukemia, Biochemical pharmacology 2023: 217: 115809.
298. ZELLE-RIESER C., THANGAVADIVEL S., BIEDERMANN R., BRUNNER A., STOITZNER P., WILLENBACHER E. et al. T cells in multiple myeloma display features of exhaustion and senescence at the tumor site, Journal of hematology & oncology 2016: 9: 116.
299. MOREIRA A., GROSS S., KIRCHBERGER M. C., ERDMANN M., SCHULER G., HEINZERLING L. Senescence markers: Predictive for response to checkpoint inhibitors, International Journal of Cancer 2019: 144: 1147-1150.
300. HENSON S. M., LANNA A., RIDDELL N. E., FRANZESE O., MACAULAY R., GRIFFITHS S. J. et al. p38 signaling inhibits mTORC1-independent autophagy in senescent human $CD8^+$ T cells, The Journal of clinical investigation 2014: 124: 4004-4016.
301. MARIN I., SERRANO M., PIETROCOLA F. Recent insights into the crosstalk between senescent cells and CD8 T lymphocytes, npj aging 2023: 9: 8.

302. LIU X., MO W., YE J., LI L., ZHANG Y., HSUEH E. C. et al. Regulatory T cells trigger effector T cell DNA damage and senescence caused by metabolic competition, Nature Communications 2018: 9: 249.
303. HENSON S. M., MACAULAY R., RIDDELL N. E., NUNN C. J., AKBAR A. N. Blockade of PD-1 or p38 MAP kinase signaling enhances senescent human CD8(+) T-cell proliferation by distinct pathways, European journal of immunology 2015: 45: 1441-1451.
304. DIETSCH G. N., RANDALL T. D., GOTTARDO R., NORTHFELT D. W., RAMANATHAN R. K., COHEN P. A. et al. Late-Stage Cancer Patients Remain Highly Responsive to Immune Activation by the Selective TLR8 Agonist Motolimod (VTX-2337), Clinical cancer research : an official journal of the American Association for Cancer Research 2015: 21: 5445-5452.
305. CHOW L. Q. M., MORISHIMA C., EATON K. D., BAIK C. S., GOULART B. H., ANDERSON L. N. et al. Phase Ib Trial of the Toll-like Receptor 8 Agonist, Motolimod (VTX-2337), Combined with Cetuximab in Patients with Recurrent or Metastatic SCCHN, Clinical cancer research : an official journal of the American Association for Cancer Research 2017: 23: 2442-2450.
306. HOYER D., CLARKE D. E., FOZARD J. R., HARTIG P. R., MARTIN G. R., MYLECHARANE E. J. et al. International Union of Pharmacology classification of receptors for 5-hydroxytryptamine (Serotonin), Pharmacological reviews 1994: 46: 157-203.
307. RAY R. S., CORCORAN A. E., BRUST R. D., KIM J. C., RICHERSON G. B., NATTIE E. et al. Impaired respiratory and body temperature control upon acute serotonergic neuron inhibition, Science (New York, NY) 2011: 333: 637-642.
308. GERSHON M. D., WADE P. R., KIRCHGESSNER A. L., TAMIR H. 5-HT receptor subtypes outside the central nervous system. Roles in the physiology of the gut, Neuropsychopharmacology : official publication of the American College of Neuropsychopharmacology 1990: 3: 385-395.
309. CLOUTIER N., ALLAEYS I., MARCOUX G., MACHLUS K. R., MAILHOT B., ZUFFEREY A. et al. Platelets release pathogenic serotonin and return to circulation after immune complex-mediated sequestration, Proc Natl Acad Sci U S A 2018: 115: E1550-e1559.
310. JIN X., LI H., LI B., ZHANG C., HE Y. Knockdown and inhibition of hydroxytryptamine receptor 1D suppress proliferation and migration of gastric cancer cells, Biochemical and biophysical research communications 2022: 620: 143-149.
311. WU W., LI Q., ZHU Z., LI C., LU P., ZHOU X. et al. HTR1D functions as a key target of HOXA10-AS/miR-340-3p axis to promote the malignant outcome of pancreatic cancer via PI3K-AKT signaling pathway, International journal of biological sciences 2022: 18: 3777-3794.
312. EFIMOVA I., CATANZARO E., VAN DER MEEREN L., TURUBANOVA V. D., HAMMAD H., MISHCHENKO T. A. et al. Vaccination with early ferroptotic cancer cells induces efficient antitumor immunity, Journal for immunotherapy of cancer 2020: 8.
313. LIAO P., WANG W., WANG W., KRYCZEK I., LI X., BIAN Y. et al. CD8(+) T cells and fatty acids orchestrate tumor ferroptosis and immunity via ACSL4, Cancer Cell 2022: 40: 365-378.e366.
314. WIERNICKI B., MASCHALIDI S., PINNEY J., ADJEMIAN S., VANDEN BERGHE T., RAVICHANDRAN K. S. et al. Cancer cells dying from ferroptosis impede dendritic cell-mediated anti-tumor immunity, Nature Communications 2022: 13: 3676.
315. JIANG L., KON N., LI T., WANG S. J., SU T., HIBSHOOSH H. et al. Ferroptosis as a p53-mediated activity during tumour suppression, Nature 2015: 520: 57-62.
316. LANG X., GREEN M. D., WANG W., YU J., CHOI J. E., JIANG L. et al. Radiotherapy and Immunotherapy Promote Tumoral Lipid Oxidation and Ferroptosis via Synergistic Repression of SLC7A11, Cancer discovery 2019: 9: 1673-1685.
317. BARATELLI F., LIN Y., ZHU L., YANG S. C., HEUZÉ-VOURC'H N., ZENG G. et al. Prostaglandin E2 induces FOXP3 gene expression and T regulatory cell function in human CD4+ T cells, Journal of immunology (Baltimore, Md : 1950) 2005: 175: 1483-1490.
318. WIERNICKI B., MASCHALIDI S., PINNEY J., ADJEMIAN S., VANDEN BERGHE T., RAVICHANDRAN K. S. et al. Cancer cells dying from ferroptosis impede dendritic cell-mediated anti-tumor immunity, Nat Commun 2022: 13: 3676.

319. LUO X., GONG H. B., GAO H. Y., WU Y. P., SUN W. Y., LI Z. Q. et al. Oxygenated phosphatidylethanolamine navigates phagocytosis of ferroptotic cells by interacting with TLR2, Cell Death Differ 2021: 28: 1971-1989.
320. CRAMER S. L., SAHA A., LIU J., TADI S., TIZIANI S., YAN W. et al. Systemic depletion of L-cyst(e)ine with cyst(e)inase increases reactive oxygen species and suppresses tumor growth, Nature medicine 2017: 23: 120-127.
321. WANG W., GREEN M., CHOI J. E., GIJÓN M., KENNEDY P. D., JOHNSON J. K. et al. CD8(+) T cells regulate tumour ferroptosis during cancer immunotherapy, Nature 2019: 569: 270-274.
322. SONG R., LI T., YE J., SUN F., HOU B., SAEED M. et al. Acidity-Activatable Dynamic Nanoparticles Boosting Ferroptotic Cell Death for Immunotherapy of Cancer, Advanced materials (Deerfield Beach, Fla) 2021: 33: e2101155.
323. XU C., SUN S., JOHNSON T., QI R., ZHANG S., ZHANG J. et al. The glutathione peroxidase Gpx4 prevents lipid peroxidation and ferroptosis to sustain Treg cell activation and suppression of antitumor immunity, Cell reports 2021: 35: 109235.

Declaration

I declare under oath that I have produced my thesis independently and without any undue assistance by third parties under consideration of the ‘Principles for the Safeguarding of Good Scientific Practice at Heinrich Heine University Düsseldorf’.

_____

Paweł Stachura, 22.07.2024